The Dissertation Committee for Andrew James Sexton certifies that this is the approved version of the following dissertation:

Amine Oxidation in CO_2 Capture Processes

Committee:

_____

Gary T. Rochelle, Supervisor

_____

David T. Allen

_____

Nicholas A. Peppas

_____

Eric V. Anslyn

_____

James E. Critchfield

Amine Oxidation in CO_2 Capture Processes

by

Andrew James Sexton, B. S.; M. Eng.

Dissertation

Presented to the Faculty of the Graduate School of

The University of Texas at Austin

in Partial Fulfillment

of the Requirements

for the Degree of

Doctor of Philosophy

The University of Texas at Austin

December 2008

To my loving parents,

Joe and Carol Sexton

Your support and encouragement has guided me and I am forever grateful.

Acknowledgements

First and foremost, I would like to thank my research advisor Dr. Gary Rochelle. I was initially drawn to Dr. Rochelle's group solely by the enthusiasm and excitement he exhibited when discussing his research. Upon joining his group, I quickly learned that Dr. Rochelle's initial impression was not just a sales pitch to attract new graduate students; he brings that eagerness to teach – and to learn – with him every single day. The door to his office is always open, literally and figuratively, to any graduate or undergraduate student – even those he does not supervise or teach. While Dr. Rochelle and I did not always agree on everything during our weekly meetings, I always felt like I left each meeting having learned at least one thing I did not know before I stepped in his office. If given the opportunity to rewind the clock four years and pick another research advisor, I would make the same decision without hesitation. Dr. Rochelle has been a great mentor and I truly appreciate everything he has done for me.

The Rochelle research group has doubled in size since I joined, yet Dr. Rochelle has always been accessible and things run as efficiently as ever in the group. For this I thank Dr. Rochelle's assistants during my time here – Jody Lester, Lane Salgado and Maeve Cooney. The three of you were always available meet any last-second requests from this self-proclaimed procrastinator when conference or quarterly report time came around. And to Jody – I am still slowly working my way through the list of restaurants you compiled for me; I have yet to be disappointed by a single one.

I would also like to acknowledge all the Rochelle group members that I have gotten to know during my time at The University of Texas: Tim Cullinane, Akin

Alawode, Chuck Okoye, Babatunde Oyenekan, Marcus Hilliard, Jennifer Lu, Fred Closmann, Thu Nguyen, Qing Xu, Xi Chen, Jorge Plaza, Sepideh Ziaii, David Van Wagener, Stephanie Freeman, Eric Chen and George Goff. I extend my gratitude to all senior group members who I could always call upon for advice while I was learning the ropes, especially George Goff. Even while writing your dissertation, you never hesitated to stop and answer a question, share your knowledge of Aspen or stay at the lab until 4AM demonstrating high gas flow experiments. You will make a great professor someday.

I think it speaks volumes that a majority of the members of the Rochelle group get along with one another and interact quite often outside of the laboratory environment. To those Rochelle group members I have befriended (John McLees, Ross Dugas, Jason Davis, and Bob Tsai), I would like to say that I have many great memories from conferences, parties, tailgates and The Posse. It was refreshing to be surrounded a number of intelligent and hard-working individuals who knew how to let loose and enjoy themselves after quitting time. It is now up to you to continue the traditions of burrito Thursday and Friday happy hour.

I have also been fortunate to have made a number of friends in the department since I moved to Austin, Texas (keep in mind that I do not use the term friend lightly). Terry Farmer, Jason Cantor, Luke Henderson, Saul Lee, Mikey Lin, Ryan Fitzpatrick and Danielle Smith are all people I will keep in touch with long after I have left the 40 Acres. To all those except Mikey and Terry, enjoy the rest of your time at UT. It will be over before you know it. Special thanks are reserved for Jason and John McLees as well – you

two had to live with me as your roommate for four years. I also want to mention those close friends of mine I met outside the College of Engineering (yes, it does happen sometimes). Paul Anderson, Paul Norwine, Greg Beatty, Jesse Sultzer, Melody Lee, Brian Talarico and Adam Johnson have all helped me retain my sanity during time spent outside of CPE.

Sometimes there are not enough hours in the day to accomplish everything; in that case you either pick it up the next day or you hire some good help. Along those lines, I would like to thank the undergraduate research assistants I have collaborated with: Humera Rafique, Dan Ellenberger, Jon Mellin, Ellie Doh, and Jang Lee. Without your assistance, I would probably be graduating in December 2009 instead of 2008.

The members of my committee – Drs. Jim Critchfield, David Allen, Nicholas Peppas, and Eric Anslyn – have been extremely helpful as this project has progressed. Dr. Anslyn has done an excellent job in providing this chemical engineer with a refresher in organic chemistry. Dr. Critchfield has been an invaluable resource over the past four years. Being a Rochelle group graduate himself, Dr. Critchfield has almost served as a second advisor. He has been able to call on his experience from grad school and provide an industry perspective on this research project. His suggestions and critiques have led to a couple of important discoveries.

I like to think of myself as a capable troubleshooter. I have taken the IC and FTIR apart so many times I think I have their internals etched into my brain. However, there were certain times where I would just have to throw my hands up and call in the professionals. Fortunately, Randy West and Donnie Lummus at Dionex and Mark

Nelson at Air Quality Analytical, Inc. always came through. They would even forgo guaranteed future business by explaining to me the underlying problem and the solution in case it ever happened again.

I do not think I would be at this point in my life without the love and support of my family. From an early age, my parents recognized my talents and encouraged me to use them. At the time, I didn't understand why I was getting up at 8AM on Saturday morning to work with a gifted children specialist, taking middle school math classes in 4th grade, or attending community college as high school freshman. Now I realize that my parents just wanted what any parent wants for their child, no matter the situation. They have raised four well-mannered and successful children who have graduated from college and started their professional careers; that is quite an accomplishment. And don't worry – I promise that I will be in Australia for only six months.

The final – and most important – thank you is reserved for my fiancée, Melissa. You have endured long hours spent in the lab and countless complaints about broken equipment and experiments gone awry. You have seen the best and the worst of me over the past three and a half years, yet you are still standing by my side. I am excited about spending the rest of my life with my best friend.

Without the financial support of our generous research sponsors – the U. S. Department of Energy, the Separations Research Program, the Industrial Associates Program for CO_2 Capture and the Luminant Carbon Management Program – this project would not have been possible.

Amine Oxidation in CO_2 Capture Processes

Publication No. _____

Andrew James Sexton, Ph.D.

The University of Texas at Austin, 2008

Supervisor: Gary T. Rochelle

Aqueous amine solutions were batch loaded into 500 mL glass jacketed reactors and subjected to oxidative degradation at both low and high gas rates. Solutions at low gas were degraded with 100 mL/min of 98%O_2/2%CO_2 with mass transfer achieved by vortexing. Samples were drawn from the reactor during the course of the experiment and analyzed for degradation using ion chromatography and HPLC with evaporative light scattering detecion. In a parallel apparatus 7.5 L/min of 15%O_2/2%CO_2 was sparged through 350 mL of solution; additional mass transfer was achieved by vortexing. A Fourier Transform Infrared Analyzer collected continuous gas-phase data on amine volatility and volatile degradation products.

Hydroxyethyl-formamide (HEF), hydroxyethylimidazole (HEI) and formate are the major carbon containing monoethanolamine (MEA) oxidation products; HEF, HEI and ammonia are the major nitrogen containing products. In terms of catalyst oxidation potential, Cu > Cr/Ni (combined) > Fe > V. The oxygen stoichiometry (ν) ranges from 1.5 mol MEA degraded/mol O_2 consumed for Cu and Fe catalyzed systems to 1.0 for V catalyzed systems. Estimation of rates from an industrial absorber show degradation costs to range from \$1.17 / metric ton (MT) CO_2 captured for a system controlled by the solubility of O_2 to \$2.22 / MT CO_2 for a mass transfer controlled system.

Inhibitors A and B (reaction mechanism inhibitors) and EDTA (a chelating agent) were established as effective MEA oxidation inhibitors. EDTA and Inhibitor A were successful inhibitors at 100 mM, while 7.5 mM Inhibitor B successfully inhibited degradation. Sodium sulfite and reaction intermediates formaldehyde and formate (expected oxygen scavengers) were unsuccessful at inhibiting MEA oxidation.

Cu catalyzes concentrated PZ oxidation, while Fe has no effect on PZ oxidation even at high catalyst concentration. MEA/PZ blends were more susceptible to oxidation than any other amine system investigated. It is believed that free radicals formed in the MEA oxidation process serve to accelerate the degradation of the PZ structure. All MEA analogs (glycine, ethylenediamine and ethylene glycol) and secondary/hindered amines (diethanolamine, diglycolamine and 2-amino-2-methyl-1-propanol) were resistant to oxidation in the presence of Fe or Cu, except for diethanolamine.

Contents

Tables

Figures

Chapter 1: Introduction

This chapter gives an overview of CO_2 emission sources and potential issues associated with these emissions. Emissions sources, along with targets for potential reductions, are identified. Information on the traditional absorption/stripping process is given, including information on solvent degradation. Lastly, the objectives and scope of the project are identified.

1.1. CO_2 Emissions

According to a study of atmospheric CO_2 concentrations, measured at Mauna Loa, Hawaii since 1958, CO_2 concentrations have risen by 19% over the last 45 years (Keeling and Whorf 2004). The Intergovernmental Panel on Climate Change has reported increasing annual average temperatures on the Earth's surface, lower

atmosphere, and oceans, in addition to retreating glaciers and reduced areas with year round snow coverage (IPCC 2001). All of these environmental observations indicate global warming. A recent report shows that recent trends in CO_2 concentrations are significantly higher than expected based on past long term trends (Ruddiman 2005).

The National Research Council supported the IPCC, stating that greenhouse gases are accumulating in the atmosphere, "most likely due to human activities" (NRC 2001). Global warming is quickly becoming a worldwide policy issue, as evidenced by the push for all industrial nations to ratify the Kyoto Protocol, which came into effect on February 16, 2005 and requires at least a 5% reduction in 1990 level CO_2 emissions by 2012 for each signatory (Kyoto Protocol 2004). Although the United States did not sign the protocol, many governmental and industrial agencies are anticipating that regulations will be put in place in the near future. As a result, there is a demand for research in the area of CO_2 capture technologies across the globe.

There are three primary sinks in the global carbon cycle: atmospheric, oceanic and terrestrial systems (Grace 2004). Almost all anthropogenic CO_2 is emitted to atmosphere, but only 40% of the CO_2 remains there. Half the remaining carbon dioxide is dissolved into oceans, while the other half ends up being sequestered in biological ecosystems.

In 2002, worldwide CO_2 emissions from anthropogenic sources were 24,533 million metric tons, 23% of which was from the United States (Energy Information Administration 2004b). Almost 98% of the CO_2 emissions comes from the consumption and flaring of fossil fuels (Energy Information Administration 2004a). The largest sources of emissions in the United States are coal-fired power plants (32.7%), transportation (32.2%), and industrial facilities (18.0%).

Targeting the transportation sector for CO_2 removal poses obstacles; in order to significantly reduce emissions, a large investment would have to be made to install CO_2 removal systems for all vehicles. Fossil fuel fired power generators provide the best opportunity to reduce emissions for point source emitters. While 50% of the electricity

comes from coal fired power plants, these electricity generators produce 83% of the CO_2 emissions.

Two different scenarios are discussed for CO_2 removal from flue gas: pre-combustion and post-combustion capture (Davison et al. 2001). Pre-combustion capture involves gasifying a fuel with oxygen to form a synthetic gas of CO and H_2. The CO can be further oxidized to CO_2 and removed from the H_2 prior to combustion. This process is associated with a coal gasified power plant, also known as IGCC (integrated gasification combined cycle).

Post-combustion capture involves removing CO_2 from flue gas at the end of a power plant cycle. This type of removal method is generally associated with a retrofit of a pulverized coal power plant with flue gas desulphurization or a natural gas combined cycle (NGCC) power plant. A fourth type of power involves burning coal with pure O_2 and recycled CO_2 to control the temperature of the boilers. The CO_2 recycle gives a significant concentration increase in the flue gas, which can reduce the cost of capture.

The most common technologies for post-combustion capture are cryogenics, membranes, adsorption, and aqueous absorption/stripping (Davison et al. 2001; IEA 1999, 2003). Cryogenic separation of CO_2 is generally only used for gas streams with high concentrations of CO_2. Due to the cold temperatures of the cryogenic solvents, the gas stream must be dehydrated, which is costly when treating the large gas volumes. Moreover, the cost of refrigeration is high in these processes and adds to the operating costs. It is difficult to achieve a high purity CO_2 product with membrane separation of flue gas without extensive (and expensive) process modifications like recycles and multiple stage separations.

Adsorbents are solids that selectively bind CO_2 from the flue gas. The adsorbent beds are regenerated by either applying heat to liberate the CO_2, temperature swing adsorption (TSA), or by reducing the pressure to allow the CO_2 to desorb from the solid, pressure swing adsorption (PSA). The heat duty associated with TSA is large, while PSA requires pulling a vacuum on the adsorbent bed or compressing the flue gas prior to the

CO_2 separation step. Currently, adsorbents are limited by low selectivity and poor CO_2 capacity (Davison et al. 2001).

Aqueous absorption/stripping involves counter-currently contacting the flue gas with an aqueous solvent that reacts reversibly with the CO_2 in an absorber column. The solvent is then regenerated in the stripper by applying heat to reverse the reaction and liberate the CO_2. Several amines are already commonly used in absorption/stripping for natural gas treating, H_2 purification, and NH_3 production to remove acidic impurities like CO_2 and H_2S (Kohl and Nielsen 1997).

Two methods of CO_2 sequestration commonly discussed include geological and oceanic storage. Geological storage is currently accepted as the best sequestration method, which includes storage in depleted oil and gas reservoirs, deep saline reservoirs, and unminable coal seams (Davison et al. 2001). An established technique known as enhanced oil recovery (EOR) consists of injecting CO_2 into depleted oil and gas reservoirs in order to capture residual fuel left in underground formations.

Injection of CO_2 into unminable coal seams recovers methane that is adsorbed on the coal. Injection into deep saline aquifers differs from other geologic sequestration methods in that there is no economic value associated with sequestration. These saline aquifers are capped by a solid rock layer with low CO_2 permeability that would ensure the CO_2 stayed permanently sequestered. Large volumes of these reservoirs have been identified as possible sinks for CO_2 sequestration, and test operations are occurring across the globe. One example is the Frio Brine Test Facility in east Texas.

1.2. CO_2 Capture Using Aqueous Absorption/Stripping

Alkanolamines are used extensively in the gas process industry to remove acid gases such as carbon dioxide and hydrogen sulfide from process gas. Aqueous monoethanolamine (MEA) is the current solvent of choice for flue gas treating because of its high capacity for CO_2 absorption, fast reaction kinetics, and high removal efficiencies (Kohl and Nielsen 1997).

Figure 1.1 shows a typical aqueous absorption/stripping process used in gas-treating processes. In a typical absorber/stripper system, a flue gas stream with 10% CO_2, 0.2% SO_2, and 5% O_2 enters the bottom of the absorber, which is operating at 55^oC and 1 atmosphere pressure (Rochelle et al. 2001). The lean amine counter currently contacts the flue gas and exits the bottom of the absorber. The CO_2 reacts reversibly with MEA to form an MEA carbamate. The rich amine solution, with a CO_2 loading (α) of approximately 0.4 mol/mol MEA, goes through a cross heat exchanger, where it is preheated by the lean amine solution before entering the top of the stripper, which operates at 120^oC and 1 atmosphere.

In the stripper, heat is provided in the reboiler by steam, which is used to reverse the chemical equilibrium between the MEA and MEA-carbamate, thus liberating the CO_2. The gas leaving the stripper is dehydrated and compressed before being pumped for sequestration. The hot lean amine solution is passed back through the cross exchanger, where it is cooled and recycled back to the top of the absorber. A reclaimer off the bottom of the stripper takes a slip stream to remove heat stable salts and high molecular weight degradation products.

Corrosion is a major issue for alkanolamine systems used in acid gas removal. MEA by itself is a known corrosion inhibitor in aqueous solutions in the absence of CO_2 (Riggs 1973). On the other hand, amine carbamates are known complexing agents, and could cause the increase in the corrosion rates (Nakayanagi 1996). Plant tests have indicated a higher than expected concentration of Fe in solution (Comeaux 1962; Hofmeyer et al. 1956; Wong et al. 1985). This increased solubility is most likely explained by the complexing of the MEA carbamate with the Fe. Corrosion inhibitors used in acid gas treating systems are primarily heavy metal based. Copper salts are the most commonly used (Cringle et al. 1987; Pearce 1984; Pearce et al. 1984; Wolcott et al. 1985). Vanadium salts are also known corrosion inhibitors for acid gas treating (Ranney 1976).

Degradation of the solvent in this absorption/stripping system can be classified into two types: thermal degradation/carbamate polymerization and oxidative degradation

(Rochelle et al. 2001). Thermal degradation does not usually occur at temperatures less than 100°C, while carbamate polymerization occurs in any process where a primary/secondary alkanolamine forms a carbamate with CO_2. The degradation products resulting from these degradation pathways are of high molecular weight.

Oxidative degradation requires the presence of oxygen; since flue gas contains at least 5% O_2, oxidative degradation can be significant. This type of degradation does not apply to acid gas treating processes, which are usually absent of oxygen. The degradation products via this process are typically oxidized fragments of the amine solvent. This project proposes to study the mechanism by which amine solutions are subjected to oxidative degradation, and how its effects impact the implementation of absorption/stripping units for CO_2 capture.

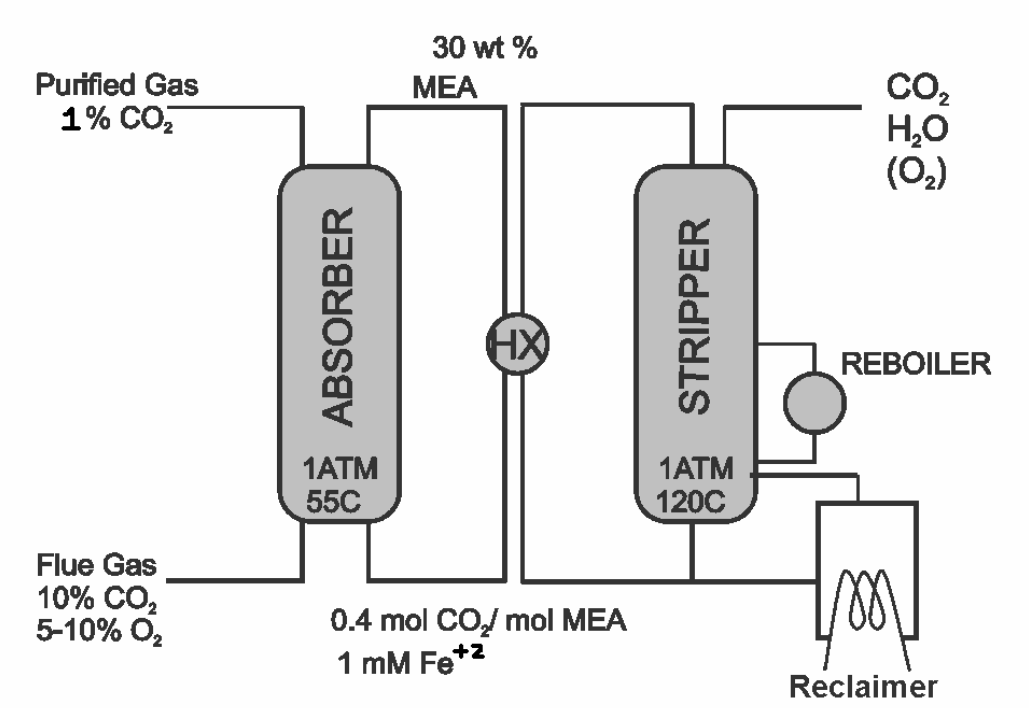

Figure 1.1 Process Flow Diagram for MEA CO_2 Capture Process

1.3. Research Objectives

Degradation is an irreversible chemical transformation of alkanolamine into undesirable compounds resulting in its diminished ability to absorb CO_2. Since most gas treating processes using alkanolamines for CO_2 removal are performed in the absence of oxygen, oxidative degradation is a source of solvent degradation that has not been properly quantified. Oxidative degradation is important because it can impact the environment and process economics and decrease equipment life due to corrosion.

The environmental effects refer to the degradation products themselves: what is being produced, how much of it is being produced, and how can it be disposed of without doing significant damage to the environment. Solvent make-up rate and design of the reclaiming operation impact process economics. If amine is continually being degraded, then fresh amine must be continually added to the process at a significant cost. In addition, CO_2 loaded amine solutions corrode carbon steel equipment, which catalyzes oxidative degradation even further. It is imperative to quantify how much of this solvent make-up rate is due to oxidative degradation.

Suspected oxidative degradation products of MEA include various aldehydes, NH_3, and nitrosamines (Rochelle et al. 2001). Nitrosamines are known carcinogens, and NH_3 forms particulates which are regulated by the U.S. EPA. Most of the degradation products are removed from the process through solvent reclaiming. The potentially hazardous liquid and solid waste from the reclaiming process must be disposed of properly.

The costs resulting from amine degradation are considerable; Rao and Rubin (2002) estimate solvent degradation to be around 10% of the total cost of CO_2 capture. Therefore, a comprehensive understanding of the fundamentals of degradation chemistry is important. Thermal reclaiming processes use steam to remove waste products. Moreover, the cost of waste disposal has not accurately been accounted for in economic models of CO_2 capture since the degradation process is not well understood.

Another significant cost is associated with equipment corrosion. MEA solvents are highly corrosive, and the degradation products can increase the rate of corrosion of process equipment (Hofmeyer et al. 1956; Tanthapanichakoon and Veawab 2003; Veawab and Aroonwilas 2002; Veawab et al. 1999). Both Fe and Cu catalyze the rate of oxidative degradation of MEA (Blachly and Ravner 1963; Chi 2000; Goff and Rochelle 2004; Goff 2005). The tradeoff and balance between corrosion and degradation is important to system performance, and these respective mechanisms are not very well understood. As a solvent degrades, it has a reduced capacity for CO_2 absorption and must be replaced. Freguia (2002) showed that the accumulation of heat stable salts can have a catalytic effect on the CO_2 absorption kinetics.

Most previous studies on the oxidative degradation of amines were long duration experiments. Some works have been focused only on identifying the liquid phase degradation products using HPLC and GC (Bello and Idem 2005; Strazisar et al. 2003), while other studies have attempted to quantify degradation rates (Lawal and Idem 2005; Lawal et al. 2005; Rooney et al. 1998). Most of these experiments were carried out at elevated temperature and pressure, which are not representative of absorber conditions.

Goff (2005) and Chi (2002) from the Rochelle group at the University of Texas quantified the rate of oxidative degradation by measuring the rate of NH_3 evolution from the degraded MEA solutions. Alawode (2005) used GC to measure piperazine (PZ) disappearance and IC to measure formation rates of ionic degradation products. This study attempts to quantify amine oxidation, at absorber conditions, using HPLC to identify liquid-phase degradation products, cation chromatography to measure amine disappearance and FTIR to measure amine volatility and gas-phase degradation products.

The expected result of this project is to identify and quantify the liquid-phase and vapor-phase oxidative degradation products of amine systems (both homogeneous systems as well as amine blends), to understand the environmental impact of the degradation products and amine solvents, and to identify conditions that minimize oxidative degradation rates.

Specific goals are as follows:

- Determine the mixture of oxidative degradation products that are formed via multivalent metal catalysis and how their oxygen stoichiometry affects degradation of monoethanolamine, piperazine, and other amine systems.
- Determine how blends of amines behave when subjected to oxidative degradation by calculating competitive degradation rates and establishing which amines degrade faster than others.
- Evaluate the effectiveness of Na_2SO_3, formaldehyde, Inhibitor A (a proprietary material) and other compounds with regards to inhibiting oxidation of these amine systems.
- Present process conditions that make commercial operation the most cost effective and environmentally safe.

Chapter 2: Literature Review

This chapter includes all relevant information pertaining to the oxidation of amines. Information of degradation chemistry and possible products is discussed. The experimental work of researchers who have studied amine oxidation is presented and its relevance is placed in the scope of this work.

2.1. MEA Degradation Chemistry

2.1.1. Electron Abstraction Mechanism

The mechanism for the fragmentation of MEA is uncertain, although MEA is the most extensively studied amine for the use of CO_2 capture. Two mechanisms are suggested for MEA degradation: electron abstraction and hydrogen abstraction.

Figure 2.1 demonstrates a proposed electron abstraction mechanism. This series of reactions is based on a group of studies performed at the Edgewood Arsenal by the U.S. Army Chemical Research and Development Laboratories. These studies focused on the oxidation of tertiary amines using chlorine dioxide and other single electron oxidants (Rosenblatt et al. 1963, Rosenblatt et al. 1967, Dennis et al. 1967, Hull et al. 1967). A reactive free radical, most likely Fe^{+3}, in the absorption/stripping system extracts an electron from the nitrogen in an unprotonated amine to produce an aminium cation radical. This electron abstraction is thought to be the rate-limiting step.

The cation radical rearranges with the loss of H^+ to produce an imine radical, which loses a free radical to produce an imine. The imine then hydrolyzes to produce an aldehyde/ketone and an amine. In the case of monoethanolamine, the final products would be ammonia and hydroxyacetaldehyde. Dennis et al. (1967) showed that ethanolamines can oxidize by fragmentation. The imine can form a resonance structure known as an enamine, which hydrolyzes to two moles of formaldehyde and one mole of ammonia.

Chi and Rochelle (2002) proposed an alternate route for the imine radical, in which it can react with oxygen to form an amino-peroxide radical. Afterwards, the amino-peroxide radical could react with another molecule of MEA to form an amino-peroxide and another aminium radical. The amino-peroxide subsequently decomposes to form hydrogen peroxide and an imine, which reacts with water to form an aldehyde and ammonia.

Communication with Dr. Eric Anslyn (2008) in the Chemistry Department at the University of Texas at Austin has suggested alternate (and more likely) routes to the production of formaldehyde (and subsequently formic acid when formaldehyde is oxidized). The amino-peroxide molecule from Figure 2.1 can lose an OH radical at highly basic conditions, leaving a free radical structure that decomposes to formamide and the free radical version of formaldehyde. In a highly basic solution (i.e. basic amine solution), the formaldehyde radical will lose an H^+, leaving a charged free radical that loses an electron and rearranges to form formaldehyde.

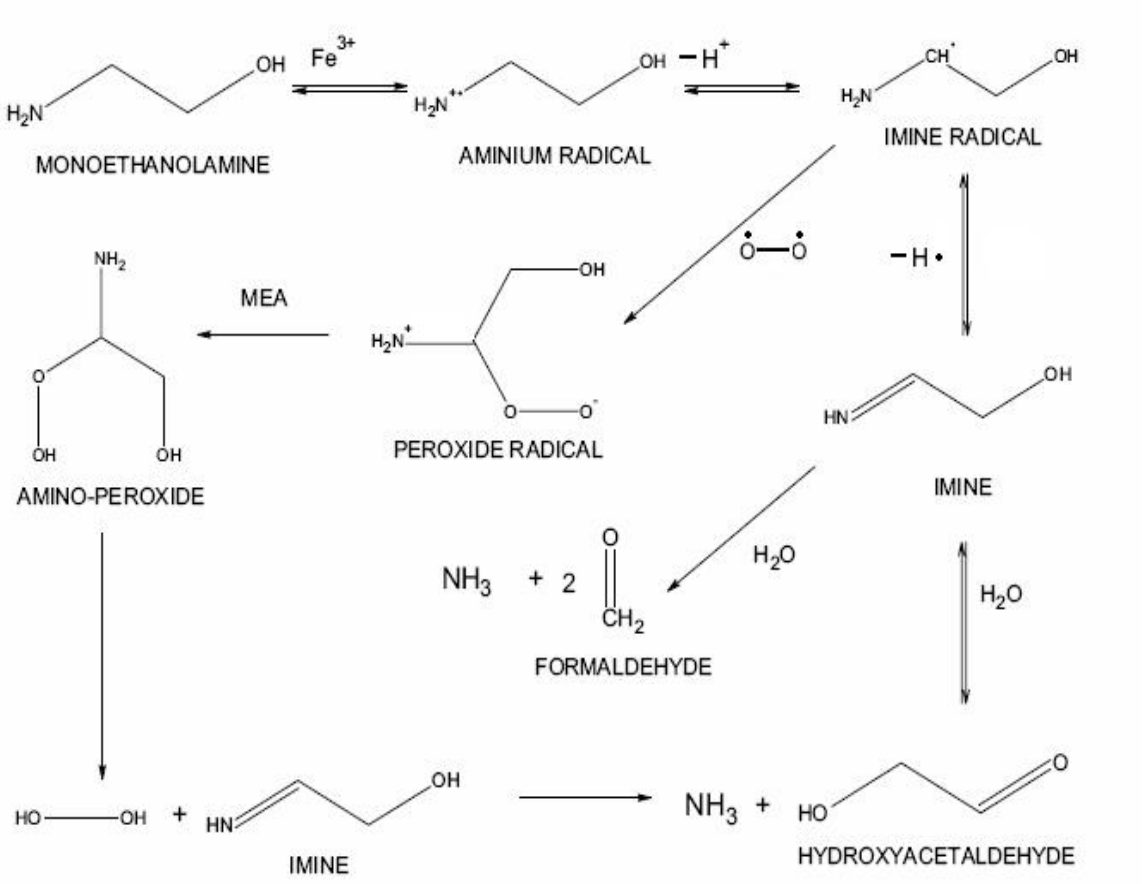

Figure 2.1 Electron Abstraction Mechanism for MEA Oxidative Degradation (Chi and Rochelle 2002)

2.1.2. Hydrogen Abstraction Mechanism

An alternative to the electron abstraction mechanism is the hydrogen abstraction mechanism, also developed at the Edgewood Arsenal (Figure 2.2), in which aqueous solutions of alkanolamines were degraded by ionization radiation as the initiation step. This was supported by Petryaev et al. (1984). The radiation formed initiating radicals such as $H^{\cdot}$, $OH^{\cdot}$, and $e^{-}(aq)$. The principal investigators proposed that the mechanism proceeded through a 5-membered cyclic, hydrogen bonded conformation of MEA at a pH greater than 6.

In aqueous solution, MEA can form a cyclic conformation by hydrogen bonds between HN---O or OH----N. Free radicals abstract a hydrogen atom from the nitrogen, the α-carbon, or the β-carbon. The newly formed amine radical can transfer the radical internally through the ring structure, which ultimately results in cleavage of the N---C bond. The resulting degradation products are ammonia and an aldehyde or aldehyde radical. The aldehyde radical would act as an initiator by abstracting another hydrogen from a second MEA molecule, forming the MEA radical and the aldehyde. The validity of the cyclic transition state, unique to MEA, is supported by several molecular simulation studies (Alejandre et al. 2000, Button et al. 1996, Vorobyov et al. 2002).

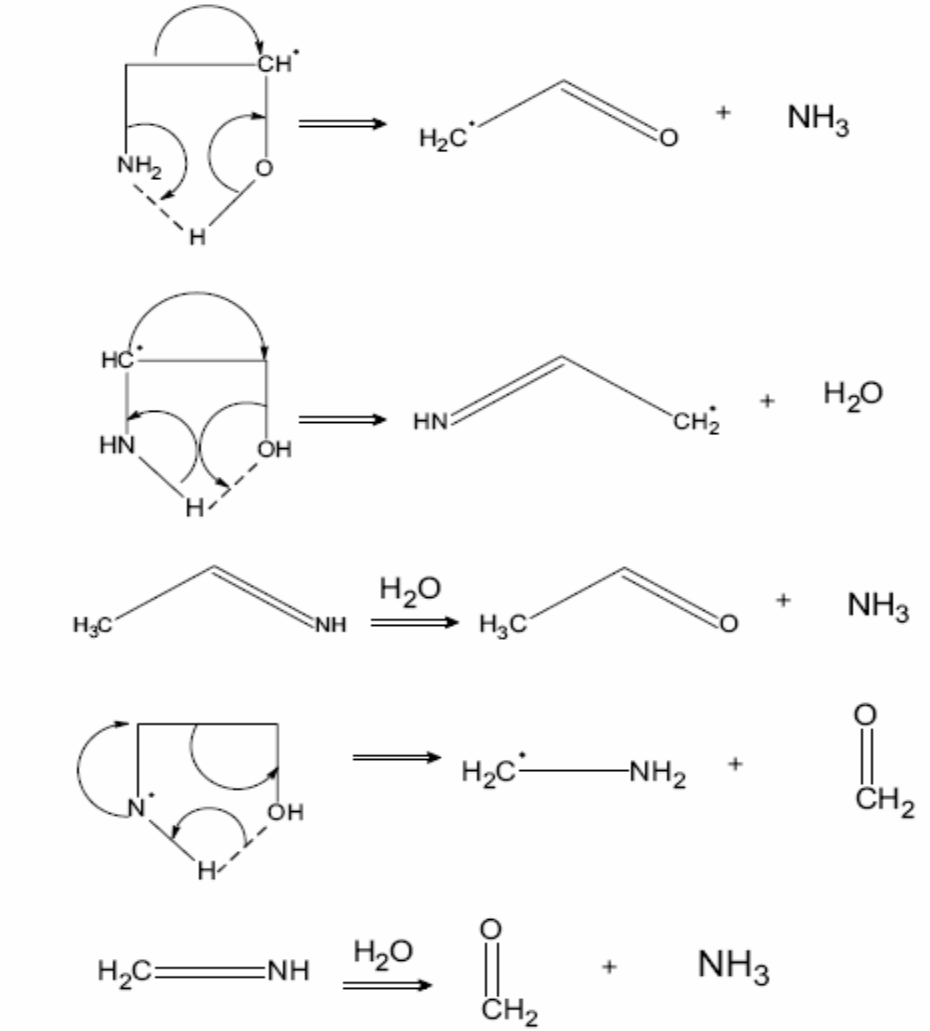

Figure 2.2 Hydrogen Abstraction Mechanism for MEA Oxidative Degradation (Petryaev et al. 1984)

2.1.3. Expected Degradation Products

Fessenden and Fessenden (1994) have established that aldehydes are very susceptible to autoxidation in the presence of oxygen. The oxygen will react with aldehydes to form carboxylic acids via a peroxy acid intermediate. Since MEA solutions have alkaline pH, the carboxylic acids formed would dissociate in solution to form heat stable salts with the amines.

The presence of organic acids in degraded MEA solutions has been documented by Rooney et al. (1998) and Strazisar et al. (2003). It is important to note that while the pathway described by both of the above mechanisms is different, the degradation products are the same. Both of the mechanisms predict the primary amino degradation product of MEA is ammonia along with aldehydes, which are oxidized to carboxylic acids in the presence of oxygen. The formation of the carboxylic acids has a strong effect on the overall oxygen stoichiometry of the system, depending on which acid is formed. The Dow study conducted by Rooney et al. (1998) recognized acetate, formate, glycolate and oxalate as heat-stable salts formed from MEA oxidation. Formate was the most prevalent carboxylic acid in all of the amine systems studied.

A major conclusion from Goff (2005) is that in the presence of metal catalysts, the rate of evolution of MEA is controlled by the rate of oxygen absorption under experimental and industrial conditions. Goff's assertion was that 1 degraded mole of MEA resulted in 1 mole of ammonia. Ammonia evolution rates increased with agitation rate and increased linearly with oxygen concentration.

Goff (2005) proposed that MEA reacts with oxygen to form ammonia and other carbon containing degradation products, which are listed in Table 2.1. Each of the major degradation products has a specific oxygen stoichiometry, which is listed below. Oxygen stoichiometry ranges from 0.0 for ammonia to 2.0 for oxalic acid. The oxygen stoichiometry for each product can be utilized to calculate an overall oxygen consumption rate for each degradation experiment.

$$C_2H_7NO + \nu O_2 \rightarrow NH_3 + \text{product} \quad (2.1)$$

$$NH_3 + \nu O_2 \rightarrow H_2O + \text{product} \quad (2.2)$$

$$\text{Rate of } O_2 \text{ Consumption (mM/hr)} = \Sigma\ \nu_i * \text{formation rate}_i \text{ (mM/hr)} \quad (2.3)$$

Table 2.1 Oxygen Stoichiometry for Important Liquid and Gas Phase Oxidative Degradation Products of MEA

Product	**Stoichiometry (ν)**
NH_3	**0.0**
Formaldehyde	**0.25**
Formic Acid	**0.75**
Hydroxyethylimidazole	**0.625**
Hydroxyethyl-formamide	**0.75**
NO	**1.25**
CO_2	**1.25**
HNO_2	**1.5**
N_2O	**2.0**
Oxalic Acid	**2.0**

At the conditions within either experimental apparatus, it is presumed MEA can react via two different pathways to form hydroxyethyl-formamide, according to communication with Dr. Eric Anslyn from the Chemistry Department at The University of Texas (2008). In the first reaction pathway, MEA reacts with formic acid to create hydroxyethyl-formamide and water. This reaction is facilitated by the presence of the Fe catalyst. The Fe actually forms a metal coordinated complex with formic acid, which is attacked by an MEA aminium radical. The resulting products are hydroxyethyl-formamide and an iron hydroxide complex.

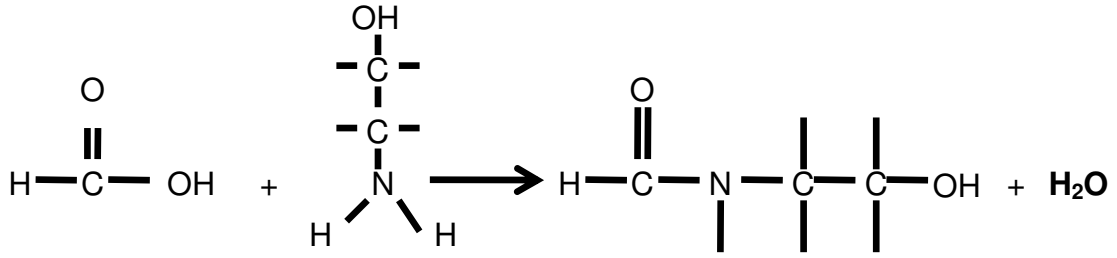

Hydroxyethyl-formamide can also be formed from the reaction of formaldehyde and MEA, both of which have been found in degraded solutions in significant concentration, as results in Chapter 5 will illustrate. MEA reacts with formaldehyde to produce an imine structure and water. The imine is hydrolyzed at basic conditions and oxidized to form hydroxyethyl-formamide. While metal catalysis is not necessary to facilitate this reaction path, it does accelerate this set of reactions. Both of these reaction pathways are valid for the reaction of MEA with oxalate, glycolate, acetate and their respective aldehydes; it is also assumed that the these pathways are valid for reactions between any carboxylic acid and any of the amine systems studied in the scope of this project.

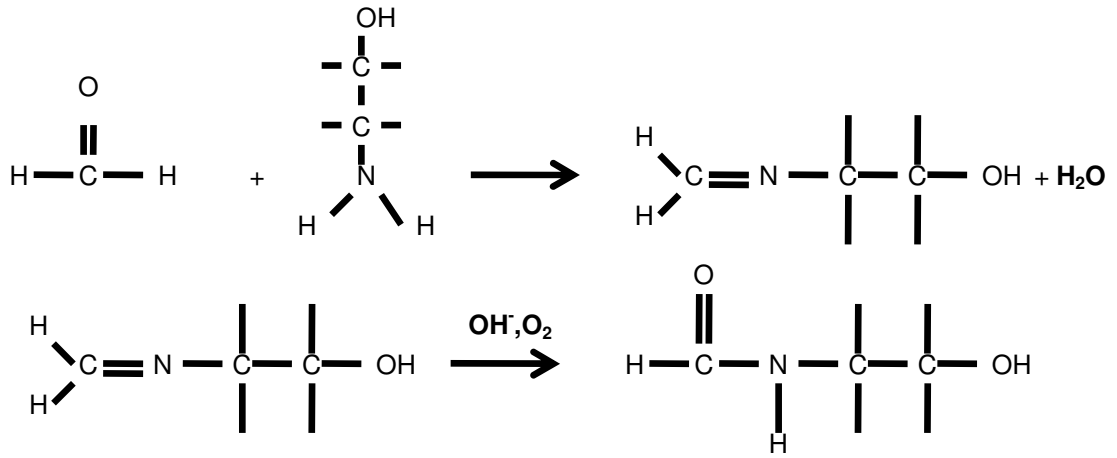

Strazisar et al. (2003) proposed a similar reaction pathway for MEA and acetic acid. MEA and acetic acid reacted with one another, in the presence of iron catalyst, to form the amide N-acetylethanolamine. The amide could then react with another MEA molecule to form a longer chain structure known as 2-hydroxyethylamino-*N*-

hydroxyethyl acetamide. With the exception of the partial amide of amine and oxalic acid, amides do not possess any carboxylic acid functionality and thus go undetected using anion chromatography analysis.

Koike et al. (1987) analyzed spent 20 wt% DEA solution used in an acid gas treating facility and discovered that a large concentration of N-formyldiethanolamine (FORMYDEA) was present in the solution. They discovered that the addition of 6 M sodium hydroxide would hydrolyze the purified FORMYDEA and recover formate and DEA.

2.2. Prior Oxidative Degradation Experiments

Several different studies have previously been performed on the oxidative degradation of MEA. These studies were performed over a wide range of experimental conditions (gas flowrates for example), making direct comparison of the results difficult. Several studies have partially or completely analyzed the liquid solution for aqueous, non-volatile degradation products using GC and/or HPLC; however, no study has been conducted that was able to close the gas and liquid phase material balances for the MEA solution. These prior experiments are summarized below by their objective.

2.2.1. General Amine Oxidation Experiments

Early studies on the oxidative degradation of alkanolamines were primarily driven by the U.S. Department of the Navy in the early 1950s (Carbon Dioxide Absorbants 1950). Alkanolamine systems were being used to remove CO_2 from the air supply of nuclear submarines. Oxidative degradation in these types of systems is important since ammonia, a known toxic air pollutant, is volatile and can be released into the closed atmosphere of the submarine.

The Girdler Corporation completed a number of screening tests in 1950. The goal of one study (Kindrick et al. 1950a) was to test the relative resistance to oxidative degradation of possible CO_2 absorbants that are to be used in the presence of oxygen.

Thirty-nine amines and eleven mixtures of amines were tested for relative resistance to oxidation.

The accelerated oxidation test involved contacting 1000 L of a gas mixture of 50% CO_2/50% O_2 at a rate of 100 mL/min with 100 mL of 2.5 N amine solution at 80°C. The experiments were performed with 25 to 60 ppm dissolved iron in the solutions. Evolved ammonia was detected by passing the reaction gas through a weak acid solution to absorb the ammonia. NH_3 concentration was quantified by titration with a strong acid. Results showed that NH_3 production occurred as follows: tertiary amines < primary < secondary.

An additional series of long-term tests was performed with 13 selected amines that showed low rates of degradation in the accelerated tests (Kindrick et al. 1950b). Amines tested include AMP (2-amino-2-methyl-1-propanol) and MDEA. 100 mL of 2.5 N amine were subjected to 100 mL/min of 5% CO_2 in air at 85°F for forty days. Dissolved iron was present at 30 to 60 ppm throughout all of the tests. Maximum degradation rates for these experiments were extremely low – approaching the detection limit of the methods.

The Navy conducted a major of study of MEA degradation to support submarine environments (Blachly and Ravner 1964). Blachly and Ravner measured the evolution of ammonia and the production of peroxides with air sparging of amine solutions at 55°C and 98°C for 3 to 13 days. Without CO_2 in the air, they observed no perceptible degradation. At 55°C, with no metals present and 1% CO_2 in the air, the rate of ammonia evolution and peroxide was about 3 mM/day.

Two studies on MEA degradation were performed by The Dow Chemical Co. The first earliest study quantified the rate of oxidative degradation by measuring the rate of NH_3 evolution from the amine solution and the basicity loss of the liquid amine solution (Hofmeyer et al. 1956; Lloyd 1956). In this study it was shown that the NH_3 loss from the MEA solution accounted for 40% of the total basicity loss of the solvent. The rest of the basicity loss came from neutralization of free MEA by the formation of heat stable

carboxylic acid salts. Corrosion tests performed with MEA solutions showed a significant increase in corrosion rate with the degraded solutions.

The study by Rooney et al. (1998) looked at the formation of carboxylic acids in loaded (α=0.25) and unloaded solutions of 20 wt % MEA, 50 wt % diglycolamine (DGA^{TM}), 30 wt % diethanolamine (DEA), as well as 30 and 50 wt % MDEA over a 28-day period. The solutions were degraded by bubbling a stream of compressed air at a flowrate of 5.5 mL/min through the amine solutions at 180^{o}F. The solutions were agitated via a magnetic stir bar. The Rooney study showed that, of the unloaded solutions, MEA degraded the fastest. The study was able to identify some of the anions being formed as acetate, formate, glycolate, and oxalate. No oxalate was observed for MEA degradation, while formate was the most prevalent anion formed – regardless of loading. In the absence of CO_2, oxidation resistance increases in the order of: 30% DEA > 50% MDEA > 30 % MDEA > 50% DGA^{TM} > 20% MEA (DEA is the most oxidation resistant). With a CO_2 loading of 0.25, oxidation resistance increases in the following order: 30% DEA > 50% DGA^{TM} > 20% MEA > 50% MDEA > 30% MDEA.

Table 2.2 Carboxylic Acid Formation in 28 Day Oxidation Experiment for Alkanolamine Solutions (Rooney et al. 1998)

	Acetate (mmol)	Formate (mmol)	Glycolate (mmol)	Oxalate (mmol)
50% MDEA Unloaded	1.76	4.90	6.38	0.00
50% MDEA Loaded	1.47	6.48	5.38	0.00
30% MDEA Unloaded	7.11	4.57	8.31	0.00
30% MDEA Unloaded	6.92	5.17	8.77	0.00
30% MDEA Loaded	4.20	4.36	6.28	0.00
30% DEA Unloaded	0.93	4.67	1.18	0.00
30% DEA Loaded	0.74	1.14	0.14	0.00
50% DGA^{TM} Unloaded	2.15	19.79	2.42	0.15
50% DGA^{TM} Loaded	3.25	4.26	0.00	0.15
20% MEA Unloaded	0.86	17.13	12.27	0.00
20% MEA Loaded	0.95	10.34	0.00	0.00

Critchfield and Jenkins (1999) reported comprehensive analyses of samples from three field systems using MDEA, all of which were exposed to trace or intermittent levels of oxidants. Oxidative degradation rates were on the order of 0.05 to 0.1 mM/hr. Organic acids, DEA, and methylmonoethanolamine (MMEA) were equally present as

degradation products. Formate represented half of the organic acid; glycolate, acetate, oxalate, and lactate were also observed. Alawode (2005) and Jones (2003) attempted to quantify the oxidative degradation of PZ by using GC for piperazine loss and anion IC to quantify the formation acetate, the observed major product of PZ degradation according to Alawode. The rate of acetate production ranged from 0.08 to 0.4 mM/hr while actual piperazine loss ranged from 1 mM/hr to 5 mM/hr.

Lloyd (1956) examined the effects of O_2 pressure, solvent concentration, pH and temperature (from 35 to 95^{o}C) on the oxidation of diethylene glycol. Lloyd calculated an oxygen consumption rate of 20 mM/hr, and observed formic acid, formaldehyde and hydroxyacetaldehyde as major degradation products.

Two studies have been performed by different principle investigators at the University of Regina. The first study was an attempt to quantify the kinetics of the oxidative degradation of MEA under conditions encountered in a typical flue gas treating process (Supap 1999; Supap et al. 2001). Experiments, involving 5 M MEA (α=0.51) solutions agitated at 500 RPM, were performed with an autoclave reactor at elevated temperatures (55 to 120^{o}C) and pressures (250 kPa O_2). Degradation was quantified by measuring the concentration of MEA using GC-MS; GC-MS and HPLC-RID were utilized to identify degradation products. Kinetics were regressed from the experiments based on the rate of MEA loss and O_2 consumption.

Products detected by GC included acetamide, acetaldehyde and imidazole; the presence of imidazole was confirmed by HPLC. Supap concluded that the presence of CO_2 in MEA/O_2 systems decreased degradation; in other words, unloaded solutions degraded faster than loaded solutions. As the O_2 was consumed, O_2 was added to the reactor to maintain constant pressure. Since the partial pressure of volatile degradation compounds, namely NH_3, was not accounted for in the total pressure measurements, there is some question as to the accuracy of the O_2 consumption rate. Additionally, some of the kinetic parameters of the degradation reactions only have a statistical significance of ~ ± 200%. Using the kinetics from this study to predict the degradation rates expected in the reactors used in this work underpredicts the degradation rate by an order of magnitude.

The second study analyzed the liquid solution to determine the degradation products and mechanism of degradation for MEA and mixtures of MEA/MDEA (Bello and Idem 2005; Lawal and Idem 2005; Lawal et al. 2005). Experiments were again performed with an autoclave reactor at temperatures of 55°C, 100°C, and 120°C and O_2 pressures of 250 or 350 kPa over a several day time frame. Degradation experiments were performed with and without O_2 and CO_2 to quantify the effect of CO_2 loading and degradation in the absence of O_2. Degradation products were identified using a GC-MS with methods developed by previous investigators in the research group (Supap 1999). Concentrations and rates of formation of the degradation products were not quantified, and MEA/MDEA degradation rates were quantified by the concentration change of the amine with time.

MEA systems (varying from 11.4 to 17.9 weight percent with loadings ranging from 0 to 0.44) were tested with and without $NaVO_3$ catalyst. Bello and Idem (2005) reported no products, but did conclude that MEA degradation rate increased in the presence of vanadium. They also observed a direct correlation between MEA degradation with increasing MEA concentration, temperature and oxygen pressure.

Lawal et al. (2005) investigated MEA/MDEA blends ranging from 5-9 M in total amine concentration, with loading ranging from 0 to 0.53 mol CO_2/mol amine. The MDEA/MEA ratio varied from 0 to 0.4. A significant number of degradation products were identified, most of which had not previously been reported in the literature. These products ranged from expected products (NH_3, ethylamine, formate, bicine) to unexpected products, such as a 15-member cyclic crown ether. Absent in the identified compounds were thermal degradation products and carbamate polymerization products that have been identified previously by several investigators (Polderman et al. 1955; Yazvikova et al. 1975).

Compound analysis was performed by doing a library search to match mass spectra in the NIST database. Supap (1999) reported that the statistical match for the MEA sample spectrum is only as good as 86%, and that the statistical match of some of the reported major degradation products is as low as 10%. This brings into question the

accuracy of the analytical method, especially because MEA is present in high concentration and could not be verified with 100% certainty.

The Lawal studies noted trends that mirrored results of the Supap studies. Oxidative degradation increased with increasing amine concentration, and decreased with the addition of CO_2, confirming that unloaded solutions faster oxidize than loaded solutions. Another important conclusion from these studies was the addition of MDEA to the MEA solutions appeared to decrease the rate of MEA oxidation as the MDEA is preferentially oxidized.

A study headed by the National Energy Technology Laboratory performed comprehensive liquid analysis on degraded samples from an industrial application (Strazisar et al. 2003). The IMC Chemicals Facility in Trona, CA removes CO_2 from a coal-fired power plant using an aqueous MEA. The purified CO_2 is used to carbonate brine for the sale of commercial sodium carbonate.

Solution analysis was performed on samples taken from three points in the process: make-up MEA (clean), lean MEA (inlet to the absorber), and the liquid waste from the reclaimer bottoms. Volatile compounds were identified using gas chromatography combined with mass spectrometry (GC-MS), FTIR, or atomic emission detection. Ionic species in the liquid were quantified using ion chromatography and inductively coupled plasma-atomic emission spectroscopy (ICP-AES).

In addition to the known carboxylic acid degradation products (specifically acetate and formate), several new degradation compounds were detected in this experiment. Notable products include propionic acid, N-butyric acid, hydroxyethyl-formamide, N-acetyl MEA, 2-oxazolidone and other longer chain amides. These products are believed to come from degradation mechanisms for $MEA/CO_2/O_2$ systems.

Because this analysis was done using an actual flue gas, many of the degradation products (not listed here) are attributable to reactions with impurities in the flue gas such as SO_x and NO_x. Sulfate was found in the liquid solution, as well as nitrosamine functional groups (see Appendix A for a detailed discussion on nitrosamines). All of the liquid-phase analysis was performed on solution extracted from the reclaimer bottoms; no

analysis was performed on the rich MEA solution. This makes it impossible to determine whether the "new" degradation products are being formed in the absorber/stripper process or in the solvent reclaimer, where MEA is present in very high concentration and is subjected to temperatures higher than in the stripper. Many of the degradation products identified in this study are likely the result of carbamate polymerization, thermal degradation in the reclaimer, or reactions between oxidation products and thermal degradation/carbamate polymerization products.

2.2.2. Amine Degradation in the Absence of Oxygen

Extensive work has been performed on a number of amine systems in the absence of oxygen. This type of degradation results in products created from thermal degradation and/or carbamate polymerization. Diethanolamine (DEA), a secondary alkanolamine, has been the most extensively studied amine system under these conditions (Polderman 1956; Choy and Meisen 1980; Kim and Sartori 1984; Kennard and Meisen 1985; Hsu and Kim 1985).

Researchers studied DEA/CO_2 systems ranging from 0-100 wt% DEA, 90 to 250^{o}C, and 1.5 to 6.9 MPa; experiments were carried out in 10mL stainless steel bombs, with experiment time ranging from a few hours to 15 days. Degradation product formation and DEA disappearance were noted using GC-MS. Observed degradation products include HEO, substituted dimers HEP and THEED, and the substituted, high-boiling trimeric compounds HAO, HAP and THEDT. Increased temperature, pressure and DEA concentration all led to higher degradation rates.

Choy and Meisen (1980) also studied DEA/CO_2/H_2S sour gas systems at 185^{o}C and 4.2 MPa of CO_2 for four hours of experiment time. Hydroxyethylpiperazine (HEP) was noted as a degradation product in these systems, in addition to four other unidentified compounds.

Polderman et al. (1956) proposed a mechanism by which MEA degrades thermally in gas-treating service to form higher molecular weight products. MEA reacts

with CO_2 to cyclize and form a ring structure known as 2-oxazolidone. This ring structure can react with another MEA molecule to form a ring structure known as HEIA. Finally, the HEIA is hydrolyzed and rearranges to form a dimer known as HEED.

Chakma and Meisen (1988) investigated MDEA degradation at elevated temperatures (100 to 200^{o}C) and pressures (1.4 to 4.2 MPa CO_2) at concentrations ranging from 20 to 50 weight percent. They concluded that MDEA thermal degradation increases rapidly as temperature and pressure are increased. Dawodu and Meisen (1996) investigated MDEA blended with MEA and DEA at similar experimental conditions. In terms of resistance to thermal degradation, they discovered MDEA < MEA < DEA, with MDEA being the most resistant.

Daptardar et al. (1994) studied MDEA and triethanolamine (TEA) systems promoted by PZ and morpholine (MOR) and found that PZ-promoted systems were less thermally stable; in terms of PZ systems, PZ/MDEA is more stable than PZ/TEA. Keeping pressure and temperature lower led to reduced degradation rates.

Holub et al. (1998) proposed a general pathway for the thermal degradation of ethanolamines in gas treating applications (in the absence of oxygen). An ethanolamine reacts with carbon dioxide to form a carbamic acid, which rearranges and loses a water to form an oxazolidone ring structure. The oxazolidone reacts with another ethanolamine to form a substituted ethylenediamine structure; this structure either rearranges to form a substituted piperazine, or reacts with another oxazolidone to form a substituted diethylenetriamine. This substituted dimer can continue to react with other species to form trimers and other higher molecular weight compounds. Suggestions to minimize degradation agrees with other researchers; lowering the temperature, pressure, CO_2 concentration and amine concentration all contribute to reducing thermal degradation. These findings for MEA are supported by Davis (2009) from the Rochelle group at the University of Texas.

2.2.3. Experiments Performed in the Presence of Metal Catalysts

Dissolved iron is the most probable metal catalyst because it is a corrosion product in systems constructed of carbon steel. With degradation products that chelate iron, as much as 160 ppm of dissolved iron has been observed in amine systems (Hall and Barron 1981); Holub et al. (1998) notes that degraded DEA solutions can dissolve up to 6000 ppm iron. Lee and Rochelle (1988) suggested that ferrous ion reacts with "peroxide" to produce two free radicals as the initiating step of oxidation. It is very likely that any organic peroxides produced by alkanolamine oxidation would be decomposed by Fe^{+2} to produce free radicals, which would then catalyze further oxidation (Russell 1960).

$$Fe^{+2} + ROOH \rightarrow Fe^{+3} + RO^{\cdot} + OH^{-\cdot} \qquad 2.4$$

The Fe^{+2} is regenerated without losing any free radicals by another parallel reaction with the peroxide:

$$Fe^{+3} + ROOH + \rightarrow Fe^{+2} + ROO^{\cdot} + H^{+} \qquad 2.5$$

The direct reaction of ferrous ion with oxygen may be an important source of free radicals (Fe^{+3}) and a way of getting oxygen into the oxidation mechanism. In water, Fe^{+2} appears to react with oxygen, forming intermediates such as hydroperoxy ($HOO^{\cdot}$) and hydrogen peroxide (Stumm and Lee 1961).

$$Fe^{+2} + O_2 \rightarrow Fe^{+3} + HOO^{\cdot} \qquad 2.6$$

$$Fe^{+2} + HOO^{\cdot} \rightarrow Fe^{+3} + H_2O_2 \qquad 2.7$$

$$Fe^{+2} + H_2O_2 \rightarrow Fe^{+3} + OH^{\cdot} + H_2O \qquad 2.8$$

$$Fe^{+2}HO^{\cdot} \rightarrow Fe^{+3} + H_2O \qquad 2.9$$

Several patents assigned to Dow Chemical address the use of cupric salts as corrosion inhibitors in alkanolamine systems, especially in the presence of oxygen (Wolcott et al. 1986, Pearce et al. 1984, Pearce 1984, Cringle et al. 1987). However, Ferris et al. (1968) have shown that Cu^{+2} and V^{+3} have catalytic properties similar to Fe^{+2} for the dealkylation of tertiary amine oxides. Due to the corrosive nature of alkanolamine solvents, corrosion inhibitors must be added to solutions to prevent equipment destruction. These corrosion inhibitors are usually heavy metal salts of vanadium or copper (White 2001; Hakka and Ouimet 2004; Ulrich 1983; Lee 1986; Kohl and Nielsen 1997). Several studies have shown that the oxidation of MEA is catalyzed by dissolved metals, including Fe, Cu and V (Rooney et al. 1998; Tanthapanichakoon et al. 2003; Jou et al. 1995; Barron et al. 1966). Degradation and corrosion are closely related since degradation products have been shown to increase corrosion rates (Conklin et al. 1988; Bengtsson et al. 1975).

Blachly and Ravner (1964) examined the effects of metals as oxidation catalysts in MEA systems. Concentrations of copper up to 15 ppm, iron up to 30 ppm and chromium up to 37 ppm were studied; effects of bulk nickel metal were also detailed in the report, but exact nickel concentration was not specified.

They determined that dissolved copper at concentrations as low as 10 ppm was sufficient to cause serious degradation of the amine solution, and that the rates of copper catalyzed degradation were higher than iron catalyzed degradation at the same concentrations. A concentration of 3.7 ppm of nickelous ion had no impact on MEA oxidation, but a tenfold increase in concentration caused noticeable degradation. Rossiter et al. (1985) concluded that the presence of Cu catalyst in aerated solutions produced the greatest degradation rate in ethylene glycol systems.

Chi and Rochelle (2002) decreased the time necessary to quantify amine degradation by instantaneously measuring the concentration of evolved ammonia by Fourier-Transform infrared analysis (FTIR). In this method, the degradation rate was quantified by analyzing the rate of evolved NH_3 normalized to the liquid volume of amine solution. Instantaneous measurements of gas phase products eliminated the need

for complex liquid-phase analysis. Studies by Chi and Rochelle found that dissolved iron, over a concentration range of 0.0001 to 3.2 mM, catalyzed degradation rates from 0.12 to 1.10 mM NH_3 evolved / liter of solution-hr.

A parallel study by Ho (2003) used a sparged reactor and combinations of V, Fe, and Cu catalyst to degrade MEA solutions. Results from the experiments show that V is a catalyst for oxidative degradation and rates reported were equivalent to rates with Fe or Cu alone. These experiments appear to be limited by the rate of O_2 mass transfer.

Goff (2005) examined O_2 mass transfer effects and reaction kinetics by changing reaction conditions; in addition, a variety of compounds were screened for effectiveness as an oxidative degradation inhibitor. The study on oxygen mass transfer showed that the rate of NH_3 evolution is controlled by the rate of O_2 absorption into the amine, not by degradation kinetics. In general, the rate of NH_3 evolution increased as the agitation rate was increased, and also increased linearly with increasing O_2 concentration. Furthermore, at high concentrations of catalyst (above 0.5 mM Fe or Cu) and MEA (above 7.0 m MEA, or 30 wt %), the rate of NH_3 evolution was controlled by the rate of O_2 mass transfer.

2.2.4. Experiments Performed in the Presence of Degradation Inhibitors

Blachly and Ravner (1966) developed an inhibitor package based on two additives, the tetra-sodium salt of ethylene-diamine-tetra-acetic acid (EDTA), and the monosodium salt of N,N-diethanol glycine (VFS, or bicine). The EDTA was used as a chelating agent to bind the Cu and other dissolved metals to prevent them from acting as catalysts, and VFS functioned as a peroxide scavenger to inhibit the degradation mechanism. These inhibitors were both found to be more effective at inhibiting Cu catalyzed degradation than for Fe, Cr and Ni. Specifications were developed for an additive package consisting of both EDTA and VFS, which was subsequently employed in nuclear submarines to minimize oxidative degradation of MEA.

To counteract the iron catalyzed degradation, Chi (2002) found that in MEA solutions with a CO_2 loading of 0.4, a ratio of EDTA to total dissolved iron of 22.5 to 1 cut the degradation rate by 40% (in terms of ammonia evolution). A second experiment confirmed the 40% reduction in MEA degradation rate.

Goff (2006) studied a number of oxygen scavengers, reaction inhibitors and chelating agents to test their effectiveness in inhibiting the Fe and Cu catalyzed oxidative degradation of MEA. These inhibiting agents included sodium sulfite, formaldehyde, hydroquinone, ascorbic acid, manganese salts, EDTA and inorganic potassium salts. Goff found that a 1:1 ratio of EDTA:Cu reduced NH_3 production by 75%, but EDTA lost inhibiting capacity over time as it continued to chelate Cu catalyst. Proprietary Inhibitor A, an inorganic compound that is stable and acts as a reaction mechanism inhibitor, was the most successful oxidation inhibitor. It was shown to be effective at inhibiting oxidation catalyzed by iron and/or copper.

2.3. Mass Transfer Effects

The simplest mass transfer theory assumes that all transport between two different phases occurs in two films of finite thickness, with each film having a different resistance to mass transfer (Lewis and Whitman 1924). When a gas-liquid system is at steady state, the concentration of a species A in the liquid at the gas-liquid interface is in equilibrium with the concentration of the gas at the interface. Since gases are sparingly soluble in most liquids, the solubility can be represented by Henry's law.

In the case of the oxidative degradation of MEA, the O_2 diffusing into the amine solution is reacting with the MEA. There are five different regimes of mass transfer with chemical reaction: Kinetic, Diffusion, Fast Reaction, Instantaneous Reaction, and Surface Reaction (Astarita 1966). The Kinetic Regime occurs when the reaction kinetics are slow enough that all of the liquid phase is saturated with the diffusing component, O_2 in this case. The kinetics in this regime still show a dependence on reactant or catalyst

concentration, but are slow enough so that all of the reactions take place in the bulk liquid.

As kinetics are increased, the system enters the Diffusion Regime. The reactions still take place in the bulk liquid, but now the kinetics are fast enough that O_2 reacts as quickly as it can diffuse into the bulk liquid. An increase in the reaction kinetics does not affect the overall rate of consumption of O_2, since the controlling process is diffusion of O_2 into the bulk liquid.

As the kinetics continue to increase, the system enters the Fast Reaction Regime. At this point the reactions are fast enough that the reaction takes place in the liquid film and not the bulk liquid. If the kinetics are increased even further, the system again becomes diffusion limited and enters the Instantaneous Reaction Regime. At this point, the kinetics are so fast that the liquid reactant is being depleted in the liquid film, and the kinetics are so fast that the reaction occurs as soon as O_2 and MEA are brought together by diffusion transport.

If kinetics are again increased so that the concentration of species A in the liquid film is negligible, the system is in the Surface Reaction Regime. At this point, the overall rate of consumption of A is controlled by the diffusion of A to the gas-liquid interface where the reaction takes place instantaneously. The rate of consumption of A can be considered gas-film controlled, and the rate of mass transfer is determined by the overall gas-film mass transfer coefficient, K_G.

Since the mechanisms for the oxidative degradation of MEA involve a series of free radical reactions, the overall reaction rate is expected to be very fast. Goff concluded that the degradation rate of MEA is controlled by the rate of O_2 mass transfer in the presence of Fe and Cu catalyst. At low catalyst concentrations, or in systems where degradation inhibitors are present, the degradation rate is slow enough to be in the Kinetic Regime. As the concentration of catalyst increases, the overall rate begins to be diffusion controlled. In this regime an increase in the catalyst concentration has little effect on the overall reaction rate. At very high catalyst concentration, the rate begins to increase again as the system enters the Fast Reaction Regime.

2.4. Conclusions

Oxidative degradation of monoethanolamine is driven by oxygen in the flue gas, resulting from free radical reactions occurring in the system. The amount of dissolved iron (in addition to other metals) and its rate of oxidation are likely to play a major role in the degradation process. Dissolved iron can react directly and quickly with oxygen and carry oxidizing potential into the stripper, or it can catalyze autoxidation by decomposing peroxides into free radicals. Copper and vanadium, both utilized as corrosion inhibitors in carbon steel systems, have been observed to present the same problem as ferrous iron in MEA systems.

Comprehensive laboratory studies of amine oxidation need to be performed to quantify the mechanisms of degradation. These studies should focus on MEA and then expand to other amine systems. The role of dissolved iron, copper, and/or vanadium on the degradation product mix and their quantities must be addressed. Once mass transfer effects are understood, the effects of degradation inhibitors and other solvent additives need to be studied. Moreover, amine blends and/or pure systems using more degradation resistant amines (piperazine, AMP, MDEA) should also be investigated.

Chapter 3: Analytical Methods and Experimental Apparatus

This chapter details the experimental apparatus used to oxidize amine solutions at absorber conditions, as well as all the analytical methods employed to measure rate of formation of products and rate of amine disappearance. Information on equipment specifications, operating procedure and data interpretation are presented in great detail.

3.1. Anion Chromatography

3.1.1. Equipment Specifications

Anionic species produced from the oxidative degradation of amines are quantified using a Dionex ICS-3000 Dual RFIC Ion Chromatography System. The system includes a DP-1 dual pump module (Serial No. 07050048), EG-2 eluent generation module (Serial

No. 07030712), and DC conductivity module (Serial No. 07030753). Attached to the ICS-3000 is an AS Autosampler (Serial No. 07040110), which eliminates the need for manual user injection.

Experimental samples are introduced from a 2 mL plastic sample vial via an injection needle in the AS Autosampler. A majority of the sample is flushed through a 25 μL injection loop to ensure that there is no cross-contamination from a previous sample. The remaining sample is passed through the injection loop and carried by the mobile phase to the inlet of the columns.

The mobile phase is an aqueous solution of potassium hydroxide in water. Water is provided by a Millipore Direct-Q 3 UV Water Purification System (Serial # F7CN14541). The Direct-Q 3 UV Water Purification System is an integrated reverse osmosis and polishing system designed to product Type III and Type I water directly from tap water. A SmartPak cartridge includes pretreatment reducing the need for feedwater pretreatment (softener) in front of the system and purification which provides ultrapure water for specific applications. The system also incorporates a dual-wave UV lamp designed to reduce TOC required by organic-sensitive applications. A built-in 6.5 liter reservoir dispenses the water at a rate of 0.6 L/min.

The distilled, deionized water is analytical grade water produced at 18.2 MΩ*cm. The water is transferred from a 2-L plastic reservoir located on top of the DC module using an isocratic pump located in the DP-1 module. Eluent is produced by mixing the water with concentrated KOH from an EluGen KOH Cartridge (Serial No. 070472109015). A specific ratio of KOH is dispensed and mixed with the water using the interface on Chromeleon software (Version 6.80).

The generated eluent is passed through a 4-mm Carbonate Removal Device (CRD-200). The CRD is an ion-exchange membrane that scrubs any carbonate out of the eluent. Carbonate can be generated if the DDI water has absorbed any CO_2. When the concentrated KOH is mixed with the water, the CO_2 reacts with KOH to form K_2CO_3 in solution. The carbonate anion formed has the potential to interfere with the analysis of other anions in the experimental sample.

After the scrubbed eluent leaves the CRD, it passes through the injection port and carries the experimental sample through a series of two ion-exchange columns: an IonPac AG15 Guard Column (4 x 50 mm) and an IonPac AS15 Analytical Column (4 x 250 mm). Both columns are packed with a cross-linked ethylbenzene/divinylbenzene resin affixed with quaternary ammonium groups. The AG15 and AS15 columns were designed specifically for the separation of low molecular weight compounds.

Any anionic species in the sample will become affixed to the resin in the columns. As the mobile phase is continually passed through the columns, the anions will be flushed off based on their affinity for the resin and replaced with fresh hydroxide ions. The stronger the bond between the species and the resin, the longer it will take to flush the species from the column. After the anionic species have been flushed from the columns, they are carried by the KOH eluent to the ASRS 4-mm suppressor.

The ASRS suppressor is a device that separates the ionic species in solution. The suppressor is an enclosed unit containing anodic and cathodic plates, separated by a permeable membrane. The suppressor is plugged into a power supply, which provides a user-specified current to the suppressor. The applied current separates the anionic and cationic species on the plates on the opposite sides of the membrane. Cationic species are carried out to the waste container. On the opposite side of the membrane, a solution of weakly ionized anions in water travels to the conductivity cell.

The suppressor is self-regenerating because nothing external is added to the system. Once the weakly ionized solution of anions passes through the conductivity cell, an ion-exchange membrane removes the anions from solution and circulates the regenerated water back to the suppressor, where it is countercurrently contacted with fresh sample entering the suppressor from the IonPac AS15 analytical column.

Once the weakly ionized solution of anions exits the suppressor, it passes through a Continuously Regenerated Anion Trap Column (CR-ATC). Like the CRD, the CR-ATC, is a selective ion exchange membrane that removes carbonate from solution. The source of the carbonate anion is the degraded amine sample loaded with CO_2 in the form of amine carbamate, which is converted to carbonate in the Dionex system.

Once the solution has been scrubbed for carbonate, it travels to a conductivity cell (Serial No. 07030816) located downstream. As the solution passes through the cell, any anionic species traveling through will produce a response (measured in microsemems, or μS) that is represented by a peak. The height and area of each peak is directly proportional to the concentration of the each anionic species in solution. Each anionic species will have a specific retention time in the system, based on its affinity for the resin in the columns. The series of peaks for a particular experimental sample is displayed on a chromatogram using Chromeleon Software (Version 6.80). After passing through the cell, the analyzed solution travels through the CR-ATC and CRD, where it picks up the scrubbed carbonate anions before it is cleaned and circulated back to the ASRS unit.

3.1.2. Standard Preparation

The following chemicals will be needed in the preparation of standards for anion chromatography analysis: acetic acid, glycolic acid, formic acid, sodium nitrate, sodium nitrite, and oxalic acid. Table 3.1 below gives the specifications for all reagents used for experimentation and analysis.

Table 3.1 Chemical Reagent Specifications

Reagent	CAS #	Supplier	Molecular Weight	Assay	Lot #
Sodium Nitrite	7632-00-0	Fisher	84.99	99.9%	905569
Sodium Nitrate	7631-99-4	Fisher	69.00	97.0%	AD-6094-29
Oxalic Acid Monohydrate	144-62-7	Spectrum	126.07	99.5% - 102.5%	IK184
Acetic Acid, Glacial	64-19-7	Acros	100.14	100.0%	B0507607
Glycolic Acid (67% in Water)	79-14-1	Acros	76.05	67.0%	2197194272
Formic Acid (88% in Water)	64-18-6	Fisher	46.03	90.0%	033186
Sodium Hydroxide (40% w/w)	1310-73-2	Ricca	40.00	100.0%	2604571
Methanesulfonic Acid	75-75-2	Fisher	96.10	99.0%	
Ethylenediamine	107-15-3	Fisher	60.10	99.0%	011047
Ammonium Sulfate	7783-20-2	EM Industries	132.15	99.0%	39027911
Piperazine	110-85-0	Fluka	86.14	98.0%	1294963
Monoethanolamine	141-43-5	Acros	61.08	99.0%	A0216802001
2-amino-2-methyl-1-propanol (AMP)	124-68-5	Acros	89.14	99.0%	A0209789001
Potassium Bicarbonate	298-14-6	Fisher	100.12	100.0%	028080
Sodium Metavanadate	13718-26-8	Acros	121.93	96.0%	A019877601
Ferrous Sulfate Heptahydrate	7782-63-0	Spectrum	278.01	99.0%	HC131
Cupric Sulfate Pentahydrate	7758-99-8	Mallinckrodt	249.68	99.5%	48444N06693
Inhibitor A		MCB		99.0%	
Hydroxyethyl-formamide		Huntsman	89.03	51.0%	
Hydroxyethylimidazole	1615-14-1	Acros	112.13	95.00%	A0195049001
Diglycolamine	929-06-6	Acros	105.14	98%	A0175139
Diethanolamine	111-42-2	Acros	105.14	99%	A019762101
Ethylene Glycol	107-21-1	Fisher	62.07	99%	933006
Glycine	56-40-6	EM Industries	75.07	98.50%	39141937
Chromium Sulfate		Pfaltz/Bauer	392.18	99.9%	123
Nickel Sulfate	10101-97-0	Alfa Aesar	262.88	98.0%	D095034
EDTA	60-00-4	Fisher	292.25	100.3%	916810
Paraformaldehyde	30525-89-4	Fisher	(30.03)n	95.0%	37435
Inhibitor B		EM		99.0%	
Sodium Sulfite	7757-83-7	Spectrum	126.04	98.0%	GD076

From the DDI water reservoir, add approximately 200 mL of water to an empty 1-L volumetric flask. Record the mass of water added to the flask. Using a scale (with three decimal accuracy) and plastic weigh boats, transfer 2.000 g each of sodium nitrate, sodium nitrate, and oxalic acid monohydrate to the 1-L volumetric flask. Record the exact mass of each reagent transferred to the flask.

Using an Eppendorf autopipette (range 2 to 10 mL), transfer the following volumes of the acids to the 1-L volumetric flask: acetic acid – 2.0 mL; formic acid – 2.3 mL; glycolic acid – 3.0 mL. Record the exact mass of each acid added to the flask. From the DDI water reservoir, add water to the line denoting the 1-L mark on the flask. Record the mass of water added to the flask and combine it with the mass of water initially added

to the flask. Label this flask as "2000 ppm stock anion standard" and cap it with a glass stopper.

Using an Eppendorf micropipette (range 100 to 1000 µL) transfer 500 µL of the 2000 ppm stock anion standard to an empty 100 mL volumetric flask. Record the mass of stock standard transferred. From the DDI reservoir, add water up to the mark on the neck of the flask denoting 100 milliliters. Record the mass of water added to the flask. Label this flask as "10 ppm stock anion standard" and cap it with a glass stopper.

Replace the micropipette tip and transfer 1.0 mL of the 2000 ppm stock anion standard to an empty 100 mL flask. Repeat the above steps and label this volumetric flask "20 ppm stock anion standard" and cap it with a glass stopper. Repeat this process with 1.5, 2.0, and 2.5 mL of the 2000 ppm stock anion standard transferred into three more 100 mL volumetric flasks. Label these flasks "30", "40", and "50 ppm stock anion standard", respectively.

3.1.3. Preparation of Control and Experimental Samples

Using an Eppendorf micropipette (range 20 to 200 µL), transfer 100 µL of 7 m MEA ($\alpha = 0$) to a 15 mL screwtop glass vial. Record the mass of MEA added to the vial. Using the Eppendorf 10 mL autopipette with a clean tip, transfer 10 mL of DDI water to the screwtop vial. Record the mass of water added and screw the cap shut. Label the vial "Unloaded MEA Control Sample".

After replacing the disposable microtip, transfer 100 µL of 7 m MEA ($\alpha = 0.40$) to an empty 15 mL screwtop glass vial with the micropipette. Record the mass of MEA added to the vial. Using the autopipette, transfer 10 mL of DDI water to the screwtop vial and record the mass. Cap the vial and label it "Loaded MEA Control Sample". (Note: If any degraded amine systems other than MEA are being analyzed, perform the above steps to create a loaded and unloaded control sample for each amine system.)

For each experimentally degraded sample to be analyzed, transfer 100 µL of the sample to an empty 15 mL screwtop glass vial with the 200 µL micropipette and record

the mass of sample added. Transfer 10 mL of DDI water to the vial, record the mass of water added, and cap the vial. Label the vial with the experimental conditions (amine concentration, catalyst and/or inhibitor concentration), the date the sample was taken, the time the sample was taken, and "100X", which denotes the sample was diluted by a factor of 100 from its original concentration. All samples – the calibration standards, control samples and experimental samples – must be transferred into 1.5 mL Dionex disposable autosampler vials. Use the 1000 μL micropipette to transfer a portion of each of the samples from the screwtop vials to the autosampler vials.

In order to analyze for amide concentration, add 1 g of 5 M sodium hydroxide to 1 g of degraded amine sample, allowing 24 hours for the reaction to go to completion at room temperature. Then repeat the above steps for sample dilution and transfer to the autosampler vial. The addition of NaOH hydrolyzes amides present in solution and recovers the respective carboxylic acids and amines. Any increase in carboxylic acid concentration between the two samples is considered to be amide that has been recovered in the form of carboxylic acid.

3.2. Cation Chromatography

3.2.1. Equipment Specifications

The presence of cationic species in degraded amine solutions is determined using a Dionex ICS-2500 Ion Chromatography System. The system includes a GP50 Gradient Pump, CD25 Conductivity Detector, and LC25 Chromatography Oven. The gradient pump allows for a step change or linear gradient in eluent, or mobile phase, concentration during sample analysis from a mixture of up to four 2-liter plastic reservoirs. The chromatography oven houses all of the consumable parts used for peak separation and controls the temperature at which they are operated. The conductivity detector takes a voltage reading from the conductivity cell and converts it to a total conductivity measurement in microsemens (μS).

The sample is introduced via a manual injection port located on the outside of the LC25 chromatography oven. A portion of the sample flushes a 25 μL injection loop and is carried via waste tubing to a waste collection container. The remaining sample travels through the cleaned injection loop to a series of columns: an IonPac CG17 Guard Column (4 x 50 mm) and an IonPac CS17 Analytical Column (4 x 250 mm). Both columns are packed with a divinylbenzene/ethylbenzene resin that separates cationic species based on their affinity for the resin. The guard column and analytical column are packed with the same resin at the same density; the guard column, or "pre-column", acts as a filter that catches any impurities before they reach the analytical column. This prefiltering process helps prolong the life of the analytical column.

The experimental sample is carried through the IonPac columns via an eluent consisting of dilute methanesulfonic acid in water. The MSA eluent is prepared with distilled, deionized water produced by a Millipore Direct-Q 3 UV Water Purifcation System (Serial No. F7CN145411). The Millipore Direct-Q system can produce up to 10 liters a day of analytical grade water at 18.2 MΩ. Before entering the Millipore system, boiler feedwater taken from The University of Texas Power Station is pretreated with a series of filters provided by Siemens Technologies. These filters consist of two mixed filters and one activated carbon filter.

All prepared eluents are kept in 2-liter plastic bottles located on top of the CD25 Conductivity Detector. All eluents and DDI water are kept inert with an 8 psig nitrogen pad in the head space above the liquid. Nitrogen, purchased from the Cryogenics lab in the Department of Physics, is available at 16.2 barg.

The MSA eluent is pumped using the GP50 from the plastic reservoirs through Gradient Mixer GM-3 to the IonPac columns. The gradient mixer is a small beaded column that ensures that the eluent is homogeneously mixed before it enters the columns. Once the cationic species in the experimental sample are pushed off the column with the eluent, the cations in the sample enter a 4-mm CSRS (Cationic Self-Regenerating Suppressor).

The suppressor is an enclosed unit containing anodic and cathodic plates, separated by a permeable membrane. The suppressor is plugged into a power supply, which provides a specified current. The applied current separates the anionic and cationic species on opposite sides of the membrane. Anionic species are carried out to the waste container. On the opposite side of the membrane, a solution of weakly ionized cations in water travels to the conductivity cell.

The suppressor is termed as a "self-regenerating" suppressor because nothing external has to be added to the system. Once the weakly ionized solution of cations passes through the conductivity cell, an ion-exchange membrane removes the cations from solution and recirculates the water back to the suppressor, where it is countercurrently contacted with fresh sample entering the suppressor from the IonPac CS17 analytical column.

As stated above, once the solution exits the suppressor, it travels to a conductivity cell located just downstream. As the solution passes through the cell, any cationic species traveling through will produce a response (measured in μS) represented by a peak. The height and area of the peak is directly proportional to the concentration of the cationic species in solution. Each cationic species will have a specific retention time in the system, based on its affinity for the resin in the columns. The series of peaks for a particular experimental sample is displayed on a chromatogram using Chromeleon Software (version 6.60).

3.2.2. Standard Preparation

Ethylenediamine, manufactured by Fisher Chemical, will be needed for preparation of a standard. From the DDI water reservoir, add approximately 200 mL of water to an empty 1-L volumetric flask. Record the mass of water added to the flask. Using an Eppendorf autopipette (range 2 to 10 mL), transfer 2.0 mL of ethylenediamine to the volumetric flask and record the mass added. From the DDI water reservoir, add water to the line denoting the 1-L mark on the flask. Record the mass of water added to

the flask and add it to the mass of water initially added to the flask. Label this flask as "2000 ppm stock EDA standard" and cap it with a glass stopper.

Using an Eppendorf micropipette (range 200 to 1000 μL) transfer 500 μL of the 2000 ppm stock EDA standard to an empty 100 mL volumetric flask. Record the mass of stock standard transferred. From the DDI reservoir, add water up to the mark on the neck of the flask denoting 100 milliliters. Record the mass of water added to the flask. Label this flask as "10 ppm stock EDA standard" and cap it with a glass stopper.

Replace the micropipette tip and transfer 1.0 mL of the 2000 ppm stock EDA standard to an empty 100 mL flask. Repeat the above steps and label this volumetric flask "20 ppm stock EDA standard" and cap it with a glass stopper. Repeat this process with 1.5, 2.0, and 2.5 mL of the 2000 ppm stock EDA standard transferred into three more 100 mL volumetric flasks. Label these flasks "30", "40", and "50 ppm stock EDA standard", respectively. Repeat this process to create calibration standards for the appropriate amine if you are performing simultaneous analysis for solvent disappearance.

3.2.3. Preparation of Control and Experimental Samples

Using an Eppendorf micropipette (range 20 to 200 μL), transfer 100 μL of 7 m MEA ($\alpha = 0$) to a 15 mL screwtop glass vial. Record the mass of MEA added to the vial. Using the autopipette, with a clean tip, transfer 10 mL of DDI water to the screwtop vial. Record the mass of water added and screw the cap shut. Label the vial "Unloaded MEA Control Sample".

After replacing the disposable tip, transfer 100 μL of 7 m MEA ($\alpha = 0.40$) to an empty 15 mL screwtop glass vial with the micropipette. Record the mass of MEA added to the vial. Using the autopipette, transfer 10 mL of DDI water to the screwtop vial and record the mass. Cap the vial and label it "Loaded MEA Control Sample". (Note: If any degraded amine systems other than MEA are being analyzed, perform the above steps to create a loaded and unloaded control sample for each amine system.)

For each experimentally degraded sample to be analyzed, transfer 100 µL of the sample to an empty 15 mL screwtop glass vial with the micropipette and record the mass of sample added. Transfer 10 mL of DDI water to the vial, record the mass of water added, and cap the vial. Label the vial with the experimental conditions (amine concentration, catalyst and/or inhibitor concentration), the date the sample was taken, the time the sample was taken, and "100X", which denotes the sample was diluted by a factor of 100 from its original concentration.

3.3. HPLC Method with Evaporative Light Scattering Detection

HPLC analysis of nonionic species is performed using evaporative light scattering detection (ELSD). The PL-ELS 2100 evaporative light scattering detector is a unique and highly sensitive detector for semi-volatile and non-volatile solutes in a liquid stream. The heated solvent stream containing the solute material is nebulized and carried heated nitrogen gas flow through an evaporation chamber. The solvent is volatilized, leaving a mist of solute particles that scatter light to a photosensitive device. When highly volatile compounds (including the solvent) are being nebulized, only its vapor passes though the light path and the amount of light scattered minimal. When a non-volatile solute is present, a particle cloud passes through the light path, causing light to be scattered. The signal is amplified and a voltage output results from the concentration of solute particles passing through the light.

The PL-ELS 2100 is interfaced through Chromeleon Software Version 6.80 on the Dionex ICS-3000 and performs parallel liquid-phase analysis independent of the anion IC system. However, calibration standards and sample dilutions are prepared in the exact manner as for anion analysis; the only difference is the dilution factor. Because the evaporative light scattering detector has a highly non-linear response, a 10X dilution factor is typically used for ELSD analysis of degraded samples (1 g sample + 9 g DDI H_2O).

Separation of nonpolar degradation products is achieved using a Waters T3 C18 column. The nebulizer and evaporator were both set at 50°C with a N_2 flowrate of 1.6 SLM and a light source intensity of 85%. The method started with 98% H_2O/2% acetonitrile (ACN) by volume at a rate of 1.0 mL/min from 0-3 minutes, ramped to 80% H_2O/20% ACN from 3-15 minutes, and held there for an additional 5 minutes.

Operation of the ELSD system is also very similar to the anion system; there are only three major differences. All batches run using the evaporative light scattering detector are found in the folder "ICS3000_ELSD Analysis". The "HEF" program is used for calibration and degraded samples – with the exception of the final sample. Similar to the anion sequences, use the "Shutdown" program for the final sample. Under the method category, choose "HEF" for all samples. The peaks of interest when using evaporative light scattering detection are hydroxyethyl-formamide (retention time = 2.66 minutes) and hydroxyethylimidazole (retention time = 5.91 minutes). When degraded samples are analyzed, there is often a large peak that appears around 2.0 minutes; this peak is any material that is not retained on the columns and passes directly through the HPLC system.

3.4. FTIR Analysis Method

The gas phase portable FT-IR analyzer and sample pump were purchased from Air Quality Analytical, Inc. The portable FT-IR analyzer, a Temet Gasmet™ Dx-4000 (Serial No. 01253), allows for simultaneous analysis of up to 50 components and the gas cell is temperature controlled at 180°C. The high temperature analysis allows for direct sample measurement without having to dry or dilute the gas stream to avoid IR interference due to water absorption. Table 3.2 gives the detailed specs for the FT-IR analyzer.

Table 3.2 Temet Gasmet™ DX-4000 FT-IR Gas Analyzer Technical Specifications

General Parameters	
Model	DX-4000
Serial Number	01253
Supplier	Air Quality Analytical, Inc. (www.airqa.com)
Measurement Principle	FT-IR (Fourier Transform Infrared)
Performance	Simultaneous analysis of up to 50 compounds
Operating Temperature	20 ± 20°C, optimum 15 - 25°C non condensing
Storage Temperature	-20 - 60°C, non condensing
Power Supply	12 VDC or 100-240 VAC / 50 - 60 Hz
Software	Calcmet™ for Windows v 4.41
Spectrometer	
Interferometer	Temet Carousel Interferometer
Resolution	8 cm^{-1} (7.76 cm^{-1})
Scan frequency	10 spectra/s
Aperture	2.54 cm
Detector	MCTP (Mercury, Cadmium, Tellurium, Pelletier Cooled)
IR-source	Ceramic, SiC, 1550 K Temperature
Beamsplitter	ZnSe
Window material	BaF_2
Wavenumber range	900 - 4200 cm^{-1}
Sample Cell	
Structure	Multi-pass, fixed path length 5.0m
Material	Gold/Ruthenium/Nickel coated extruded Aluminum
Mirrors	fixed, protected gold coating
Volume	1.0 L nominal
Connectors	Swagelok 6.35 mm (1/4")
Gaskets	Teflon® coated Viton®
Temperature	180°C
Maximum sample gas pressure	2 bar
Flow rate	1-5 L/min
Response time	3 cell flushes (depends on gas rate)
Required gas filtration	Filtration of particulates (2 microns)
Sample condition	non condensing
Measuring parameters	
Zero point calibration	Every 24 hours calibrate with N_2 (minimum)
Zero point drift	2% of smallest measuring range per zero point calibration interval
Sensitivity drift	None
Accuracy	2% of smallest measuring range
Temperature drift	2% of smallest measuring range per 10°C temperature change
Pressure influence	1% change of measuring value for 1% sample pressure change
Enclosure	
Material/Weight	Aluminum / 16 kg
Dimensions (nm)	433 * 185 * 425

The gas sampler has dual temperature controls (for the sample pump and the heated sample line) as well as pressure gauges for the sample inlet and the vent line. The heated sample line is a 15 foot long insulated Teflon® tube with PFA tubing for the gas sample. Both the sample pump and the sample line are controlled at a temperature of 180^{o}C to avoid any liquid entrainment into the gas sample cell or condensation of liquid onto the gold plated mirrors.

3.4.1. Infrared Spectroscopy Analytical Method

The composition of gas leaving the high gas flow degradation reactor is quantified using the Temet Gasmet™ Dx-4000 gas analyzer detailed above. The application of infrared radiation (600 – 4200 cm^{-1}) to a molecule excites both the rotational and vibrational energy levels of the molecule. The transition from a lower energy level to a higher energy level requires a discrete amount of energy, which corresponds to a given wavelength, or wavenumber (inverse wavelength), in the infrared region. Every molecule absorbs radiation over a distinct set of wavelengths, providing a unique spectrum with which to identify the molecule. In order for a molecule to undergo a transition in its vibrational or rotational energy level, it must exhibit a net dipole moment to allow interaction with the electric field of the infrared radiation. Since homo-nuclear diatomic molecules do not exhibit a net dipole moment with any vibrational or rotational changes, these molecules are IR inactive and show no absorption spectra in the IR region.

The absorption spectra from IR radiation can be used quantitatively to determine the concentration of a compound using the Beer-Lambert law. Radiation of a known intensity is measured before and after the radiation has come in contact with the gas sample. The Beer-Lambert law states that for a given optical path length (b), the absorbance (A) is proportional to the concentration (c) of the species in the gas sample at a fixed wavelength. This is only true if the molar absorptivity (a) does not change with concentration. At high concentrations, this relationship will no longer be true.

$$A = \log_{10}(I_0/I) = \log(1/T) = abc \qquad 3.1$$

where: T = transmittance

I_0 = incident radiation intensity

I = intensity of radiation after contacting sample

Reactions between gas species generally do not occur; therefore, the total absorbance of the gas sample is the sum of absorbance by each species present. This allows for simultaneous analysis of multiple components in the gas sample. Quantification of the gas species and their concentrations requires the availability of reference absorption spectra for each component over the concentration range of interest. Simple compounds over small concentration ranges require fewer spectra since the molar absorptivity is nearly constant, but other species such as water and CO_2 will require more reference spectra to account for the changing molar absorptivity at some wavelengths.

Using the Beer-Lambert law, an absorbance of 1.0 corresponds to a transmittance of 10%, meaning that the compound is absorbing 90% of the incident radiation at that wavelength. Two problems occur at an absorbance above 1.0. First, above 1.0 absorbance units, the compound is generally not obeying the Beer-Lambert law any more, and the molar absorptivity for that wave number is no longer a linear function of concentration. In order to account for this, reference spectra must be generated over much smaller concentration intervals.

Additionally, the Temet Gasmet™ Dx-4000 has a noise level of ~ 2% (absorbance basis), resulting in a maximum absorbance of 1.2 absorbance units. Therefore, a spectrum containing an absorbance above 1.2 units will not contain useful information. As a result, for this study, a maximum absorbance of 1.0 units was used in order to account for noise level fluctuations. For very strongly absorbing compounds like water and CO_2, the absorbance is set below 1.0.

3.4.2. Reference Spectra

Reference spectra for gas compounds were generated by blending the gas with nitrogen in known ratios using the mass flow controllers. The spectra were recorded using the FT-IR until the concentration reached steady state. These steady state spectra were then examined and the cleanest average spectrum was selected to be the reference spectrum in the software library for that particular concentration.

Compounds that are a liquid at standard conditions must be vaporized in order to obtain reference spectra. An apparatus supplied by Air Quality Analytical Inc. was used to generate reference spectra for MEA and other liquids. The apparatus consists of a syringe connected to a gear pump, a Brooks mass flow controller, a furnace, and a heated sample line run at 180^{o}C. The liquid is loaded onto the syringe, and a volumetric flowrate is set for the gear pump. The liquid is pumped into the furnace, where it is evaporated and mixed with N_2 (at a rate determined by the mass flow controller) before passing through the heated line to the FT-IR. As with the gas compounds, the cleanest steady state spectra was chosen as reference spectra.

3.4.3. Multiple Component Analysis

Each compound in an experimental gas sample absorbs infrared radiation independently of each of the other compounds, resulting in a cumulative absorption spectrum. Specifically, the FT-IR detects the transmittance of the infrared radiation from 900 to 4200 cm^{-1} and converts this to absorbance via the Beer-Lambert law. This absorbance spectrum is the sum of the absorbance spectra for each compound in the gas sample. Multiple components can be resolved from this combined spectrum by multiplying a reference spectrum by a factor (X_i) and subtracting the result from the combined absorbance spectrum. The multipliers and reference spectra are changed to minimize the residual absorbance spectrum that is left after all the components have been subtracted from the absorbance spectrum.

In order to properly resolve multiple components, different analysis areas (wavenumber regions) can be set for each component. The Calcmet™ software allows for up to 3 analysis areas to be set for each compound, each with a different absorbance maximum. If the absorbance of the sample spectrum goes above the set maximum, the software will no longer use the analysis region for that compound. The analysis regions are also determined by choosing regions where absorption peaks for multiple compounds do not overlap or interfere with one another. Table 3.3 shows the regions used for each compound in the multi-component analysis for the High Gas Flow Degradation Apparatus along with the associated absorbance limit for each measuring range and the number of references used for each component.

Table 3.3 Analysis Regions and Absorbance Limits for Compounds Studied

Compound	Concentration	Range 1			Range 2			Range 3			
		cm^{-1}		Abs. Limit	cm^{-1}		Abs. Limit	cm^{-1}		Abs. Limit	Refs.
Water	vol %	1883	2161	1.0	3142	3319	0.5				13
CO_2	vol %	980	1130	1.0	1999	2208	0.5	2450	2650	0.5	3
CO	ppm_v	2007	2207	0.5	2624	2750	1.0				8
N_2O	ppm_v	2107	2246	0.5	2647	2900	0.5				5
NO	ppm_v	1760	1868	0.8	1869	1991	0.8	2550	2650	1.0	4
NO_2	ppm_v	2550	2933	0.5							3
NH_3	ppm_v	910	964	1.0	980	1196	0.5	3219	3396	0.5	4
Formaldehyde	ppm_v	988	1111	1.0	2450	2600	0.6	2650	3211	0.5	3
Acetaldehyde	ppm_v	1034	1243	1.0	2638	2916	1.0				3
MEA	ppm_v	980	1119	1.0	2624	3150	1.0				1
Methylamine	ppm_v	980	1303	1.0	2450	2650	1.0	2800	3450	1.0	3

Since the absorbance peaks for different compounds can overlap, it is necessary to specify possible interferences from other compounds. For example, water has two major absorption peaks that stretch over almost the entire IR region. These major peaks of water will interfere with every component in the analysis, and must be specified as a possible interference for these compounds. This interference analysis was completed for all of the components and entered into the Calcmet™ software prior to sample analysis. A correlation matrix of interferences between the compounds studied in the high gas flow oxidative degradation experiments is presented in Table 3.4.

Table 3.4 Correlation Matrix for Interfering Compounds for FT-IR Analysis

	Water	CO_2	CO	N_2O	NO	NO_2	NH_3	Formaldehyde	Acetaldehyde	MEA	Methylamine
Water	-	X	X	X	X		X			X	
CO_2	X	-	X	X		X	X		X	X	X
CO	X	X	-	X	X	X		X	X	X	X
N_2O	X	X	X	-	X	X		X	X	X	X
NO	X	X	X	X	-		X		X	X	
NO_2	X	X		X		-		X	X	X	X
NH_3	X	X		X		X	-	X	X	X	X
Formaldehyde	X	X		X		X	X	-	X	X	X
Acetaldehyde	X	X		X		X	X	X	-	X	X
MEA	X	X		X		X	X	X	X	-	X
Methylamine	X	X		X		X	X	X	X	X	-

3.5. HPLC Analysis with Electrochemical Detection

Total glycine concentration was determined using electrochemical detection (ED) with a fixed gold electrode calibrated with a pH/Ag/AgCl reference. The analytical method uses a pair of AminoPac PA10 columns in series. The mobile phase consists of a mixture of water, sodium hydroxide and sodium acetate at 1.0 mL/min and 30^{o}C, starting with 50 mM sodium hydroxide from 0 to 12 minutes and increasing linearly to 80 mM NaOH at 16 minutes. From time 16 to 24 minutes, NaOH concentration decreases to 60 mM while sodium acetate concentration increases to 400 mM, where the concentrations remain until t = 40 minutes.

The ED system is interfaced through Chromeleon Software Version 6.80 on the Dionex ICS-3000 and performs parallel liquid-phase analysis independent of the anion IC system; in fact, it is actually interchangeable with the ELS-2100 system. In order to switch over from ELSD to ED (and vice versa) all the lines must be flushed, the proper column must be placed in the detection oven and the outlet to the column must be routed to the proper detector. Calibration standards and sample dilutions are prepared in the exact manner as for anion analysis.

Operation of the electrochemical detection system is also very similar to the anion system; there are only three major differences – the same differences that existed for the ELSD system. All batches run using the electrochemical detector are found in the folder named “ICS3000_ELD Analysis”. The “Amino_1” program is used for calibration and degraded samples – with the exception of the final sample. Similar to the anion

sequences, use the "Shutdown" program for the final sample. Under the method category, choose "Glycine" for all samples. The only peak of interest when using electrochemical detection is glycine (retention time = 5.23 minutes).

3.6. Total Carbon and Nitrogen Analysis

Total nitrogen content in selected degraded amine solution was determined using EPA Method 351.4 (1978). Total Kjeldahl nitrogen is determined potentiometrically using an ion selective electrode; this method is favored because interference from metals (which are present in the form of catalyst) is eliminated with the addition of NaI.

Total organic carbon from selected samples of interest is measured using a Shimadzu 5050A TOC Analyzer. The Shimadzu TOC can be used to measure both inorganic (TIC) and total carbon (TC); TOC is calculated from the difference between the two measurements. For the TIC carbon measurement, 25 wt % phosphoric acid is used to evolve the CO_2 gas from the solvent. The stream of CO_2 is analyzed with an NDIR detector. For total organic carbon analysis, a precisely metered slipstream of the sample is combusted over platinum catalyst at 680°C with ultra pure air. The resulting CO_2 is measured with the NDIR detector. The Shimadzu has a detection limit of four ppb and a range up to 4000 ppm for TOC and 5000 ppm for IC. A 1000 ppm IC standard was prepared from a mixture of Na_2CO_3, $NaHCO_3$ and deionized (DI) water. Refer to Appendix of the Chen dissertation (2007) at The University of Texas for an exact operating procedure regarding the Shimadzu TOC analyzer.

3.7. Solution Loading

All of the solutions in this study were prepared gravimetrically. Amine solutions were loaded with CO_2 by sparging pure CO_2 through the solutions inside 1000 mL LG-3675 gas washing bottles purchased from Wilmad Glass Laboratories. Each unit consists of a 1000 mL bottle and a 40/35 stopper with an inlet tube sealed through the center of a

fritted glass disc. The disc is approximately 1/2" above the bottom of the bottle. Pure CO_2 provided by Matheson Tri-Gas travels through the inlet tube and the fritted disc, which disperses the gas into tiny bubbles into the amine solution, providing more efficient solution loading.

The CO_2 gas flowrate is kept low in order to prevent it from heating the solution excessively (the reaction of amine with CO_2 is exothermic). CO_2 loadings are quantified by placing the gas washing bottle on a scale while loading the CO_2 and recording the mass difference. CO_2 loadings were also verified by TIC (total inorganic carbon) analysis using a Model 525 Analyzer from Oceanography International Corporation. Solutions were run with a loading corresponding to 2 volume% of CO_2 partial pressure in the vapor space above the solution at 55^{o}C. For example, in 7 m MEA solutions, this corresponds to a loading of α = 0.4 mol CO_2 / mol MEA.

3.8. Low Gas Apparatus Description

Experiments performed in the low gas flow degradation apparatus achieve appreciable mass transfer by introducing gas into the vapor space above an agitated amine solution in a temperature-controlled semi-batch reactor. The agitation vortexes the reaction gas into the solution and transfers the oxygen needed to degrade the amine into solution. Figure 3.1 depicts the setup of the low gas flow apparatus. Reaction gas, consisting of a mixture of CO_2 and O_2, is bubbled through water to pre-saturate the gas before being introduced into the vapor space above the amine solution in order to minimize water losses in the reactor.

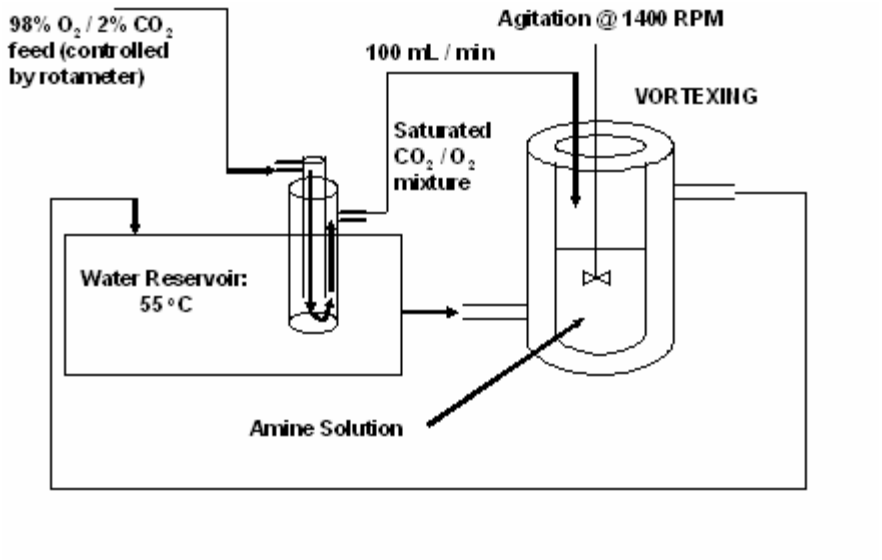

Figure 3.1 Low Gas Flow Degradation Apparatus

An Ace Glass 5196 Vacuum Adapter (250 mm, with 24/40 size joints) serves as the pre-saturator for both low gas flow degradation apparatuses. Reaction gas enters a glass connection on the adapter and flows down a ¼" tube immersed in the water. The saturated gas bubbles through the water and out a glass connection on the body of the vacuum adapter. Figure 3.1 depicts the flow path through the pre-saturator. Distilled, deionized water from the Millipore unit is used to refill the pre-saturators.

Gas flowrates are controlled differently in the two low gas flow apparatuses. In Low Gas Flow Apparatus #1, gas flow rate is controlled by a ColeParmer model EN-03217-06 Correlated Flowmeter with Valves (Aluminum/SS Flowmeter, 131 mL/min O_2). The flowmeter is a rotameter with a spherical stainless steel float that illustrates how far the valve on the flowmeter is open. The flowmeter is set by measuring the volume displacement of soap bubbles in a graduated burette as a function of time. A displacement of 10 mL over 6 seconds correlates to a gas flowrate of 100 mL/min. The reaction gas in apparatus #1 is a pre-mixed cylinder of 2% CO_2, balance O_2 (168 ft^3, 1600 psig, CGA outlet 296), provided by Matheson Tri-Gas.

Gas flowrates in Low Gas Flow Apparatus #2 are regulated using Brooks mass flow controllers (model 5850E) connected to a Brooks Instrument Co. 4-channel Brose

control box (Model 5878A1B1, Serial No. 8507H27518/2) with 15-pin D connectors. The control box displays a digital readout corresponding to the % open of the mass flow controller. O_2 is controlled by a 100 SCCPM flow controller (Brooks model 5850E, Serial No. 9103HCO37044/4) and CO_2 is controlled with a 20 SCCPM flow controller (Brooks model 5850E, Serial No. 9103HCO37044/2). Flow controllers are calibrated every 12 months. Calibrations are performed by connecting the flow controllers to the appropriate gas source, changing the setting on the control box, and measuring the volume displacement of soap bubbles in a graduated burette as a function of time. The volumetric flowrate of gas is then converted to a molar flowrate based on the Ideal Gas Law. Figure 3.2 shows a typical calibration curve for the 100 SCCPM mass flow controller and O_2.

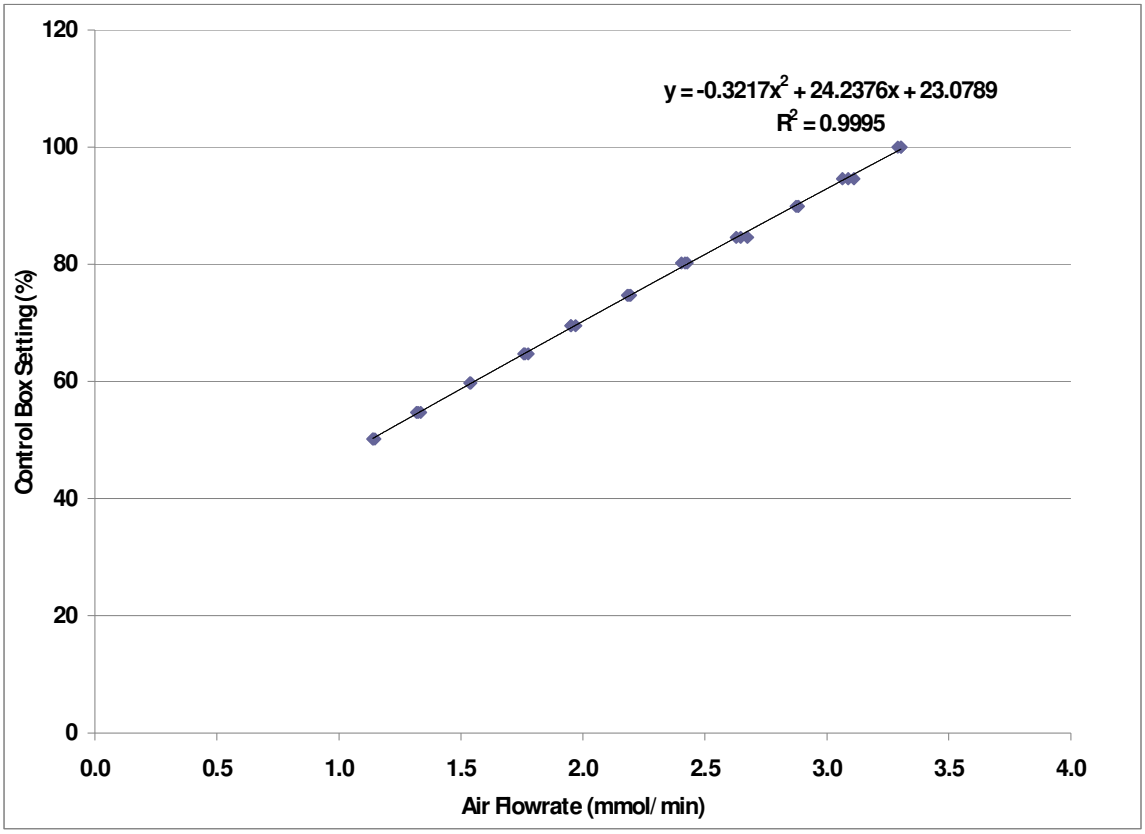

Figure 3.2 Calibration Curve for the 100 SCCPM Brooks Mass Flow Controller and O_2

Compressed O_2 (Zero Grade, 337 ft^3, 2640 psig @ 70°F, CGA Outlet 540) and CO_2 (60 lbs, 830 psig @ 70°F, CGA Outlet 320) are both provided by Matheson Tri-Gas Inc. For both low gas flow apparatus, the reaction gas mixture travels through ¼" OD Parker Perflex PE tubing (120 psig max, 150°F max).

Once the saturated gas exits the pre-saturator, it moves through the PE tubing into the vapor space above the reactor. Each low gas flow reactor is an Ace Glass 600 mL jacketed reactor (7.5 cm ID, 11 cm OD, 14 cm height). Each reactor is sealed with a size 14 rubber stopper. In each rubber stopper, three ¼" holes have been cut. Inserted into one of the holes is a Fisherbrand thermometer that measures the temperature of the solution in each reactor. The thermometer is coated with vacuum grease and placed inside of a rubber septum, which is placed into the hole. Inside the second hole is the Parker Perflex PE tubing carrying the reaction gas. The tubing is coated with vacuum grease and threaded through a rubber septum, which is inserted into the hole. The tubing should extend 1" from the top of the rubber stopper into the vapor space above the amine solution.

The third hole in each septum is necessary for the agitator shafts. In Low Gas Flow Degradation Apparatus #1, the shaft is powered by a StedFast™ Stirrer (model SL1200) by Fisher Scientific International, capable of agitation speeds up to 1450 RPM. The stainless steel agitator is 30 cm long and 0.5 cm in diameter; four curved impeller blades, each measuring 1.5 cm in length and 1cm in width, are located at the bottom of the agitator shaft. The agitator shaft is coated with vacuum grease and threaded through a rubber septum, which is inserted into the third hole. The impeller blades should sit 1" from the bottom of the reactor. The rubber tops are not meant to completely seal the reactors; they are merely covers to prevent any liquid entrainment or vortexing that may extend above the top of the reactor. The apparatus is actually open to atmosphere and venting at all times.

In Low Gas Flow Degradation Apparatus #2, the shaft is powered by a Maxima™ Stirrer by Fisher Scientific International, capable of agitation speeds up to 2000 RPM. The stainless steel agitator is 35 cm long and 0.8 cm in diameter; four curved impeller

blades, each measuring 2.2 cm in length and 0.8 cm in width, are located at the bottom of the agitator shaft. The agitator shaft is coated with vacuum grease and threaded through a rubber septum, which is inserted into the third hole. The impeller blades should sit 1" from the bottom of the reactor.

The reactor temperatures are kept constant at 55^{o}C using Ecoline Lauda Heating Circulators with E-100 series controllers and 003 series stainless steel baths. The heat transfer fluid is boiler feedwater from the faucet in the laboratory. The water is circulated from the stainless steel bath to the glass reactor via 3/8" ID (with 1/16" wall thickness) Fisherbrand Tygon® tubing. Covers are kept on the stainless steel baths in order to minimize evaporative losses from the heated reservoirs.

3.9. High Gas Apparatus Description

Experiments are performed in the high gas flow degradation apparatus by sparging gas through an agitated amine solution in a temperature controlled semi-batch reactor. Figure 3.3 shows an illustration of the high gas flow apparatus. Reaction gas, consisting of a mixture of house air, nitrogen, and CO_2 is bubbled through water to presaturate the gas before it is sparged through the amine solution in order to minimize water losses in the reactor.

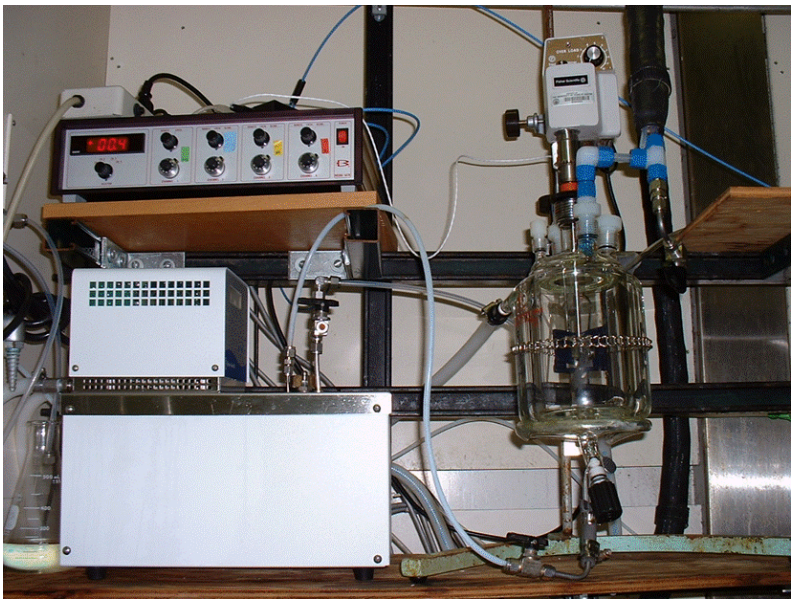

Figure 3.3 High Gas Flow Degradation Apparatus

A Parr 1108 Oxygen Combustion Bomb served as the water presaturator. A 1/8" stainless steel tube on the inside of the presaturator carries the gas mixture into the water reservoir ¼" above the bottom of the presaturator bomb. The gas bubbles through the heated water and out the presaturator bomb. The bomb and its contents are kept at 55°C in a water bath heated by a Lauda Econoline E-100 Series Heating Circulator.

Water level in the presaturator is controlled using a series of Masterflex peristaltic pumps. The inlet pump is a ColeParmer Masterflex Model 7520-50 (range 1-100 RPM). Affixed to the pump is a Masterflex Model 7013-20 pump head. Distilled, deionized water from the Millipore Direct-Q 3 system is contained in an atmospheric reservoir located on top of the inlet pump. The water is pumped into the presaturator through Masterflex 6409-13 Tygon tubing (0.03" ID) at a flowrate of 1 mL/min. This exceeds the rate at which water evaporates from the presaturator.

A ColeParmer Masterflex Model 7521-40 (range 6-600 RPM) with an Easy-Load II variable speed drive (Model 77200-50) serves as the outlet pump motor. Affixed to the pump is a Masterflex Model 7016-20 pump head threaded with Masterflex Model 6409-16 Tygon tubing (0.123" ID). The outlet pump is set at a flowrate of 2 mL/min; the

outlet flowrate is set at twice the inlet flowrate to ensure that the presaturator does not flood and send water directly to the reactor.

A ¼" stainless steel tube extends 1" down from the top of the presaturator into the reservoir. If the water level in the presaturator is below the bottom of the tube, the outlet pump will only pull the reaction gas mixture at 2 mL/min out of the bomb. Once the water level reaches the bottom of the tube, the outlet pump will begin to pull water out of the reservoir and keep the level in the presaturator bomb constant. Refer to Figures 3.4 and 3.5 for diagrams depicting the connections and flow paths on the presaturator.

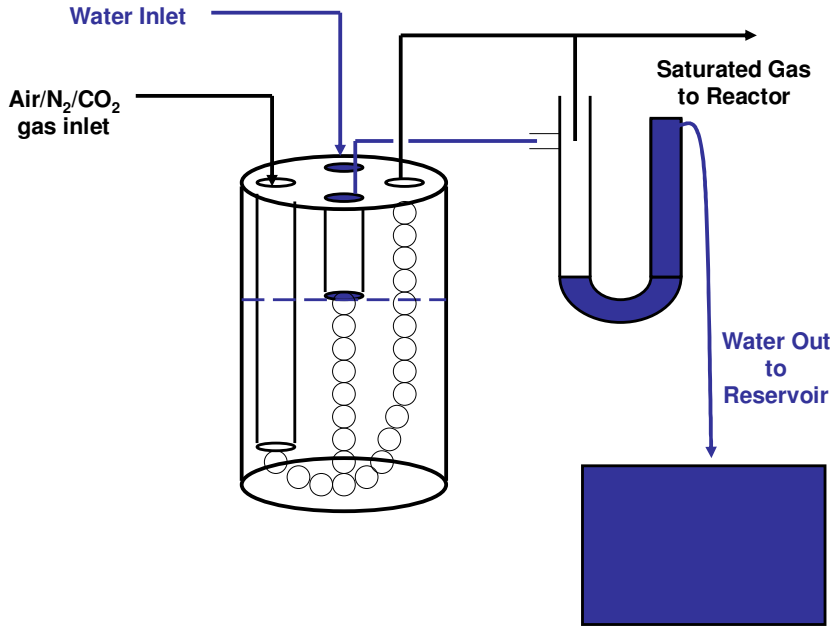

Figure 3.4 Presaturator for High Gas Flow Degradation Apparatus

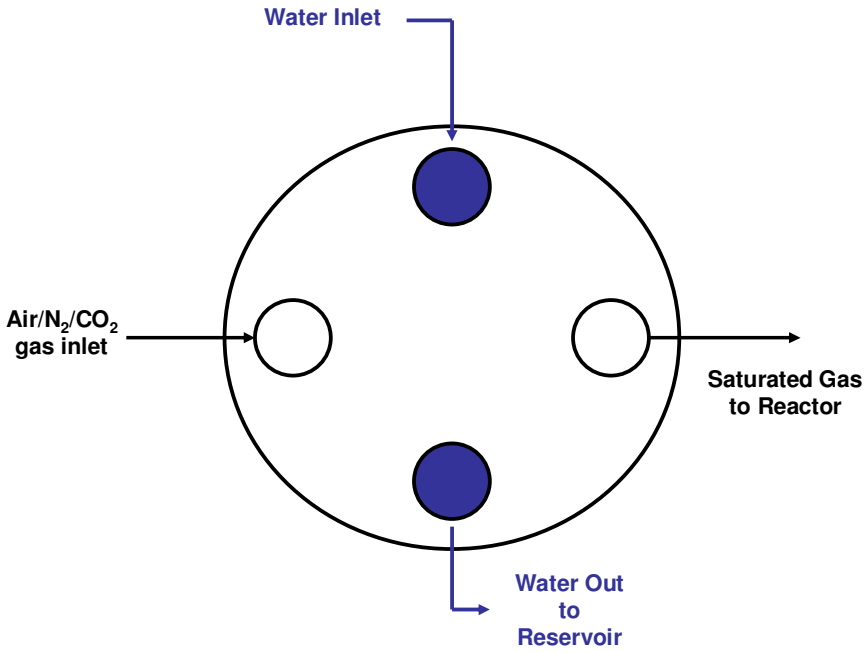

Figure 3.5 Top View of Presaturator for High Gas Flow Degradation Apparatus

The outlet pump carries the gas/water mixture into a 500 cc flash tank (16 cm OD, 30.5 cm height). Any entrained water drops to the bottom of the tank through a U-tube (1/4" ID) and a gate valve cracked open. Static pressure from the water level slowly forces the water through the U-tube and out the valve, where the water falls back into the DDI reservoir. Reaction gas exits the top of the tank and flows through ¼" PE tubing (max 150^{o}F, 120 psig) to a Swagelok tee, where it recombines with saturated gas exiting the presaturator on its way to the reactor.

Gas flowrates were regulated using Brooks mass flow controllers (model 5850E) connected to a Brooks Instrument Co. 4-channel Brose control box (Model 5878A1B1, Serial No. 8507H27518/4). The control box displays a digital readout corresponding to the % open of the mass flow controller. Air and nitrogen flowrates are controlled by a 15 SLPM flow controller (Brooks model 5850E) and CO_2 is controlled with 1.0 SLPM flow controller (Brooks model 5850E). Flow controllers are calibrated every 12 months. Calibrations are performed by connecting the flow controllers to the appropriate gas source, changing the setting on the control box, and measuring the volume displacement

of soap bubbles in a graduated burette as a function of time. The volumetric flowrate of gas is then converted to a molar flowrate based on the Ideal Gas Law. Figure 3.6 shows a typical calibration curve for the 15 SLPM mass flow controller and air.

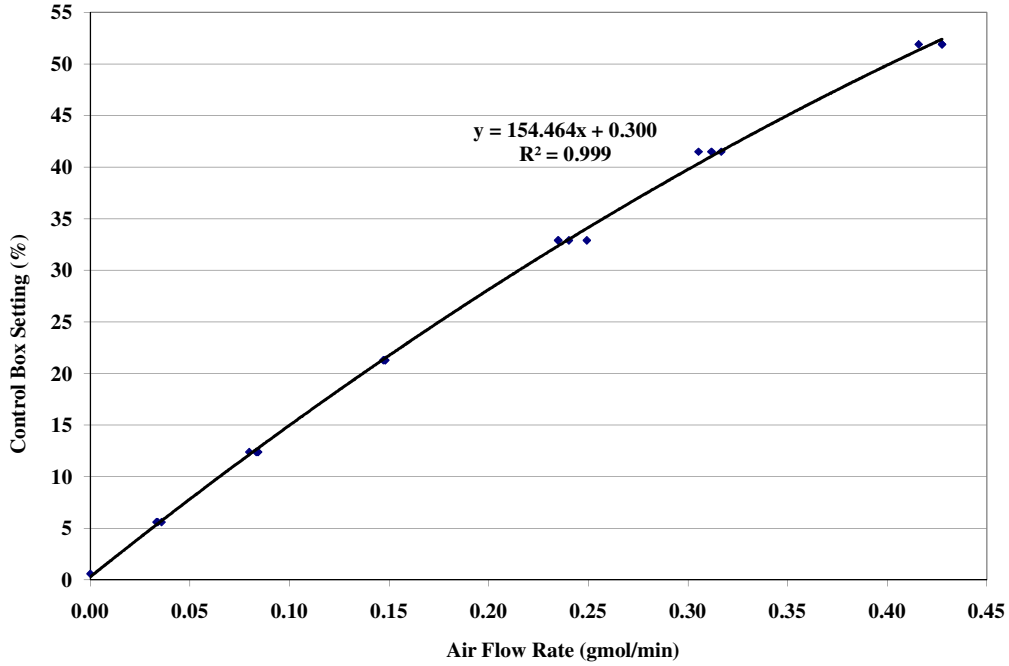

Figure 3.6 Calibration Curve for the 15 SLPM Brooks Mass Flow Controller and Air

Temperature is continuously monitored throughout each high gas flow experiment, and the temperature of the heat baths were adjusted to keep the reactor at a constant temperature of 55^{o}C. Temperature in the jacketed reactor is kept constant using an IsoTemp 3016H temperature bath manufactured by Fisher Scientific International. The heat transfer fluid is dimethyl silicone oil (50 cSt viscosity) purchased from Krayden, Inc. Temperature was controlled within ± 1^{o}C by monitoring the temperature with a PT-100 immersion probe (Class B, 4x150 mm) connected to PicoLog Recorder software (Version 5.13.9) through a PT-104 converter. For this system, in order to maintain a reactor temperature of 55^{o}C, the temperature bath and presaturator bath are set at a temperature of approximately 63^{o}C (depending on ambient conditions).

Figure 3.3 shows the entire high gas flow apparatus and associated equipment. The jacketed reactor, purchased from Ace Glass Inc., was a 1-L reactor with a 5 neck (threaded, 1 large, 3 medium, 1 small) top and an 8-mm bottom drain tube, which served as the gas inlet to the reactor. The reactor is rated for a pressure of 45 psig at 100^{o}C and has an inside diameter of 10 cm and a depth of 15 cm. The reactor jacket is equipped with 2 threaded "Ace-Safe" taps for easy connection to tubing. All o-rings and rubber seals are made of CHEMRAZ® perfluorelastomer polymers in order to ensure chemical compatibility.

The center neck of the reactor was equipped with a Maxima™ Stirrer manufactured by Fisher Scientific International, capable of agitation speeds of up to 2000 RPM. The agitator uses a stainless steel stir shaft with a single flat-blade paddle. The impeller blade rotates parallel to the axis of the drive shaft, and is 5 cm wide and 13 mm high. The reactor is sealed by inserting the stir shaft through a #15 Ace Glass threaded adapter. Both ends of the adapter are sealed using Teflon® connectors fitted with CHEMRAZ® o-rings.

One of the three medium necks is used for inserting the thermocouple into the reactor, and a second one is used as the gas outlet. The remaining two openings (sealed while the experiment is in progress) are used for periodic additions to the reactor throughout the course of the experiment (if necessary). Plugs and connectors are made of either nylon or Teflon®, and both have proven to be compatible with MEA. The plug for the gas outlet is packed with air filter media (NaturalAire Cut-to-fit) to serve as a mist eliminator and eliminate liquid entrainment into the heated sample line.

Chapter 4: Raw Experimental Data

This chapter provides a matrix for all long-term oxidative degradation experiments performed in both the low gas and high gas degradation apparatus. All of the raw data for formation of degradation products and disappearance of amines during these experiments is also tabulated.

4.1. Summary of Results

Table 4.1 provides an experimental matrix for all long-term oxidation experiments performed on both the high gas flow and low gas flow degradation apparatus. Short-term degradation experiments performed using the high gas flow apparatus are tabulated in Appendix E. For each experiment, the following information is listed: the month and year in which the experiment was conducted, the concentration of

the solvent subjected to degradation, the apparatus in which the experiment was conducted and catalyst and/or inhibitor concentration added to solution.

The standard experimental condition at low gas is 100 mL/min of a saturated 98%O_2/2%CO_2 gas mixture being vortexed into 350 mL amine solution by agitation at 1400 RPM. A water bath circulating through the jacket of the reactor keeps the solution temperature at 55^oC. The standard high gas flow experimental condition consists of 7.5 L/min of a saturated 15%O_2/2%CO_2 gas mixture sparged through 350 mL of amine solution, which is also agitated at 1400 RPM. A silicone oil bath circulated through the jacket of the reactor keeps amine solution temperature at 55^oC in the high gas apparatus.

Derived results included in the table are total carbon product formation rate, total nitrogen product formation rate and solvent loss rate. Total carbon and nitrogen was calculated from concentrations of degradation products as determined by anion IC, HPLC-ELSD and FTIR (for high gas experiments only). Total carbon formation is reported as C_1, while it is quantified as C_2 in solvent losses. For example, for the experiment performed on 7/08 using MEA/Fe/Cu, 70% of the nitrogen and 96% of the carbon from solvent losses is accounted for in known degradation products.

Amine losses were determined using cation chromatography, using sulfate as an internal standard to account for any change in water concentration. MEA concentration was calculated by taking the difference between initial and final experimental samples. Experimental error for cation analysis is ± 5%, so the expected error for MEA losses is ± 0.3 mM/hr. That rate was normalized by total experimental time in order to compare MEA losses to product formation rates.

With the exception of vanadium, catalyst is added to each amine solution as inorganic, hydrated sulfate salt (vanadium is added as sodium metavanadate). Sulfate is not consumed in any of the degradation reactions, so it is assumed that sulfate is conserved. Sulfate concentration is quantified and used as an internal standard using the anion chromatography analytical method. Sulfate appears on the anion chromatogram directly before oxalate.

For the high gas experiments, overall MEA loss was calculated using cation chromatography and volatile MEA loss was calculated using FTIR analysis. The difference between these two rates gave an MEA degradation loss rate. Carbon and nitrogen formation rates were calculated for each of the degradation experiments by adding up the total number of carbons and nitrogens contained in each liquid and gas phase product.

Table 4.1 Summary of Results

Date	Solvent (m)	Catalyst (mM)	Inhibitor (mM)	Apparatus	Total Carbon (mM/hr)	Total Nitrogen (mM/hr)	Solvent Loss (mM/hr)
07/08	4 DGA	1 Fe		Low Gas	0.0	0.0	
07/08	4 DEA	1 Fe		Low Gas	0.8	0.1	2.1
07/08	7 MEA	0.1 Fe/5 Cu		Low Gas	20.0	7.1	10.3
07/08	7 Ethylene Glycol / 1 $KHCO_3$	1 Fe		Low Gas	0.0	0.0	
07/08	4 AMP	5 Cu		Low Gas	0.0	0.0	
06/08	7 MEA	0.1 Fe/5 Cu	(700 RPM)	Low Gas	9.6	0.3	17.0
06/08	7 MEA	1 Fe	7.5 B	Low Gas	0.2	0.1	1.2
06/08	7 MEA	1 Fe	(6% CO_2)	Low Gas	2.7	0.4	6.4
05/08	7 MEA	0.6 Cr/0.1 Ni	100 A	Low Gas	0.0	0.0	1.0
05/08	7 MEA	1 Fe	2 EDTA	Low Gas	3.8	1.4	8.6
05/08	7 MEA	1 V		Low Gas	1.6	0.6	2.1
05/08	7 MEA	1 Fe	100 Na_2SO_3	Low Gas	5.4	2.0	5.1
05/08	7 MEA	0.1 Fe/5 Cu		High Gas	5.0	4.0	5.3
04/08	7 MEA	1 Fe	10 EDTA	Low Gas	0.7	0.2	1.5
04/08	7 MEA	5 Cu	500 Formaldehyde	Low Gas	14.6	5.3	8.0
04/08	7 MEA	0.6 Cr/0.1 Ni		Low Gas	5.3	2.1	8.0
04/08	7 MEA	1 Fe		High Gas	1.1	2.0	3.8
04/08	2 Potassium Glycinate	1 Fe		Low Gas	0.0	0.0	
03/08	2 Potassium Glycinate	5 Cu		Low Gas	0.1	0.0	
03/08	3.5 EDA	1 Fe		Low Gas	0.4	0.2	
02/08	3.5 EDA	5 Cu		Low Gas	0.6	0.2	
01/08	7 MEA	1 Fe	100 EDTA	Low Gas	0.0	0.0	0.1
12/07	7 MEA	0.1 Fe/5 Cu		High Gas	4.8	3.5	3.5
12/07	7 MEA	1 Fe	500 Formate	Low Gas	4.5	2.0	4.5

Table 4.1 Summary of Results (Continued)

Date	Solvent (m)	Catalyst (mM)	Inhibitor (mM)	Apparatus	Total Carbon (mM/hr)	Total Nitrogen (mM/hr)	Solvent Loss (mM/hr)
11/07	7 MEA	1 Fe	500 Formaldehyde	Low Gas	5.8	2.3	5.1
09/07	7 MEA	1 Fe		Low Gas	6.3	2.5	3.8
09/07	5 PZ	5 Fe		Low Gas	0.1	0.0	
08/07	7 MEA/2 PZ	0.1 Fe		Low Gas	8.3	3.0	
08/07	5 PZ	0.1 Fe	100 A	Low Gas	0.1	0.1	
08/07	5 PZ	0.1 Fe		Low Gas	0.1	0.0	
07/07	7 MEA	1 Fe		High Gas	1.5	2.0	8.0
07/07	7 MEA/2 PZ	0.1 Fe	100 A	Low Gas	0.9	0.3	
07/07	7 MEA/2 PZ	0.1 Fe/5 Cu	100 A	Low Gas	2.1	0.8	
06/07	7 MEA	0.1 Fe/5 Cu		Low Gas	28.4	9.8	
05/07	5 PZ	0.1 Fe/5 Cu	100 A	Low Gas	0.1	0.1	
04/07	5 PZ	0.1 Fe/5 Cu		Low Gas	0.8	0.5	
04/07	4 AMP	1 Fe		Low Gas	0.0	0.0	
12/06	2.5 PZ	5 V	100 A	Low Gas	0.3	0.3	
12/06	2.5 PZ / 5 $KHCO_3$	5 V		Low Gas	0.0	0.0	
10/06	7 MEA/2 PZ	0.1 Fe/5 Cu		Low Gas	35.5	12.5	
09/06	9 MEA	0.1 Fe		Low Gas	0.5	0.5	
04/06	2.5 PZ / 5 $KHCO_3$	5 V		Low Gas	0.0	0.1	
03/06	7 MEA	0.6 Fe		Low Gas	0.5	0.5	
01/06	7 MEA	0.6 Fe/0.6 Cu	100 A	Low Gas	0.1	0.0	
11/05	2.5 PZ	5 V		Low Gas	0.4	0.4	
09/05	7 MEA	0.6 Fe/0.6 Cu		Low Gas	0.9	0.3	
12/04	7 MEA	0.6 Cu		Low Gas	0.5	0.2	

4.2 Long-Term Oxidation Experiments Raw Data

Tables 4.3 through 4.49 lists all of the raw experimental data compiled from liquid-phase analysis for all long-term oxidation experiments. Additionally, an overall concentration for volatile products was determined by constructing a continuous plot of concentration (in ppm_v) versus experiment time and approximating the area under the

curve. This value was then converted into a production rate (using total experiment time, molar gas rate and solution volume) in units of mM/hr. This rate was multiplied by the total experiment time to give a total accumulation in mM. MEA volatility was calculated and quantified in the same manner.

All carboxylic acids (formate, oxalate, acetate and glycolate) and their respective general amide (formamide, oxamide, acetamide and glycolamide) concentrations were calculated using anion chromatography. Amide concentrations were calculated by taking the difference in organic acid concentration in the degraded samples before and after treatment with concentrated sodium hydroxide. Sulfate, used as an internal standard to account for water concentration, was also determined using anion chromatography.

The concentration profile of each amine/solvent through the course of each experiment was calculated using cation chromatography. Hydroxyethyl-formamide and hydroxyethylimidazole concentrations were calculated using HPLC with evaporative light scattering detection. All other HPLC peaks that have not been positively identified were reported by retention time and raw peak area. In later chapters, these unknown peaks are assumed as HEI using the following equations:

$$\text{Concentration (mM)} = 6.49 * (\text{Raw Area})^{0.519} \quad 4.1$$

$$\text{Concentration (mM)} = 64.9 * (\text{Dilute Area})^{0.519} \quad 4.2$$

Table 4.2 Explanation of Methods Used for Product Concentrations

Experiment	Sample High Gas Experiment			
Experiment Time (Hours)	0	X	X	Final
Formate (mM)	Anion IC			
Formamide (mM)	NaOH Hydrolysis/Anion IC			
Oxalate (mM)	Anion IC			
Oxamide (mM)	NaOH Hydrolysis/Anion IC			
Acetate (mM)	Anion IC			
Acetamide (mM)	NaOH Hydrolysis/Anion IC			
Glycolate (mM)	Anion IC			
Glycolamide (mM)	NaOH Hydrolysis/Anion IC			
Nitrate (mM)	Anion IC			
Nitrite (mM)	Anion IC			
Sulfate (mM)	Anion IC			
MEA (m)	Cation IC			
Hydroxyethyl-formamide (mM)	HPLC-ELSD			
Hydroxyethylimidazole (mM)	HPLC-ELSD			
Unknown #1, RT=3.2 min (raw area)	HPLC-ELSD			
CO (mM)	FTIR			
CH_4 (mM)	FTIR			
N_2O (mM)	FTIR			
NO (mM)	FTIR			
NO_2 (mM)	FTIR			
NH_3 (mM)	FTIR			
C_2H_4 (mM)	FTIR			
Formaldehyde (mM)	FTIR			
Acetaldehyde (mM)	FTIR			
MEA Volatility (mM)	FTIR			
Methanol (mM)	FTIR			
Methylamine (mM)	FTIR			

Table 4.3 Raw Data – DGA/Fe Low Gas Experiment, 7/08

Experiment	4m DGA / 1mM Fe					
Experiment Time (Hours)	0	120	172	215	285	336
Formate (mM)	1.27	1.47	1.50	1.79	2.27	3.64
Formamide (mM)	0.00	1.46	2.59	4.30	5.01	6.02
Oxalate (mM)	0.00	0.01	0.01	0.02	0.03	0.03
Oxamide (mM)	0.02	0.13	0.25	0.38	0.52	0.65
Acetate (mM)	0.15	0.04	0.04	0.16	0.06	0.06
Acetamide (mM)	0.10	0.26	0.32	0.19	0.34	0.39
Glycolate (mM)	0.00	0.00	0.00	0.00	0.00	0.00
Glycolamide (mM)	0.00	0.00	0.00	0.00	0.00	0.00
Nitrate (mM)	0.00	0.27	0.28	0.42	0.49	0.75
Nitrite (mM)	0.00	0.18	0.28	0.39	0.57	0.90
Sulfate (mM)	2.17	2.12	1.98	1.92	1.86	1.89
DGA (m)	4.0	4.0	4.3	4.0	4.1	4.2
Unknown #1, RT=4.7 min (raw area)						10.63
Unknown #2, RT=5.5 min (raw area)						1.84
Unknown #3, RT=14.1 min (raw area)						3.93

Table 4.4 Raw Data – DEA/Fe Low Gas Experiment, 7/08

Experiment	4m DEA / 1mM Fe					
Experiment Time (Hours)	0	43	113	174	220	292
Formate (mM)	0.66	14.50	27.18	32.34	35.62	48.56
Formamide (mM)	0.58	58.62	93.32	110.90	117.03	139.99
Oxalate (mM)	0.01	0.36	1.26	1.80	2.34	3.96
Oxamide (mM)	0.02	4.46	9.63	11.11	12.32	14.02
Acetate (mM)	0.02	0.70	1.00	1.21	1.23	1.57
Acetamide (mM)	0.02	0.82	1.79	1.27	2.48	2.56
Glycolate (mM)	0.00	0.00	0.12	0.20	0.26	0.36
Glycolamide (mM)	1.64	97.92	56.21	28.30	17.05	3.71
Nitrate (mM)	0.00	2.83	3.93	4.72	4.26	5.53
Nitrite (mM)	0.00	8.84	13.10	12.95	11.87	12.19
Sulfate (mM)	2.01	1.88	1.90	1.65	1.71	1.40
DEA (m)	4.0	3.0	2.9	2.5	2.6	2.8
Unknown #1, RT=2.4 min (raw area)						75.07
Unknown #2, RT=3.2 min (raw area)						32.04
Unknown #3, RT=13.2 min (raw area)						13.71

Table 4.5 Raw Data – MEA/Fe/Cu Low Gas Experiment, 7/08

Experiment	7m MEA/1mM Fe/5mM Cu					
Experiment Time (Hours)	0	43	113	174	220	292
Formate (mM)	0.52	29.79	81.59	120.25	146.36	213.22
Formamide (mM)	0.44	358.42	530.83	580.41	593.48	684.77
Oxalate (mM)	0.00	1.10	4.44	7.32	9.28	12.57
Oxamide (mM)	0.00	45.94		119.73		121.70
Acetate (mM)	0.00	0.84	0.94	0.90	0.77	0.77
Acetamide (mM)	0.00	0.36	0.47	0.45	2.14	1.10
Glycolate (mM)	0.00	0.05	0.24	0.47	0.57	0.99
Glycolamide (mM)	13.68	15.14	16.75	11.87	19.94	12.14
Nitrate (mM)	0.00	0.00	17.97	21.97	20.11	27.65
Nitrite (mM)	0.16	38.91	65.64	78.30	76.72	96.30
Sulfate (mM)	8.21	7.95	7.67	8.15	8.80	7.61
MEA (m)	7.0	4.7	2.8	2.1	1.9	2.8
Hydroxyethyl-formamide (mM)						949
Hydroxyethylimidazole (mM)						497
Unknown #1, RT=2.4 min (raw area)						5.73
Unknown #2, RT=3.2 min (raw area)						3.18
Unknown #3, RT=4.6 min (raw area)						3.43
Unknown #4, RT=13.2 min (raw area)						5.91

Table 4.6 Raw Data – Ethylene Glycol/Fe Low Gas Experiment, 7/08

Experiment	7m Ethylene Glycol/1m $KHCO_3$/1mM Fe					
Experiment Time (Hours)	0	24	122	170	290	313
Formate (mM)	0.02	0.24	0.46	0.53	0.76	1.08
Formamide (mM)	2.37	1.03	0.74	0.64	0.56	0.35
Oxalate (mM)	0.00	0.01	0.04	0.06	0.08	0.10
Oxamide (mM)	0.00	0.03	0.04	0.05	0.05	0.06
Acetate (mM)	0.00	0.02	0.02	0.03	0.05	0.05
Acetamide (mM)	0.22	0.05	0.06	0.06	0.07	0.08
Glycolate (mM)	0.00	0.06	0.08	0.07	0.08	0.08
Glycolamide (mM)	0.17	0.11	0.08	0.10	0.10	0.13
Nitrate (mM)	0.00	0.00	0.00	0.00	0.00	0.00
Nitrite (mM)	0.00	0.00	0.00	0.00	0.05	0.02
Sulfate (mM)	1.72	1.83	1.73	1.74	1.72	1.91
Ethylene Glycol (m)	7.0	7.0	7.7	7.3	8.2	7.9

Table 4.7 Raw Data – AMP/Cu Low Gas Experiment, 7/08

Experiment	4m AMP/5mM Cu					
Experiment Time (Hours)	0	24	96	144	264	287
Formate (mM)	0.71	0.83	1.73	1.94	2.59	3.15
Formamide (mM)	1.26	1.07	1.33	1.68	1.40	0.56
Oxalate (mM)	0.00	0.02	0.11	0.16	0.29	0.31
Oxamide (mM)	0.00	0.03	0.11	0.14	0.24	0.15
Acetate (mM)	0.00	0.04	0.08	0.07	0.07	0.10
Acetamide (mM)	0.07	0.04	0.06	0.08	0.11	0.02
Glycolate (mM)	0.00	0.00	0.00	0.00	0.00	0.00
Glycolamide (mM)	0.00	0.00	0.00	0.00	0.00	0.00
Nitrate (mM)	0.00	0.21	0.33	0.33	0.38	0.31
Nitrite (mM)	0.00	0.10	0.15	0.16	0.21	0.17
Sulfate (mM)	7.81	7.90	7.82	8.27	8.09	7.75
AMP (m)	4.0	4.0	4.0	3.8	3.9	3.9
Unknown #1, RT=5.1 min (raw area)						16.95

Table 4.8 Raw Data – MEA/Fe/Cu/700 RPM Low Gas Experiment, 6/08

Experiment	7m MEA/1mM Fe/5mM Cu/700 RPM				
Experiment Time (Hours)	0	46	118	164	214
Formate (mM)	1.47	25.08	62.47	88.98	94.14
Formamide (mM)	0.02	0.95	5.10	8.67	11.34
Oxalate (mM)	1.38	247.38	483.77	559.87	606.39
Oxamide (mM)	0.02	50.38	147.26	264.79	336.66
Acetate (mM)	0.08	0.71	0.78	0.90	0.66
Acetamide (mM)	0.20	0.15	0.36	0.81	0.36
Glycolate (mM)	0.02	0.14	0.49	0.79	2.08
Glycolamide (mM)	4.14	15.76	29.51	35.22	25.46
Nitrate (mM)	0.00	4.77	12.69	16.32	16.08
Nitrite (mM)	0.15	11.10	30.67	37.72	36.38
Sulfate (mM)	5.77	5.81	6.30	6.65	7.45
MEA (m)	7.0	5.5	3.6	2.6	1.9

Table 4.9 Raw Data – MEA/Fe/B Low Gas Experiment, 6/08

Experiment	7m MEA/1mM Fe/7.5mM Inhibitor B				
Experiment Time (Hours)	0	46	118	164	214
Formate (mM)	1.96	2.02	5.18	8.05	10.22
Formamide (mM)	10.62	12.32	18.76	25.96	32.64
Oxalate (mM)	0.00	0.00	0.06	0.12	0.17
Oxamide (mM)	0.60	1.16	2.14	4.87	7.57
Acetate (mM)	0.02	0.09	0.00	0.00	0.00
Acetamide (mM)	0.37	0.06	0.00	0.03	0.00
Glycolate (mM)	0.00	0.00	0.00	0.00	0.00
Glycolamide (mM)	4.41	2.75	2.34	3.22	4.07
Nitrate (mM)	0.00	0.00	0.97	0.82	1.02
Nitrite (mM)	0.16	0.07	0.14	0.23	0.32
Sulfate (mM)	11.41	11.33	12.26	11.34	10.86
MEA (m)	7.0	7.0	6.8		6.6

Table 4.10 Raw Data – MEA/Fe/6% CO_2 Low Gas Experiment, 6/08

Experiment	7m MEA/1mM Fe/6% CO_2				
Experiment Time (Hours)	0	46	137	183	233
Formate (mM)	1.94	11.61	34.54	57.42	72.28
Formamide (mM)	0.00	68.32	145.70	182.68	175.68
Oxalate (mM)	0.00	0.73	3.61	6.77	9.70
Oxamide (mM)	0.06	33.30	105.37	155.18	170.46
Acetate (mM)	0.14	0.44	1.40	0.59	0.61
Acetamide (mM)	0.07	1.23		0.97	1.01
Glycolate (mM)	0.00	0.00	0.34	0.00	0.44
Glycolamide (mM)	1.23	4.10	8.78	13.95	9.33
Nitrate (mM)	0.00	6.90	17.57	26.11	27.23
Nitrite (mM)	0.03	23.56	58.07	73.14	73.35
Sulfate (mM)	2.22	2.02	1.58	1.46	1.86
MEA (m)	7.0	6.5	6.7	5.9	4.9

Table 4.11 Raw Data – MEA/Cr/Ni/A Low Gas Experiment, 5/08

Experiment	7m MEA/0.6mM Cr/0.1mM Ni/100mM Inhibitor A				
Experiment Time (Hours)	0	46	138	190	236
Formate (mM)	0.21	0.28	0.40	0.39	0.59
Formamide (mM)	0.45	0.42		1.13	1.21
Oxalate (mM)	0.03	0.03	0.04	0.05	0.05
Oxamide (mM)	0.01	0.04	0.01	0.10	0.13
Acetate (mM)	0.05	0.04	0.04	0.03	0.01
Acetamide (mM)	0.20	0.25		0.31	0.23
Glycolate (mM)	0.00	0.00	0.00	0.00	0.00
Glycolamide (mM)	0.00	0.00	0.00	0.00	0.00
Nitrate (mM)	0.00	0.00	0.00	0.00	0.06
Nitrite (mM)	0.00	0.03	0.00	0.04	0.06
Sulfate (mM)	0.92	1.17	1.07	1.11	1.03
MEA (m)	7.0				6.7

Table 4.12 Raw Data – MEA/Fe/EDTA (1:2) Low Gas Experiment, 5/08

Experiment	7m MEA/1mM Fe/2mM EDTA				
Experiment Time (Hours)	0	46	138	190	236
Formate (mM)	0.61	1.66	4.40	10.10	12.25
Formamide (mM)	0.50	18.57	44.20		49.43
Oxalate (mM)	0.02	0.08	0.28	0.72	1.09
Oxamide (mM)	0.09	3.84	12.75		21.99
Acetate (mM)	0.17	0.03	0.15	0.05	0.22
Acetamide (mM)	0.02	0.01	0.07	0.13	0.00
Glycolate (mM)	0.00	0.00	0.00	0.00	0.00
Glycolamide (mM)	1.86	3.33	4.05		6.02
Nitrate (mM)	0.00	0.41	1.74		3.68
Nitrite (mM)	0.04	0.82	2.78		4.70
Sulfate (mM)	1.92	2.00	1.82	1.86	2.47
MEA (m)	7.0	6.3	6.7	6.2	4.2
Hydroxyethyl-formamide (mM)					118.64
Hydroxyethylimidazole (mM)					87.85
Unknown #1, RT=2.4 min (raw area)					112.21
Unknown #2, RT=3.2 min (raw area)					9.98
Unknown #3, RT=3.5 min (raw area)					79.48
Unknown #4, RT=4.6 min (raw area)					30.13
Unknown #5, RT=13.2 min (raw area)					89.52

Table 4.13 Raw Data – MEA/V Low Gas Experiment, 5/08

Experiment	7m MEA/1mM V				
Experiment Time (Hours)	0	46	138	190	236
Formate (mM)	0.14	2.29	4.96	9.87	13.60
Formamide (mM)	1.20	4.44	18.49	23.28	28.08
Oxalate (mM)	0.02	1.01	0.49	1.10	1.59
Oxamide (mM)	0.06	3.99	19.02	27.77	37.26
Acetate (mM)	0.04	0.25	0.14	0.16	0.29
Acetamide (mM)	0.31	0.14	0.02	0.00	0.00
Glycolate (mM)	0.00	0.00	0.00	0.12	0.06
Glycolamide (mM)	0.22	2.17	3.11	3.00	3.11
Nitrate (mM)	0.09	2.02	6.59	9.42	11.65
Nitrite (mM)	0.05	1.95	6.74	9.73	12.17
MEA (m)	7.0	6.5	6.6	6.6	6.3
Hydroxyethyl-formamide (mM)					23.55
Hydroxyethylimidazole (mM)					24.99
Unknown #1, RT=2.4 min (raw area)					91.93
Unknown #2, RT=3.6 min (raw area)					145.5
Unknown #3, RT=4.6 min (raw area)					5.14
Unknown #4, RT=13.2 min (raw area)					5.99

Table 4.14 Raw Data – MEA/Fe/Na_2SO_3 Low Gas Experiment, 5/08

Experiment	7m MEA/1mM Fe/100mM Na_2SO_3				
Experiment Time (Hours)	0	46	138	190	236
Formate (mM)	0.26	2.48	6.34	12.98	19.41
Formamide (mM)	0.25	21.24	45.77	69.66	81.77
Oxalate (mM)	0.00	0.03	0.45	8.23	2.49
Oxamide (mM)	0.00	8.69	29.82	49.10	71.98
Acetate (mM)	0.09	0.42	0.30	0.64	0.45
Acetamide (mM)	0.14	0.00	0.13	0.00	0.00
Glycolate (mM)	0.00	0.00	0.00	0.05	0.07
Glycolamide (mM)	0.08	1.20	1.54	2.46	2.48
Nitrate (mM)	0.08	4.15	5.88	7.55	10.07
Nitrite (mM)	0.04	5.98	15.31	25.91	31.29
Sulfate (mM)	110.84	112.31	108.10	112.20	112.70
MEA (m)	7.0	6.3	5.9	5.6	5.3
Unknown #1, RT=2.4 min (raw area)					50.46
Unknown #2, RT=3.2 min (raw area)					0.24
Unknown #3, RT=3.6 min (raw area)					1.03
Unknown #4, RT=13.2 min (raw area)					0.47

Table 4.15 Raw Data – MEA/Fe/Cu High Gas Experiment, 5/08

Experiment	7m MEA/0.1mM Fe/5mM Cu High 5/08			
Experiment Time (Hours)	0	46	121	145
Formate (mM)	0.29	5.91	23.49	31.50
Formamide (mM)	3.17	68.59	141.96	152.15
Oxalate (mM)	0.00	0.05	0.32	0.50
Oxamide (mM)	0.07	3.79	15.96	16.25
Acetate (mM)	0.03	0.12	0.12	0.14
Acetamide (mM)	0.00	0.15	1.88	3.00
Glycolate (mM)	0.00	0.00	0.00	0.02
Glycolamide (mM)	1.70	6.89	8.20	5.59
Nitrate (mM)	0.00	1.12	2.86	3.36
Nitrite (mM)	0.15	1.93	4.30	3.10
Sulfate (mM)	6.70	6.67	6.50	6.53
MEA (m)	7.0	6.3	5.8	5.5
Hydroxyethyl-formamide (mM)				126
Hydroxyethylimidazole (mM)				34
Unknown #1, RT=3.2 min (raw area)				39.13
Unknown #2, RT=3.6 min (raw area)				35.76
Unknown #3, RT=4.6 min (raw area)				54.05
Unknown #4, RT=13.2 min (raw area)				13.67
CO (mM)				0.00
CH_4 (mM)				4.79
N_2O (mM)				20.30
NO (mM)				9.14
NO_2 (mM)				0.00
NH_3 (mM)				285.51
C_2H_4 (mM)				0.00
Formaldehyde (mM)				1.60
Acetaldehyde (mM)				2.61
MEA Volatility (mM)				271.44
Methanol (mM)				0.00
Methylamine (mM)				0.15

Table 4.16 Raw Data – MEA/Fe/EDTA (1:10) Low Gas Experiment, 4/08

Experiment	7m MEA/1mM Fe/10mM EDTA						
Experiment Time (Hours)	0	80	104	149	203	268	364
Formate (mM)	0.45	4.34	6.76	18.27	19.13	12.38	21.56
Formamide (mM)	2.33	28.75	29.90	28.60	31.54	20.86	35.09
Oxalate (mM)	0.00	0.02	0.05	0.18	0.23	0.39	0.32
Oxamide (mM)	0.08	1.83	2.22	3.29	3.36	4.73	5.47
Acetate (mM)	0.24	0.08	0.03	0.00	0.00	0.25	0.00
Acetamide (mM)	0.00	0.00	0.00	0.33	0.10	0.76	2.56
Glycolate (mM)	0.00	0.00	0.00	0.00	0.00	0.00	0.00
Glycolamide (mM)	0.79	1.08	0.56	0.00	0.68	0.92	1.52
Nitrate (mM)	0.00	0.09	0.11	0.29	0.37	0.41	0.41
Nitrite (mM)	0.04	0.91	0.90	1.00	1.33	1.17	1.38
Sulfate (mM)	1.57	1.57	1.71	1.56	1.66	1.79	1.76
MEA (m)	7.0	7.6	7.5	6.9	6.3	6.4	6.2
Hydroxyethyl-formamide (mM)							23.31
Hydroxyethylimidazole (mM)							21.33
Unknown #1, RT=3.6 min (raw area)							27.95
Unknown #2, RT=4.6 min (raw area)							9.68
Unknown #3, RT=13.2 min (raw area)							6.51

Table 4.17 Raw Data – MEA/Cu/Formaldehyde Low Gas Experiment, 4/08

Experiment	7m MEA/5mM Cu/500mM Formaldehyde							
Experiment Time (Hours)	0	90	126	169	219	269	417	435
Formate (mM)	1.56	74.23	101.51	108.38	112.94	140.91	165.92	156.66
Formamide (mM)	16.13	290.30	325.36	296.43	270.68		343.75	330.51
Oxalate (mM)	0.03	1.29	2.66	3.97	4.38	6.53	7.60	8.33
Oxamide (mM)	0.00	45.68	71.27				74.70	89.98
Acetate (mM)	0.75	1.30	1.43	1.71	1.53	1.53	1.27	1.40
Acetamide (mM)	0.00	0.28	0.73	0.66	0.84	1.53	1.17	1.06
Glycolate (mM)	0.00	0.13	0.31	0.48	0.55	0.84	0.90	1.03
Glycolamide (mM)	0.13	12.05	14.71	15.40	14.14	18.30	11.31	10.85
Nitrate (mM)	0.06	3.43	5.48	6.82	6.45	9.36	9.11	9.81
Nitrite (mM)	0.01	38.88	55.46	61.88	54.60	75.21	73.52	75.47
Sulfate (mM)	8.04	7.90	7.01	8.15	8.28	7.77	6.31	7.93
MEA (m)	7.0	4.0	3.2	2.7	2.0	2.4	2.1	2.1
Hydroxyethyl-formamide (mM)								987
Hydroxyethylimidazole (mM)								555
Unknown #1, RT=2.4 min (raw area)								6.24
Unknown #2, RT=3.2 min (raw area)								5.52
Unknown #3, RT=4.6 min (raw area)								2.38
Unknown #4, RT=13.2 min (raw area)								1.83

Table 4.18 Raw Data – MEA/Cr/Ni Low Gas Experiment, 4/08

Experiment	7m MEA/0.6mM Cr/0.1mM Ni						
Experiment Time (Hours)	0	49	100	146	194	267	332
Formate (mM)	0.56	7.76	17.56	37.23	49.63	70.83	95.04
Formamide (mM)	1.61	58.90	68.66	106.66	105.19	120.64	145.55
Oxalate (mM)	0.01	0.09	0.39	1.05	1.69	3.09	6.36
Oxamide (mM)	0.03	6.78	14.05	27.39	36.34	46.39	63.21
Acetate (mM)	0.10	0.38	0.00	0.51	0.52	0.79	0.52
Acetamide (mM)	0.28	0.33	1.14	1.00	2.60	0.81	0.62
Glycolate (mM)	0.00	0.00	0.00	0.03	0.08	0.15	0.34
Glycolamide (mM)	0.79	1.78	1.67	1.60	3.11	1.32	1.84
Nitrate (mM)	0.00	1.09	2.25	4.27	4.77	6.65	13.29
Nitrite (mM)	0.03	13.08	23.12	45.90	51.65	69.13	76.55
Sulfate (mM)	1.26	1.33	1.67	1.42	1.47	1.41	1.36
MEA (m)	7.0	5.4	3.4	3.9	3.5	2.9	3.3
Hydroxyethylimidazole (mM)							195
Unknown #1, RT=2.4 min (raw area)							122.13
Unknown #2, RT=3.2 min (raw area)							1.3
Unknown #3, RT=3.6 min (raw area)							2.14
Unknown #4, RT=13.2 min (raw area)							1.26

Table 4.19 Raw Data – MEA/Fe High Gas Experiment, 4/08

Experiment	7m MEA/1mM Fe High 4/08		
Experiment Time (Hours)	0	173	216
Formate (mM)	0.28	22.55	28.34
Formamide (mM)	1.41	66.32	69.08
Oxalate (mM)	0.00	0.66	0.87
Oxamide (mM)	0.04	13.01	15.46
Acetate (mM)	0.11	2.03	1.74
Acetamide (mM)	0.23	0.00	0.00
Glycolate (mM)	0.00	0.06	0.07
Glycolamide (mM)	0.42	1.93	1.52
Nitrate (mM)	0.00	1.70	1.82
Nitrite (mM)	0.00	5.60	5.76
Sulfate (mM)	1.70	1.60	1.56
MEA (m)	7.0	6.0	5.9
Unknown #1, RT=3.6 min (raw area)			95.84
Unknown #2, RT=4.6 min (raw area)			32.51
Unknown #3, RT=13.2 min (raw area)			2.85
CO (mM)			2.81
CH_4 (mM)			4.32
N_2O (mM)			0.22
NO (mM)			16.85
NO_2 (mM)			12.10
NH_3 (mM)			395.93
C_2H_4 (mM)			4.32
Formaldehyde (mM)			0.00
Acetaldehyde (mM)			0.43
MEA Volatility (mM)			244.73
Methanol (mM)			1.51
Methylamine (mM)			0.22

Table 4.20 Raw Data – Potassium Glycinate/Fe Low Gas Experiment, 4/08

Experiment	2m Potassium Glycinate/1mM Fe						
Experiment Time (Hours)	0	47	95	143	190	239	268
Formate (mM)	0.43	1.46	2.34	3.82	3.01	5.20	6.43
Oxalate (mM)	0.03	0.05	0.07	0.09	0.07	0.13	0.16
Acetate (mM)	0.25	0.16	0.03	0.04	0.05	0.01	0.115
Nitrate (mM)	0.02	0.03	0.05	0.03	0.04	0.07	0.057
Nitrite (mM)	0.02	0.03	0.04	0.05	0.04	0.06	0.07
Glycine (m)	1.9	1.9	1.9	1.8	1.8	1.9	1.9

Table 4.21 Raw Data – Potassium Glycinate/Cu Low Gas Experiment, 3/08

Experiment	2m Potassium Glycinate/5mM Cu							
Expeiment Time (Hours)	0	46	94	142	188	232	275	295
Formate (mM)	2.63	3.53	4.90	6.23	7.60	9.15	11.09	12.00
Oxalate (mM)	0.07	0.10	0.13	0.17	0.20	0.22	0.27	0.30
Acetate (mM)	0.78	2.35	2.86	3.57	4.08	4.56	5.17	5.63
Nitrite (mM)	0.01	0.03	0.03	0.04	0.04	0.05	0.06	0.06
Glycine (m)	1.9	1.8	1.9		1.9	1.7	1.6	1.8

Table 4.22 Raw Data – EDA/Fe Low Gas Experiment, 3/08

Experiment	3.5m EDA/1mM Fe					
Experiment Time (Hours)	0	47	146	215	313	383
Formate (mM)	0.15	0.18	0.96	1.57	2.59	3.37
Formamide (mM)	0.00	0.00	0.00	0.00	0.00	0.00
Oxalate (mM)	0.00	0.00	0.02	0.03	0.05	0.08
Oxamide (mM)	0.07	0.08	0.27	0.37	0.49	0.04
Acetate (mM)	0.00	0.03	0.00	0.00	0.03	0.02
Nitrate (mM)	0.02	0.04	0.25	0.39	0.48	0.62
Nitrite (mM)	0.07	0.17	0.92	1.21	1.63	1.65
DETA (mM)	0.29	1.53	3.64	4.10	4.94	4.43
EDA (m)	3.3		3.0	3.2	3.3	
Hydroxyethyl-formamide (mM)						47.38

Table 4.23 Raw Data – EDA/Cu Low Gas Experiment, 2/08

Experiment	3.5m EDA/5mM Cu					
Experiment Time (Hours)	0	47	145	249	314	335
Formate (mM)	0.20	0.56	1.37	2.05	3.07	3.26
Formamide (mM)	2.17	3.01	3.78	3.56	3.98	4.14
Oxalate (mM)	0.00	0.01	0.02	0.04	0.08	0.09
Oxamide (mM)	0.08	0.31	0.41	0.54	0.94	0.85
Acetate (mM)	0.07	0.04	0.05	0.05	0.08	0.19
Acetamide (mM)	0.13	0.22	0.12	0.21	0.24	0.41
Glycolate (mM)	0.01	0.02	0.04	0.08	0.14	0.13
Nitrate (mM)	0.25	0.44	0.66	0.83	0.96	0.95
Nitrite (mM)	0.07	0.56	0.91	1.15	1.31	1.32
EDTA (mM)	0.24	5.32	5.34	5.55	6.25	6.21
EDA (m)	3.4		3.5	3.5	3.4	3.4
Hydroxyethyl-formamide (mM) - HPLC						51.65
Unknown #1, RT=2.4 min (raw area)						1.82

Table 4.24 Raw Data – MEA/Fe/EDTA (1:100) Low Gas Experiment, 1/08

Experiment	7m MEA/1mM Fe/100mM EDTA						
Experiment Time (Hours)	0	122	168	217	286.5	336	382.5
Formate (mM)	0.31	0.96	1.18	1.75	2.24	2.56	2.96
Formamide (mM)	0.41	1.09	1.61	1.38	1.68	2.15	0.00
Oxalate (mM)	0.00	0.00	0.00	0.00	0.00	0.00	0.00
Oxamide (mM)	0.00	0.00	0.00	0.00	0.00	0.00	0.00
Acetate (mM)	0.00	0.00	0.00	0.00	0.00	0.00	0.00
Acetamide (mM)	0.00	0.00	0.05	0.04	0.00	0.02	0.00
Glycolate (mM)	0.00	0.00	0.00	0.00	0.00	0.00	0.00
Glycolamide (mM)	0.00	0.00	0.05	0.06	0.07	0.09	0.00
Nitrate (mM)	0.00	0.00	0.00	0.00	0.00	0.53	0.00
Nitrite (mM)	0.00	0.00	0.04	0.05	0.00	0.14	0.05
Sulfate (mM)	2.35	2.14	2.30	2.26	2.22	2.47	2.38
MEA (m)	7.0	7.2	7.3	7.2	7.3	6.6	6.9
Hydroxyethyl-formamide (mM)							4.47
Unknown #1, RT=3.6 min (raw area)							10.94

Table 4.25 Raw Data – MEA/Fe/Cu High Gas Experiment, 12/07

Experiment	7m MEA/0.1mM Fe/5mM Cu High 12/07					
Experiment Time (Hours)	0	22	45	92	154	191
Formate (mM)	1.71	11.29	16.84	34.77	60.65	102.49
Formamide (mM)	2.32	46.71	75.64	139.07	152.79	175.70
Oxalate (mM)	0.06	0.62	0.00	0.91	1.67	3.58
Oxamide (mM)	0.00	0.34	2.44	3.56	8.10	9.73
Acetate (mM)	0.00	0.34	0.24	0.43	1.04	2.42
Acetamide (mM)	0.00	0.19	0.76	1.77	2.49	2.35
Glycolate (mM)	0.00	0.29	0.27	0.33	0.67	0.38
Glycolamide (mM)	0.00	7.28	8.60	6.60	8.32	1.31
Nitrate (mM)	0.00	1.24	1.62	3.56	4.83	4.66
Nitrite (mM)	1.18	2.12	4.08	5.16	3.27	0.60
Sulfate (mM)	7.22	7.22	7.08	7.17	6.98	6.06
MEA (m)	7.0	6.8	6.4	6.1	5.6	5.2
Hydroxyethyl-formamide (mM)						174
Hydroxyethylimidazole (mM)						55
Unknown #1, RT=3.2 min (raw area)						42.57
Unknown #2, RT=3.6 min (raw area)						32.27
Unknown #3, RT=4.6 min (raw area)						81.65
Unknown #4, RT=13.2 min (raw area)						13.31
CO (mM)						0.00
CH_4 (mM)						6.10
N_2O (mM)						30.10
NO (mM)						22.29
NO_2 (mM)						0.00
NH_3 (mM)						322.71
C_2H_4 (mM)						0.00
Formaldehyde (mM)						4.57
Acetaldehyde (mM)						12.19
MEA Volatility (mM)						601.22
Methanol (mM)						0.00
Methylamine (mM)						2.48

Table 4.26 Raw Data – MEA/Fe/Formate Low Gas Experiment, 12/07

Experiment	7m MEA/1mM Fe/500mM Formic Acid						
Experiment Time (Hours)	0	22	77	153	223	319	366
Formate (mM)	327.52	301.56	348.15	278.25	264.11	300.07	376.89
Formamide (mM)	0.00	28.41	163.42	105.39	152.86	189.82	153.50
Oxalate (mM)	0.00	0.00	0.63	1.23	1.95	3.47	5.42
Oxamide (mM)	0.00	1.50	9.14	2.85	27.09	31.38	
Acetate (mM)	0.85	1.02	1.55	1.42	1.36	1.58	1.96
Acetamide (mM)	0.09	0.44	0.27	0.14	0.65	0.24	0.09
Glycolate (mM)	0.00	0.00	0.00	0.05	0.11	0.19	0.38
Glycolamide (mM)	1.03	1.16	1.76	2.20	2.70	2.40	0.88
Nitrate (mM)	0.00	1.99	8.23	45.15	14.30	22.72	31.42
Nitrite (mM)	0.30	12.48	49.35	57.50	70.58	83.21	108.10
Sulfate (mM)	1.97	2.02	1.65	1.75	1.26	2.00	1.43
MEA (m)	7.0	6.5	6.3	5.7	4.3	4.3	4.5
Hydroxyethylimidazole (mM)							201
Unknown #1, RT=2.4 min (raw area)							103.31
Unknown #2, RT=3.2 min (raw area)							0.6
Unknown #3, RT=3.6 min (raw area)							1.58
Unknown #4, RT=13.2 min (raw area)							0.46

Table 4.27 Raw Data – MEA/Fe/Formaldehyde Low Gas Experiment, 11/07

Experiment	7m MEA/1mM Fe/500mM Formaldehyde				
Experiment Time (Hours)	0	139	192	309	333
Formate (mM)	0.60	52.60	52.82	60.77	73.40
Formamide (mM)	5.57	204.69	220.53	209.12	231.57
Oxalate (mM)	0.00	1.24	1.50	1.87	2.25
Oxamide (mM)	0.00	14.27	15.24	18.87	22.29
Acetate (mM)	0.00	0.58	0.61	0.63	0.67
Acetamide (mM)	0.00	0.23	2.44	0.19	0.30
Glycolate (mM)	0.00	0.10	0.07	0.10	0.14
Glycolamide (mM)	0.00	1.51	1.34	1.85	2.24
Nitrate (mM)	0.00	9.42	10.07	11.82	14.25
Nitrite (mM)	0.00	72.50	72.10	72.87	82.17
Sulfate (mM)	1.61	1.68	1.68	1.75	1.64
MEA (m)	7.0	4.7	4.4	4.6	4.8
Hydroxyethylimidazole (mM)					213
Unknown #1, RT=2.4 min (raw area)					107.33
Unknown #2, RT=3.6 min (raw area)					1.27
Unknown #3, RT=4.6 min (raw area)					0.78
Unknown #4, RT=13.2 min (raw area)					0.48

Table 4.28 Raw Data – MEA/Fe Low Gas Experiment, 9/07

Experiment	7m MEA/1mM Fe				
Experiment Time (Hours)	0	144	213	445	496
Formate (mM)	0.44	38.44	73.69	115.80	143.57
Formamide (mM)	1.26	110.99	150.82	195.50	176.19
Oxalate (mM)	0.00	1.65	3.98	7.94	10.06
Oxamide (mM)	0.00	16.20	29.14	58.62	44.34
Acetate (mM)	0.00	0.55	0.64	0.72	0.95
Acetamide (mM)	0.00	0.30	0.43	0.82	0.46
Glycolate (mM)	0.00	0.01	0.14	0.34	0.43
Glycolamide (mM)	0.00	0.61	1.30	1.76	1.37
Nitrate (mM)	0.00	12.66	26.36	37.76	42.03
Nitrite (mM)	0.00	56.12	80.76	90.59	89.39
Sulfate (mM)	0.78	0.90	1.10	1.12	1.25
MEA (m)	7.0	4.4	4.1	3.9	4.4
Hydroxyethyl-formamide (mM)					383
Hydroxyethylimidazole (mM)					287
Unknown #1, RT=2.4 min (raw area)					88.33
Unknown #2, RT=3.6 min (raw area)					0.68
Unknown #3, RT=13.2 min (raw area)					0.4

Table 4.29 Raw Data – PZ/Fe Low Gas Experiment, 9/07

Experiment	5m PZ/5mM Fe						
Experiment Time (Hours)	0	47	96	142	219	267	291
Formate (mM)	0.33	0.43	0.84	1.03	1.40	1.52	1.99
Formamide (mM)	0.00	0.00	0.84	6.18	1.68	1.40	1.09
Oxalate (mM)	0.00	0.00	0.00	0.00	0.00	0.06	0.09
Oxamide (mM)	0.00	0.00	0.11	0.21	0.16	0.00	0.00
Acetate (mM)	0.00	0.00	0.00	0.00	0.00	0.00	0.00
Acetamide (mM)	0.00	0.00	0.00	0.00	0.00	0.00	0.00
Glycolate (mM)	0.00	0.00	0.00	0.00	0.00	0.00	0.00
Glycolamide (mM)	0.00	0.00	0.00	0.00	0.00	0.00	0.00
Nitrate (mM)	0.00	0.00	0.00	0.00	0.00	0.00	0.00
Nitrite (mM)	0.00	0.00	0.00	0.00	0.00	0.00	0.00
EDA (mM)	0.45	0.84	1.36	1.76	3.31	5.12	
Sulfate (mM)	7.37	9.05	8.56	8.29	8.14	7.54	7.62
PZ (m)	5.0	4.6	4.4	5.4	4.3	5.0	5.0

Table 4.30 Raw Data – MEA/PZ/Fe Low Gas Experiment, 8/07

Experiment	7m MEA/2m PZ/0.1mM Fe							
Experiment Time (Hours)	0	46	88	139	185	233	310	363
Formate (mM)	0.38	4.46	10.61	19.12	29.96	42.55	51.05	62.47
Formamide (mM)								73.73
Oxalate (mM)	0.02	0.21	0.54	1.01	1.45	2.42	3.05	2.41
Oxamide (mM)								25.72
Acetate (mM)	0.00	0.15	0.19	0.32	0.00	0.28	0.30	0.88
Acetamide (mM)								0.00
Glycolate (mM)	0.00	0.00	0.00	0.01	0.02	0.06	0.09	0.02
Glycolamide (mM)								0.24
Nitrate (mM)	0.04	4.13	6.87	8.84	10.38	13.38	13.33	20.35
Nitrite (mM)	0.07	3.41	5.47	6.75	6.97	8.39	7.85	9.51
EDA (mM)	0.19	0.80	1.27	1.50	1.43	1.55	1.45	2.54
PZ (m)	2.0	1.7	1.8	1.6	1.8	1.6	1.5	1.3
MEA (m)	7.0	5.7	4.8	5.4	4.0	3.3	3.4	2.7
Hydroxyethyl-formamide (mM)								539
Hydroxyethylimidazole (mM)								203
Unknown #1, RT=2.4 min (raw area)								70.13
Unknown #2, RT=3.2 min (raw area)								0.9
Unknown #3, RT=3.6 min (raw area)								1.9
Unknown #4, RT=4.6 min (raw area)								2.51
Unknown #5, RT=13.2 min (raw area)								0.81

Table 4.31 Raw Data – PZ/Fe/A Low Gas Experiment, 8/07

Experiment	5m PZ/0.1mM Fe/100mM Inhibitor A							
Experiment Time (Hours)	0	46	88	139	185	233	306	352
Formate (mM)	0.31	0.26	0.56	0.65	0.89	0.24	0.64	0.33
Formamide (mM)								0.22
Oxalate (mM)	0.00	0.01	0.02	0.02	0.07	0.07	0.03	0.02
Oxamide (mM)								0.34
Acetate (mM)	0.07	0.02	0.16	0.05	0.06	0.01	0.08	0.01
Acetamide (mM)								0.44
Glycolate (mM)	0.00	0.00	0.01	0.01	0.01	0.00	0.01	0.00
Glycolamide (mM)								0.20
Nitrate (mM)	0.00	0.00	0.00	0.00	0.00	0.00	0.00	0.07
Nitrite (mM)	0.00	0.00	0.00	0.00	0.01	0.00	0.00	0.00
EDA (mM)	0.24	0.25	0.26	0.27	0.36	0.28	0.33	0.34
PZ (m)	5.0	5.3	5.3	5.3	5.2	4.9	5.4	5.2

Table 4.32 Raw Data – PZ/Fe Low Gas Experiment, 8/07

Experiment	5m PZ/0.1mM Fe						
Experiment Time (Hours)	0	67	119	169	261	313	333
Formate (mM)	0.36	1.10	1.75	1.99	3.11	4.02	4.04
Oxalate (mM)	0.00	0.06	0.07	0.11	0.14	0.15	0.25
Acetate (mM)	0.00	0.00	0.00	0.00	0.00	0.00	0.00
Glycolate (mM)	0.00	0.00	0.00	0.00	0.00	0.00	0.00
Nitrate (mM)	0.00	0.14	0.07	0.10	0.14	0.18	0.00
Nitrite (mM)	0.00	0.00	0.00	0.00	0.01	0.01	0.00
EDA (mM)	0.00	0.63	2.34	3.24	5.16	6.24	6.88

Table 4.33 Raw Data – MEA/Fe High Gas Experiment, 7/07

Experiment	7m MEA/1mM Fe High 7/07							
Experiment Time (Hours)	0	24	74	105	126.5	151	170.5	193
Formate (mM)	0.64	2.15	6.68	9.41	12.60	15.01	23.44	19.93
Formamide (mM)	0.36	1.03	3.03	4.50	6.01		11.98	30.62
Oxalate (mM)	0.02	0.06	0.18	0.27	0.36	0.47	0.79	0.63
Oxamide (mM)	0.01	0.02	0.03	0.05	0.08		0.10	1.58
Acetate (mM)	0.08	0.20	0.49	0.75	1.00	0.98	2.02	1.07
Acetamide (mM)	0.25	0.24	0.27	0.21	0.19		0.35	0.04
Glycolate (mM)	0.00	0.00	0.00	0.01	0.02	0.04	0.09	0.09
Glycolamide (mM)	0.12	0.21	0.29	0.38	0.50	0.12	0.71	1.28
Nitrate (mM)	0.16	0.24	0.51	0.63	0.79	0.33	1.80	1.46
Nitrite (mM)	0.10	0.05	0.51	1.33	1.80	0.84	6.98	5.86
Sulfate (mM)	1.60	1.41	1.29	1.32	1.24	1.23	1.32	1.16
MEA (m)	7.0	6.9	6.2	6.0	5.6	5.3	5.6	4.8
Unknown #1, RT=3.6 min (raw area)								27.27
Unknown #2, RT=4.6 min (raw area)								11.19
Unknown #3, RT=13.2 min (raw area)								2.26
CO (mM)								57.71
CH_4 (mM)								0.00
N_2O (mM)								0.00
NO (mM)								22.97
NO_2 (mM)								1.35
NH_3 (mM)								353.96
C_2H_4 (mM)								46.90
Formaldehyde (mM)								16.41
Acetaldehyde (mM)								30.49
MEA Volatility (mM)								478.45
Methanol (mM)								0.00
Methylamine (mM)								0.39

Table 4.34 Raw Data – MEA/PZ/Fe/A Low Gas Experiment, 7/07

Experiment	7m MEA/2m PZ/0.1mM Fe/100mM Inhibitor A					
Experiment Time (Hours)	0	72	120	165	261	333
Formate (mM)	0.37	17.35	31.91	42.77	60.31	68.44
Formamide (mM)						40.55
Oxalate (mM)	0.00	0.21	0.46	0.80	1.83	2.70
Oxamide (mM)						21.32
Acetate (mM)	0.00	0.03	0.04	0.05	0.07	0.00
Acetamide (mM)						2.97
Glycolate (mM)	0.00	0.00	0.00	0.00	0.00	0.00
Glycolamide (mM)						2.23
Nitrate (mM)	0.00	4.11	6.15	7.44	8.88	9.78
Nitrite (mM)	0.03	2.98	4.04	4.60	5.51	5.67
EDA (mM)	0.00	0.39	0.51	0.53	0.67	0.66
Hydroxyethylimidazole (mM)						47.43
Unknown #1, RT=2.4 min (raw area)						128.92
Unknown #2, RT=3.6 min (raw area)						121.89
Unknown #3, RT=4.6 min (raw area)						55.24
Unknown #4, RT=13.2 min (raw area)						7.8

Table 4.35 Raw Data – MEA/PZ/Fe/Cu/A Low Gas Experiment, 7/07

Experiment	7m MEA/2m PZ/0.1mM Fe/5mM Cu/100mM Inhibitor A					
Experiment Time (Hours)	0	72	120	165	261	333
Formate (mM)	1.53	39.33	63.19	71.19	96.63	102.62
Formamide (mM)						116.26
Oxalate (mM)	0.00	0.23	0.53	0.76	2.05	2.95
Oxamide (mM)						27.39
Acetate (mM)	0.00	0.15	0.11	0.05	0.05	0.04
Acetamide (mM)						3.39
Glycolate (mM)	0.00	0.00	0.00	0.06	0.19	0.23
Glycolamide (mM)						1.45
Nitrate (mM)	0.00	5.46	7.52	7.05	8.06	8.02
Nitrite (mM)	0.04	1.32	1.70	1.41	1.55	1.37
EDA (mM)	2.82	14.24	16.12	16.14	18.10	18.97
Hydroxyethyl-formamide (mM)						92.35
Hydroxyethylimidazole (mM)						58.26
Unknown #1, RT=2.9 min (raw area)						2.29
Unknown #2, RT=3.2 min (raw area)						3.59
Unknown #3, RT=3.6 min (raw area)						17.25
Unknown #4, RT=4.6 min (raw area)						127.74
Unknown #5, RT=13.2 min (raw area)						23.65

Table 4.36 Raw Data – MEA/Fe/Cu Low Gas Experiment, 6/07

Experiment	7m MEA/0.1mM Fe/5mM Cu						
Experiment Time (Hours)	0	67	119	169	261	313	333
Formate (mM)	4.20	13.20	39.69	95.56	160.38	201.12	223.41
Formamide (mM)							601.14
Oxalate (mM)	0.00	0.12	1.03	4.27	10.79	15.52	17.56
Oxamide (mM)							236.59
Acetate (mM)	0.20	0.53	1.16	1.46	1.26	1.44	1.50
Glycolate (mM)	0.00	0.00	0.00	0.55	1.59	2.41	2.67
Glycolamide (mM)							37.57
Nitrate (mM)	1.35	2.86	12.29	24.24	35.42	40.98	43.99
Nitrite (mM)	0.78	0.58	4.12	15.17	31.05	35.76	37.19
Hydroxyethyl-formamide (mM)							1483
Hydroxyethylimidazole (mM)							839

Table 4.37 Raw Data – PZ/Fe/Cu/A Low Gas Experiment, 5/07

Experiment	5m PZ/0.1mM Fe/5mM Cu/100mM Inhibitor A				
Experiment Time (Hours)	0	123	175	290	340
Formate (mM)	0.28	0.77	0.88	1.39	4.73
Formamide (mM)					4.91
Oxalate (mM)					0.91
Oxamide (mM)					0.29
Acetate (mM)					0.62
Acetamide (mM)					0.00
Glycolate (mM)					0.10
Glycolamide (mM)					0.06
Nitrate (mM)					0.33
Nitrite (mM)					0.30
EDA (mM)	4.30	10.87	11.28	14.12	14.51

Table 4.38 Raw Data – PZ/Fe/Cu Low Gas Experiment, 4/07

Experiment	5m PZ/0.1mM Fe/5mM Cu					
Experiment Time (Hours)	0	77	143	244	298	413
Formate (mM)	1.14	30.57	65.26	76.19	90.98	93.29
Formamide (mM)						62.38
Oxalate (mM)	0.00	0.40	1.63	3.04	3.69	5.50
Oxamide (mM)						14.41
Acetate (mM)	0.00	0.00	0.00	0.00	0.00	0.00
Acetamide (mM)						2.80
Glycolate (mM)	0.00	0.00	0.00	0.00	0.00	0.00
Glycolamide (mM)						0.94
Nitrate (mM)	1.32	2.03	3.65	2.01	2.55	2.45
Nitrite (mM)	0.00	3.47	4.17	4.03	4.93	4.27
EDA (mM)	7.38	71.10	81.54	97.52	100.10	111.54
Unknown #1, RT=2.6 min (raw area)						128.24
Unknown #2, RT=2.9 min (raw area)						60.76
Unknown #3, RT=3.4 min (raw area)						11.62

Table 4.39 Raw Data – AMP/Fe Low Gas Experiment, 4/07

Experiment	4m AMP/1mM Fe									
Experiment Time (Hours)	0	53	99	171	195	243	320	364	412	504
Formate (mM)	0.44	0.77	1.24	1.43	1.67	2.12	2.15	2.45	2.56	2.93
Oxalate (mM)	0.24	0.09	0.14	0.23	0.32	0.48	0.51	0.67	0.57	1.16
Acetate (mM)	0.00	0.08	0.07	0.07	0.05	0.08	0.08	0.07	0.11	0.13
Glycolate (mM)	0.14	0.15	0.16	0.16	0.15	0.20	0.18	0.23	0.20	0.22
Nitrate (mM)	0.00	0.34	0.40	0.44	0.59	0.55	0.53	0.68	0.87	0.82
Nitrite (mM)	0.00	0.17	0.24	0.34	0.38	0.41	0.45	0.47	0.50	0.60

Table 4.40 Raw Data – PZ/V/A Low Gas Experiment, 12/06

Experiment	2.5m PZ/5mM V/100mM Inhibitor A			
Experiment Time (Hours)	0	44	92	186
Formate (mM)	0.03	3.99	3.32	11.39
Oxalate (mM)	0.06	0.09	0.18	0.11
Acetate (mM)	0.10	0.00	0.00	0.00
Glycolate (mM)	0.00	0.00	0.00	0.00
Nitrate (mM)	0.17	0.55	1.84	6.30
Nitrite (mM)	0.00	1.13	1.79	5.03
EDA (mM)	0.00	2.62	6.27	20.57
Unknown #1, RT=2.6 min (raw area)				9.3
Unknown #2, RT=2.9 min (raw area)				28.44
Unknown #3, RT=3.4 min (raw area)				1.46
Unknown #4, RT=13.2 min (raw area)				2.58

Table 4.41 Raw Data – PZ/V/$KHCO_3$ Low Gas Experiment, 12/06

Experiment	2.5m PZ/5mM V/5m $KHCO_3$			
Experiment Time (Hours)	0	147	195	310
Formate (mM)	0.23	5.54	1.60	2.46
Oxalate (mM)	0.29	0.69	0.34	0.29
Acetate (mM)	0.00	0.00	0.00	0.75
Glycolate (mM)	0.00	0.00	0.00	0.00
Nitrate (mM)	0.19	0.42	1.29	0.30
Nitrite (mM)	0.00	0.00	0.00	0.00
EDA (mM)	0.17			0.42

Table 4.42 Raw Data – MEA/PZ/Fe/Cu Low Gas Experiment, 10/06

Experiment	7m MEA/2m PZ/0.1mM Fe/5mM Cu				
Experiment Time (Hours)	0	130	185	256	282
Formate (mM)	3.60	375.71	496.54	589.38	665.37
Oxalate (mM)	0.00	9.00	15.84	23.36	25.80
Acetate (mM)	0.00	0.75	1.02	0.96	4.65
Glycolate (mM)	0.00	3.64	7.32	5.78	8.23
Nitrate (mM)	0.00	18.62	25.91	41.14	37.46
Nitrite (mM)	1.10	2.35	1.42	1.41	1.06
EDA (mM)	3.23	14.88	11.58	8.23	7.05
Hydroxyethyl-formamide (mM)					1144
Hydroxyethylimidazole (mM)					974
Unknown #1, RT=2.4 min (raw area)					84.63
Unknown #2, RT=3.2 min (raw area)					12.82
Unknown #3, RT=3.6 min (raw area)					12.61
Unknown #4, RT=4.6 min (raw area)					95.52
Unknown #5, RT=13.2 min (raw area)					39.09

Table 4.43 Raw Data – MEA/Fe Low Gas Experiment, 9/06

Experiment	9m MEA/0.1mM Fe				
Experiment Time (Hours)	0	144	257	311	334
Formate (mM)	36.27	51.30	103.48	133.55	173.86
Oxalate (mM)	0.42	2.11	6.06	8.10	7.73
Acetate (mM)	0.00	4.05	3.03	3.11	9.24
Glycolate (mM)	0.00	0.00	0.00	0.00	0.00
Nitrate (mM)	5.37	4.47	12.90	19.53	22.43
Nitrite (mM)	5.76	3.87	18.45	62.42	159.92

Table 4.44 Raw Data – PZ/V/$KHCO_3$ Low Gas Experiment, 4/06

Experiment	2.5m PZ/5mM V/5m $KHCO_3$					
Expeiment Time (Hours)	0	114	133	160	251	266
Formate (mM)		0.50	0.29			
Oxalate (mM)	1.53	0.70		1.32	1.04	1.16
Glycolate (mM)	6.73	5.59	4.98	6.66	5.36	5.27
Nitrate (mM)	0.19	0.19		0.24		
EDA (mM)	0.49	1.06	0.73	0.74	0.36	0.19

Table 4.45 Raw Data – MEA/Fe Low Gas Experiment, 3/06

Experiment	7m MEA/0.6mM Fe					
Experiment Time (Hours)	0	50	50	122	186	235
Formate (mM)	2.13	18.67	19.11	48.30	77.74	97.63
Oxalate (mM)	2.42	3.25	3.56	4.16	6.08	8.03
Acetate (mM)	3.52	3.47	3.77	4.90	5.07	0.26
Nitrate (mM)	0.00	9.52	10.25	22.20	31.49	37.73
Nitrite (mM)	0.24	1.07	3.15	28.32	52.02	55.71

Table 4.46 Raw Data – MEA/Fe/Cu/A Low Gas Experiment, 1/06

Experiment	7m MEA/0.6mM Fe/0.6mM Cu/100mM Inhibitor A				
Experiment Time (Hours)	0	21	69	139	155
Formate (mM)	0.93	2.29	3.57	6.76	7.37
Oxalate (mM)	0.00		1.24		0.99
Acetate (mM)					2.52
Nitrate (mM)	1.25	2.66	2.82	3.11	1.27
Nitrite (mM)	0.00	2.03	2.93	4.43	

Table 4.47 Raw Data – PZ/V Low Gas Experiment, 11/05

Experiment	2.5m PZ/5mM V				
Experiment Time (Hours)	0	95	191	239	263
Formate (mM)	0.00	16.79	27.89	36.47	29.13
Oxalate (mM)	0.00	6.30	20.67	7.37	3.74
Acetate (mM)	0.00	0.60	0.62	0.64	0.38
Glycolate (mM)	9.44		10.94	9.98	6.58
Nitrate (mM)	0.00	13.47	23.95	31.95	49.34
Nitrite (mM)	0.00	0.00	7.53	9.37	
EDA (mM)	2.57	8.36	16.89	20.45	33.94
Unknown #1, RT=2.9 min (raw area)					6.84
Unknown #2, RT=3.4 min (raw area)					1.76
Unknown #3, RT=13.2 min (raw area)					9.1

Table 4.48 Raw Data – MEA/Fe/Cu Low Gas Experiment, 9/05

Experiment	7m MEA/0.6mM Fe/0.6mM Cu		
Experiment Time (Hours)	0	120	335
Formate (mM)	27.37	181.79	268.04
Oxalate (mM)		10.89	13.16
Acetate (mM)	5.30	6.99	5.09
Nitrate (mM)	0.93	25.23	45.70
Nitrite (mM)	0.30	0.00	60.85

Table 4.49 Raw Data – MEA/Cu Low Gas Experiment, 12/04

Experiment	7m MEA/0.6mM Cu					
Experiment Time (Hours)	72	122	169	243	282	306
Formate (mM)	36.78	61.74	85.40	93.85	108.93	129.31
Oxalate (mM)	6.98	9.12	11.24	11.94	14.31	11.80
Acetate (mM)	4.86	2.99	3.84	2.88	3.12	4.59
Nitrate (mM)	8.56	12.05	14.40	15.22	16.15	23.42
Nitrite (mM)	20.96	29.70	36.86	41.87	46.42	59.68

Chapter 5: Reaction Products from the Oxidative Degradation of MEA

Aqueous monoethanolamine (MEA) solutions were subjected to oxidative degradation in 500 mL agitated reactors at both low and high gas rates. Solutions were degraded with 100 mL/min of 98%O_2/2%CO_2 and mass transfer was achieved by vortexing. Samples were drawn from the reactor during the course of the experiment and analyzed for degradation using ion chromatography and HPLC with evaporative light scattering detection (ELSD). In a parallel apparatus 7.5 L/min of 15% O_2/2% CO_2 was sparged through 350 mL of solution; additional mass transfer was achieved by vortexing. A Fourier Transform Infrared Analyzer collected continuous gas-phase data on amine volatility and volatile degradation products.

Formate, hydroxyethyl-formamide and HEI account for 92% of the degraded carbon that has been quantified at low gas flow. These species account for 18% to 59%

of the degraded carbon at high gas flow. Oxalate, its respective MEA amide, glycolate and acetate are also present, but at much lower concentrations.

Ammonia, hydroxyethyl-formamide and HEI are the dominant nitrogen-containing degradation products; they account for 84% of the degraded nitrogen at low gas flow and 83% to 92% at high gas flow. At high gas rate, NO_x is produced and stripped from the solution. At low gas rate, NO_x is retained in the solution and oxidized to nitrite and nitrate. At high gas rate, NO_x/N_2O production is 15% of the rate of ammonia production. At low gas rate, nitrite/nitrate production occurs at the same rate as NO_x/N_2O production at high gas rate. Other volatile degradation products include CO, C_2H_4, formaldehyde and acetaldehyde.

A comparison of total carbon and nitrogen production rates to MEA losses show that 25 to 50% of oxidative degradation products currently remain unaccounted for. Oxygen consumption rates vary from 1 to 2 mM/hr.

5.1. Introduction

Aqueous monoethanolamine (MEA) solutions were batch loaded into 500 mL glass jacketed reactors and subjected to oxidation at both low and high gas rates. Solutions were degraded with 100 mL/min of $98\%O_2/2\%CO_2$ with mass transfer achieved by vortexing. Samples were drawn from the reactor during the course of the experiment and analyzed for degradation using ion chromatography and HPLC with evaporative light scattering detection (ELSD). In a parallel apparatus 7.5 L/min of 15% O_2/2% CO_2 was sparged through 350 mL of solution; additional mass transfer was achieved by vortexing. A Fourier Transform Infrared Analyzer collected continuous gas-phase data on amine volatility and volatile degradation products. Samples were also drawn intermittently from the high gas flow reactor and analyzed for liquid phase degradation products.

Once all the major degradation products were identified and quantified, total rates of carbon and nitrogen formation from degradation products were compared to rates of

MEA disappearance, which was determined using cation chromatography, Kjeldahl and TOC analysis. Results from all of these analytical techniques were compiled in order to calculate an overall material balance for each baseline experiment (where applicable). An overall oxygen stoichiometry and consumption rate was calculated for each degradation experiment.

Carbon and nitrogen formation rates were calculated for each of the degradation experiments by adding up the total number of carbons and nitrogens contained in each liquid and gas phase product. If the material balance for each experiment were to close 100%, then the MEA degradation rate (in mM/hr) would equal the nitrogen formation rate and two times the carbon formation rate. That means that each and every nitrogen and carbon from the fragmented MEA molecules would be accounted for in degradation products.

A major conclusion from Goff (2005) is that in the presence of metal catalysts, the rate of evolution of MEA is controlled by the rate of oxygen absorption under experimental and industrial conditions. Goff's assertion was that 1 degraded mole of MEA resulted in 1 mole of ammonia. Ammonia evolution rates increased with agitation rate and increased linearly with oxygen concentration.

Goff (2005) proposed that MEA reacts with oxygen to form ammonia and other carbon containing degradation products, which are listed in Table 5.1. Ammonia can further react with oxygen to form water and a host of nitrogen containing degradation products. Each of the major degradation products has a specific oxygen stoichiometry, which is listed below.

$$C_2H_7NO + \nu O_2 \rightarrow NH_3 + \text{product} \qquad 5.1$$

$$NH_3 + \nu O_2 \rightarrow H_2O + \text{product} \qquad 5.2$$

A total oxygen consumption rate for the final low gas flow experiment and the two high gas flow experiments was determined by multiplying the rate of formation for

each degradation product by its oxygen stoichiometry (needed to form one mole of product). The first two low gas flow experiments were not considered for total oxygen analysis because amide hydrolysis was not performed and a sulfate internal standard was not used to account for changes in water concentration over the course of the experiment. The O_2 consumption rate only takes into account degradation products that have been discovered and quantified.

Table 5.1 Oxygen (O_2) Stoichiometry for Important Liquid and Gas Phase Oxidative Degradation Products of MEA

Product	**Stoichiometry (ν)**
NH_3	0.0
Formaldehyde	0.25
Formic Acid	0.75
Hydroxyethylimidazole	0.625
Hydroxyethyl-formamide	0.75
NO	1.25
CO_2	1.25
HNO_2	1.5
NO_2	1.75
N_2O	2.0
Oxalic Acid	2.0
HNO_3	2.0

5.2. Experimental Results

Five experiments (three at low gas and two at high gas) were performed at baseline conditions – 7 m MEA with ferrous sulfate added as an oxidation catalyst. Analysis was performed using HPLC and FTIR to quantify amine product degradation and MEA disappearance rates.

5.2.1. Degradation Profiles

Figure 5.2 illustrates the accumulation of liquid phase degradation products over time for a representative low gas flow experiment. Hydroxyethyl-formamide, hydroxyethylimidazole and formate were the most concentrated oxidation products.

Amide concentrations were calculated using two methods: by taking the difference in organic acid concentration in the degraded samples before and after treatment with concentrated sodium hydroxide, and by direct quantification of the amides using HPLC with the ELSD. Analysis shows that for the low gas flow experiment in Table 6.1, the NaOH method underpredicted hydroxyethyl-formamide concentration by approximately 55%. HPLC gave a hydroxyethyl-formamide rate of 0.77 mM/hr, while NaOH addition coupled with anion IC gave a formamide rate of 0.35 mM/hr.

It is possible that the reaction of concentrated NaOH with the degraded MEA sample did not completely reverse the reaction back to MEA and formate, or the amide broke down into other products. Another explanation is that the products formed from the hydrolysis of the hydroxyethyl-formamide reacted with any of the other degradation products in solution to disguise the formate as another substance. Hydroxyethyl-formamide concentration by HPLC-ELSD and formamide by NaOH hydrolysis will be reported separately. Purified solution of the MEA-oxamide cannot be obtained for HPLC verification. Therefore, all oxamide rates reported are reported using the NaOH hydrolysis technique.

HEI, a 5-membered ring structure, is present in the low gas experiment at concentrations similar to hydroxyethyl-formamide. HEI was only found in the low gas flow experiment – it was not detected in the high gas flow experiments. The absence of HEI at high gas rates could be attributed to the stripping of ammonia needed for HEI synthesis. The structure of HEI is shown in Figure 5.1.

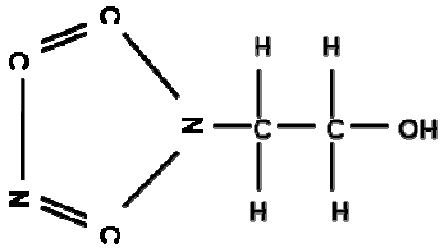

Figure 5.1 Hydroxyethylimidazole Structure

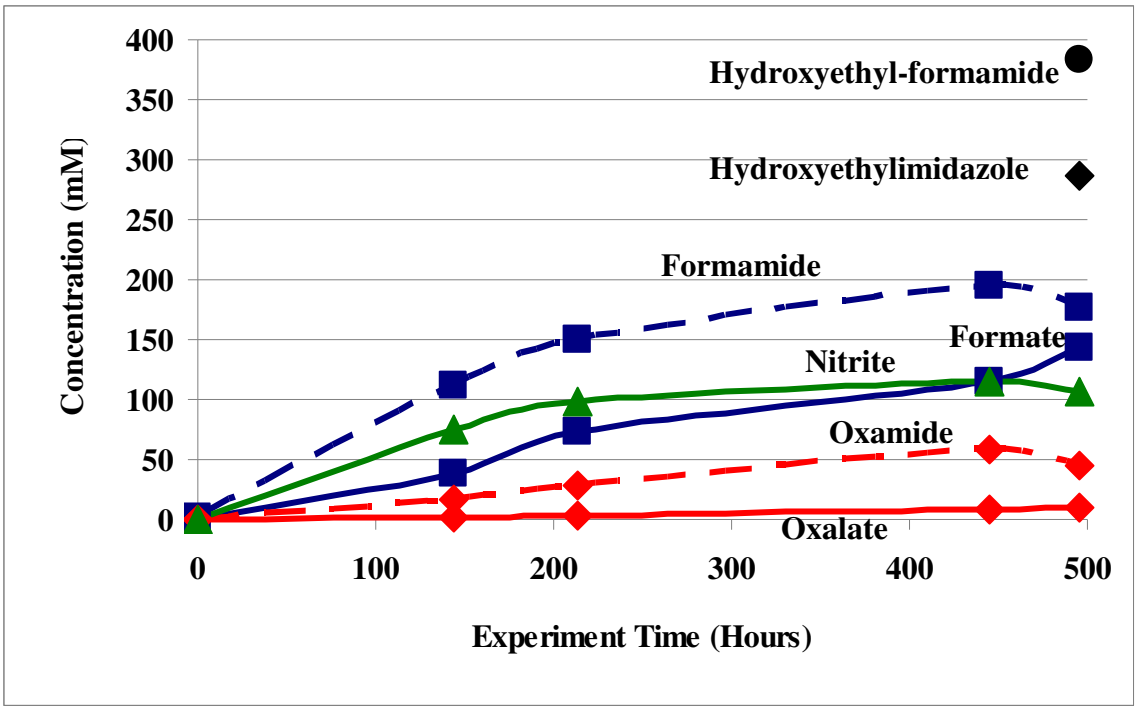

Figure 5.2 Oxidative Degradation of 7 m MEA, 1 mM Fe^{+2}, 0.40 mol CO_2/mol MEA, 55°C, 1400 RPM, 100 cc/min 98%O_2/2%CO_2, Sulfate Correction Included

Figures 5.3 and 5.4 illustrate the concentration profiles of liquid phase oxidative degradation products of MEA at high gas flow. Both experiments were run for approximately 10 days using 15%O_2/2%CO_2 at a flowrate of approximately 7.5 L/min. Formate is the most abundant degradation product; other ionic products were observed in lower concentrations.

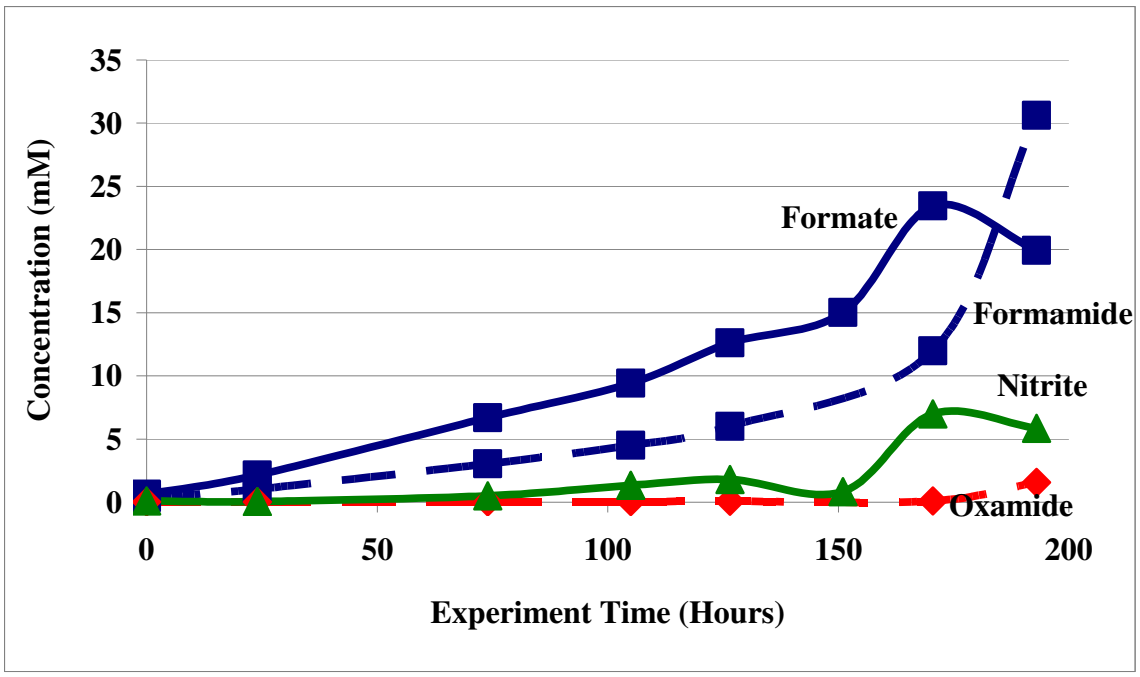

Figure 5.3 Oxidative Degradation of 7 m MEA, 1 mM Fe^{+2}, 0.40 mol CO_2/mol MEA, 55°C, 1400 RPM, 7.5 L/min 15%O_2/2%CO_2, Sulfate Correction Included

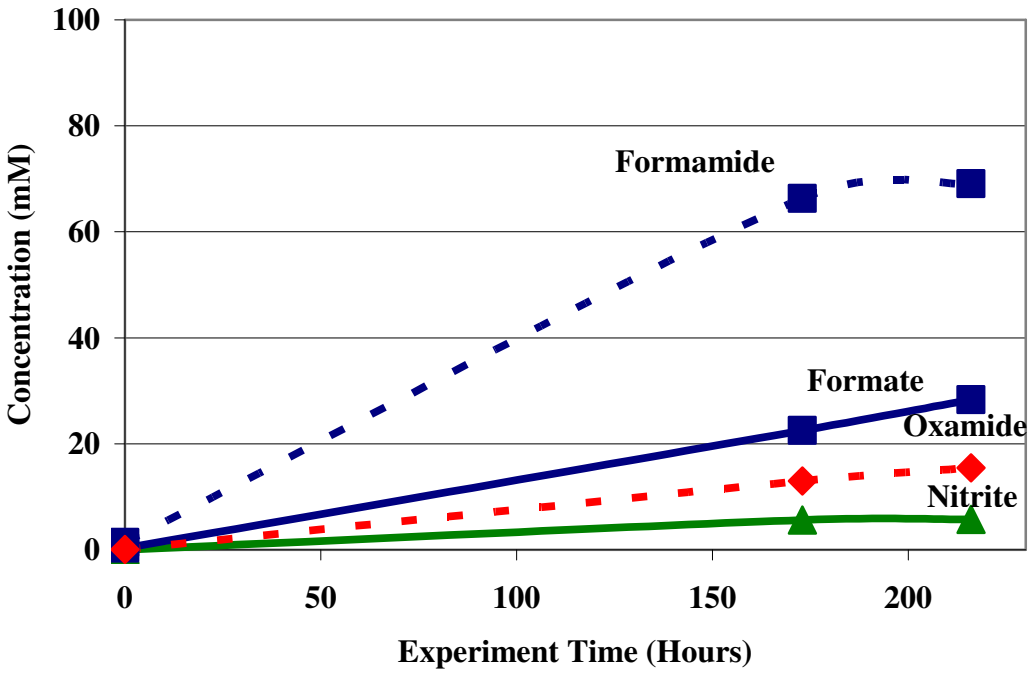

Figure 5.4 Oxidative Degradation of 7 m MEA, 1 mM Fe^{+2}, 0.40 mol CO_2/mol MEA, 55°C, 1400 RPM, 7.5 L/min 15%O_2/2%CO_2, Sulfate Correction Included

Figure 5.5 illustrates the MEA losses versus time for the noted experiments. All MEA disappearance rates appear to be fairly linear. One high gas experiment produced a significantly faster MEA disappearance rate as opposed to the other two experiments; MEA entrainment was problematic in this experiment and may account for this enhanced loss rate. At approximately 200 hours, MEA losses vary by 35% between the other two experiments.

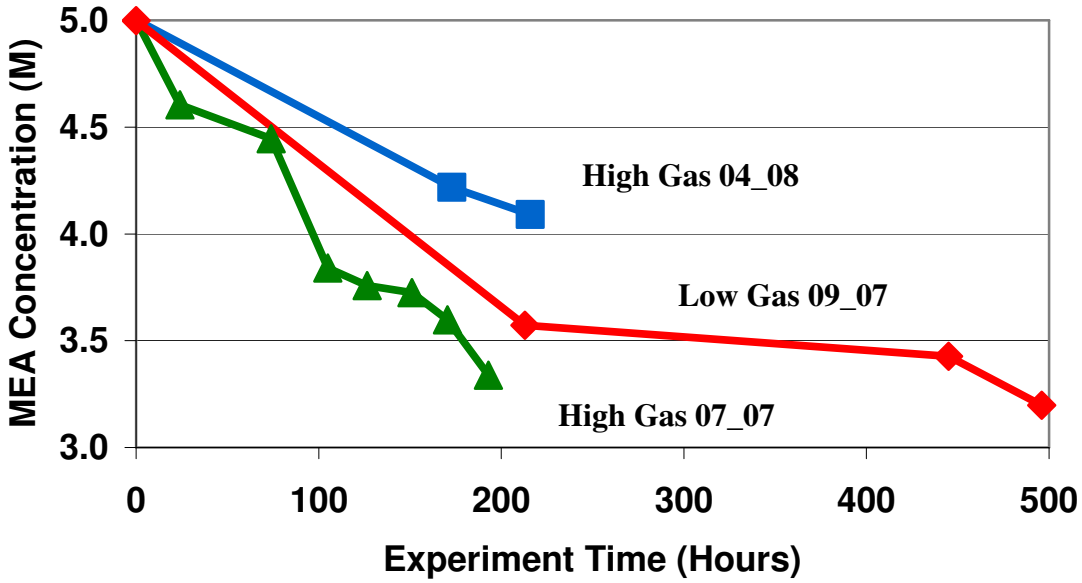

Figure 5.5 MEA Concentration Losses During Degradation Experiments

5.2.2. Material Balance Calculations

Tables 5.2 and 5.3 list formation rates of all quantifiable MEA oxidation products catalyzed by iron. Table 5.2 details rates of formation of major liquid phase products produced at low gas, while Table 5.3 lists significant liquid and vapor phase products detected at high gas. Liquid phase product rates were calculated by dividing the final concentration of each individual component by the total experiment time.

For each volatile component, a continuous plot of concentration (in ppm_v) versus experiment time was constructed and the area under the curve was approximated so that a total concentration of each component evolved during the course of the experiment could be calculated. This value was then converted into a production rate (using total experiment time, molar gas rate and solution volume) in units of mM/hr. MEA volatility was calculated and quantified in the same manner. These volatility measurements were verified by directly injecting vaporized aqueous MEA solutions at known concentrations (carried by nitrogen gas) into the FTIR.

Results from the formation of degradation products listed in Table 5.2 shows that there is a variance in reproducibility between the low gas degradation experiments. Formate and nitrite/nitrate products both vary by approximately 25% between the two low gas experiments conducted in the presence of 7 m MEA. This variance may be accounted for by sample aging – not all samples were analyzed directly after they were withdrawn from the reactor.

Iron catalyst varied between 5 and 50 ppm for all experiments, yet ionic product formation rates were all on the same order of magnitude. It appears that there is a minimum concentration of iron (less than or equal to 5 ppm) in solution that catalyzes degradation controlled by oxygen mass transfer.

Table 5.2 Summary of Oxidative Degradation Product Rates (mM/hr), Low Gas Flow (55°C, 100 cc/min 98%O_2/2%CO_2, α = 0.40, 1400 RPM)

MEA Concentration (m)	**7**	**9**	**7**
Iron Concentration (mM)	**0.6**	**0.1**	**1.0**
Products (mM/hr)			
Hydroxyethyl-formamide			**0.77**
Hydroxyethylimidazole	**N/A**	**N/A**	**0.66**
Formamide	**N/A**	**N/A**	**0.35**
Formate	**0.40**	**0.41**	**0.29**
Nitrite	**0.24**	**0.46**	**0.21**
Nitrate	**0.16**	**0.05**	**0.09**
Oxamide	**N/A**	**N/A**	**0.09**
HPLC Unknown #1, RT=2.4 min			**88.33**
HPLC Unknown #2, RT=3.6 min			**0.68**
HPLC Unknown #3, RT=13.2 min			**0.40**
Derived Results			
Nitrogen Products (mM N/hr)	**0.4**	**0.5**	**2.5**
Carbon Products (mM C/hr)	**0.7**	**0.5**	**6.3**
MEA Loss (mM/hr)	**N/A**	**N/A**	**3.8**
O_2 Consumption Rate (mM/hr)	**1.2**	**1.2**	**1.9**

MEA losses were determined using cation chromatography, using sulfate as an internal standard to account for any changes in water concentration. MEA concentration was calculated by taking the difference between initial and final experimental samples. That rate was normalized by total experimental time in order to compare MEA losses to product formation rates. For example, low gas flow experiment number 3 experienced MEA losses of approximately 4 mM/hr over the course of a 500 hour degradation experiment. That equates to 40% ($\pm$3%) loss of MEA over the course of the experiment (12 weight percent of total solution).

Table 5.3 Summary of Oxidative Degradation Product Rates (mM/hr), High Gas Flow (7 m MEA, 7.5 L/min 15%O_2/2%CO_2, α = 0.40, 1 mM Fe^{+2}, 1400 RPM)

Experiment Date	Jul-07	Apr-08
Products		
NH_3 (g)	1.83	1.69
Formamide (aq)	0.16	0.49
Formate (aq)	0.10	0.18
NO (g)	0.12	0.12
Formaldehyde (g)	0.09	0.02
Acetaldehyde (g)	0.16	0.06
CO (g)	0.30	0.00
N_2O (g)	0.00	0.16
C_2H_4 (g)	0.24	0.00
Oxamide (aq)	0.01	0.10
HPLC Unknown Area, RT=3.6 min	27.27	95.84
HPLC Unknown Area, RT=4.6 min	11.19	32.51
HPLC Unknown Area, RT=13.2 min	2.26	2.85
Derived Results		
MEA Volatile Loss (mM/hr)	2.5	1.1
MEA Degradation Loss (mM/hr)	5.8	2.5
Carbon Products (mM C/hr)	1.5	1.1
Nitrogen Products (mM N/hr)	2.2	2.5
O_2 Consumption Rate (mM/hr)	0.9	1.0

For the high gas experiments, overall MEA loss was calculated using cation chromatography and volatile MEA loss was calculated using FTIR analysis. The difference between these two rates gave an MEA degradation loss rate. The first high gas experiment experienced 32% MEA loss by solution mass, while the second experiment experienced 16% MEA loss. An applicable cation chromatography method was not in place when the first two low gas flow experiments were performed, so MEA loss rates are not available.

Kjeldahl and TC analysis were run on the second high gas experiment to verify the FTIR measurements. FTIR results show that 13% of total nitrogen in solution was lost to either volatility or gas phase degradation, while total nitrogen analysis showed

29% nitrogen losses. TC analysis showed a better agreement than Kjeldahl. FTIR showed 3% carbon losses to the gas phase, while FTIR showed 5% carbon losses.

A total oxygen consumption rate for the final low gas flow experiment and the two high gas flow experiments was determined by multiplying the rate of formation for each degradation product by its oxygen stochiometry (needed to form one mole of product). The first two low gas flow experiments were not considered for total oxygen analysis because amide hydrolysis was not performed and a sulfate internal standard was not used to account for changes in water concentration over the course of the experiment. It is imperative to note that the O_2 consumption rate only takes into account degradation products that have been discovered and quantified.

The oxygen consumption rate calculated for each degradation experiment reveals that despite the differences in the two degradation apparatus, mass transfer capabilities are quite similar. Oxygen consumption rates range from 1.15 to 1.93 mM/hr in the low gas apparatus; in the high gas apparatus, oxygen consumption ranged from 0.93 to 1.15 mM/hr. These oxygen rates only take into account identified products; the rate would increase with the discovery of any additional products. For perspective on how much oxygen is being consumed, 1 mM/hr of oxygen consumption equates to approximately 0.16 cc/min of O_2. Theoretically, oxygen consumption rates will increase as more products are discovered and the gap in the material balance closes.

Carbon and nitrogen formation rates were calculated for each of the degradation experiments by adding up the total number of carbons and nitrogens contained in each liquid and gas phase product. If the material balance for each experiment were to close 100%, then the MEA degradation rate (in mM/hr) would equal the nitrogen formation rate and two times the carbon formation rate. That means that each and every nitrogen and carbon from the fragmented MEA molecules would be accounted for in degradation products.

For the high gas experiments, only 13% to 23% of the degraded MEA carbons have been accounted for in noted degradation products. In the case of degraded MEA nitrogens, 37% to 100% of them are accounted for in degradation products. For the fully

analyzed low gas flow experiment, 65% of the degraded nitrogens and 83% of the degraded carbons are accounted for.

Two conclusions can be drawn from these percentages; first, the material balance is not completely closing for all of the experiments. Next, degradation products with high C to N ratios (or products with zero nitrogens, such as CO_2) have not been identified.

HPLC analysis of the degraded MEA solutions reveals unknown peaks other than HEF and HEI. For example, at low gas conditions in the presence of iron, there is an unknown peak with an area of approximately 88; the peak area for HEI, which was formed at a rate of 0.66 mM/hr during this experiment, was 4.4.

It is important to note that the response of the ELSD is highly non-linear. On average, a tenfold increase in peak area equates to double the actual concentration. The identification and quantification of these unknown peaks would assist in closing the material balance.

The carbon to nitrogen ratio of MEA is 2:1, but in the high gas apparatus the overall C:N ratio from discovered products ranges from 0.45:1 to 0.69:1. On the other hand, in the low gas apparatus (where gas phase products are not analyzed), carbon to nitrogen ratio ranges from 1:1 to 2.5:1. It needs to also be noted that in the first two low gas experiments, sulfate was not used to account for any changes in water concentration. For these experiments, error due to water concentration is upwards of 20%, compared to 2% for experiments conducted with sulfate analysis.

5.3. Conclusions

Formate, hydroxyethyl-formamide and HEI account for 92% of the degraded carbon that has been quantified in the low gas apparatus; they account for 18% to 59% of the degraded carbon in the high gas apparatus. Oxalate (and its respective amide), glycolate and acetate are also present, but at much lower concentrations. The ratio of MEA-formamide to formate varies from 1.2:1 to 2.7:1, while MEA-oxamide to oxalate

varies from 4.5:1 to 10:1. Formate and its hydroxyethyl-formamide are approximately six times more abundant than oxalate in the high gas apparatus and ten times more in the low gas apparatus. We believe the formation of these amides is reversible, especially at stripper conditions. The reversibility of the formation of HEI is unknown at this point in time.

Ammonia, hydroxyethyl-formamide and HEI are the dominant nitrogen-containing degradation products; they account for 84% of the degraded nitrogen in the low gas apparatus and 83% to 92% in the high gas apparatus. At high gas rate, NO_x are produced and stripped from the solution. On the other hand, at low gas rate where gas is not stripped from solution, NO_x is retained in the solution and oxidized to nitrite and nitrate. At high gas rate, NO_x/N_2O production occurs at approximately 15% of the rate of ammonia production. At low gas rate, nitrite/nitrate production occurs at the same rate as NO_x/N_2O production at high gas rate. For the three experiments in which amides were accounted for, the NO_x/N_2O/nitrite/nitrate to formate/formamide ratio is approximately 30% to 45%.

Since ammonia production is 6 times greater than NO_x/N_2O at high gas conditions, it is probably produced at low gas rates as well. This ammonia may exist in gaseous form, in the solution as ammonium cation or tied up with carboxylic acid as formamide or oxamide. Using our current cation chromatography analytical method, ammonium is eluted around the same time as MEA, which is present in concentration at least 100X greater than ammonia. As a result the ammonium peak is hidden under the MEA peak and cannot be effectively separated.

Other volatile degradation products include CO, C_2H_4, formaldehyde and acetaldehyde. In one high gas experiment, these combined product concentrations comprised of 43% of total ammonia production. In the other high gas experiment, they made up 7% of the total ammonia production. Despite the high gas phase product concentrations and inexplicable high MEA losses in the first high gas experiment, overall total carbon and nitrogen production are similar for the two experiments.

The elevated combined concentration of formate, formaldehyde and CO in the first high gas experiment is similar to formate and formaldehyde concentration in the second experiment. Formate is essentially CO dissolved in solution, while formaldehyde is an intermediate in formate production. Likewise, the combination of gas and liquid-phase products containing two carbons from both experiments is similar in total concentration. The data suggests that the first high gas experiment stripped more of the degradation products out of the apparatus.

For all of the products that have been identified using our current analytical capabilities, a number of liquid-phase products that we believe to exist have not been confirmed or dispelled as oxidative degradation products of MEA. The first group of compounds that have yet to be quantified are aldehydes. Organic acids are confirmed present in great quantities, and result from the oxidation of aldehydes in solution.

We attempted to quantify aldehyde concentration per methods developed by Nascimento (1997), but only found aldehydes in trace concentrations in bulk degraded solution. Formaldehyde, acetaldehyde, hydroxyacetaldehyde and glyoxal should be present in measureable quantities, either in pure form or tied up with MEA as imine or amide complexes. Gloxylic acid, an intermediate with carboxylic acid functionality in the formation of oxalic acid, has not been identified either.

Several gas phase products could be passing through the FTIR undetected as well. If the solution possesses high redox potential, then CO_2 and N_2 could be present in the off-gas. Nitrogen gas cannot be detected by the FTIR; however, CO_2 is easily detected using our current methods. According to TIC analysis, an unloaded 7 m MEA experiment run in the presence of 1 mM of iron and 0.5 M potassium formate in the high gas apparatus produced CO_2 at a rate of 0.10 mM/hr. This rate of CO_2 production is not enough to close the carbon gap in the material balance. It is very likely that the gap in the material balance lies with the unidentified peaks that appear using evaporative light scattering detection. A comparison of total carbon and nitrogen production rates to MEA losses show that 25 to 50% of oxidative degradation products currently remain unaccounted for.

Chapter 6: Effect of Catalysts and Inhibitors on the Oxidative Degradation of MEA

Aqueous monoethanolamine (MEA) solutions were batch loaded into 500 mL glass jacketed reactors and subjected to oxidative degradation at both low and high gas rates. Solutions were degraded with 100 mL/min of 98%O_2/2%CO_2 with mass transfer achieved by vortexing. Samples were drawn from the reactor during the course of the experiment and analyzed for degradation using ion chromatography. In a parallel apparatus 7.5 L/min of 15% O_2/2% CO_2 was sparged through 350 mL of solution; additional mass transfer was achieved by vortexing. A Fourier Transform Infrared Analyzer collected continuous gas-phase data on amine volatility and volatile degradation products.

Low gas flow experiments show that hydroxyethyl-formamide and hydroxyethylimidazole (HEI) are the major oxidation products of MEA. In the presence

of Fe and Cu, hydroxyethyl-formamide, HEI and MEA losses increase by a factor of 3 as compared to a system in the absence of iron. Data from the high gas flow experiments support these findings.

Chromium and nickel, two metals present in stainless steel alloys, also catalyze the oxidative degradation of MEA. Observed carbon and nitrogen product rates are 20% lower than in an iron catalyzed system, but MEA losses are 55% greater. MEA systems catalyzed by 1 mM vanadium degrade at a rate 50% slower than in the presence of iron. In terms of oxidative degradation potential: copper > chromium/nickel > iron > vanadium.

Inhibitors A and B and EDTA are effective degradation inhibitors. The presence of 100 mM Inhibitor A decreases the formation of known degradation products by 90% in an MEA system catalyzed by Fe and Cu and by 99% in Cr/Ni systems. FTIR analysis from high gas experiments shows a similar decrease in ammonia production.

Inhibitor B decreases product rates by 97% and MEA losses by 75%. A 100:1 ratio of EDTA to Fe is necessary to sufficiently inhibit the oxidation of MEA. At this ratio, no observable MEA losses or oxidative degradation products are detected.

The addition of formaldehyde, formate or sodium sulfite had an unintended effect on MEA losses. They actually increased the rate at which MEA degraded. While observed products decreased, MEA losses increased by 20% to 30% in the presence of these potential inhibitors.

Total carbon and nitrogen analysis shows that with the exception of the low gas experiment performed in the presence of Cr and Ni catalyst, there is over a 90% material balance on all selected low and high gas flow experiments.

6.1. Introduction

The oxidation potential of Fe, Cu, Cr, Ni and V were all evaluated at low gas rate; only Fe and Cu were evaluated at high gas as well. Sulfite, EDTA, formaldehyde, formate and proprietary inhibitors A and B were tested at low gas conditions.

Due to the corrosive nature of alkanolamine solvents, corrosion inhibitors must be added to solutions to prevent equipment destruction. These corrosion inhibitors are usually heavy metal salts of vanadium or copper (Asperger et al. 1998; Mago et al. 1984; Pearce 1984; Pearce et al. 1984; Ranney 1976). Several studies have shown that the oxidation of MEA is catalyzed by dissolved metals, including Fe, Cu and V (Girdler 1950; Blachly and Ravner 1964; Blachly and Ravner 1963; Chi and Rochelle 2002; Hofmeyer et al. 1956). Degradation and corrosion are closely related since degradation products have been shown to increase corrosion rates (Polderman et al. 1955; Tanthapanichakoon et al. 2003).

Blachly and Ravner (1963) examined the effects of metals as oxidation catalysts in MEA systems. Concentrations of copper up to 15 ppm, iron up to 30 ppm and chromium up to 37 ppm were studied; effects of bulk nickel metal were also detailed in the report, but exact nickel concentration was not specified.

They determined that dissolved copper at concentrations as low as 10 ppm was sufficient to cause serious degradation of the amine solution, and that the rates of copper catalyzed degradation were higher than iron catalyzed degradation at the same concentrations. A concentration of 3.7 ppm of nickelous ion had no impact on MEA oxidation, but a tenfold increase in concentration caused noticeable degradation.

Goff (2004) focused studies on Cu and Fe catalyzed degradation since vanadium is not known to be used commercially in any MEA applications. Goff found that for a given set of reaction conditions, copper had a greater catalytic effect than iron on MEA systems.

6.2. Experimental Results

Oxidation experiments were performed at high and low gas rates under varying inhibitor and catalyst conditions. Tables 6.2 through 6.7 list formation rates of all quantifiable oxidative degradation products. Liquid phase product rates were calculated

by dividing the final concentration of each individual component by the total experiment time.

For each volatile component, the continuous production rate is integrated over the entire experiment and reported as an average rate (mM/hr). MEA volatility was calculated and quantified in the same manner.

Amide concentrations were determined by both HPLC (HEF only) and anion IC (all general amides). However, HPLC is believed to give a more reliable concentration for formamide. Therefore, it has been used in all material balances. Concentrations for unknown peaks from HPLC were estimated using the calibration curve for HEI.

Total MEA loss is calculated from initial and final MEA as determined by cation IC; loss rates less than 0.3 mM/hr are too small to detect using this method. For the high gas experiments, overall MEA loss was calculated using cation chromatography and volatile MEA loss was calculated using FTIR. The difference between these two rates gave an MEA degradation loss rate.

The total carbon and nitrogen in products was calculated without including formamide by IC or unknowns by HPLC. Nitrogen in solution was determined using Kjeldahl analysis; total organic carbon in solution was calculated using a Shimadzu TOC analyzer. The nitrogen imbalance is nitrogen unaccounted for after MEA nitrogen and product nitrogen concentrations are subtracted from total nitrogen in solution; the carbon imbalance is calculated in a similar manner.

A major conclusion from Goff (2005) is that in the presence of metal catalysts, the rate of evolution of NH_3 is controlled by the rate of oxygen absorption under experimental and industrial conditions. Goff's assertion was that 1 degraded mole of MEA resulted in 1 mole of ammonia. Ammonia evolution rates increased with agitation rate and increased linearly with oxygen concentration.

Goff (2005) proposed that MEA reacts with oxygen to form ammonia and other carbon containing degradation products. Each of the major degradation products has a specific oxygen stoichiometry, which is listed in Table 6.1.

$$C_2H_7NO + \nu O_2 \rightarrow NH_3 + \text{product} \quad 6.1$$

$$NH_3 + \nu O_2 \rightarrow H_2O + \text{product} \quad 6.2$$

A total oxygen consumption rate was determined by multiplying the rate of formation for each degradation product by its oxygen stoichiometry (needed to form one mole of product). Low gas flow experiments shown in Table 6.3 were not considered for total oxygen consumption analysis because amide hydrolysis was not performed and a sulfate internal standard was not used to account for changes in water concentration over the course of the experiment. The O_2 consumption rate only takes into account degradation products that have been discovered and quantified.

Table 6.1 Oxygen Stoichiometry for Important Liquid and Gas Phase Oxidative Degradation Products of MEA

Product	Stoichiometry (ν)
NH_3	0.0
Formaldehyde	0.25
Formic Acid	0.75
Hydroxyethylimidazole	0.625
Hydroxyethyl-formamide	0.75
NO	1.25
CO_2	1.25
HNO_2	1.5
N_2O	2.0
Oxalic Acid	2.0

6.2.1. Effect of Catalyst at Low Gas Rates

Low gas experiments detailed in Table 6.2 were performed in an attempt to quantify how metal catalysts affect the oxidative degradation of MEA. The effects of vanadium on MEA are unknown. Blachly and Ravner (1963) detailed the catalytic

effects of dissolved Fe, Cu, Cr and Ni on MEA oxidation. Fe is a corrosion product in carbon steel systems, while Cu has been suggested as a corrosion inhibitor. If stainless steel construction were used on the absorber, it is possible that Cr and Ni could leach into the amine system.

Figures 6.1 and 6.2 illustrate the formation of major oxidative degradation products for systems catalyzed by Fe only as well as Fe and Cu. Major degradation products include hydroxyethylimidazole, hydroxyethyl-formamide, and formate. Amide concentrations were calculated using two methods: by taking the difference in organic acid concentration in the degraded samples before and after treatment with concentrated sodium hydroxide, and by direct quantification of the amides using HPLC with the ELSD. HEF and HEI concentrations are available only for final experimental samples.

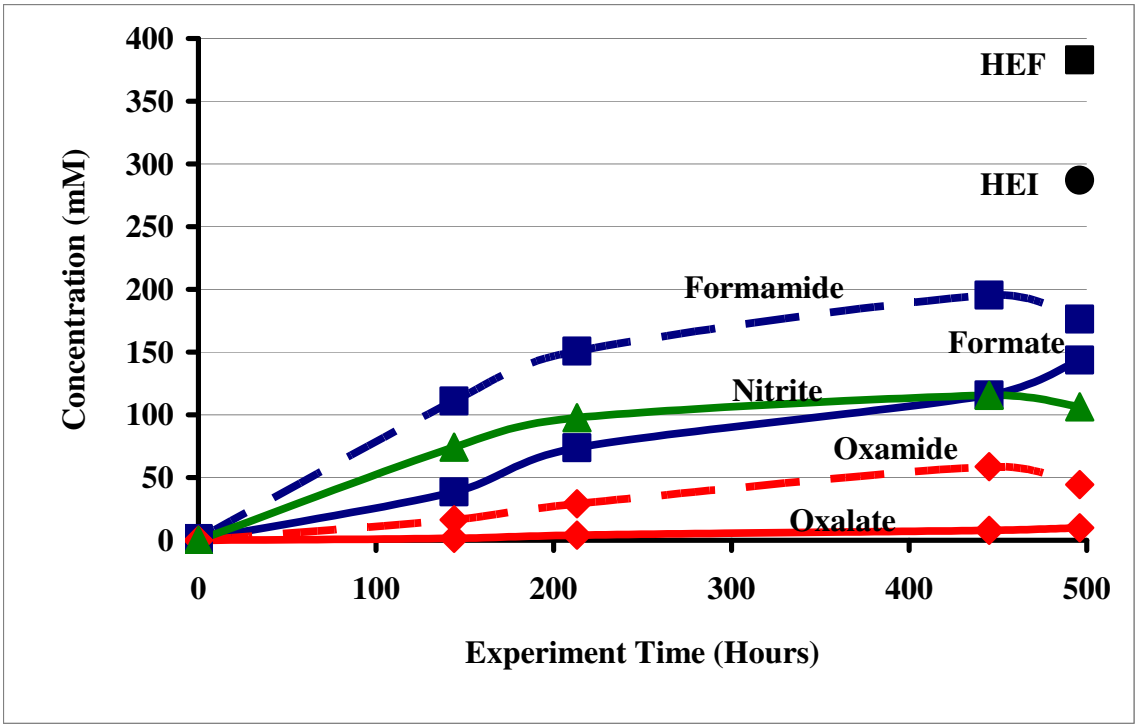

Figure 6.1 Oxidative Degradation of 7 m MEA, 1 mM Fe^{+2}, 0.40 mol CO_2/mol MEA, 55°C, 1400 RPM, 100 cc/min 98%O_2/2%CO_2, Sulfate Correction Included

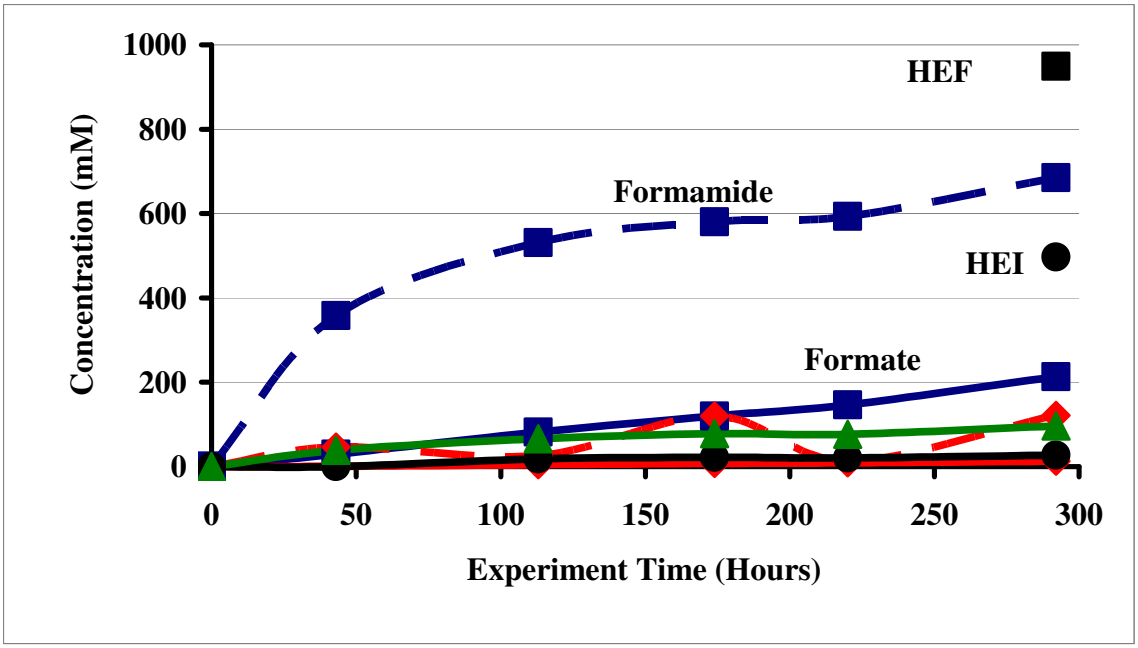

Figure 6.2 Oxidative Degradation of 7 m MEA, 0.1 mM Fe^{+2}, 5 mM Cu^{+2}, 0.40 mol CO_2/mol MEA, 55°C, 1400 RPM, 100 cc/min 98%O_2/2%CO_2, Sulfate Correction Included

Low gas experiments detailed in Table 6.2 were performed in an attempt to quantify how metal catalysts affect the oxidative degradation of MEA. In the case of all four catalyst combinations, HEI, formamide and formate are the most abundant degradation products. The production rate of hydroxyethyl-formamide is almost an order of magnitude higher in the presence of Fe and Cu when compared to the Fe catalyzed experiment, while the production of hydroxyethylimidazole increases by a factor of three. This results in a carbon formation rate that is approximately three times greater, and an MEA loss rate that is over double from when copper is absent from solution.

The addition of copper to an oxidized MEA solution appears to enhance the mass transfer characteristics of the solution; the oxygen consumption rate of this system is considerably higher than the other catalyzed systems. On the other hand, vanadium catalyzed systems exhibit lower MEA losses and oxygen consumption rates. Goff's major conclusion was that all catalyzed systems were oxygen mass-transfer controlled, but the data does not reflect that. However, the unidentified degradation products may

affect these calculated oxygen consumption rates. In terms of greatest to lowest oxidation potential for MEA systems, Fe/Cu (combined) > Cr/Ni (combined) > Fe > V.

Table 6.2 shows that 7m MEA catalyzed with 1 mM of sodium metavanadate is degraded less than in the presence of 1 mM Fe, which serves as our base case for comparison. There is a noticeable shift from the production of formate to oxalate (as well as their respective amides), but overall formation of carbon products is 75% lower in the presence of vanadium. Nitrogen production (in the form of nitrite/nitrate) is also 75% lower in the vanadium catalyzed experiment, and MEA losses are approximately cut in half as opposed to the iron catalyzed experiment. This decrease in carbon and nitrogen products is attributed the two major degradation products: hydroxyethyl-formamide and hydroxyethylimidazole (HEI).

Analysis shows formamide analysis by anion IC does not agree with direct HPLC analysis for hydroxyethyl-formamide. It is possible that the reaction of concentrated NaOH with the degraded MEA sample did not completely reverse the reaction back to MEA and formate, or the amide broke down into other products. Another explanation is that the products formed from the hydrolysis of the hydroxyethyl-formamide reacted with any of the other degradation products in solution to disguise the formate as another substance. As a result, these two formamide numbers will be reported separately.

Carbon and nitrogen formation rates in the experiment catalyzed by both chromium and nickel are approximately 15% lower than in the iron catalyzed experiment; most of this is accounted for by the decreased production of hydroxyethylimidazole. There is once again a noticeable shift from formate (and formamide) to oxalate production. However, measured MEA losses are 53% greater. This suggests that there are signifcant degradation products unaccounted for in this experiment.

Table 6.2 Effect of Metal Catalyst on Oxidative Degradation Product Rates (mM/hr), Low Gas (350 mL, 7 m MEA, 55°C, 100 cc/min 98%O_2/2%CO_2, α = 0.40, 1400 RPM)

Catalyst Concentration (mM)	**1 Fe**	**1 V**	**0.6 Cr / 0.1 Ni**	**0.1 Fe / 5 Cu**
Results (mM/hr)				
MEA Loss	**3.8**	**2.1**	**8.0**	**10.3**
Carbon in Products	**6.3**	**1.6**	**5.3**	**20.0**
Nitrogen in Products	**2.5**	**0.6**	**2.1**	**7.1**
O_2 Consumption	**1.9**	**0.7**	**1.8**	**5.6**
HPLC (mM/hr)				
HEI	**0.66**	**0.11**	**0.59**	**1.70**
HEF	**0.77**	**0.10**	**0.00**	**3.25**
Total Unknowns	**2.28**	**0.49**	**2.91**	**1.49**
HPLC Unknowns (Dilute Area)				
Unknown #1, RT=2.4 min	**88.33**	**91.93**	**122.13**	
Unknown #2, RT=3.2 min			**1.30**	**39.13**
Unknown #3, RT=3.6 min	**0.68**	**145.50**		**35.76**
Unknown #4, RT=4.6 min		**5.14**	**2.14**	**54.05**
Unknown #5, RT=13.2 min	**0.40**	**5.99**	**1.26**	**13.67**
Anion IC (mM/hr)				
Formate	**0.29**	**0.06**	**0.29**	**0.73**
Formamide	**0.35**	**0.12**	**0.43**	**2.35**
Oxamide	**0.09**	**0.15**	**0.19**	**0.42**
Nitrite	**0.21**	**0.05**	**0.23**	**0.29**
Derived Results				
N in Solution (M)			**4.14**	
C in Solution (M)		**10.00**	**9.82**	**8.73**
N Imbalance (mM/hr)			**3.31**	
C Imbalance (mM/hr)		**2.88**	**10.15**	**0.00**

$$\text{Carbon in Products} = \Sigma\,(\text{Number of Carbon Atoms})_i * \text{Production Rate}_i\ (\text{mM/hr}) \quad 5.3$$

$$\text{Nitrogen in Products} = \Sigma\,(\text{Number of Nitrogen Atoms})_i * \text{Production Rate}_i\ (\text{mM/hr}) \quad 5.4$$

$$O_2\ \text{Consumption} = \Sigma\,\nu_i * (\text{Production Rate})_i * \text{Production Rate}_i\ (\text{mM/hr}) \quad 5.5$$

$$\text{N Imbalance} = (\text{Kjeldahl Solution N} - \text{MEA N} - \text{Degradation Product N}) / \text{Time} \quad 5.6$$

$$\text{C Imbalance} = (\text{TOC Solution C} - \text{MEA C} - \text{Degradation Product C}) / \text{Time} \quad 5.7$$

Where:
i = individual degradation product
ν = oxygen stoichiometry
Note: U denotes an undiluted HPLC peak area; other areas are from 10X diluted samples

Volatile carbon from low gas experiments is determined using TC analysis. Undegraded 7 m MEA (α = 0.4) was run using TC analysis and used as a control for carbon concentration. Any difference in TC for the low gas experiments was assumed to be carbon that had escaped either as amine volatility or a carbon-containing gaseous product. MEA carbon was calculated by determining the MEA concentration in each of the final degraded samples. With the exception of the experiment performed in the presence of chromium and nickel, the carbon material balance ranges from 87% to 104%.

Volatile nitrogen is determined using Kjeldahl analysis. Undegraded 7 m MEA (α = 0.4) was analyzed using Kjeldahl analysis and used as a control for total nitrogen count. Any loss of total nitrogen in solution for the low gas experiments was assumed to be nitrogen that had escaped either as amine volatility or a nitrogen-containing gaseous product (NH_3 or NO_x). MEA nitrogen was calculated by determining the MEA concentration in each of the final degraded samples. The nitrogen material balance ranges from 92% to 101% for the selected low gas experiments.

If the material balance for each experiment were to close completely, then the MEA degradation rate (in mM/hr) would equal the nitrogen formation rate and two times the carbon formation rate. That means that each and every nitrogen and carbon from the fragmented MEA molecules would be accounted for in degradation products. The gap in the overall carbon and nitrogen material balances is attributed to peaks that still have not been identified using HPLC with the evaporative light scattering detector. While HEF and HEI have been positively identified, unknown peaks consistently show up when degraded MEA samples are analyzed using HPLC-ELSD.

The evaporative light scattering detector gives a highly non-linear response. On average, a dilution factor of ten reduces peak response by a factor of 100. That is why some samples were analyzed undiluted on the HPLC; any dilution decreased peak areas to the noise range. Most degraded samples containing Fe only have at least 90% of raw peak area unidentified. On the other hand, only 18% to 52% of peak area remains unidentified for degradation experiments conducted in the presence of copper catalyst. This information suggests that the formation of HEF is favored when Cu is present.

Oxygen consumption rates range from 0.7 to 5.6 mM/hr for low gas experiments performed in the absence of effective oxidative degradation inhibitors; mass transfer of oxygen into the interfacial layer of liquid determines the degradation rate for these low gas experiments. The presence of copper enhances mass transfer such that the reaction is taking place in the boundary layer.

Experiments performed in the presence of iron as well as a combination of chromium and nickel gave similar O_2 rates. The low rate produced in the presence of vanadium suggests MEA degradation may not be completely mass transfer controlled in the presence of vanadium catalyst. It is important to note that oxygen rates do not take unidentified products into account.

Table 6.3 lists liquid-phase degradation product formation rates for a group of low gas experiments performed prior to the development of amide and total amine analysis. 7 m MEA was degraded in the presence of iron, copper and a combination of the two. In addition, low gas degradation experiments were carried out in the presence of iron, copper and Inhibitor A. Formate was the most abundant carbon-containing ionic product, while nitrite was the major nitrogen-containing ionic product.

An MEA solution degraded in the presence of an equimolar mixture of Fe and Cu behaves similarly to a degraded 7 m MEA solution degraded in the presence of minimal iron (0.1 mM) and high copper (5 mM), which was chosen to represent an industrial system in which copper is added to inhibit corrosion. Formate production rates are very similar, and they both exceed MEA systems which contain copper only and iron only. Moreover, carbon and nitrogen formation rates are on the same order of magnitude – they were not expected to be identical because a complete material was not available.

The major difference is in the amount of nitrite/nitrate production. In the equimolar Fe/Cu catalyst system, nitrite/nitrate production rate is approximately halfway between nitrite/nitrate production for iron only and copper only systems. The Fe/Cu catalyst system with a 50:1 Cu to Fe ratio produced nitrite/nitrate formation rates very similar to a copper only system. The combination of iron and copper has an additive effect on the production of formate, the major ionic carbon containing liquid phase

degradation product, while nitrite/nitrate production is an average effect determined by the copper to iron ratio.

The data also suggests that there is a minimum concentration of catalyst that oxidizes MEA. A 7 m MEA solution containing over 5 mM of metal catalyst is oxidized at approximately the same rate as a 7 m MEA solution containing approximately 1mM of total catalyst. Any catalyst concentration above this minimum threshold has no additional effect on amine oxidation.

The addition of 100 mM Inhibitor A to the same Fe/Cu catalyzed system proved successful in slowing down the formation of observed products. The formation of all carbon and nitrogen containing products was decreased by approximately 90%.

Table 6.3 Oxidative Degradation Product Rates (mM/hr), Low Gas Flow (7 m MEA, 55°C, 100 cc/min 98%O_2/2%CO_2, α = 0.40, 1400 RPM)

Iron Concentration (mM)	**0.6**	**-**	**0.6**	**0.1**	**0.1**
Copper Concentration (mM)	**-**	**0.6**	**0.6**	**5**	**5**
Inhibitor A Concentration (mM)	**-**	**-**	**-**	**-**	**100**
Products (mM/hr)					
Formate	**0.40**	**0.39**	**0.67**	**0.66**	**0.04**
Derived Results					
Nitrogen Products (mM/hr N)	**0.46**	**0.21**	**0.33**	**0.24**	**0.04**
Carbon Products (mM/hr C)	**0.54**	**0.52**	**0.85**	**0.78**	**0.10**

6.2.2. Effect of Catalyst at High Gas Rates

Table 6.4 lists both liquid-phase and gas-phase product rates for MEA degradation experiments conducted in the high gas flow apparatus. For each volatile component, the continuous production rate is integrated over the entire experiment and reported as an average rate (mM/hr). MEA volatility was calculated and quantified in the same manner. Overall MEA loss was calculated using cation chromatography and volatile MEA loss was calculated using FTIR analysis. The difference between these two rates gave an MEA degradation loss rate.

Table 6.4 Effect of Iron and Copper Catalyst on Oxidative Degradation Product Rates (mM/hr), High Gas (350 mL, 7 m MEA, 7.5 L/min 15%O_2/2%CO_2, α = 0.40, 1400 RPM)

Catalyst (mM)	1 Fe		0.1 Fe / 5 Cu	
Experiment Date	Jul-07	Apr-08	Nov-07	May-08
Results (mM/hr)				
MEA Loss	5.8	3.8	3.5	5.3
C in Products	1.5	1.1	4.8	5.0
N in Products	2.0	2.0	3.5	4.0
O_2 Consumption	0.9	1.1	1.9	1.8
HPLC (mM/hr)				
HEF	0.00	0.00	0.87	0.91
HEI	0.00	0.00	0.23	0.29
Unknown Peaks	0.54	0.50	0.60	0.45
HPLC Unknown Peaks (Raw Area)				
Unknown #1, RT=3.2 min			42.57	39.13
Unknown #2, RT=3.6 min	27.27	95.84	32.27	35.76
Unknown #3, RT=4.6 min	11.19	32.51	81.65	54.05
Unknown #4, RT=13.2 min	2.26	2.85	13.31	13.67
Anion IC (mM/hr)				
Formate	0.10	0.18	0.53	0.22
Formamide	0.16	0.49	0.92	1.05
Oxamide	0.01	0.10	0.05	0.11
FTIR (mM/hr)				
NH_3	1.83	1.69	1.69	1.97
CO	0.30	0.00	0.00	0.00
N_2O	0.00	0.16	0.16	0.14
NO	0.12	0.12	0.12	0.06
C_2H_4	0.24	0.00	0.00	0.00
Formaldehyde	0.09	0.02	0.02	0.01
Acetaldehyde	0.16	0.06	0.06	0.02
MEA Volatile Loss	2.5	3.2	3.2	1.9
Derived Results				
N in solution (M)		4.33		4.39
C in solution (M)		9.52		9.78
N Imbalance (mM/hr)		0.46		1.66
C Imbalance (mM/hr)		3.94		8.90

Note: All unknown HPLC peak areas are from undiluted samples

The major difference, product wise, between the iron catalyzed experiment and the combined iron and copper catalyzed experiment is the increase in formate and HEF production. HEF production increases by factor of two when copper is added in the high gas apparatus. Hydroxyethylimidazole is only detected in the high gas apparatus in the presence of iron and copper. HEI is present in much lower concentrations when MEA is degraded at high gas conditions. The decrease in HEI concentration at high gas rates could be attributed to the stripping of ammonia needed for HEI synthesis.

Gas-phase aldehydes, whose concentrations are minor compared to the amides, decrease in production when MEA is degraded in the presence of iron and copper. This suggests that the aldehydes are reacting faster in the presence of both iron and copper, leaving a lower concentration in solution subjected to being stripped out of solution. All other major degradation product formation rates, including ammonia, are similar between the two systems. This disagrees with Goff's assertion that both copper and iron individually produced different steady-state ammonia formation rates for MEA.

In experiments with high gas flow, TC analysis was compared to total carbon concentration calculated from vapor products and amine volatility, and the results matched within 5%. For the selected high gas experiments, Kjeldahl analysis was compared to total nitrogen concentration calculated from vapor products and amine volatility, and the results matched within 5%.

For high gas degradation experiments conducted in the presence of iron and copper, 48% to 68% of the degraded MEA carbons have been accounted for measured degradation products; 75% to 100% of the nitrogen loss has been accounted for in degradation products. Although the material balance is not closed, the gap is smaller for the experiments conducted in the presence of iron and copper. The carbon to nitrogen ratio ranges from 1.25:1 to 1.38:1 for this set of experiments.

In the high gas apparatus, oxygen consumption ranged from 0.9 to 1.9 mM/hr. Rates increased by approximately 85% in the presence of copper and iron versus iron only. These oxygen rates only take into account identified products; the larger gap in the material balance for the iron experiments should account for this oxygen difference.

6.2.3. Successful Inhibitors at Low Gas Rates

Results listed in Tables 6.5 through 6.7 represent catalyzed MEA systems run under inhibited conditions. Na_2SO_3 is a known oxygen scavenger that is used in a range of applications varying from boiler feedwater treating to food packaging (Somogyi 2008; White 2001; Hakka and Ouimet 2004). The kinetics of sulfite oxidation in aqueous solutions are known to be very fast, and the rate of oxidation is controlled by the rate of oxygen absorption (Ulrich 1983; Lee 1986). SO_2 reacts quickly with O_2 in MEA solutions to form sulfate (SO_4^{-2}), forming a heat stable salt with MEA (Kohl and Nielsen 1997). Previous studies have shown that sulfite oxidation shows a square root dependence on catalyst concentration, independent of the metal being used (Barron et al. 1966; Conklin et al. 1988; Bengtsson et al. 1975; Chen et al. 1972).

Formaldehyde is an expected intermediate in the oxidative degradation of MEA (Goff 2004; Goff 2005; Chi 2000; Rochelle et al. 2001). Moreover, formate is an observed degradation product that comes from the oxidation of formaldehyde (Fessenden and Fessenden 1994; Rooney et al. 1998). Since both of these products likely compete with MEA for oxygen, they are suitable compounds to screen as degradation inhibitors. Although formaldehyde itself is considered toxic under the Clean Air Act (2008), the presence of oxygen should oxidize the formaldehyde to formate, or it may react with MEA to form hydroxyethyl-formamide.

Goff (2005) and Table 6.3 have proven Inhibitor A to be effective under iron and copper catalyzed MEA systems, so it was necessary to test its effectiveness in the presence of Cr and Ni. Inhibitor B is another inorganic additive that was tested for effectiveness as a degradation inhibitor in the presence of iron. EDTA has been identified as an excellent chelating agent in the presence of copper and iron catalyst (Blachly and Ravner 1964; Chi 2000; Blachly and Ravner 1965; Goff et al. 2003). EDTA has four active sites that can react with metals in solution and effectively bind the metal ions, thereby preventing them from catalyzing free radical reactions that promote oxidative

degradation. Chelation constants have been determined for Fe-EDTA and Cu-EDTA complexes (Sunda and Huntsman 2003; Olivieri and Escandar 1997).

Fe is a known catalyst for EDTA oxidation (Seibig et al. 1997). Iminodiacetic acid (diglycine), glyoxylic acid and cyanate have all been identified as anionic degradation products of EDTA in the presence of UV and H_2O_2 (Sorensen et al. 1998). All of these anions were tested as the unknown peak and came back negative. However, Sorensen also states that in oxidation processes where iron is present, EDTA can degrade into ethylenediaminetriacetate (ED3A), ethylenediaminediacetate (EDDA) and ethylenediaminemonoacetate (EDMA).

It is also important to determine if EDTA is being oxidized from a cost standpoint. EDTA is an expensive additive – an order of magnitude more expensive than MEA. Even if EDTA is being oxidized very slowly, the cost of continually adding EDTA to a commercial system outweighs its benefits as an amine oxidation inhibitor. EDTA does give a peak using anion chromatography, but it has a very strong response.

Table 6.5 shows that Inhibitor A is an extremely effective oxidative degradation inhibitor for MEA systems in the presence of chromium and nickel (over a 99% decrease in the formation of all detectable products). Moreover, MEA loss rate was decreased by a factor of eight and is approaching the detection limits of the cation chromatography system.

Experimental results also show Inhibitor B to be extremely effective at inhibiting degradation in the presence of iron catalyst. Carbon and nitrogen-containing products are decreased by 97%, while MEA loss rates were reported in the range of the inhibited Cr/Ni system – only 25% the MEA loss rate of an uninhibited system catalyzed by iron. Rates for experiments performed under inhibited conditions ranged from 0.0 to 0.9 mM/hr; the degradation rate in these types of experiments is expected to be limited by reaction kinetics.

Figure 6.3 illustrates the effect of EDTA:Fe ratio on nitrogen and carbon production, as well as MEA losses. The figure shows that the addition of EDTA has an exponential effect as an oxidative degradation inhibitor. A concentration of 100 mM

EDTA completely inhibits any MEA degradation. Table 6.6 lists details the product rates illustrated in Figure 6.3. Both degradation product formation and MEA loss decrease as EDTA concentration is increased. This suggests that in high enough concentrations, EDTA is effective at chelating Fe and inhibiting the formation of observable oxidative degradation products. The major issue with using EDTA in an industrial application as an inhibitor is corrosion. Corrosion creates an endless supply of Fe to complex with EDTA, and the EDTA will continue to complex the iron until all of its active sites are unavailable. The EDTA/Fe complex would have to be reclaimed or fresh EDTA would have to be added to the solution – the latter of which is not an economically viable option.

Table 6.5 Effect of Successful Degradation Inhibitors on Oxidative Degradation Product Rates (mM/hr), Low Gas (350 mL, 7 m MEA, 55°C, 100 cc/min 98%O_2/2%CO_2, α = 0.40, 1400 RPM)

Catalyst Concentration (mM)	**1 Fe**	**0.6 Cr / 0.1 Ni**	**1 Fe**
Inhibitor Concentration (mM)	**-**	**100 A**	**7.5 B**
Results (mM/hr)			
MEA Loss	**3.8**	**1.0**	**1.2**
Carbon in Products	**6.3**	**0.0**	**0.1**
Nitrogen in Products	**2.5**	**0.0**	**0.0**
O_2 Consumption	**1.9**	**0.0**	**0.2**
HPLC (mM/hr)			
HEI	**0.66**	**0.00**	**0.00**
HEF	**0.77**	**0.00**	**0.00**
Total Unknowns	**2.28**	**0.00**	**0.00**
Anion IC (mM/hr)			
Formate	**0.29**	**0.00**	**0.04**
Formamide	**0.35**	**0.00**	**0.10**
Oxamide	**0.09**	**0.00**	**0.03**
Nitrite	**0.21**	**0.00**	**0.00**
Derived Results			
N in solution (M)		**4.77**	**4.77**
C in solution (M)		**5.00**	**5.00**
N Imbalance (mM/hr)		**0.00**	**0.09**
C Imbalance (mM/hr)		**1.91**	**2.15**

Table 6.6 Effect of EDTA Concentration on Oxidative Degradation Product Rates (mM/hr), Low Gas (350 mL, 7 m MEA, 1 mM Fe^{+2}, 55°C, 100 cc/min 98%O_2/2%CO_2, α = 0.40, 1400 RPM)

EDTA Concentration (mM)	0	2	10	100
Results (mM/hr)				
MEA Loss	3.8	8.6	1.5	0.1
Carbon in Products	6.3	3.8	0.7	0.0
Nitrogen in Products	2.5	1.4	0.2	0.0
O_2 Consumption	1.9	0.9	0.2	0.0
HPLC (mM/hr)				
HEI	0.66	0.37	0.06	0.00
HEF	0.77	0.50	0.09	0.01
Total Unknowns	2.28	0.53	0.10	0.06
HPLC Unknowns (Raw Area)				
Unknown #1, RT=2.4 min	88.33 (D)	112.21		
Unknown #2, RT=3.2 min		9.98		
Unknown #3, RT=3.6 min	0.68 (D)	79.48	27.95	10.94
Unknown #4, RT=4.6 min		30.13	9.68	
Unknown #5, RT=13.2 min	0.40 (D)	89.52	6.51	
Anion IC (mM/hr)				
Formate	0.29	0.05	0.06	0.01
Formamide	0.35	0.21	0.10	0.00
Oxamide	0.09	0.09	0.02	0.00
Nitrite	0.21	0.02	0.00	0.00
Derived Results				
N in solution (M)				4.91
C in solution (M)				9.47
N Imbalance (mM/hr)				0.00
C Imbalance (mM/hr)				0.00

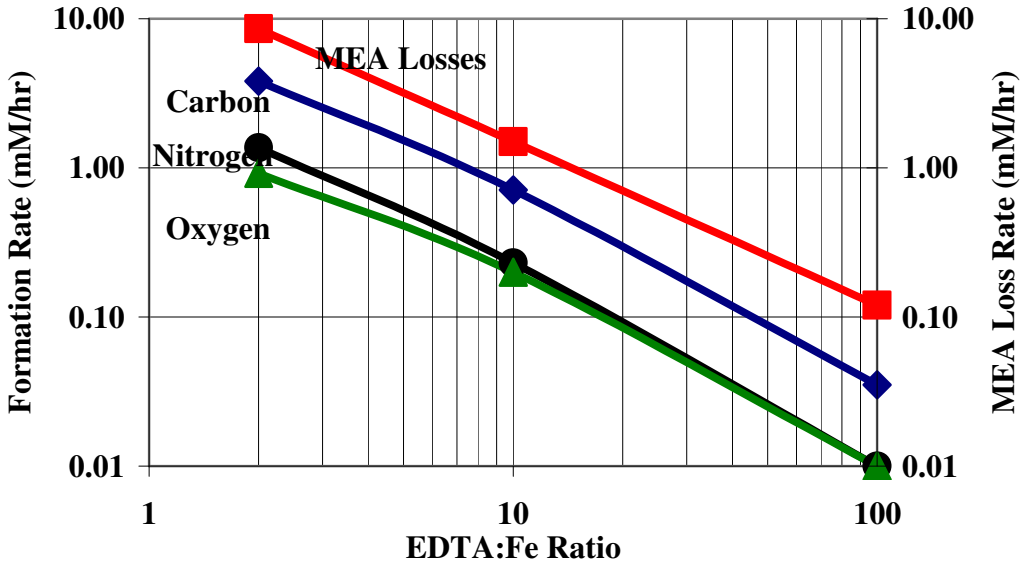

Figure 6.3 Effect of EDTA Concentration on Product Rates and MEA Losses (mM/hr), Low Gas (350 mL, 7 m MEA, 1 mM Fe^{+2}, 55°C, 100 cc/min 98%O_2/2%CO_2, α = 0.40, 1400 RPM)

6.2.4. Unsuccessful Inhibitors at Low Gas Rates

Data reported in Table 6.7 show that sodium sulfite, formaldehyde and formate were all ineffective as degradation inhibitors for the observed MEA systems. For the first 50 to 75 hours of the sodium sulfite experiment, it appears that oxidative degradation products were being formed at a decreased rate, suggesting that sulfite was oxidizing to sulfate and was nominally protecting the MEA from oxidative degradation. However, once all of the sulfite was consumed and oxidized, oxidation products formed at a rate similar to an MEA/Fe solution oxidized with no inhibitors added. While observed products were down by approximately 15% to 20%, the MEA loss rate increased by about 30% over an iron catalyzed solution in the absence of sodium sulfite.

Figure 6.4 illustrates the formation of degradation products over time for a low gas experiment conducted in the presence of iron and formaldehyde. The hypothesis is that the reaction intermediate (formaldehyde) would react faster with the available oxygen and be consumed quicker than the MEA, thereby protecting it from oxidative

degradation. However, results from Table 6.7 show the addition of formaldehyde had little impact on reducing product rates, and increased the MEA loss rate by about 30% - similar to the sodium sulfite experiment. In the presence of copper, hydroxyethyl-formamide rates double, while hydroxyethylimidazole formation rates increase by a factor of 3. The MEA loss rate approaches the rate of an MEA system catalyzed by iron and copper in the absence of formaldehyde.

Unlike other experiments, Figure 6.4 reveals that degradation products are not formed at a constant rate in the presence of formaldehyde. A large concentration of formamide is produced at the beginning of the experiment; this supports the theory that MEA formamide can be produced by directly reacting MEA with formaldehyde at these experimental conditions. The figure also shows that after the initial formation of products, all ionic product concentrations appear to be reaching some type of steady-state concentration. After degradation began, the ratio of MEA formamide to formate stayed constant at a 4:1 ratio.

Figure 6.5 illustrates the concentration of observed degradation products during the course of a low gas experiment testing 500 mM formate as an oxidation inhibitor. Initially, formate is observed at a concentration of 330 mM according to anion IC, even though 500 mM was added. During the first 75 hours of the experiment, while formate concentration remains constant, formamide concentration increases to approximately 170 mM – thus accounting for the "missing" formate. This behavior suggests that some of the initial formate is undetectable because it complexes with the iron metal in solution. Once the solution begins to oxidize, the iron-formate complex reacts with MEA to create formamide, supporting the reaction pathway that suggests metals in solution catalyze the reaction of carboxylic acid with amine.

During the middle of the experiment, formate (and formamide) concentration decreased, suggesting formate was oxidizing faster than it was being produced. At 150 hours, formate concentrations begins to increase once again, suggesting formate production occurred faster than formate oxidation.

The copper-catalyzed MEA system containing 500 mM formaldehyde behaved quite similarly to the MEA/Fe/formaldehyde system. A large percentage of formaldehyde added at the beginning of the experiment reacted with the MEA to form hydroxyethyl-formamide. After the rapid initial production period, degradation product concentrations continue to increase during the course of the experiment at a drastically slower rate. Similar to the formaldehyde experiment conducted in the presence of iron, hydroxyethyl-formamide is present at a 4:1 ratio with formate. Rates in Table 6.7 show formate performs slightly better than formaldehyde in the presence of iron, but worse than a system in the absence of formate. Observed carbon and nitrogen products are 20 to 30% lower, but MEA losses are 20% higher.

Table 6.7 Effect of Unsuccessful Oxygen Scavengers on Oxidative Degradation Product Rates (mM/hr), Low Gas (350 mL, 7 m MEA, 55°C, 100 cc/min 98%O_2/2%CO_2, α = 0.40, 1400 RPM)

Catalyst Concentration (mM)	1 Fe	1 Fe	5 Cu	1 Fe	1 Fe
Inhibitor Concentration (mM)	-	500 Formaldehyde	500 Formaldehyde	100 Na_2SO_3	500 Formate
Results (mM/hr)					
MEA Loss	3.8	5.1	8.0	5.1	4.5
Carbon in Products	6.3	5.8	14.6	5.4	4.5
Nitrogen in Products	2.5	2.3	5.3	2.0	2.0
O_2 Consumption	1.9	1.7	3.6	1.6	1.6
HPLC (mM/hr)					
HEI	0.66	0.64	1.28	0.59	0.55
HEF	0.77	0.00	2.27	0.00	0.00
Total Unknowns	2.28	2.64	0.96	2.87	2.40
HPLC Unknowns (Dilute Area)					
Unknown #1, RT=2.4 min	88.33	50.46	6.24	107.33	103.31
Unknown #2, RT=3.2 min		0.24	5.52		0.60
Unknown #3, RT=3.6 min	0.68	1.03		1.27	1.58
Unknown #4, RT=4.6 min			2.38	0.78	
Unknown #5 RT=13.2 min	0.40	0.47	1.83	0.48	0.46
Anion IC (mM/hr)					
Formate	0.29	0.22	0.36	0.08	0.14
Formamide	0.35	0.68	0.76	0.35	0.42
Oxamide	0.09	0.06	0.21	0.31	0.09
Nitrite	0.21	0.25	0.17	0.13	0.30
Derived Results					
N in solution (M)		4.52			4.24
C in solution (M)		9.44	9.54		9.53
N Imbalance (mM/hr)		1.26			0.19
C Imbalance (mM/hr)		2.79	1.1		2.65

Note: All unknown HPLC peak areas are samples diluted by a factor of ten

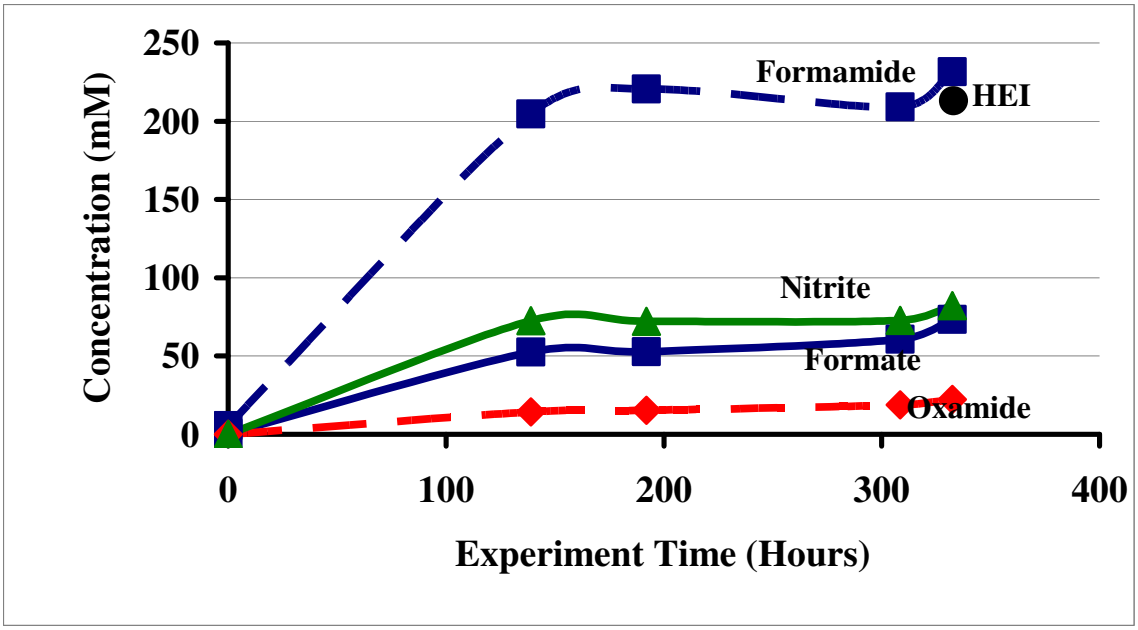

Figure 6.4 Oxidative Degradation of 7 m MEA, 1 mM Fe^{+2}, 500 mM Formaldehyde, 0.40 mol CO_2/mol MEA, 55°C, 1400 RPM, 100 cc/min 98%O_2/2%CO_2, Sulfate Correction Included

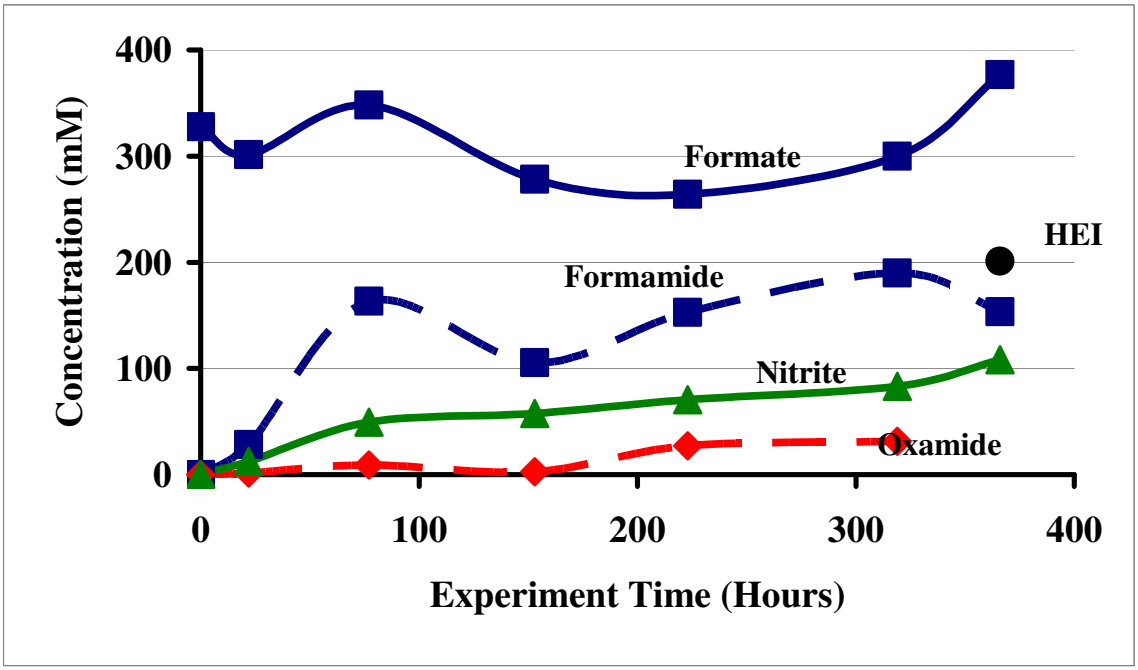

Figure 6.5 Oxidative Degradation of 7 m MEA, 1 mM Fe^{+2}, 500 mM Formic Acid, 0.40 mol CO_2/mol MEA, 55°C, 1400 RPM, 100 cc/min 98%O_2/2%CO_2, Sulfate Correction Included

6.2.5. Effect of Inhibitors at High Gas Rates

A set of experiments were run using the high gas flow apparatus to further investigate the effects of Inhibitor A on MEA degradation. One experiment was run at a lean loading (α) of 0.15 with 4.3 mM Cu present. Another experiment was run at the same lean loading with 0.3 mM Fe and 4.3 mM Cu present. The final experiment was run at a rich loading of 0.40 with both Fe and Cu in solution.

For each experiment, once the initial ammonia evolution rate reached steady state, subsequent amounts of Inhibitor A were added until the ammonia evolution rate approached baseline levels. Figure 6.6 illustrates this behavior for one of the experiments – the figure shows the ammonia evolution rate in mM/hr as a function of time. Each vertical red line represents the time at which Inhibitor A was added to the solution – first at a concentration of 10 mM, then 30 mM, 100 mM and 200 mM concentrations. The steady state ammonia evolution rate decreases from 8 mM/hr to 0.6 mM/hr with the addition of 200 mM of Inhibitor A for this particular high gas experiment.

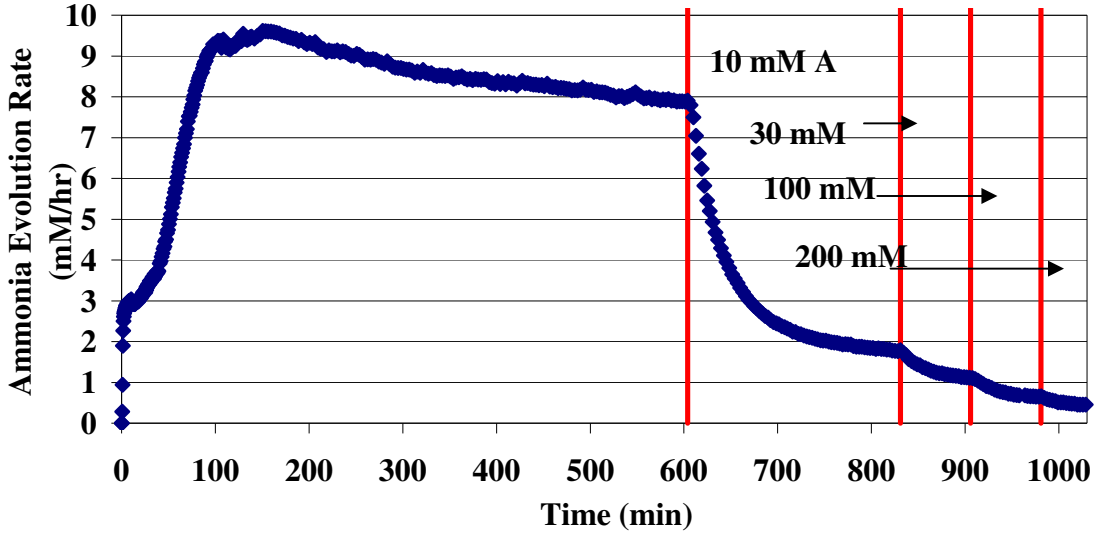

Figure 6.6 Effect of Inhibitor A on NH_3 Evolution Rate, 7 m MEA, 4.3 mM Cu^{+2}, 0.15 mol CO_2/mol MEA, 55°C, 1400 RPM, 7.5 L/min 15%O_2/2%CO_2

Figure 6.7 depicts the ammonia evolution rate as a function of Inhibitor A concentration. The baseline ammonia evolution rate, which was determined to be 0.15 mM/hr, was determined by conducting a high gas flow degradation experiment at zero loading with no corrosion inhibitors added. Figure 6.7 shows that the addition of a small amount of Fe to Cu at lean loading significantly increases the initial degradation rate. However, the addition of 200 mM Inhibitor A drops the ammonia evolution rate close to baseline levels. These results support conclusions drawn from the low gas apparatus – at concentration of 100 mM or greater, Inhibitor A is an effective agent for preventing the oxidative degradation of MEA.

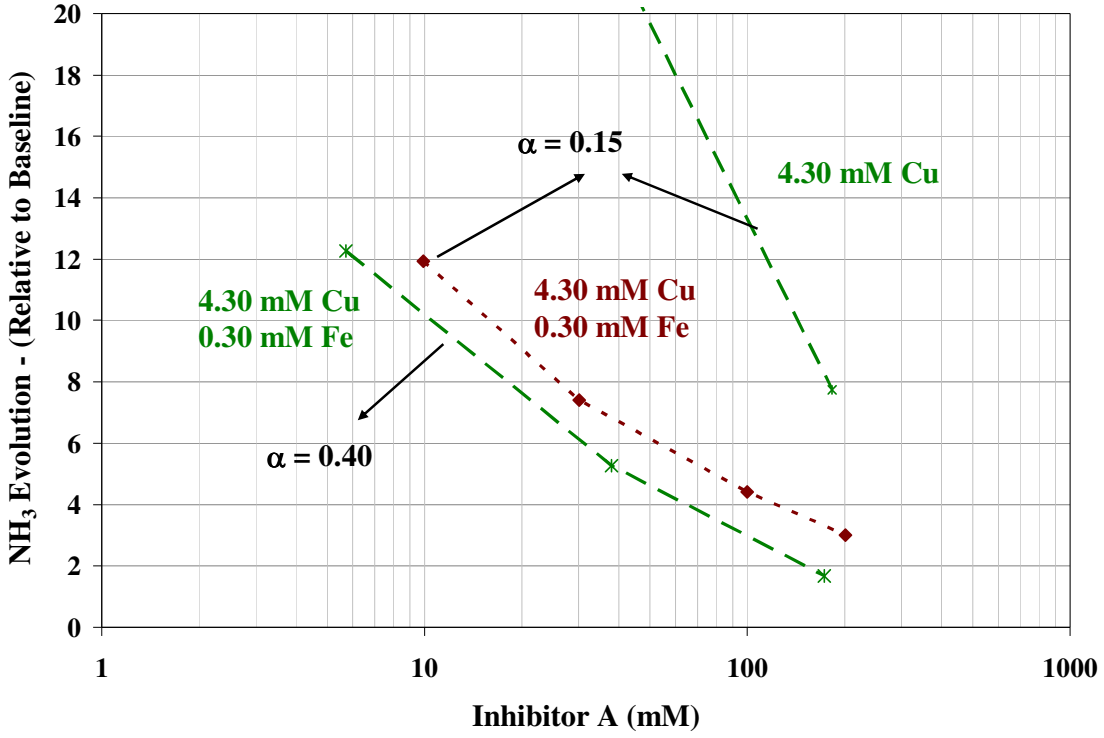

Figure 6.7 Effect of Inhibitor A on the Oxidative Degradation of MEA in the Presence of Copper and/or Iron – High Gas (55°C, 7 m MEA, 1400 RPM, Baseline = 0.15 mM/hr)

6.3. Conclusions

Experiments with low gas flow reveal that hydroxyethyl-formamide and hydroxyethylimidazole are the major oxidation products of MEA. MEA systems catalyzed by 1 mM vanadium produce much less formate (as well as formamide) and HEI, but more MEA oxamide than systems catalyzed by iron. Overall, carbon and nitrogen formation rates were lower, as well as MEA losses. Chromium and nickel, two metals present in stainless steel alloys, also catalyze the oxidative degradation of MEA. Observed carbon and nitrogen product rates are 20% lower than in an iron catalyzed system, while MEA losses are 55% greater. This suggests that chromium and nickel combined has a greater catalytic effect than iron by itself.

When both iron and copper are present as oxidation catalysts in solution, hydroxyethyl-formamide, HEI and MEA losses increase by a factor of 3 as compared to a system in the absence of iron. In terms of oxidative degradation potential: copper > chromium and nickel > iron > vanadium.

Data from experiments with high gas flow show that a combination of copper and iron creates more hydroxyethyl-formamide (the major carbon-containing degradation product) and hydroxyethylimidazole than iron by itself. The presence of copper in aqueous MEA solution enhances the production of both formate and hydroxyethyl-formamide, which experiments show is created from either the reaction of formaldehyde or a metal-formate complex with MEA.

Ammonia is the dominant nitrogen-containing degradation product. At high gas rate, NO_x is produced and stripped from the solution. On the other hand, at low gas rate where gas is not stripped from solution, NO_x is retained in the solution and oxidized to nitrite and nitrate. High gas flow experiments show that average ammonia production is independent of metal catalyst, which disagrees with Goff's findings.

The presence of 100 mM Inhibitor A decreases the formation of known degradation products by 90% in an MEA system catalyzed by both iron and copper; Inhibitor A decreases the formation of known products by over 99% and cuts MEA losses

by a factor of eight in Cr/Ni catalyzed systems. High gas experiments performed with FTIR analysis confirmed the effectiveness of Inhibitor A. From this analysis, one can conclude that Inhibitor A is an attractive option as an agent for inhibiting MEA degradation. Inhibitor screening has also targeted Inhibitor B as an effective oxidative degradation inhibitor for iron-catalyzed systems. In the presence of iron, it decreases product rates by 97% and MEA losses by 75%. Its effectiveness in other metal catalyzed systems needs to be tested.

A set of low gas flow experiments involving EDTA show that a 100:1 ratio of EDTA to Fe is necessary to sufficiently inhibit the oxidation of MEA. At this ratio, no observable MEA losses or oxidative degradation products are detected. However, it is still unknown whether EDTA itself degrades at these reaction conditions

The addition of formaldehyde, formate or sodium sulfite had an unintended effect on MEA losses. They actually increased the rate at which MEA degraded. While observed products decreased, MEA losses increased by 20% to 30% in the presence of these potential inhibitors.

Under assumed mass transfer conditions in the low gas apparatus, oxygen stoichiometry ranges from 1.6 to 1.9 mM/hr in all experiments performed in the presence of Fe and Cr/Ni, 3.6 to 5.6 mM/hr for experiments performed in the presence of Cu, and 0.7 mM/hr in the presence of V. Oxygen consumption rates were 0.2 mM/hr or less under assumed inhibited conditions. In the high gas apparatus, the presence of copper doubled the oxygen consumption rate. However, these rates cannot be accurately compared because HPLC analysis shows a large amount of unknown raw peak area for experiments performed in the presence of Fe and the combination of Cr/Ni.

Total carbon and nitrogen analysis shows that with the exception of the low gas experiment performed in the presence of Cr and Ni catalyst, there is over a 90% material balance on all selected low and high gas flow experiments.

Chapter 7: Effect of Catalysts and Inhibitors on the Oxidative Degradation of PZ

Aqueous piperazine (PZ) solutions were batch loaded into 500 mL glass jacketed reactors and subjected to oxidative degradation at low gas rates. Solutions were degraded with 100 mL/min of 98%O_2/2%CO_2 with mass transfer achieved by vortexing. Samples were drawn from the reactor during the course of the experiment and analyzed for degradation using ion chromatography and HPLC with evaporative light scattering detection.

Aqueous piperazine solutions do degrade in the presence of metal catalysts, albeit at much lower rates than MEA solutions. In terms of greatest to least catalyst oxidation potential, Cu > V > Fe. In concentrated PZ solutions, 5 mM of Cu was sufficient to create appreciable concentrations of EDA and formate, while 5 mM of Fe has virtually no

effect on degradation. In 2.5 m PZ solutions, 5 mM V catalyst resulted in carbon and nitrogen formation rates at about 60% of the rates produced by Cu catalyst.

The addition of 100 mM of Inhibitor A to concentrated PZ solutions in the presence of Fe and Cu decreased formate and EDA concentrations by over 90%. Degradation was completely inhibited by the addition of 100 mM Inhibitor A to PZ solutions catalyzed by Fe only. Therefore, it may be more advisable to minimize iron concentration in PZ solutions to inhibit corrosion, as opposed to adding Cu to inhibit corrosion and Inhibitor A to inhibit degradation.

For 2.5 m PZ solutions, the addition of 100 mM A to vanadium catalyzed solutions was not nearly as effective. Carbon and nitrogen formation rates were only decreased by 25%. However, the addition of 5 molal $KHCO_3$ to 2.5 m PZ (in the presence of 5 mM V) completely inhibited oxidative degradation. It is believed that the addition of the potassium bicarbonate alters the ionic strength of the solution and severely limits oxygen solubility and mass transfer capabilities.

7.1. Introduction

Cullinane (2002; 2005) proposed a new solvent containing a blend of piperazine (PZ) and aqueous potassium carbonate. Piperazine is a cyclic diamine, which means it can absorb two moles of CO_2 per mole of amine and potentially results in a higher capacity for CO_2. It also has a fast CO_2 absorption rate that is comparable or even faster than MEA. When piperazine is blended with K_2CO_3, the amount of amine protonation is reduced by the buffering capacity of the potassium bicarbonate/carbonate, which leaves more amine free to react with CO_2. PZ also has a higher pK_a than MEA, which generally translates into a fast rate of absorption.

Based on his bench-scale work, Cullinane found that a solution of 5 m K^+/2.5 m PZ has an absorption rate of CO_2 that is 1–1.5 times faster than 7 m MEA. Also, the heat of absorption is also approximately 10–25% less than MEA, as reported by Austgen (1989). The capacity of this solution is comparable or slightly less than that of 30 wt%

MEA. However, pilot plant experiments show that the heat duty requirement for desorption of CO_2 from the stripper may be slightly higher than MEA (Chen 2007).

Some prior work on PZ as a CO_2 absorbent has been published in literature (Bishnoi and Rochelle 2002; Eramtchkov et al. 2003; Kamps et al. 2003; Aroua and Salleh 2004; Hilliard 2008). Most of the VLE data are at CO_2 loadings above 0.75 mol CO_2/mol amine, as compared to the 0.1 to 0.5 range encountered in flue gas treating. Bishnoi (2000) presents some data on PZ, but the majority of his work focuses on PZ/MDEA blends. The most comprehensive study of aqueous PZ is given by Ermatchkov (2003), who reports speciation data for 0.1 to 1.45 m PZ and CO_2 loadings of 0.1 to 1.0 mol CO_2/mol PZ. Kamps (2003) reports total pressure data of CO_2/PZ mixtures from 40 to 120^{o}C. Unfortunately, most of this data are above loadings of 1.0 mol CO_2/mol PZ limiting its use in this work. Aroua and Salleh (2004) give equilibrium CO_2 partial pressure data for aqueous PZ under similar conditions. Dang (2001) gives date for the absorption rate of CO_2 into PZ/MDEA, in which PZ is used as a rate promoter.

PZ is more expensive than MEA, so it is imperative that PZ have a lower rate of degradation than MEA if it is to be economically viable. Hull (1969) proposed a mechanism for tertiary amines from experimental work with oxidants such as chlorine dioxide and hexacyanoferrate. It is believed that by this route PZ would form ethylenediamine monoacetaldehyde or ammonia and an amine that has an acetaldehyde group. The aldehyde constituents can be readily oxidized to their carboxylate counterparts (Denisov et al. 1977; Sajus and Seree de Roch 1980).

Alawode (2005) and Jones (2003) attempted to quantify the oxidative degradation of PZ by using GC for piperazine loss and anion IC to quantify the formation acetate, the observed major product of PZ degradation according to Alawode. The rate of acetate production ranged from 0.08 to 0.4 mM/hr while actual piperazine loss ranged from 1 mM/hr to 5 mM/hr.

Several studies were conducted involving the metabolism of compounds on the shoots of barley plants (Rouchaud et al. 1977; Rouchaud et al. 1978a). Piperazine was

discovered as a metabolic product of [^{3}H]-triforine, which was often used as a fungicide. A subsequent study on the metabolism of PZ identified diglycine, glycine and oxalic acid as metabolic products. Another study on the photodecomposition of PZ confirmed the presence of glycine as a product from the breakdown of PZ (Rouchaud et al. 1978b).

7.2. Experimental Results

Oxidative degradation experiments were run at low gas rates with several catalysts and inhibitors. Tables 7.1 and 7.2 list approximate formation rates of all quantifiable oxidative degradation products of piperazine under these conditions. Table 7.1 lists results for concentrated 5 m PZ, while Table 7.2 displays rates for 2.5 m PZ. Liquid phase product rates were calculated by dividing the final concentration of each individual component by the total experiment time. Amide analysis was not performed on the degraded 2.5 m PZ samples because samples from the experiments were deemed too old and unreliable for analysis.

All amide concentrations reported in Table 7.1 have been calculated by taking the difference in organic acid concentration in the degraded samples before and after treatment with concentrated sodium hydroxide – not from direct identification of the amides themselves.

Carbon and nitrogen formation rates were calculated for each of the degradation experiments by adding up the total number of carbons and nitrogens contained in each liquid and gas phase product. If the material balance for each experiment were to close completely, then the PZ degradation rate (in mM/hr) would equal two times the nitrogen formation rate and four times the carbon formation rate. That means that each and every nitrogen and carbon from the fragmented PZ molecules would be accounted for in degradation products.

7.2.1. Effect of Catalyst and Inhibitor on Concentrated PZ Systems

Figure 7.1 illustrates an aqueous 5m PZ low gas experiment at high iron concentration (5 mM), which represents catalyst conditions for an industrial system with carbon steel material of construction and no corrosion inhibitors added. Observed products include ethylenediamine (EDA), formate and formamide, all of which are in concentrations of 5 mM or less after 250 experiment hours. This suggests that Fe catalyst has no effect on the oxidative degradation of piperazine.

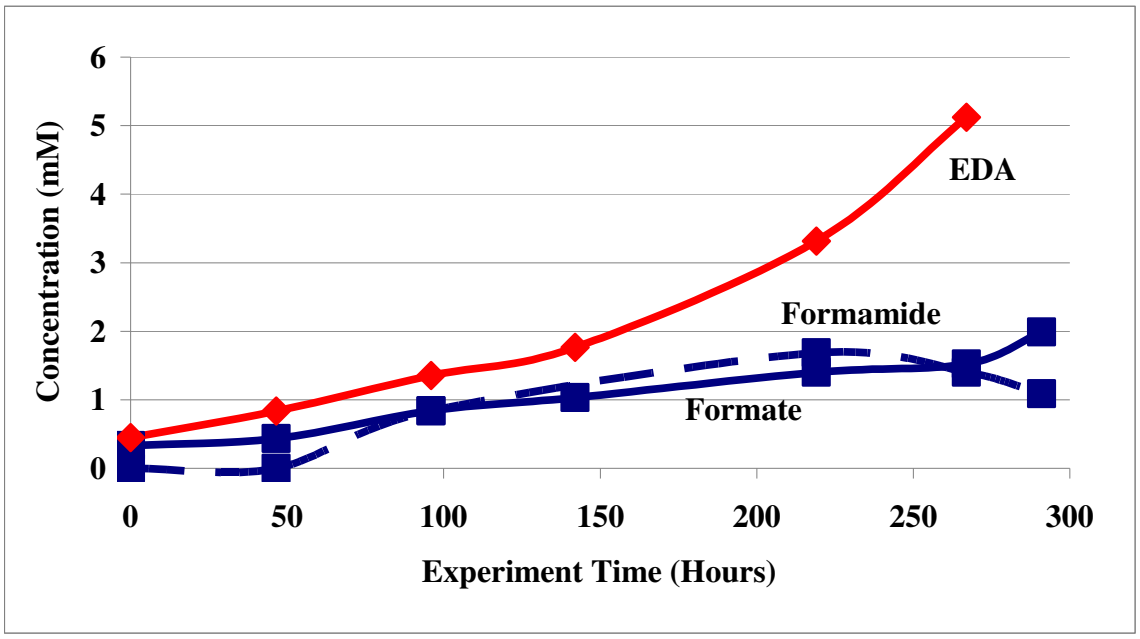

Figure 7.1 Oxidative Degradation of 5 m PZ, 5 mM Fe^{+2}, 0.30 mol CO_2/mol PZ, 55°C, 1400 RPM, 100 cc/min 98%O_2/2%CO_2, Sulfate Correction Included

Figure 7.2 contains results from two experiments, both of which involved the oxidation of 5 m PZ in the low gas apparatus and in the presence of 0.1 mM Fe and 5 mM Cu. The difference was that one experiment was conducted in the presence of 100 mM of Inhibitor A (solid lines), while the other was carried out in the absence of A (dashed lines). The main observed products were once again ethylenediamine and formate (amide analysis was not performed on these samples) for both experiments.

In the absence of Inhbitor A, formate and EDA concentrations were approximately 90 and 110 mM, respectively. Oxalate, nitrate, and nitrite were also present in final concentrations of 5 mM or less. Adding 100 mM of inhibitor A to the solution decreased degradation greatly. EDA and formate were the only products present in detectable quantities. Final concentrations for these species were 14.5 mM and 1.5 mM, respectively. This correlates to over a 90% reduction for both of these species. Although the presence of copper catalyst appears to have a greater catalytic effect on piperazine degradation than iron, the addition of 100 mM of Inhibitor A significantly decreases the presence of formate and EDA in solution.

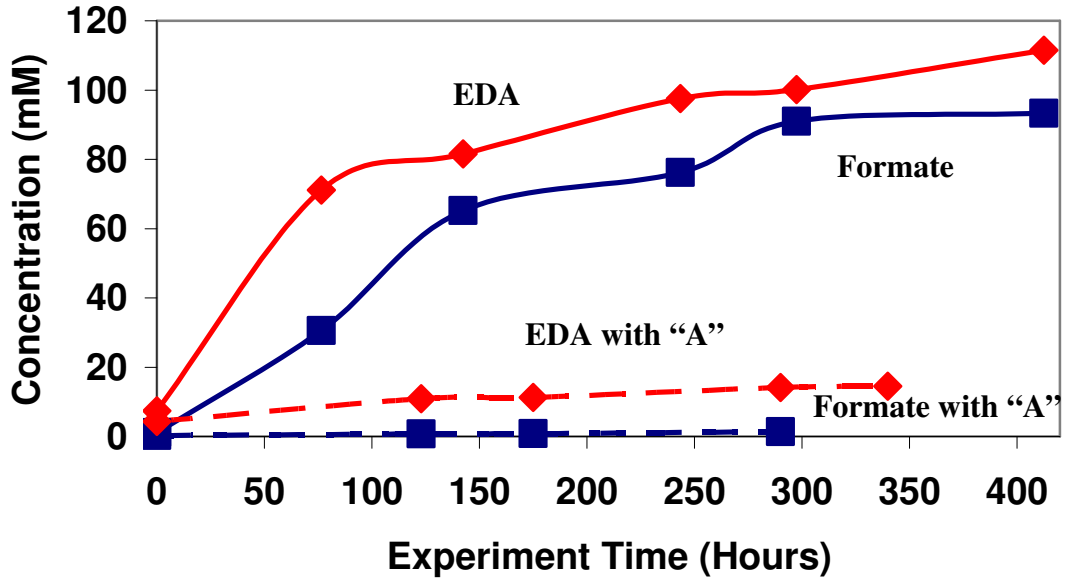

Figure 7.2 Effect of Inhibitor A (100 mM) on the Oxidative Degradation of 5 m PZ, 0.1 mM Fe^{+2}, 5 mM Cu^{+2}, 0.30 mol CO_2/mol PZ, 55°C, 1400 RPM, 100 cc/min 98%O_2/2%CO_2

Table 7.1 shows the results of the five concentrated PZ experiments performed at low gas rate. In the absence of Inhibitor A and in the presence of iron and copper catalyst, an appreciable amount of EDA and formate was produced; however, very little nitrate or nitrite is present. The addition of 100 mM of Inhibitor A decreased the formation rates of formate and EDA by 90%, and lowered the other species below detection limits.

In the presence of Fe only, PZ oxidation is minimal. Furthermore, the concentration of iron added to the system was irrelevant. The addition of 0.1 mM of Fe catalyst had the same effect as 5 mM of Fe catalyst. When 100 mM of Inhibitor A is added to either iron catalyst system, degradation is essentially zero; only EDA is observed in minute concentration.

Four unknown peaks were revealed when degraded PZ samples were analyzed by HPLC. Even in raw, undiluted samples, no HPLC peaks were observed in any PZ degradation conducted in the presence of Fe only (with or with out Inhibitor A) or in the presence of 5 m $KHCO_3$. Additionally, the experiment in which Inhibitor A was added to the 5 m PZ solution with Fe and Cu added as catalysts revealed no HPLC peaks. This is consistent with IC results, which revealed little to no accumulation of ionic degradation products.

Only three experiments possessed these peaks – PZ degraded in the presence of Fe and Cu, and PZ degraded in the presence of V (with and without Inhibitor A). This is also consistent with IC results, which show that Fe and Cu catalyst produce the most ionic degradation products with regards to PZ oxidation. Overall area is small for the other two experiments, considering these samples were not diluted prior to analysis. It is likely that these unknown peaks are some type of PZ amide structure. These raw peak areas are reported in Tables 7.1 and 7.2.

Table 7.1 Effect of Catalyst and Inhibitor Concentration on Oxidative Degradation Product Rates (mM/hr), Low Gas Flow (5 m PZ, 55°C, 100 cc/min 98%O_2/2%CO_2, α = 0.30, 1400 RPM)

Iron Concentration (mM)	**0.1**	**0.1**	**5**	**0.1**	**0.1**
Copper Concentration (mM)	**5**	**5**	**-**	**-**	**-**
Inhibitor A Concentration (mM)	**-**	**100**	**-**	**100**	**-**
Products (mM/hr)					
Formamide	**N/A**	**N/A**	**0.01**	**N/A**	**N/A**
Formate	**0.22**	**0.00**	**0.01**	**0.00**	**0.01**
EDA	**0.25**	**0.03**	**0.02**	**0.00**	**0.02**
Unknown #1, RT=2.6 min (raw area)	**128.24**				
Unknown #2, RT=2.9 min (raw area)	**60.76**				
Unknown #3, RT=3.4 min (raw area)	**11.62**				
Derived Results					
Carbon Products (mM/hr C)	**0.76**	**0.06**	**0.05**	**0.00**	**0.05**
Nitrogen Products (mM/hr N)	**0.52**	**0.06**	**0.04**	**0.01**	**0.04**
Piperazine Loss (mM/hr)	**N/A**	**N/A**	**0.00**	**N/A**	**N/A**

7.2.2. Effect of Catalyst and Inhibitor on 2.5m PZ Systems

Figure 7.3 details the important degradation products for two 2.5 m PZ low gas experiments carried out in the presence of vanadium catalyst. One experiment was carried out in the absence of Inhibitor A (solid lines) while the other was carried out in the presence of Inhibitor A (dashed lines). Figure 7.3 shows that the addition of 100 mM inhibitor A to an aqueous PZ/V system decreases formate concentration by approximately 70%, but has no effect on EDA concentration.

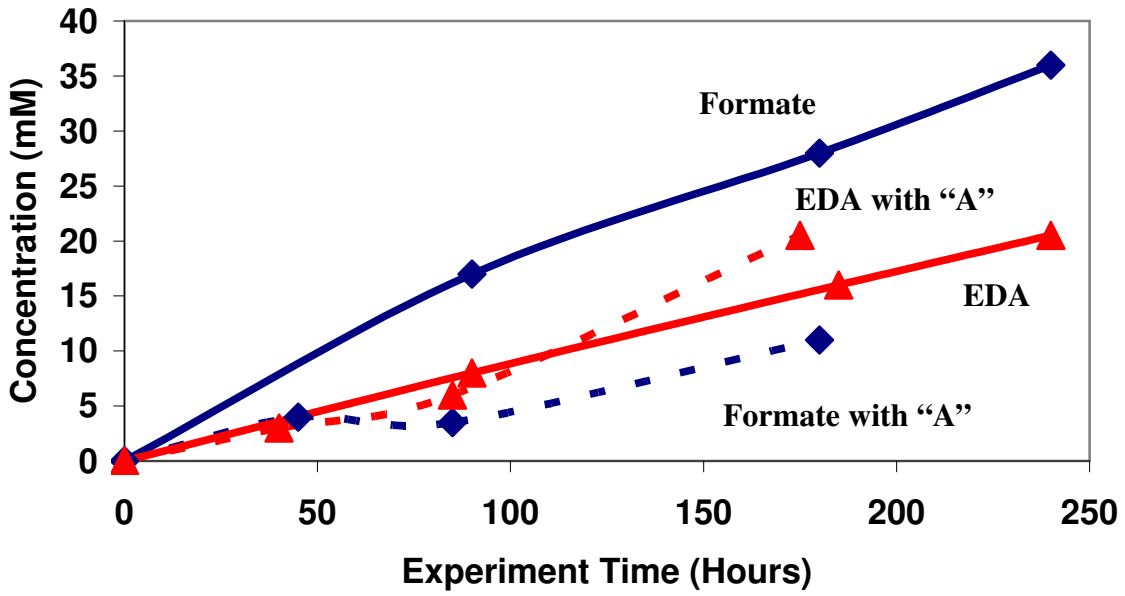

Figure 7.3 Effect of Inhibitor A (100 mM) on the Oxidative Degradation of PZ, 5 mM V^{+5}, 0.30 mol CO_2/mol PZ, 55°C, 1400 RPM, 100 cc/min 98%O_2/2%CO_2

Table 7.2 provides major degradation product formation rates (in mM/hr) for the aqueous PZ/vanadium systems analyzed in the low gas apparatus. When 2.5 m PZ is degraded in the presence of vanadium catalyst, nitrite, nitrate, EDA and carboxylic acids are all present as degradation products. The addition of 100 mM of Inhibitor A provides a 40% decrease in the overall formation of oxidative degradation products, which is attributed to the reduction of formate, nitrate and nitrite in solution; in the presence of V catalyst, EDA concentration is unaffected by the addition of Inhibitor A.

The addition of 5 m $KHCO_3$ lowers product formation rates by over an order of magnitude. Final degradation product concentrations are 3 mM or less for all identified products. It is believed that the addition of the high concentration of potassium carbonate decreases the mass transfer capabilities of the solution by significantly increasing the ionic strength of the solution. This change in ionic strength increases the Henry's constant for oxygen in solution, which decreases the oxygen solubility. The reduced oxygen mass transfer is reflected by the absence of degradation products.

When comparing all the PZ systems degraded in the low gas apparatus, Cu catalyst has the greatest catalytic effect, followed by V and Fe catalyst. This is slightly different from the observation made in MEA systems, in which Fe was a more potent catalyst than V. Similar to MEA systems, 100 mM of Inhibitor A is effective at decreasing the rate of PZ oxidation in the presence of all metal catalysts studied.

Table 7.2 Effect of Vanadium Catalyst and Inhibitor Concentration on Oxidative Degradation Product Rates (mM/hr), Low Gas Flow (2.5 m PZ, 55°C, 100 cc/min 98%O_2/2%CO_2, α = 0.30, 1400 RPM)

Vanadium Concentration (mM)	5	5	5	5
Inhibitor A Concentration (mM)	-	100	-	-
$KHCO_3$ Concentration (m)	-	-	5	5
Products (mM/hr)				
Formate	0.18	0.06	0.01	0.00
EDA	0.09	0.11	0.00	0.00
Unknown #1, RT=2.6 min (raw area)		9.3		
Unknown #2, RT=2.9 min (raw area)	6.84	28.4		
Unknown #3, RT=3.4 min (raw area)	1.76	1.5		
Unknown #4, RT=13.2 min (raw area)	9.1	2.6		
Derived Results				
Carbon Products (mM/hr C)	0.36	0.28	0.01	0.03

7.3. Conclusions

Aqueous piperazine solutions do degrade in the presence of metal catalysts, albeit at much lower rates than MEA solutions. In terms of catalyst oxidation potential, copper has the greatest potential, followed by vanadium and iron. In concentrated PZ solutions, 5 mM of Cu was sufficient to create appreciable concentrations of EDA and formate, while 5 mM of Fe has virtually no effect on degradaton. In 2.5 m PZ solutions, 5 mM V

catalyst resulted in carbon and nitrogen formation rates at about 60% of the rates produced by Cu catalyst.

The addition of 100 mM Inhibitor A to concentrated PZ solutions in the presence of Fe and Cu decreased formate and EDA concentrations by over 90%. Degradation was completely inhibited by the addition of 100 mM Inhibitor A to PZ solutions catalyzed by Fe only. Therefore, it may be more advisable to minimize iron concentration in PZ solutions to inhibit corrosion, as opposed to adding Cu to inhibit corrosion and Inhibitor A to inhibit degradation.

For 2.5 m PZ solutions, the addition of 100 mM A to vanadium catalyzed solutions was not nearly as effective. Carbon and nitrogen formation rates were decreased by 25%. However, the addition of 5 molal $KHCO_3$ to 2.5 m PZ (in the presence of 5 mM V) completely inhibited oxidative degradation. It is believed that the addition of the potassium bicarbonate alters the ionic strength of the solution and severely limits mass transfer capabilities.

Chapter 8: Solvent Screening

Aqueous amine solutions were batch loaded into 500 mL glass jacketed reactors and subjected to oxidative degradation at both low and high gas rates. Solutions were degraded with 100 mL/min of 98%O_2/2%CO_2 with mass transfer achieved by vortexing. Samples were drawn from the reactor during the course of the experiment and analyzed for degradation using ion chromatography with conductivity detection, HPLC with electrochemical detection and HPLC with evaporative light scattering detection.

Aqueous monoethanolamine (MEA) systems promoted by piperazine (PZ) are not an attractive option for CO_2 capture due to their high degradation rates. In the absence of Inhibitor A, degradation rates in the presence of Fe and Cu are four times as high as in the presence of Fe only. Even with a 90% to 94% decrease in degradation due to the addition of 100 mM of Inhibitor A, carbon and nitrogen production still occurs at

significant rates. The free radical products formed in the oxidation of MEA appear to attack PZ as well as other MEA molecules.

Low gas flow degradation experiments performed on potassium glycinate, ethylene glycol/potassium bicarbonate and ethylenediamine (EDA) solutions illustrate the importance of the ethanolamine structure in oxidative degradation. In terms of accumulation of degradation products and solvent losses, all of these solvent systems are resistant to oxidative degradation in the low gas flow apparatus. This suggests that the ethanolamine structure is susceptible to oxidative degradation. It was also learned that diethylenetriamine (DETA), the dimerization product of EDA, is an oxidative degradation product unique to EDA systems that could be used as potential marker in future experiments involving EDA.

Hindered amines, secondary amines and longer-chain amines subjected to oxidation in the low gas flow apparatus reinforced the susceptibility of the alkanolamine structure to oxidative degradation. DEA, a secondary alkanolamine, oxidized to form N-formyldiethanolamine, formate and other unknown HPLC products in the presence of Fe. However, amine losses were approximately half of an MEA system subject to the same conditions.

AMP, a sterically hindered amine, and DGA, an alkanolamine with a four carbon backbone and an ester linkage, were both resistant to oxidative degradation in the presence of Fe catalyst; AMP was resistant to oxidative degradation in the presence of Cu as well. This was confirmed by the absence of oxidative degradation products and virtually no solvent losses during the course of the experiments.

8.1. Introduction

Oxidation experiments were conducted to test the oxidative resistance of MEA solutions promoted by PZ. PZ is more expensive than MEA, so it is imperative that PZ have a lower rate of degradation than MEA if it is to be economically viable. Dang (2001) gives date for the absorption rate of CO_2 into PZ/MDEA, in which PZ is used as a

rate promoter. Preliminary results from Okoye (2005) show that MEA solutions promoted with PZ may have greater capacity and rates than homogeneous MEA systems.

If the less expensive MEA were to degrade preferentially to the PZ in the presence of oxygen (thus protecting the more valuable rate promoter), then blended MEA/PZ solvents could be an attractive alternative for CO_2 capture.

Another group of oxidation experiments were performed with the purpose of understanding how chemical structure affects susceptibility to oxidative degradation. MEA is an ethanolamine; it has a two carbon backbone with a hydroxyl group attached at one end and an NH_2 group on the other end. EDA, glycine and ethylene glycol are three compounds that are structurally similar to MEA – but have different functional groups attached to the ends of the two carbon backbone.

EDA is a diamine; the hydroxyl group on the α-carbon of the MEA structure is replaced with a second NH_2 group. EDA is also a degradation product of PZ; studying the degradation of EDA would be beneficial to understanding PZ as well. A concentration of 3.5 molal EDA, loaded to 0.3 mol CO_2 / mol EDA, was chosen as a baseline concentration for these experiments.

Glycine is an amino acid; the hydroxyl group of MEA is oxidized to a carboxylic acid functional group while the rest of the structure remains the same. van Holst (2006) proposes that salts of amino acids are an attractive alternative for CO_2 capture. Sorensen (1997) states that the degradation products of glycinate in the presence of UV and H_2O_2 are glyoxylate, oxalate and formate.

Ethylene glycol is different from MEA in that the NH_2 group is replaced with a second hydroxyl group. Thermal oxidation experiments performed on ethylene glycol systems found that the presence of Cu in aerated solutions produced the greatest amount of degradation (Rossiter et al. 1985). Low-temperature oxidation experiments performed on diethylene glycol revealed formic acid, formaldehyde and hydroxyacetaldehyde as major degradation products (Lloyd et al. 1956). This conclusion was confirmed in experiments studying the degradation of ethylene glycol in photo Fenton systems (McGinnis et al. 2000; McGinnis et al. 2001).

Another set of experiments was performed on amines that literature has suggested to be resistant to oxidation. Figure 8.1 illustrates the chemical structure of AMP, which is a sterically hindered amine. The two methyl groups on the alpha-carbon are believed to inhibit the free radical formation necessary to initiate the amine oxidative degradation. The resistance of AMP to degradation was observed by the Girdler Corporation (Kindrick et al. 1950a; 1950b). The effects of steric hinderance have been studied and noted in terms of CO_2 absorption and resistance to thermal degradation (Hook 1997; Kim 1988).

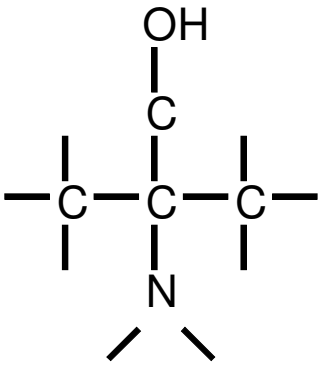

Figure 8.1 AMP Structure

Diethanolamine (DEA) is a secondary alkanolamine whose structure is shown in Figure 8.2. The mechanisms and pathways for the thermal degradation of DEA (Hsu and Kim 1985; Choy and Meisen 1980; Polderman and Steele 1956; Kim and Sartori 1984; Kennard and Meisen 1985), MDEA (Chakma and Meisen 1988; 1997) and DEA/MDEA blends (Dawodu and Meisen 1996; Holub et. al 1998) in the absence of oxygen are well understood. Moreover, high-temperature oxidation (with GC analysis) has been studied for MEA (Bello and Idem 2006; Supap et al. 2006; Supap 1999) and MEA/MDEA (Lawal and Idem 2006; Lawal et al. 2004) blended amine systems. However, no information is available on the oxidation of DEA.

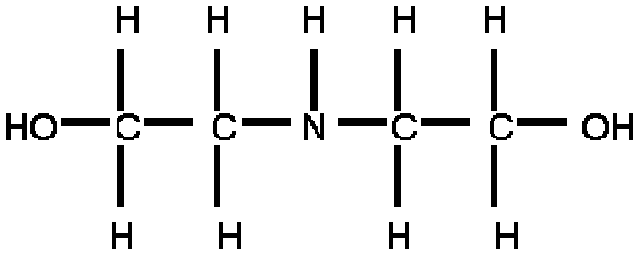

Figure 8.2 DEA Structure

Diglycolamine (DGA), also known as 2-(2-aminoethoxy)ethanol, is a longer chain alkanolamine with an ester linkage. The longer chain structure of DGA, shown in Figure 8.3, is believed to prevent the cyclizing that plagues MEA. Whereas MEA has the tendency to form stable 5-membered rings, DGA forms 8 and 9-membered rings, which are much more unstable. Rooney et al. (1998) observed the production of formate from DGA at approximately the same rate as MEA.

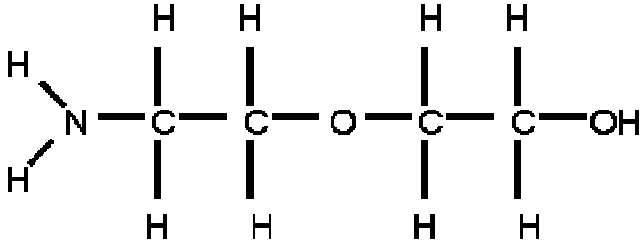

Figure 8.3 DGA Structure

8.2. Experimental Results

Oxidative degradation experiments were run on the low gas apparatus for a number of solvents that have been suggested as viable for CO_2 capture from gas streams. Liquid phase oxidation product rates were calculated by dividing the final concentration of each individual component by the total experiment time.

All reported amide rates have been calculated by taking the difference in organic acid concentration in the degraded samples before and after treatment with concentrated

sodium hydroxide. The only exception is the MEA/PZ degradation experiments; hydroxyethyl-formamide rates were calculated by direct HPLC analysis.

Amine losses were determined using cation chromatography, using sulfate as an internal standard; glycine losses were determined using HPLC with electrochemical detection. Total amine loss was calculated by taking the difference between initial and final experimental samples. That rate was normalized by total experimental time in order to compare solvent losses to product formation rates.

Carbon and nitrogen formation rates were calculated for each of the degradation experiments by adding up the total number of carbons and nitrogens contained in each liquid and gas phase product.

8.2.1. Oxidation of Blended MEA/PZ Systems

Figure 8.4 shows ionic degradation product formation rates for a 7 m MEA/2 m PZ amine solution subjected to Fe and Cu catalyst. The major ionic degradation product is formate; in fact, formate is present at 700 mM at the end of the experiment – a concentration thirty times greater than any other ionic species in solution.

Figure 8.5 illustrates the product formation rates for a low gas experiment in which 100 mM Inhibitor A was added to a 7 m MEA/2 m PZ solution degraded in the presence of Fe and Cu. While nitrate and oxalate (minor product) rates remained virtually the same, formate concentration was decreased by over 85%.

Table 8.1 summarizes the degradation product formation rates for two MEA/PZ experiments in the presence of Fe only and Fe/Cu combined catalysts systems; these same systems were degraded in the presence of 100 mM Inhibitor A. In the absence of Inhibitor A, hydroxyethyl-formamide and hydroxyethylimidazole are the most abundant degradation products. In the presence of Inhibitor A, formamide and HEI concentrations are greatly decreased and formate is the most concentrated degradation product. Very little ethylenediamine, a cationic degradation product unique to the oxidation of PZ, is

present in any of these experiments. This suggests that either the PZ is being protected by the MEA, or EDA reacts in these systems to form other degradation products.

Catalytic activity (as determined by the accumulation of carbon and nitrogen from degradation products) is four times greater in the presence of Fe and Cu catalyst versus Fe only. In fact, if carbon and nitrogen accumulation continued at the rate listed in Table 8.1, all MEA and PZ would be consumed by the oxidative degradation in the presence of Fe and Cu in 510 hours. The addition of 100 mM of inorganic additive Inhibitor A proved to be quite effective once again. In the presence of Fe only, carbon and nitrogen formation was decreased by 90%; in the presence of Fe and Cu catalyst, rates were decreased by 94% overall. In terms of oxidative degradation, MEA/PZ blended systems are not a viable option unless Inhibitor A is added to the system.

7 m MEA base case experiments are also included in Table 8.1. Carbon and nitrogen product rates are 25% greater for blended MEA/PZ systems in the presence of Fe, and 75% higher for systems in the presence of Fe and Cu. Amine losses were not calculated for the blended MEA/PZ systems.

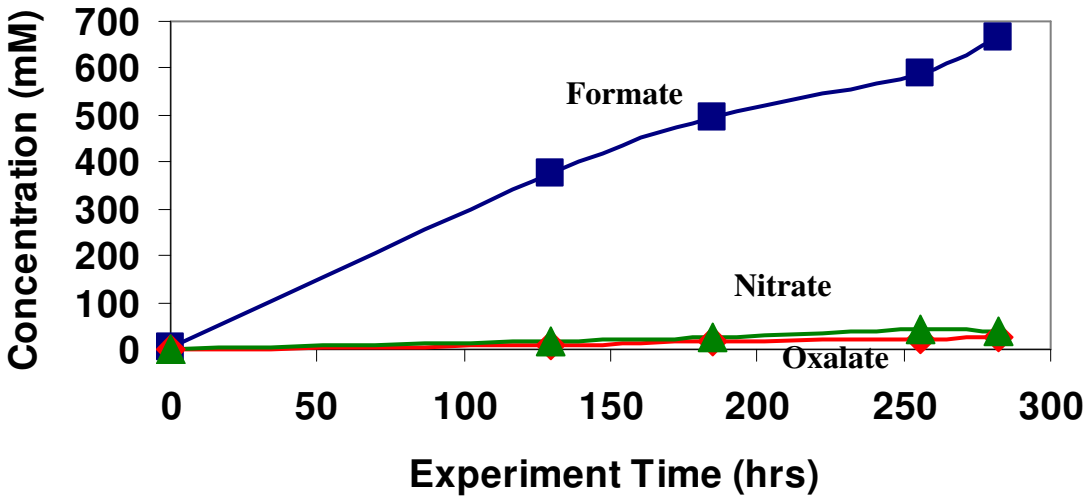

Figure 8.4 Oxidative Degradation of 7 m MEA/2 m PZ, 0.1 mM Fe^{+2}, 5 mM Cu^{+2}, 55°C, 1400 RPM, 100 cc/min 98%O_2/2%CO_2

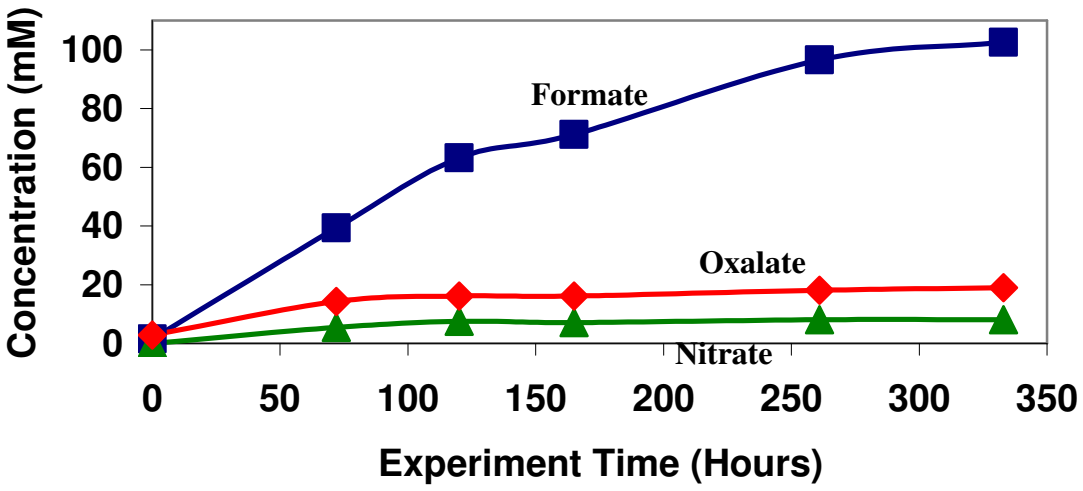

Figure 8.5 Oxidative Degradation of 7 m MEA/2 m PZ, 0.1 mM Fe^{+2}, 5 mM Cu^{+2}, 100 mM Inhibitor A, 55°C, 1400 RPM, 100 cc/min 98%O_2/2%CO_2

Table 8.1 Effect of Catalyst and Inhibitor Concentration on Oxidative Degradation Product Rates (mM/hr), Low Gas Flow (7 m MEA/2 m PZ, 55°C, 100 cc/min 98%O_2/2%CO_2, 1400 RPM)

Iron Concentration (mM)	1 (7m MEA)	0.1	0.1	0.1 (7m MEA)	0.1	0.1
Copper Concentration (mM)	-	-	-	5	5	5
Inhibitor A Concentration (mM)	-	-	100	-	-	100
Products (mM/hr)						
Hydroxyethylimidazole	0.66	0.70	0.14	1.70	4.13	0.17
Hydroxyethyl-formamide	0.77	1.49	0.00	3.25	4.06	0.28
Formate	0.29	0.17	0.20	0.73	2.35	0.30
EDA	N/A	0.01	0.00		0.03	0.05
Derived Results						
Carbon Products (mM/hr C)	6.3	8.3	0.9	20.0	35.5	2.1
Nitrogen Products (mM/hr N)	2.5	3.0	0.3	7.1	12.5	0.7

8.2.2. Oxidation of MEA Analogs

Table 8.2 presents the experimental results from the oxidation of solvents structurally similar to MEA. A 2 molal potassium glycinate solution was created using glycine, potassium carbonate and potassium hydroxide such that solution loading was 0.4

mol CO_2 / mol glycine. Since there is no NH_2 group, ethylene glycol cannot form a carbamate with CO_2. Furthermore, the physical solubility of CO_2 in ethylene glycol is extremely low. In order to obtain a representative solution loading and to bring the solution pH in the basic range, 1 molal of $KHCO_3$ was added to the aqueous ethylene glycol solution.

Table 8.2 shows the oxidation of potassium glycinate results in a minimal amount of formate production; all other products are present in trace concentrations. 3.5 m EDA degraded to a slightly greater extent. The major degradation product of EDA was hydroxyethyl-formamide, with a minor product being DETA. DETA (diethylenetriamine) is the dimerization product of EDA. Ethylene glycol, promoted with potassium bicarbonate, showed no major oxidative degradation products at low gas flow reaction conditions. Cation IC analysis showed ethylene glycol and EDA degradation to be less than 2%, while HPLC with electrochemical detection showed glycine degradation to be less than 4%. Therefore, it appears that the combination of both primary amine and primary alcohol is needed to promote MEA degradation.

Table 8.2 Oxidation Product Rates (mM/hr) of MEA Analogs, Low Gas Flow (55°C, 100 cc/min 98%O_2/2%CO_2, 1400 RPM)

Solvent Concentration	2m Potassium Glycinate	2m Potassium Glycinate	3.5m EDA	3.5m EDA	7m Ethylene Glycol
Catalyst Concentration (mM)	1mM Fe	5mM Cu	1mM Fe	5mM Cu	1mM Fe
Products (mM/hr)					
Hydroxyethyl-formamide	N/A	N/A	0.12	0.15	0.00
Formate	0.02	0.04	0.00	0.02	0.00
DETA	N/A	N/A	0.01	0.02	0.00
Derived Results					
Carbon Products (mM/hr C)	0.03	0.06	0.41	0.56	0.01
Nitrogen Products (mM/hr N)	0.00	0.00	0.16	0.21	0.00
Solvent Losses (mM/hr)	0.12	0.11	0.18	0.21	0.00

8.2.3. Oxidation of Secondary and Hindered Amines

Table 8.3 details results of low gas flow screening experiments for these amines. AMP was degraded in the presence of Fe and Cu catalyst separately, where as DEA and

DGA were only degraded in the presence of 1 mM Fe. IC and HPLC analysis revealed that in the presence of either catalyst, AMP is resistant to oxidative degradation. Formate was the most concentrated degradation product, and it was present at a concentration of less than 3 mM for either experiment. DGA degraded in the presence of Fe exhibited similar results. A small amount of formamide was detected by NaOH hydrolysis, but otherwise product concentrations remain in trace amounts. Cation analysis showed virtually no degradation loss.

DEA, possessing the ethanollamine structure that appears to be susceptible to oxidative degradation, was not as degradation resistant as the other two amines that were studied. Anion IC revealed the presence of formate, and NaOH hydrolysis showed the presence of 3 times as much N-formyldiethanolamine. According to cation analysis, amine losses for 30 wt% DEA are 45% less than amine losses for 30 wt% MEA degraded in the presence of 1 mM Fe.

An interesting phenomena observed only in the DEA experiment was the initial formation – and subsequent disappearance – of the amide formed from the reaction of glycolate (or hydroxyacetate) and MEA. Initial degraded sample analysis did not reveal the presence of any glycolate in solution. However, after NaOH hydrolysis, IC analysis showed that 100 mM of glycolate is present after 50 hours. During the remainder of the degradation experiment, the glycolate disappears at a fairly linear rate, as shown in Figure 8.6. This suggests that the DEA glycolamide is an intermediate that participates in another reaction with either DEA or some other reaction product.

Table 8.3 Amine Screening - Oxidative Degradation Product Rates (mM/hr), Low Gas Flow (55°C, 100 cc/min 98%O_2/2%CO_2, 1400 RPM)

Solvent Concentration (molal)	4m AMP	4m AMP	4m DEA	4m DGA
Catalyst Concentration (mM)	1mM Fe	5mM Cu	1mM Fe	1mM Fe
Products (mM/hr)				
Formamide	0.00	0.00	0.48	0.02
Formate	0.01	0.01	0.16	0.01
Derived Results				
Carbon Products (mM/hr C)	0.02	0.02	0.79	0.03
Nitrogen Products (mM/hr N)	0.00	0.00	0.06	0.01
Solvent Loss (mM/hr)	N/A	N/A	2.12	N/A

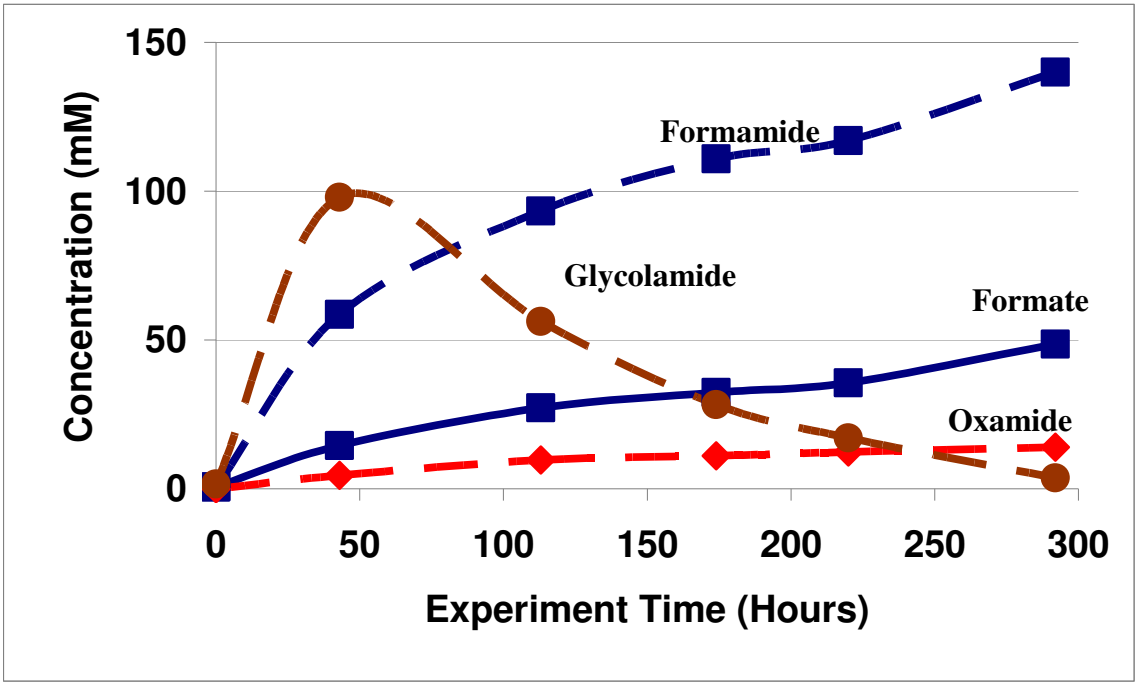

Figure 8.6 Oxidative Degradation of 4 m DEA, 1 mM Fe^{+2}, 55°C, 1400 RPM, 100 cc/min 98%O_2/2%CO_2, Sulfate Correction Included

8.2.4. HPLC-ELSD Analysis of Degraded Solvent Systems

While hydroxyethyl-formamide and HEI have been positively identified as oxidative degradation products for MEA/PZ and EDA systems, unknown peaks

consistently show up in these solvent systems – in addition to AMP, DGA and DEA systems. Table 8.4 illustrates the relative abundance of these unknown peaks in terms of their raw areas.

The total known area refers to the combined raw areas of hydroxyethyl-formamide and hydroxyethylimidazole, while total unknown area refers to the combined raw areas of all HPLC peaks that have not been positively identified. The samples are grouped into two categories: diluted and undiluted samples. The evaporative light scattering detector gives a highly non-linear response. On average, a dilution factor of ten reduces peak response by a factor of 100. That is why some samples were analyzed undiluted on the HPLC; any dilution decreased peak areas to the noise range.

In terms of the diluted samples, the uninhibited MEA/PZ experiments have at least 67% of the HPLC raw peak area unidentified. However, this doesn't necessarily correlate to 67% of raw concentration, since each of these unidentified compounds have a completely different response on the ELSD as opposed to hydroxyethyl-formamide and HEI. Furthermore, there is also an appreciable amount of peak area unidentified for the DEA low gas degradation experiment. It's possible that some of this peak area is actually N-formyldiethanolamine, which has not been positively identified using HPLC with ELSD.

For undiluted samples, 58% to 80% of peak area remains unidentified for inhibited MEA/PZ experiments. However, since these samples are undiluted, the overall concentration of these unidentified peaks is fairly small. The amount of unidentified peak area for the EDA, DGA and AMP degradation experiments are fairly small, reinforcing the assertion that these solvent systems are resistant to oxidative degradation at these reaction conditions.

Table 8.4 Area Comparison for Raw HPLC Peaks

Experiment	Total Known Area	Total Unknown Area	HPLC Area in Unknowns(%)
10X Diluted Samples			
7m MEA/2m PZ/0.1mM Fe	**20**	**76**	**79%**
7m MEA/2m PZ/0.1mM Fe/5mM Cu	**126**	**251**	**67%**
4m DEA/1mM Fe	**0**	**121**	**100%**
Undiluted Samples			
7m MEA/2m PZ/0.1mM Fe/5mM Cu/100mM A	**126**	**177**	**58%**
7m MEA/2m PZ/0.1mM Fe/100mM A	**46**	**188**	**80%**
4m AMP/5mM Cu	**0**	**17**	**100%**
4m DGA/1mM Fe	**0**	**14**	**100%**
3.5m EDA/5mM Cu	**20**	**2**	**8%**
3.5m EDA/1mM Fe	**17**	**0**	**0%**

8.3. Conclusions

Aqueous MEA/PZ systems are not an attractive option for CO_2 capture due to their high degradation rates. In the absence of Inhibitor A, degradation rates in the presence of Fe and Cu are four times as high as in the presence of Fe only. Even with the 90% to 94% decrease in degradation with the addition of 100 mM of Inhibitor A, carbon and nitrogen production still occurs at significant rates. The free radical products formed in the oxidation of MEA appear to attack PZ as well as other MEA molecules.

Low gas flow degradation experiments performed on potassium glycinate, ethylene glycol/potassium bicarbonate and EDA solutions illustrate the importance of the ethanolamine structure in oxidative degradation. In terms of accumulation of degradation products and solvent losses, all of these solvent systems are resistant to oxidative degradation in the low gas flow apparatus. It was also learned that diethylenetriamine (DETA), the dimerization product of EDA, is an oxidative degradation product unique to EDA systems that could be used as potential marker in future experiments involving EDA.

Hindered amines, secondary amines and longer-chain amines subjected to oxidation in the low gas flow apparatus reinforced the susceptibility of the ethanolamine

structure to oxidative degradation. DEA, a secondary ethanolamine, oxidized to form N-formyldiethanolamine, formate and other unknown HPLC products in the presence of Fe. However, amines losses were approximately half of an MEA system subject to the same conditions.

AMP, a sterically hindered amine, and DGA, an alkanolamine with a four carbon backbone and an ester linkage, were both resistant to oxidative degradation in the presence of Fe catalyst; AMP was resistant to oxidative degradation in the presence of Cu as well. This was confirmed through minimal formation of degradation products and amine stability. A summary of product formation rates and amine losses for these amine screening experiments is listed in Table 8.5.

Table 8.5 Summary of Results for Amine Screening

Experiment	Carbon Products (mM/hr)	Nitrogen Products (mM/hr)	Amine Losses (mM/hr)
7m MEA/1mM Fe (Base Case)	**6.3**	**2.5**	**3.8**
4m DEA/1mM Fe	**0.8**	**0.1**	**2.1**
4m DGA/1mM Fe	**0.0**	**0.0**	
4m AMP/1mM Fe	**0.0**	**0.0**	
4m AMP/5mM Cu	**0.0**	**0.0**	
7m MEA/2m PZ/0.1mM Fe	**8.3**	**3.0**	
7m MEA/2m PZ/0.1mM Fe/100mM A	**0.9**	**0.3**	
7m MEA/2m PZ/0.1mM Fe/5mM Cu	**35.5**	**12.5**	
7m MEA/2m PZ/0.1mM Fe/5mM Cu/100mM A	**2.1**	**0.7**	
3.5m EDA/1mM Fe	**0.4**	**0.2**	**0.2**
3.5m EDA/5mM Cu	**0.6**	**0.2**	**0.2**
2m K Glycinate/1mM Fe	**0.0**	**0.0**	**0.1**
2m K Glycinate/5mM Cu	**0.1**	**0.0**	**0.1**
7m Ethylene Glycol/1mM Fe	**0.0**	**0.0**	**0.0**

Chapter 9: Conclusions and Recommendations

This chapter details the key findings of this study on amine degradation at low and high gas conditions with various catalysts and inhibitors. Results are presented at conditions controlled by oxygen mass transfer and by reaction kinetics. These experimental results are utilized to estimate industrial degradation rates with an Aspen Plus absorber model. Finally, recommendations are made for future work on amine oxidation.

9.1. Conclusions Summary

Aqueous amine solutions were batch loaded into 500 mL glass jacketed reactors and subjected to oxidative degradation at both low and high gas rates. Solutions at low gas were degraded with 100 mL/min of 98%O_2/2%CO_2 with mass transfer achieved by

vortexing. Samples were drawn from the reactor during the course of the experiment and analyzed for degradation using ion chromatography and HPLC with evaporative light scattering detecion. In a parallel apparatus 7.5 L/min of 15%O_2/2%CO_2 was sparged through 350 mL of solution; additional mass transfer was achieved by vortexing. A Fourier Transform Infrared Analyzer collected continuous gas-phase data on amine volatility and volatile degradation products.

The first part of the work focused on the oxidation of monoethanolamine (MEA). Major liquid and gas-phase products were identified and quantified, and the effect of catalysts (Fe, Cu, Cr, Ni and V) and inhibitors (A, B, EDTA, sulfite, formaldehyde and formate) on MEA were studied extensively. Carbon and nitrogen material balances were conducted, and the overall oxygen stoichiometry for each reaction conditions was determined.

The second part of the study focused on expanding the knowledge of oxidation chemistry to other solvent systems. Catalysts and inhibitor effects on concentrated piperazine (PZ) and MEA/PZ blends were investigated. The effects of iron and copper catalyst were examined for MEA analogs (glycine, ethylenediamine and ethylene glycol) and secondary/hindered amines (diethanolamine, diglycolamine and 2-amino-2-methyl-1-propanol).

Hydroxyethyl-formamide (HEF), hydroxyethylimidazole (HEI) and formate are the major carbon containing MEA oxidation products; HEF, HEI and ammonia are the major nitrogen containing degradation products. In terms of catalyst oxidation potential, Cu > Cr/Ni (combined) > Fe > V. The oxygen stoichiometry (ν) ranges from 1.5 mol MEA degraded/mol O_2 consumed for Cu and Fe catalyzed systems to 1.0 for vanadium catalyzed systems.

Inhibitors A and B (reaction mechanism inhibitors) and EDTA (a chelating agent) were established as effective MEA oxidation inhibitors. Sodium sulfite and reaction intermediates formaldehyde and formate (all expected oxygen scavengers) were unsuccessful at inhibiting MEA oxidation.

Cu catalyzes concentrated PZ oxidation, while Fe has no effect on PZ oxidation even at high catalyst concentration. MEA/PZ blends were more susceptible to oxidation than any other amine system investigated. It is believed that free radicals formed in the MEA oxidation process serve to accelerate the degradation of the PZ structure. All MEA analogs and secondary/hindered amines were resistant to oxidation in the presence of Fe or Cu, except for diethanolamine (DEA). This suggests that the alkanolamine structure is more susceptible to oxidative degradation.

9.2. O_2 Mass Transfer Conditions

Experiments performed at high and low gas flow rate revealed HEF, HEI, formate and ammonia as the major MEA oxidation products. At catalyst conditions (with the exception of vanadium), MEA degradation is oxygen mass transfer controlled. The presence of copper catalyst is believed to accelerate kinetics such that degradation is taking place in the boundary layer in addition to the bulk solution.

9.2.1. MEA Oxidation Products in the Presence of Fe Catalyst

Formate, HEF and HEI account for 92% of the degraded carbon that has been quantified in the low gas apparatus; they account for 18% to 59% of the degraded carbon in the high gas apparatus. Ammonia, HEF and HEI are the dominant nitrogen-containing degradation products; they account for 84% of the degraded nitrogen in the low gas apparatus and 83% to 92% in the high gas apparatus.

Oxalate (and its respective amide), glycolate and acetate are also present, but at much lower concentrations. The ratio formamide to formate varies from 1.2 to 2.7, while oxamide to oxalate varies from 4.5 to 10. Formate/Formamide is approximately six times more abundant than oxalate/oxamide in the high gas apparatus and ten times more in the low gas apparatus. We believe the formation of the amides is reversible, especially at

stripper conditions. The reversibility of the formation of HEI is unknown at this point in time.

At high gas rate, NO_x is produced and stripped from the solution. At low gas rate, NO_x is retained in the solution and oxidized to nitrite and nitrate. At high gas rate, NO_x/N_2O production occurs at approximately 15% of the rate of ammonia production. At low gas rate, nitrite/nitrate production occurs at the same rate as NO_x/N_2O production at high gas rate.

Since ammonia production is six times greater than NO_x/N_2O at high gas conditions, it is probably produced at low gas rates as well. This ammonia may exist in gaseous form, in the solution as ammonium cation or tied up with carboxylic acid as formamide or oxamide. Using our current cation chromatography analytical method, ammonium is eluted around the same time as MEA, which is present in concentration at least 100X greater than ammonia. As a result the ammonium peak is hidden under the MEA peak and cannot be effectively separated.

Other volatile degradation products include CO, C_2H_4, formaldehyde and acetaldehyde. In one experiment at high gas rate in the presence of Fe catalyst, these combined product concentrations comprised of 43% of total ammonia production. In another experiment, they made up 7% of the total ammonia production. Despite the high gas phase product concentrations and inexplicable high MEA losses in the first high gas experiment, overall total carbon and nitrogen production are similar for the two experiments.

9.2.2. Effect of Catalyst on MEA Oxidation

In terms of oxidative degradation potential, at low gas rates: copper > chromium and nickel > iron > vanadium. Experiments at high gas flow also show that copper is a more potent oxidation catalyst than iron.

Experiments with low gas flow reveal that HEF and HEI are the major oxidation products of MEA in all systems – with the exception of vanadium. MEA systems

catalyzed by 1 mM vanadium produce much less formate, HEF and HEI, but more oxamide. Overall, carbon and nitrogen formation rates were lower, as well as MEA losses. Chromium and nickel, two metals present in stainless steel alloys, also catalyze the oxidative degradation of MEA. Observed carbon and nitrogen product rates are 20% lower than in an iron catalyzed system, while MEA losses are 55% greater. This suggests that chromium and nickel combined has a greater catalytic effect than iron by itself.

When both iron and copper are present as oxidation catalysts in solution, HEF, HEI and MEA losses increase by a factor of three as compared to a system in the absence of iron.

Data from experiments with high gas flow show that a combination of copper and iron creates more HEF (the major carbon-containing degradation product) and HEI than iron by itself. The presence of copper in aqueous MEA solution enhances the production of both formate and HEF, which is believe to be created from either the reaction of formaldehyde or a metal-formate complex with MEA.

Ammonia is the dominant nitrogen-containing degradation product. At high gas rate, NO_x is produced and stripped from the solution. On the other hand, at low gas rate where gas is not stripped from solution, NO_x is retained in the solution and oxidized to nitrite and nitrate. High gas flow experiments show that average ammonia production is independent of metal catalyst, which disagrees with the findings of Goff.

9.2.3. Unsuccessful Inhibitors

The addition of formaldehyde, formate or sodium sulfite had an unintended effect on MEA losses in systems catalyzed by iron. They actually increased the rate at which MEA degraded. While observed products decreased, MEA losses increased by 20% to 30% in the presence of these potential inhibitors.

9.2.4. Oxygen Consumption

Under assumed mass transfer conditions in the low gas apparatus, oxygen consumption ranges from 1.6 to 1.9 mM/hr in all experiments performed in the presence of Fe and Cr/Ni (including unsuccessful inhibitor experiments), 3.6 to 5.6 mM/hr for experiments performed in the presence of Cu, and 0.7 mM/hr in the presence of V. At high gas conditions, O_2 consumption ranged from 0.9 to 1.1 mM/hr in the presence of Fe only, and 1.8 to 1.9 mM/hr in the presence of both Fe and Cu.

It is possible that vanadium catalyst has a weak effect on MEA systems, and degradation is controlled by a combination of reaction kinetics and oxygen mass transfer. On the other hand, it is also possible that when Cu is present, enhanced mass transfer is taking place in the boundary layer, which explains the enhanced oxidation rate.

Total carbon and nitrogen analysis shows that with the exception of the low gas experiment performed in the presence of Cr and Ni catalyst, there is over a 90% material balance on all selected low and high gas flow experiments.

9.2.5. Other Amine Systems

Aqueous MEA/PZ systems are not an attractive option for CO_2 capture due to their high degradation rates. DEA, a secondary alkanolamine, oxidized to form N-formyldiethanolamine (FORMYDEA), formate and other unknown HPLC products in the presence of Fe. However, amines losses were approximately half of an MEA system subject to the same conditions.

MEA/PZ systems exhibit degradation rates 25 to 75% greater than analogous MEA systems. In the absence of Inhibitor A, degradation rates in the presence of Fe and Cu are four times as high as in the presence of Fe only. Even with the 90% to 94% decrease in degradation rates with the addition of 100 mM of Inhibitor A, carbon and nitrogen production still occurs at significant rates. The free radical products formed in the oxidation of MEA appear to attack PZ as well as other MEA molecules.

9.3. Kinetics Controlled Conditions

Experiments performed at low gas flow show Inhibitors A and B, along with EDTA, to be effective oxidation inhibitors for MEA and PZ systems. MEA analogs and hindered amines were also tested and proved to be resistant to oxidative degradation.

9.3.1. Successful Inhibitors

Concentrations of 100 mM Inhibitor A, 7.5 mM Inhibitor B and 100 mM EDTA independently proved to be successful in inhibiting MEA oxidation.

The presence of 100 mM Inhibitor A decreases the formation of known degradation products by 90% in an MEA system catalyzed by both iron and copper; Inhibitor A decreases the formation of known products by over 99% and cuts MEA losses by a factor of eight in Cr/Ni catalyzed systems. High gas experiments performed with FTIR analysis confirmed the effectiveness of Inhibitor A in MEA systems.

From this analysis, one can conclude that Inhibitor A is an attractive option as an agent for inhibiting MEA degradation. Inhibitor screening has also targeted Inhibitor B as an effective oxidative degradation inhibitor for iron-catalyzed systems. In the presence of iron, 7.5 mM B decreases product rates by 97% and MEA losses by 75%. Its effectiveness in other metal catalyzed systems needs to be tested.

A set of low gas flow experiments involving EDTA revealed that a 100:1 ratio of EDTA to Fe is necessary to sufficiently inhibit the oxidation of MEA. At this ratio, no observable MEA losses or oxidative degradation products are detected. However, it is still unknown whether EDTA itself degrades at these reaction conditions. Oxygen consumption rates were 0.2 mM/hr or less under assumed inhibited conditions, which suggests that these systems are now limited by reaction kinetics and not oxygen mass transfer

9.3.2. MEA Analogs and Hindered Amines

MEA analogs (ethylene glycol, glycine and ethylenediamine), cyclic amines (piperazine) and other amines (DGA and AMP) were all resistant to oxidation at low gas rates.

Aqueous piperazine solutions do degrade in the presence of metal catalysts, albeit at much lower rates than MEA solutions. In terms of catalyst oxidation potential, Cu > V > Fe. In concentrated PZ solutions, 5 mM of Cu catalyst was sufficient to create appreciable concentrations of EDA and formate, while 5 mM of Fe has no effect on oxidation. In 2.5 m PZ solutions, 5 mM V catalyst resulted in carbon and nitrogen formation rates at about 60% of the rates produced by Cu catalyst.

The addition of 100 mM of Inhibitor A to concentrated PZ solutions in the presence of Fe and Cu decreased formate and EDA concentrations by over 90%. Degradation was completely inhibited by the addition of 100 mM Inhibitor A to PZ solutions catalyzed by Fe only. Therefore, it may be more advisable to minimize iron concentration in PZ solutions to inhibit corrosion, as opposed to adding Cu to inhibit corrosion and Inhibitor A to inhibit degradation.

For 2.5 m PZ solutions, the addition of 100 mM A to vanadium catalyzed solutions was not effective. Carbon and nitrogen formation rates were decreased by 25%. However, the addition of 5 m $KHCO_3$ to 2.5 m PZ (in the presence of 5 mM V) completely inhibited oxidative degradation. It is believed that the addition of the potassium bicarbonate alters the ionic strength of the solution and severely limits mass transfer capabilities.

Low gas flow degradation experiments performed on MEA analogs (potassium glycinate, ethylene glycol/potassium bicarbonate and EDA) illustrate the importance of the alkanolamine structure in oxidative degradation. In terms of accumulation of degradation products and solvent losses, all of these solvent systems are resistant to oxidative degradation in the low gas flow apparatus at low gas flow. Diethylenetriamine (DETA), the dimerization product of EDA, is an oxidative degradation product unique to

EDA systems that could be used as potential marker in future experiments involving EDA.

AMP, a sterically hindered amine, and DGA, an alkanolamine with a four carbon backbone and an ester linkage, were both resistant to oxidative degradation in the presence of Fe catalyst; AMP was resistant to oxidative degradation in the presence of Cu as well. This was confirmed through minimal formation of degradation products and no detected amine losses.

9.4. Estimation of Rates for an Industrial Absorber

Using experimental data collected within the scope of this project, a comparison of predicted degradation rates for an industrial application was made with literature values of observed degradation rates. In order to make this calculation, details of the physical performance of an absorber column must be known. The information for this calculation came from a selected case of a rigorous absorber model developed by Plaza (2008) for modeling CO_2 removal from flue gas using MEA.

The calculations were made assuming 81.5% CO_2 removal from a flue gas containing 13.3% CO_2 and 5% O_2 on a wet volume basis. The solvent was 9 m MEA (35 weight %) and the absorber operated with a lean CO_2 loading of 0.40 and a rich loading of 0.51. The column had 6.1 m (20 ft.) of stainless steel Flexipac structured packing, and operated at atmospheric pressure. The absorber, with a diameter of 11.3 m, operated with a nominal temperature of 55°C. The superficial liquid and gas velocities were 5.3×10^4 kg/m^2-hr and 6.4×10^3 kg/m^2-hr respectively. Rates for three separate scenarios were predicted: mass transfer controlled conditions, physical solubility of oxygen controlled conditions, and reaction kinetics controlled conditions.

9.4.1. Mass Transfer Controlled Conditions

In order to complete the estimation of the degradation rates at mass transfer controlled conditions, the following assumptions were made regarding the absorber:

- Degradation occurs only in the absorber packing. No degradation occurs in the absorber sump.
- The bulk liquid O_2 concentration was negligible. This assumed fast reaction kinetics, but not fast enough to have enhanced mass transfer (i.e. reaction occurring in the boundary layer, which is believed to happen when Cu catalyst is present).
- Mass transfer coefficients and wetted packing area were estimated using Onda et al. (1968) in order to calculate the performance of the packing.
- The revised Aspen model estimated the viscosity and density of the amine solution using the correlations by Weiland (1996), surface tension of MEA using data gathered by Vazquez et al. (1997), and the diffusion coefficient of O_2 in MEA using the Wilke-Chang Equation (Seader and Henley 1997).
- Physical solubility of O_2 in the amine solution was assumed to be the same as the solubility in water, 1116 L-atm/mol (Dean 1992). The Henry's Constant was then corrected for the effect of ionic strength on the physical solubility to 1436 L-atm/mol, using the values of the van Krevelan Constants for aqueous MEA species (Weiland 1996).
- The amount of fractional liquid holdup in the packing was set at 5% in Aspen.

The absorber model was created using the rate-based RADFRAC program, in which the 20 ft of packing was divided into 20 equal segments (N_s). The kinetic holdup in absorber packing was calculated at 3.94 m^3 per segment, which gave a liquid residence time of 1 minute in the packing.

The absorber model estimates k_xaV (where k_x is the liquid mass transfer coefficient, and aV is the interfacial area in the packing) to be 462.2 kmol/s. Dividing by

the average interfacial area (a_i) and molar liquid density per segment gives a k_c (liquid film coefficient with a concentration driving force) of 0.031 cm/s. Cullinane (2005) estimated k_c values of 0.007 to 0.014 in the wetted wall column for piperazine/potassium carbonate systems. The average O_2 absorption rate for the entire column was calculated using Equation 9.1:

$$O_2 \text{ Consumption Rate} = N_s*(k_x aV)*(P_{O2}/H_{O2}) \quad 9.1$$

Using the results from the absorber model, O_2 consumption was calculated to be 2.91×10^{-4} kmol/s. Dividing this by the total volume of liquid holdup gives an O_2 consumption rate of 13 mM/hr. CO_2 removal is calculated from inlet gas conditions (13.3% CO_2 at 6.1 kmol/s) and removal rate (81.5%) to be 0.66 kmol/s. The ratio of kmol O_2 absorbed/kmol CO_2 removed is 4.40×10^{-4}.

In order to relate the O_2 absorption to MEA loss, the stoichiometry (ν) must be known. According to Chapter 6, the stoichiometry is 1.5 kmol MEA/kmol O_2 at oxygen mass transfer controlled conditions. Multiplying this oxygen stoichiometry by the ratio of O_2/CO_2 gives a rate of 6.60×10^{-4} kmol MEA/kmol CO_2 removed, or 0.92 kg MEA per metric ton (MT) CO_2 captured. In economic terms, this amounts to \$2.22 per ton CO_2 captured - assuming a price of \$2.42/kg MEA (Grigsby 2008). This number doubles if Cu, which is believed to cause enhanced mass transfer in the boundary layer, is present as catalyst in solution. The degradation rate estimated for the physical absorption of O_2 in an amine scrubber unit is an order of magnitude greater than experimental rate observed at low and high gas conditions.

Literature values for MEA degradation rates agree with rates estimated from the Plaza absorber model. One literature value reports a degradation rate of 3.6 kg MEA per MT CO_2 captured (Arnold et al. 1982). This value is reported for CO_2 capture using a 5.4 m MEA solution (20 weight %), and includes MEA losses from other types of degradation, evaporative losses, spills, etc. A more recent estimate of degradation losses is 0.45 kg MEA per MT CO_2 captured for the same solvent system (ABB 1998). It should

also be noted that the literature values of MEA degradation also include MEA loss from the formation of heat stable salts and from the reaction of MEA with SO_2 in the flue gas. Goff (2005) estimated a rate of 0.29 to 0.73 kg MEA per MT CO_2 captured.

Literature values for MEA solvent makeup in industrial applications are either within the range or larger than the rates predicted when assuming physical absorption of O_2 into MEA. This would support Goff's conclusion that the oxidative degradation of MEA is controlled by the rate of O_2 absorption and not the kinetics of the degradation reactions in an industrial process. Additionally it would suggest that the O_2 is not completely depleted in the bulk solution since this assumption causes an over-estimation of the degradation rates.

9.4.2. Degradation Controlled by the Physical Solubility of Oxygen

In order to complete the estimation of the degradation rates controlled by the physical solubility of oxygen, the following assumptions were made regarding the absorber:

- The system is no longer oxygen-mass transfer controlled, either by the removal of catalyst or from the addition of a degradation inhibitor to the system.
- Degradation occurs only in the absorber sump. No degradation occurs in the absorber packing.
- Physical solubility of O_2 in the amine solution was assumed to be the same as the solubility in water, 1116 L-atm/mol (Dean 1992). The Henry's Constant was then corrected for the effect of ionic strength on the physical solubility to 1436 L-atm/mol, using the values of the van Krevelan Constants for aqueous MEA species (Weiland 1996).
- The holdup time in the absorber sump was estimated to be slightly higher than the holdup time in the absorber packing – 3 minutes.

With these assumptions, the physical solubility of oxygen in the absorber sump is equal to the concentration of O_2, which is defined at the partial pressure of O_2 over the

solution in the sump (P_{O2}) divided by Henry's Constant for oxygen, H_{O2}. The concentration of O_2 in the absorber sump, which has a volume of approximately 80 m^3, is 0.35 mM. However, since the residence time in the sump is three minutes, the entire liquid volume in the sump is turned over twenty times an hour. Therefore, the rate of oxygen absorption by physical solubility is 7 mM/hr. Using the same calculations detailed in the previous section, this O_2 absorption rate equates to an MEA degradation cost of $1.17 per MT CO_2 captured.

9.4.3. Kinetics Controlled

In order to estimate the degradation rates controlled by the reaction kinetics in the absorber, the following assumptions were made:

- The system is no longer oxygen-mass transfer controlled, either by the removal of catalyst or from the addition of a degradation inhibitor.
- Degradation occurs only in the absorber sump. No degradation occurs in the absorber packing.
- Degradation kinetics have been reduced to a rate such that O_2 consumption is less than the rate as calculated from the consumption of oxygen in the absorber sump.

Therefore, any oxygen consumption rate below 7 mM/hr would be considered kinetics controlled. For example, oxygen consumption rates at inhibited conditions at low gas conditions range from 0 to 0.5 mM/hr O_2. This equates to a cost of $0.00 to $0.08 per MT CO_2 removed due to MEA degradation.

However, there is another concern with systems controlled by reaction kinetics. Any absorbed oxygen that does not react in the absorber is carried over to the cross exchanger and the stripper, and creates the potential for high temperature oxidation. At this point in time, the effects of elevated temperature on MEA oxidation have not been studied. It is not known how product rates and O_2 stoichiometry would be affected.

9.4.4. Industrial Process Design Implications

When designing and optimizing a CO_2 capture process, the rate of solvent degradation is important from an economic and environmental standpoint. The concentration of O_2 in the gas to be treated should be minimized. Goff (2005) proved that the rate of oxidative degradation of MEA increases linearly with O_2 concentration. The combustion process should be optimized to operate as close as possible to the stoichiometric O_2 concentration. If additional dilution gas is needed, such as in natural gas fired power plants, the CO_2 recycle (O_2/CO_2 power plant) option could be a very attractive alternative.

The specific design of the absorber depends upon what is the limiting factor for amine degradation. If the process is oxygen mass transfer controlled, then the CO_2 absorber should not be over-designed. Since both CO_2 and O_2 absorption into MEA solutions is controlled by the rate of mass transfer across the liquid film, over-design of the absorber (for increased CO_2 recovery) will result in increased solvent degradation due to an increased mass transfer area for a given liquid film MT coefficient. Packing should be selected that has a high wetted area, but gives low liquid hold-up inside the tower.

If amine degradation is controlled by a combination of oxygen mass transfer and reaction kinetics (or reaction kinetics only), the holdup time in the absorber is an important parameter. In this case, degradation kinetics are slow enough that amine solution was assumed to be saturated with O_2 as it entered the sump, and the O_2 was consumed after the solution was no longer contacting the flue gas. In this case, a shorter residence time in the sump results in reduced degradation rates.

Chakravarti and Gupta (2001) proposed sparging the absorber sump with an inert gas, like N_2, to strip out the dissolved O_2 before it could react with MEA. In the latter case, O_2 stripping could have a beneficial effect on reducing solvent degradation.

Process equipment should be constructed from corrosion resistant materials if possible. At low gas conditions, it has been shown that Cu enhances MEA degradation to a greater extent than iron and vanadium. Cu, in the absence of a degradation inhibitor,

should be avoided as a corrosion inhibitor. The combined effect of Fe and V catalysts should be investigated. The addition of Inhibitors A, B or EDTA would significantly decrease amine degradation costs, but their impact on raw material costs and reclaiming costs are not understood at this time.

Building the process equipment out of materials resistant to corrosion, possibly stainless steel, FRP, or more expensive metal alloys, will increase the capital investment for the process but could result in decreased operating costs associated with solvent make-up and reclaiming. While stainless steel is corrosion resistant, Cr and Ni may leach into the amine system and still cause oxidation.

Solvents with high viscosity and/or ionic strength should have lower oxidative degradation rates. While it is expected that secondary and tertiary amines have faster degradation kinetics, the decreased O_2 absorption rates in these solvents should result in an overall decrease in the rate of oxidative degradation. Experimental data shows that hindered or longer-chain amines are resistant to oxidation, even in the absence of oxidation inhibitors.

9.4.5. Environmental Impact

MEA degradation costs may not be the most important factor in the CO_2 removal process. Important gaseous degradation products include NH_3, N_2O, NO_x, CH_4 and volatile amine. NH_3 is important because it reacts with nitric and sulfuric acids in the atmosphere to form particulate matter with a diameter of 2.5 microns or less ($PM_{2.5}$), which has a concentration limit of 15.0 $\mu g/m^3$ according to the National Ambient Air Quality Standards as set by the Clean Air Act. Several recent health studies indicate that significant respiratory and cardiovascular problems are associated with exposure to $PM_{2.5}$.

NO_x (NO and NO_2 specifically), also listed as one of the criteria air pollutants by the Clean Air Act, can react with volatile organic compounds (VOC's) in the presence of

sunlight to form ground level ozone; it can also react to form particulate matter, acid rain and toxic chemicals in the air.

N_2O and CH_4 concentrations are important because they are both classified as greenhouse gases along with CO_2. In fact, both of these gases have a greenhouse warming potential (GWP) greater than that of CO_2. The GWP compares the amount of heat trapped by a greenhouse gas to the heat trapped by an equivalent volume of carbon dioxide over a specific period of time (100 years). CH_4 has a GWP 21 times greater than that of CO_2, while the GWP of N_2O is 310 times greater.

Using data collected at high gas conditions from the FTIR and Plaza's absorber model, calculations show that CH_4 emitted to the atmosphere from the top of the absorber would contribute 0.005% of the GWP that would be removed by capturing the CO_2. While CH_4 concentrations were independent of catalyst, N_2O concentrations were greater in the presence of Cu catalyst. However, for this worst case scenario, N_2O emitted from the top of the absorber would contribute only 1% of the GWP removed by capturing CO_2.

Calculations show that NO_x production (primarily NO) would be 0.038 lb NO_x per MT CO_2 captured. Using an emission factor of approximately 210 lb CO_2 / MM BTU for coal produced electricity, NO_x emissions from the absorber would be 0.004 lb NO_x / MM BTU. This is well below the upper limits for NO_x emissions.

Ammonia emissions from the absorber appears to be the largest concern. Selective catalytic reduction (SCR) is a means of converting NO_x to produce N_2 and H_2O. Anhydrous ammonia is added to the flue gas stream and adsorbed onto a catalyst bed, which allows the ammonia to react with NO_x at flue gas temperatures. Target slip NH_3 concentrations are 5 to 10 ppm for SCR systems and 20 to 30 ppm for NCSR (non-catalytic) systems. Average ammonia emissions at high gas conditions were 40 ppm, which exceeds these target concentrations.

In order for amine absorption/stripping to be viable from an environmental standpoint, ammonia emissions must be decreased by one of two measures:

1. Adding an oxidation inhibitor to the system
2. Placing a reflux condenser on top of the absorber (additional operating costs)

If the second scenario takes place, then a slip must be taken from the middle of the stripper to prevent accumulation of ammonia in the system. The recovered ammonia could then be recycled back to the SCR for NO_x removal.

9.4.6. Comparison with Previous Oxidation Studies

Goff (2005) re-examined several key degradation studies along with his work to conclude that all previous degradation studies that had been reported as kinetics controlled were actually oxygen mass transfer controlled. A comparison between studies was made by using an apparent overall gas phase mass transfer coefficient K_G' (defined as the rate of oxygen consumption normalized by the partial pressure of oxygen) and the space time (liquid volume / gas flow rate). All prior studies, with the exception of Goff and this current study, were performed by sparging a gas through the amine solution with no additional agitation.

At low space times, the system should have a relatively high amount of agitation and mixing, and therefore a higher value of K_G'. Conversely, at high space times, the gas is very slowly sparged through the solution, and there is likely minimum mixing and agitation, resulting in much lower values of K_G'. While it is recognized that most of the methods for predicting mass transfer coefficients in gas-liquid contactors depend on the superficial gas velocity (Gaddis 1999; Van't Riet 1979), the space time was used in the analysis since the geometry of the degradation reactor was not reported in any of the compared studies.

Figure 9.1 illustrates Goff's findings that the apparent mass transfer coefficient does in fact correlate with the space time, and that K_G', the apparent mass transfer coefficient, depends on the square root of the space time. All of the studies fit this trend with the exception of Goff and this current study. This is easily explained as these studies used additional agitation which accounts for the much higher values of K_G' for a similar space time.

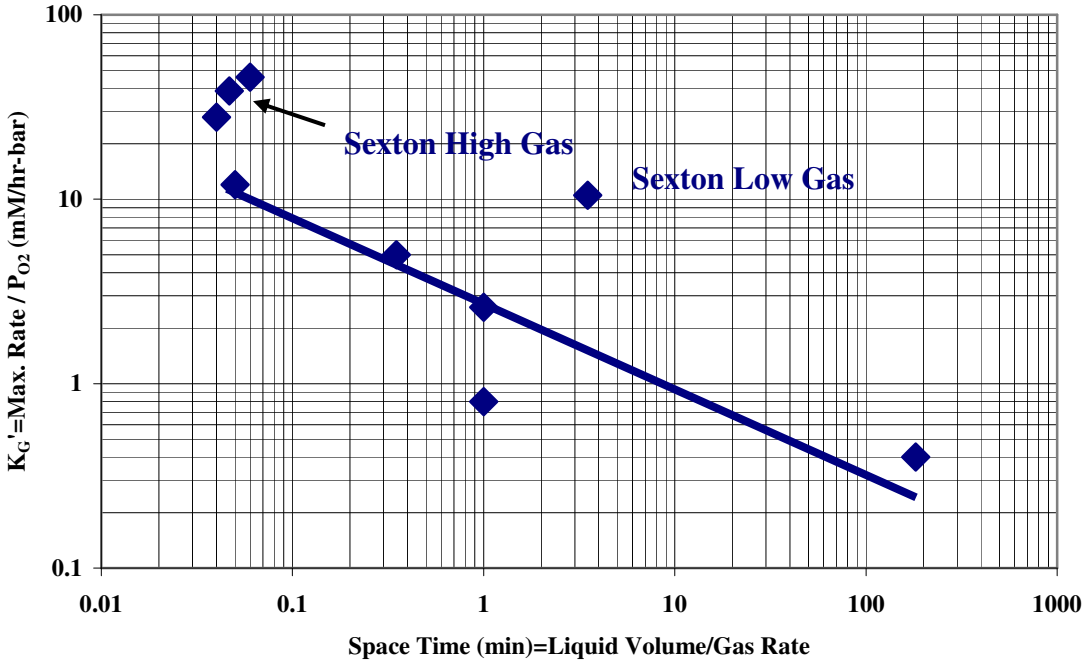

Figure 9.1 Correlation of Space Time and the Apparent Mass Transfer Coefficient, K_G', from Various Studies on the Oxidation of MEA

9.5. Recommendations

9.5.1. Characterization of Agitated Reactor Mass Transfer Conditions

The mass transfer characteristics of the reactors at both high gas and low gas should be measured and correlated. Extensive amounts of literature are available on predicting mass transfer coefficients in agitated reactors that do not vortex or have gas back mixing (Gaddis 1999; Garcia-Ochoa and Gomez 1998; Linek and Vacek 1981; Van't Riet 1979). Most of these studies explicitly state that correlations for the mass transfer coefficients are no longer valid for reactors that form a vortex; unfortunately, both reaction apparatus experience vortexing, and experiments performed at low gas also experience significant foaming, which is believed to act as a barrier to oxygen mass transfer. The effects of foaming on mass transfer should be studied as well.

Several literature studies state that measuring mass transfer coefficients in one solvent and extending the correlations to other solvents, even solvents with similar physical properties, can result in significant error in estimating mass transfer coefficients. O_2 absorption rates cannot be measured in situ with MEA solutions since the O_2 immediately begins to react with MEA. In order to pick a suitable solvent to measure equivalent O_2 uptake rates, data should be collected to provide a better understanding of the physical properties of MEA solutions. The O_2 solubility in MEA solutions is also currently unknown and has to be approximated. In order to accurately model absorption rate in a system that is in the Diffusion Regime, the bulk liquid concentration of O_2 must be known.

9.5.2. Kinetic Study

An experimental study should be performed to quantify the kinetics for the rate of formation of formate, HEF and HEI, all of which have been identified as major liquid-phase oxidation products. The oxidation state of the metals in solution as well as what amine species the metal is complexed to can have a significant affect on the catalytic properties of the metal; it is believed that ferrous ion is oxidize to ferric in the absorber, and reduced back to ferrous in the stripper. Rate constants and activation energies for the primary reactions will allow for direct calculation of changing O_2 stoichiometry based on the selectivity of the reactions at different process conditions.

The Aspen Plus simulation developed by Plaza allows for prediction of process performance of CO_2 absorption with MEA. The addition of reaction kinetics for the primary degradation reaction into this model would allow for more accurate estimation of oxidative degradation rates under actual operating conditions in a CO_2 capture process. This model could be used for a systematic study to identify beneficial process modifications to minimize the degradation rates. Additionally, this model would allow for more accurate quantification of solvent makeup rates and would improve the accuracy of the CO_2 capture economics.

9.5.3. High Temperature Oxidation Study

Experiments in this study only investigated the effects of amine oxidation at absorber temperature and pressure. It is believed that if degradation in the absorber is controlled by reaction kinetics, there can be a carryover of dissolved oxygen to the cross exchanger and the stripper. Oxidation rates of amines (and their product mixes) at high temperatures have not yet been investigated. A study investigating the oxidation of MEA at 80 to 100^{o}C should be conducted. Moreover, the effect of the interaction of oxidation products with carbamate polymerization products reported by Davis (2009) is unknown. Additional studies should be performed at high temperature to investigate amine oxidation in the presence of thermal degradation products. Finally, in order to mimic the absorption/stripping, amine solutions should be oxidized while varying temperature and pressure during the course of the experiment.

9.5.4. Additional Experiments

Diglycolamine (DGA) was shown to be resistant to oxidation in the presence of iron catalyst at low gas rates. A similar experiment should be run in the presence of iron and copper to test its resistance to degradation in the presence of a stronger catalyst. Inhibitor B, proven to be effective in inhibiting MEA oxidation in the presence of Fe, should also be tested in the presence of Cu, Cr and Ni catalysts. Lastly, NO_x and SO_x should be introduced to the feed gas at low and high gas conditions in order to simulate an industrial flue gas.

9.5.5. Analytical Techniques

HEI has been confirmed as an MEA oxidation product, but the mechanism for its formation has not been verified. The synthesis of HEI per Arduengo (2001) should be replicated in an attempt to verify the mechanism. In addition to HEI and HEF, there are

five other unknown peaks on the HPLC using evaporative light scattering detection. Mass spectroscopy should be utilized to identify these unknown oxidation products. Total carbon and nitrogen balances could be resolved by synthesizing MEA using ^{13}C and or ^{15}N and using isotope NMR to track all of the carbons and nitrogens.

9.5.6. General Lab Considerations

The current high gas system uses house air as a source of oxygen. It is recommended that future studies use a blend of N_2, O_2, and CO_2. NO_x species have been observed at appreciable concentrations throughout all high gas MEA oxidation experiments; in addition, nitrite and nitrate has been detected in low gas experiments. NO_x is most likely formed during the degradation reactions, but a small amount could theoretically come from the house air supply. NO_x are known free radicals, which can initiate the degradation reactions, and also form nitrosamines by reacting with secondary amines. By artificially creating a synthesis gas of N_2, O_2, and CO_2 any baseline NO_x could be removed from gas-phase analysis.

Liquid droplet entrainment is still an issue at high gas experimental conditions. If the level in the reactor is too high, then the entrained droplets from the vortex on the reactor wall carry over to the FTIR. If level is too low, the agitator blades skim the surface of the liquid and create entrainment by splashing. A more effective mist eliminator needs to be created to replace the air filter packing that is currently being used.

Appendix A: Literature Review of Nitrosamines

This appendix provides a literature review on the toxicology of nitrosamine compounds. It also presents reaction conditions at which nitrosamines are most likely to form, and describes how nitrosamine production can be inhibited.

Anion chromatography analysis has revealed nitrite and nitrate as major oxidative degradation products of monoethanolamine, and more importantly, piperazine. If nitrates – and nitrites especially – are present in substantial quantities in piperazine solution, it is possible that nitrite (or some other type of nitrogen compound) could react with piperazine to form a class of compounds known as nitrosamines.

In the pilot plant located at the Pickle Research Center, CO_2 capture is simulated by an absorption/stripping system by which CO_2 is removed from a synthetic flue gas using an amine solvent (Chen 2005). One amine solvent is an aqueous solution of 2.5 molal piperazine promoted by 5 molal of K^+ ion (in the form of potassium carbonate/bicarbonate). Oxidative degradation takes place in the middle of the absorber, and has been confirmed using anion and cation analysis. Therefore, nitrosamine formation from the oxidative degradation of piperazine solvent is a legitimate concern in the post-combustion removal of CO_2.

Toxicological studies have shown that piperazine can nitrosate to form *N*-mononitrosopiperazine (MNPz) and *N, N'*-dinitrosopiperazine (DNPz) in animals in vitro (Tricker et al. 1991). The formation of these compounds can come about by exposure to both nitrites and piperazine in the body. MNPz has been reported to be non-carcinogenic in rats (Love et al. 1977); conversely, the fact that significant levels of its carcinogenic metabolite NHPYR (Nitroso-3-hyrdoxypyrrolidine) can be detected in urine provides ample justification of the limited use of piperazine in medicine. Unlike its precursor, DNPz is both mutagenic and carcinogenic in experimental animals (Elespuru and Lijinsky 1976).

Under in vitro conditions (1 mM of piperazine with 2 mM sodium nitrite in 1 M citrate/HCl buffer) at 37^{o}C, piperazine nitrosated to form MNPz and DNPz over the range of pH 0.5 to 5.5. At pH maxima of 3.0, a 51% yield of MNPz and 3.8% yield of DNPz were obtained, corresponding to a 9.3% yield of DNPz from MNPz. Nitrosamine concentrations were determined using a gas chromatograph with a thermal energy analyzer (Dawson and Lawrence 1986).

In general, carcinogenous nitrosamines may be produced by the reactions of NO_x and secondary amines. Nitrosamines prepared from primary amines degrade at less than room temperature (Challis and Challis 1982). Tertiary amines do not directly form stable nitrosamines, but they can react with NO_x to produce secondary nitrosamines. Tertiary amines react with aqueous nitrous acid, contrary to common belief, and undergo dealkylation to form a carbonyl compound, a secondary nitrosamine, and nitrous oxide (Smith and Loeppky 1967).

The most probable mechanism is reaction of NO with an aminium radical or radical ion formed by amine oxidation with a free radical. This mechanism requires that the amine be in the process of oxidizing and that there be a sufficient concentration of NO in the solution. NO is not very soluble and would not be readily absorbed in an aqueous solution. It is present in low concentration in the flue gas, in contrast to percent or higher levels in studies that produce nitrosamines (Challis and Challis 1982).

$$R_2N^{\cdot} + NO \rightarrow R_2N\text{-}NO \qquad \text{A.1}$$

Gaseous N_2O_3 and N_2O_4 are effective reactants for making nitrosamines (Lovejoy and Vasper 1968). Kinetic studies of both diazotization (conversion of an aromatic primary amine into a diazonium compound) and deamination (removal of an NH group from an amino compound) in dilute solutions have given the following equation.

$$\text{Rate} = k\,[\text{amine}]\,[HNO_2]^2 \qquad \text{A.2}$$

Similarly, the combination of air and NO results in quick conversion of secondary amines to nitrosamines (Challis and Kyrtopoulos 1979), probably by oxidation of NO to N_2O_3. However, concentration of N_2O_3 and the oxidation of NO are both second order or higher processes. At the low concentrations of NO_x in the flue gas there is very little N_2O_3 and very little opportunity for oxidizing NO to NO_2.

Both N_2O_4 and N_2O_3 reacted with aqueous piperidine (similar in structure to piperazine) in aqueous 0.1 M NaOH give substantial amounts of *N*-nitrosopiperidine, plus smaller amounts of *N*-nitropiperidine in the case of N_2O_4. All these reactions are considered to occur predominantly in the aqueous phase and to be complete in a few seconds. With excess amine, yields of *N*-nitrosopiperidine reach maximum values. The dependence of product yields suggests that *N*-nitrosopiperidine formation follows equation A.3.

$$\text{Rate} = k_p\,[\text{piperidine}]\,[N_2O_x] \qquad \text{A.3}$$

Formation of *N*-nitrosopiperidine from the gaseous reactants occurs predominantly in the gas phase. N_2O_3 is nominally 3.3 times more reactive than N_2O_4 towards piperidine (Challis and Kyrtopoulos 1979).

A pH of 2 to 5 is required for the production of nitrosamines from nitrite, where some free amine is left and HNO_2 can decompose to the active reagent N_2O_3. Nitrosamine formation is generally presumed to require acidic conditions (pH < 5) where nitrite is converted to nitrous acid and H_2ONO^+ (nitrous acidium ion) exists at low concentration. With one or two exceptions, nitrosation appears to involve the unprotonated amine and a reagent such as N_2O_3, NOCl, H_2ONO^+, or NO^+ existing in equilibrium with both HNO_2 and NO_2^-. These reactions appear to be encounter-controlled and therefore very rapid. The oxidation of NO to a more reactive entity brought about by slow diffusion of air into the reaction vessel appears to be the rate-limiting process (Challis and Challis 1982).

While these studies provide insight into nitrosamines, they do not apply to pilot plant conditions because the absorber and stripper are run at basic pH. However, Keefer and Roller (1973) have shown that formaldehyde will catalyze the reaction of nitrite and diethylamine at pH 6.4 - 11 to produce diethylnitrosamine. The paper postulates that the nitrite reacts with the iminium salt produced by the interaction of the aldehyde and the

secondary amine. Yield is almost independent of hydrogen ion concentration in basic medium, the quantity of product at pH 11.0 being 40 percent of that found at pH 7.5.

Piperidine, similar in structure to piperazine, has shown to be one of the most reactive secondary amines. In the absence of formaldehyde, no nitrosamine could be detected above pH 7.5 under these conditions. Any nitrite present in the system could generate nitrosamines by this mechanism. This study is important because formaldehyde has been hypothesized as an intermediate degradation product in the oxidative degradation of amines.

Calle et al. (1992) studied the nitrosation of sixteen secondary amines by nitropropane (PrONO) and nitrobutane (BuONO) in a strongly alkaline medium (0.10 M NaOH with sodium perchlorate) – including piperazine. Nitrites were not formed in the actual bulk of the reaction medium, but rather isolated, purified and used in pure form. The following rate equations were determined

$$\text{Rate} = k_{2obs} [\text{amine}] [\text{nitrite}] \qquad \text{A.4}$$

$$\text{Rate} = k_2 [\text{amine}] [\text{nitrite}] / (1 + [H^+]/K_a), \text{ where } [H^+] << K_a \qquad \text{A.5}$$

In another experimental study, the vapor pressures of 30 *N*-nitrosamines were calculated between the temperatures of 0 and 40°C using the Hass/Newton equation (Klein 1982):

$$\Delta t = (273.1 + t) (\log 760 - \log p)/ \phi + 0.15 (\log 760 - \log p) \qquad \text{A.6}$$

Δt = to be added to the temperature at the observed pressure to yield the boiling point at 760 mmHg (°C)

t = temperature determined at pressure p (°C)

log p = $\log_{10}$ of the observed pressure (mmHg)

ϕ = the entropy of vaporization at 760 mmHg (a function of temperature and structure)

Based upon these calculations, pure nitrosopiperidine (very similar in structure to mononitrosopiperazine) has a vapor pressure of 0.44 mmHg at 40°C (or 580 ppm in air at saturation). For three of the thirty nitrosamines, the vapor pressure of pure compounds were obtained by gas phase analysis from the saturated atmosphere above a layer of nitrosamine. Experimental results were determined to be within 10% of the calculated values. In conclusion, the volatility of nitrosamines is not insignificant; it cannot be excluded that if nitrosamines are being formed, they are somewhat volatile and their vapors could be inhaled (Klein 1982).

There are basic conditions at which nitrosamine formation can be prevented. U.S. Patent No. 5,223,644 (Blezard and Jones 1993) proposed to use bicarbonates and/or carbonates to inhibit the formation of nitrosamines during the preparation, storage, and/or use of amine oxides. Amine oxides are conventionally prepared by reacting a tertiary amine with hydrogen peroxide; sodium bicarbonate (usually below 1% by weight) is used to catalyze this reaction. This patent proposes to use 2.5% to 20% by weight of a bicarbonate/carbonate stabilizer to inhibit nitrosamine formation (a by-product of amine oxide production) below levels of 100 parts per billion (ppb).

Although this process was proposed for tertiary amines, *N*-substituted piperazines may be treated by this process as well. Previously, temperature rise was a significant problem in the formation of amine oxides; the bicarbonate/carbonate stabilizer renders the solution heat resistant with respect to the formation of nitrosamine impurities. Total nitrosamine contents were determined as total NO by a chemiluminescence method, whereby the sample, after destruction of nitrite ions by sulphuric acid, is denitrosated and the NO gas liberated therefrom is fed into a chemiluminescence analyzer (Blezard and Jones 1993).

Similarly, Kirsch et al. (2000) performed experiments using bicarbonate ion to inhibit nitrosamine formation by carbamate formation. Both morpholine and piperazine were tested; since the formation of an amine carbamate depends on the pK_a value of the corresponding ammonium ion, experiments with piperazine [pK_{a1} = 5.55] were carried out at pH 7.4. At a concentration of 1 mM piperazine with 25 mM HCO_3^-, nothing was

detected via ^{13}C NMR. However at a concentration of 2 mM piperazine, formation of piperazine carbamate is evident. The concentration of piperazine carbamate increases with increasing piperazine concentrations, until at 100 mM all of the applied $^{13}CO_2$ is completely converted.

To further demonstrate that formation of piperazine carbamate is responsible for the depleted yield of nitrosopiperazine, additional experiments with piperazine (2 mM) and various concentrations of HCO_3^- were performed at pH 7.4. In the presence of 200 mM HCO_3^-, *N*-nitrosation of piperazine (2mM) was inhibited by about 66% (from 300 μM nitrosopiperazine in the absence of HCO_3^- to 115 μM at 200 mM HCO_3^-).

$NaNO_3$ was used in control experiments as an additive to show that alterations in the ionic strength cannot induce a decrease in the yield of nitrosopiperazine. When the HCO_3^- concentration is increased from 50 to 200 mM, piperazine carbamate concentration doubled and nitrosopiperazine concentration was halved. This leads to the conclusion that piperazine carbmate formation is most likely responsible for the diminished yield of nitrosopiperazine (Kirsch et al. 2000).

Although formaldehyde is likely present in basic conditions in the absorber/stripper system, the presence of potassium carbonate should prevent the formation of nitrosamines by the formation of carbamates – which can be confirmed by NMR analysis. Furthermore, MNPz is an unstable compound and the formation reaction can be reversed back to piperazine and nitrate. The major uncertainty involves the concentration of piperazine; most studies involve dilute quantities of all the reactants involved, while the pilot plant uses 30% by weight piperazine.

Appendix B: NMR Analysis

Appendix B provides NMR analysis performed on degraded monoethanolamine and piperazine solutions catalyzed by iron, copper and vanadium. Speciation of MEA is noted, and carboxylic acid degradation products and EDA are identified using ^{1}H and ^{13}C analysis.

Nuclear magnetic resonance, or NMR, identifies unique ^{1}H atoms and/or ^{13}C atoms based on structure (double/triple bonds, attachment to acid/amine/etc. groups). Sealed liquid samples are subjected to a magnetic pulse, and each unique atom is characterized by a "chemical shift" on the readout. If the structure(s) in the solution is unknown, it may be necessary to construct a 2-D carbon-hydrogen correlation in order to determine the structure. Samples must be prepared with approximately 10% D_2O (by weight) and DSS (Shoulders 2005). D_2O, or deuterium oxide, is heavier than water and enhances the signal, thereby making the analysis easier. DSS, or Sodium 2,2-Dimethyl-2-Silapentane-5-Sulfonate, is used as a reference peak for aqueous solutions containing organic materials.

In order to prepare samples for NMR analysis, prepare a solution of D_2O/DSS by adding 0.5 g of DSS to 25 g of deuterium oxide (available from Cambridge Isotope Laboratories, CAS# 7789-20-0, 99.9% assay). This will ensure that all peaks will be referenced relative to the DSS peak, which is set at a shift of 0. In a screwtop vial, add 0.5 g of the D_2O/DSS solution to 3.5 g of a degraded amine sample. Using an Eppendorf micropipette, transfer approximately 500 μL of the solution to a 507-PP NMR tube made by Wilmad. The height of liquid in the tube should be approximately 2 inches. The samples are delivered to the NMR spectroscopy lab at the University of Texas at Austin, which operates under the instruction of Ben Shoulders. Steve Sorey and Jim Wallin are the technicians responsible for running the NMR analysis. Samples submitted for NMR analysis can be separated into three categories:

1. Degraded MEA samples containing organic acid degradation products or clean MEA samples with organic acids added.
2. Loaded MEA samples with and without formaldehyde added.
3. Unloaded MEA samples with and without formaldehyde added.

Recall that most of the degraded solutions contain some concentration of iron and/or copper. Magnetic metals have a tendency to broaden and distort NMR scans. The scans from a degraded MEA sample containing 5 mM Cu contained badly distorted peaks for both the ^{1}H and ^{13}C analysis. This is illustrated in Figures B.1 and B.2.

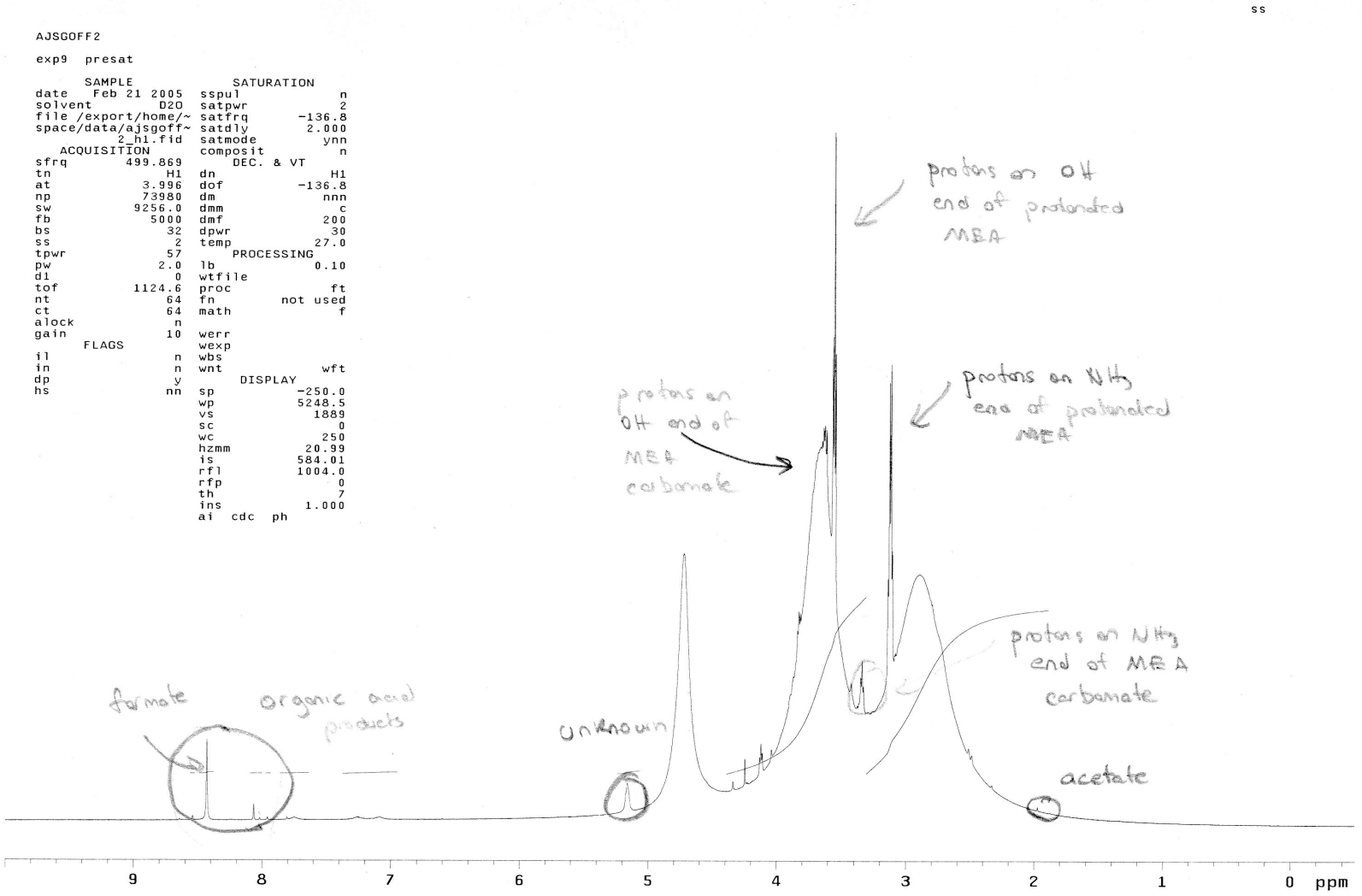

Figure B.1 ^{1}H NMR Analysis of Degraded MEA: 7 m MEA, 55^{o}C, α = 0.15, 5 mM Cu^{+2}, 1400 RPM

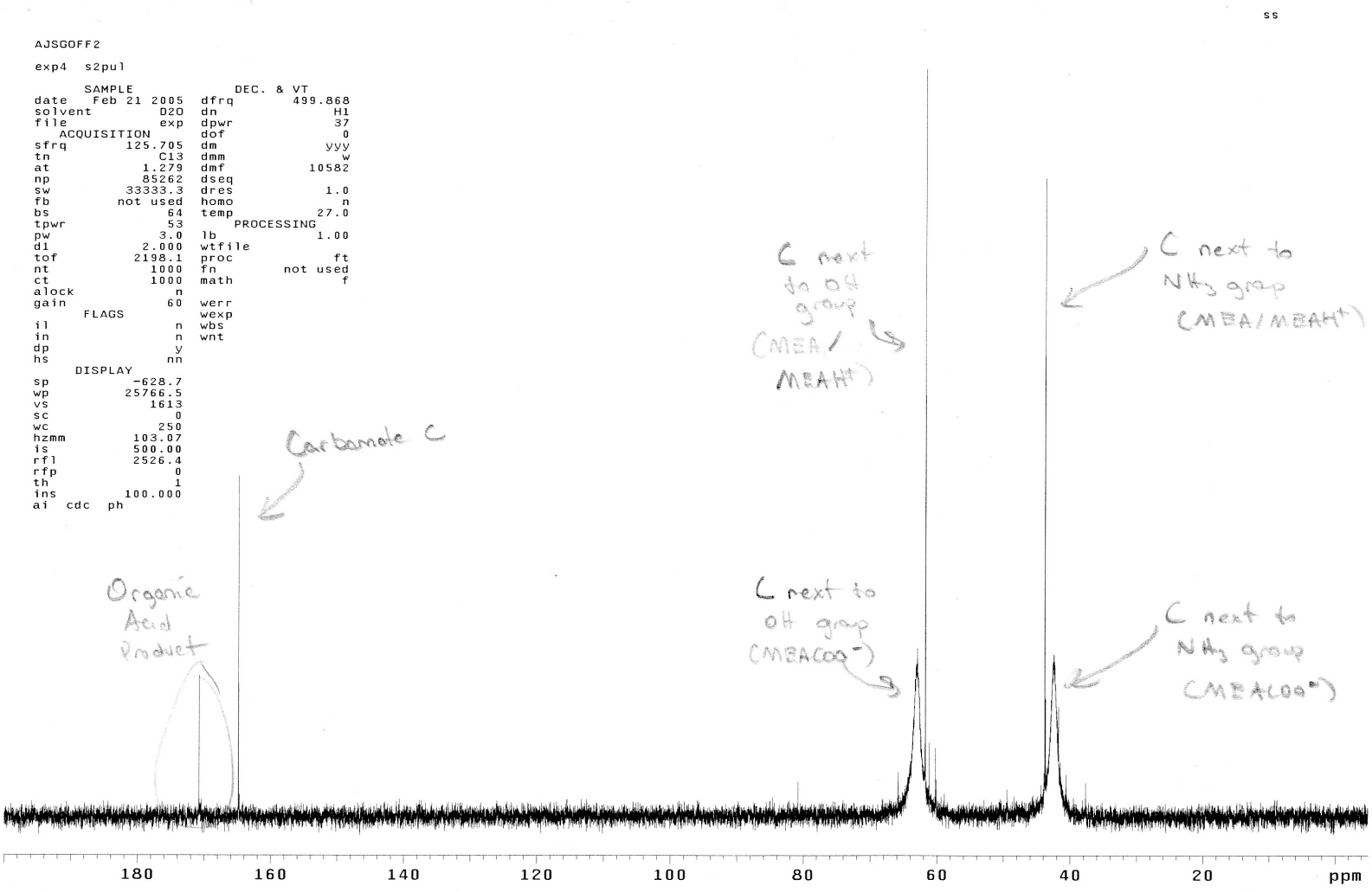

Figure B.2 ^{13}C NMR Analysis of Degraded MEA: 7 m MEA, 55°C, $\alpha = 0.15$, 5 mM Cu^{+2}, 1400 RPM

Table B.1 lists some of the significant peaks associated with this degraded MEA sample. Included are large peaks associated with the hydrogens on MEA and MEA carbamate. Minor peaks include formate and acetate according to the Aldrich Library of NMR spectra.

Table B.1 NMR Peak Summary for Degraded 7 m MEA, 55°C, $\alpha = 0.15$, 5 mM Cu^{+2}, 1400 RPM

Sample Name	Retention Time (ppm)	NMR Type
Acetic Acid	2.00	^{1}H
MEA/MEAH+ (next to nitrogen)	3.20	^{1}H
MEACOO- (next to nitrogen)	3.30	^{1}H
MEA/MEAH+ (next to OH group)	3.60	^{1}H
MEACOO- (next to OH group)	3.65	^{1}H
Water	4.75	^{1}H
Unknown	5.15	^{1}H
Unknown Organic Acid	8.00	^{1}H
Unknown Organic Acid	8.10	^{1}H
Formic Acid	8.40	^{1}H
MEACOO- (next to nitrogen)	42.0	^{13}C
MEA/MEAH+ (next to nitrogen)	43.5	^{13}C
MEACOO- (next to OH group)	61.5	^{13}C
MEA/MEAH+ (next to OH group)	62.5	^{13}C
Carbamate C	164.5	^{13}C
Unknown Organic Acid	170.5	^{13}C

NMR analysis of another degraded 7 m MEA sample exhibits similarities to the first sample. Like the previoius sample, this one was extracted from an MEA degradation experiment that contained approximately 0.6 mM Cu. The glaring difference is that this sample, even though it contained copper, did not really distort the ^{1}H or ^{13}C scan. Moreover, the peak locations might be somewhat different because, beginning with this sample, DSS was used to lock the peaks in place for ^{1}H NMR analysis. Figures B.3 and B.4 display the ^{1}H and ^{13}C scans; Table B.2 summarizes the peaks of significance.

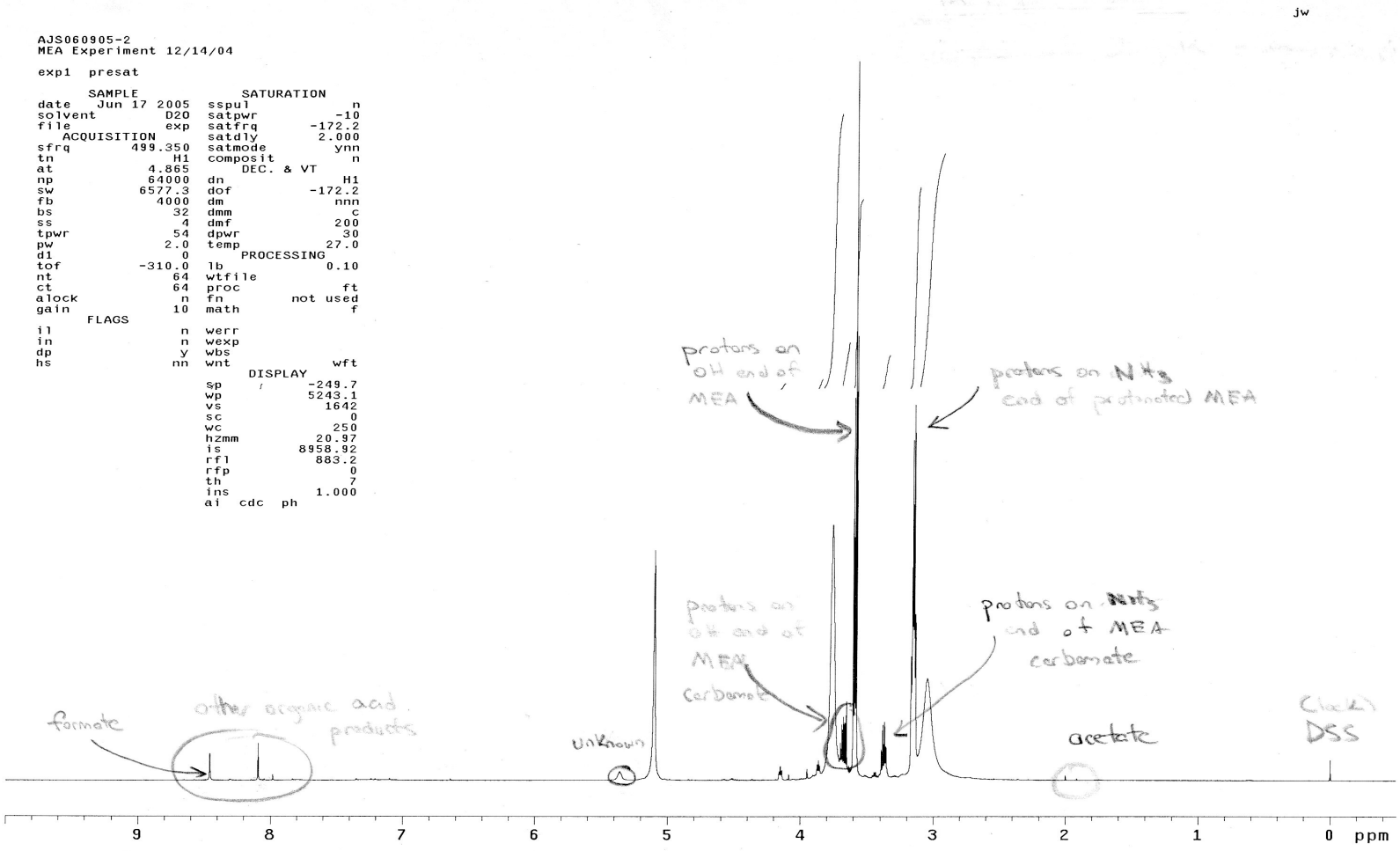

Figure B.3 ^{1}H NMR Analysis of Degraded 7 m MEA, 55^{o}C, α = 0.40, 0.6 mM Cu^{+2}, 1400 RPM

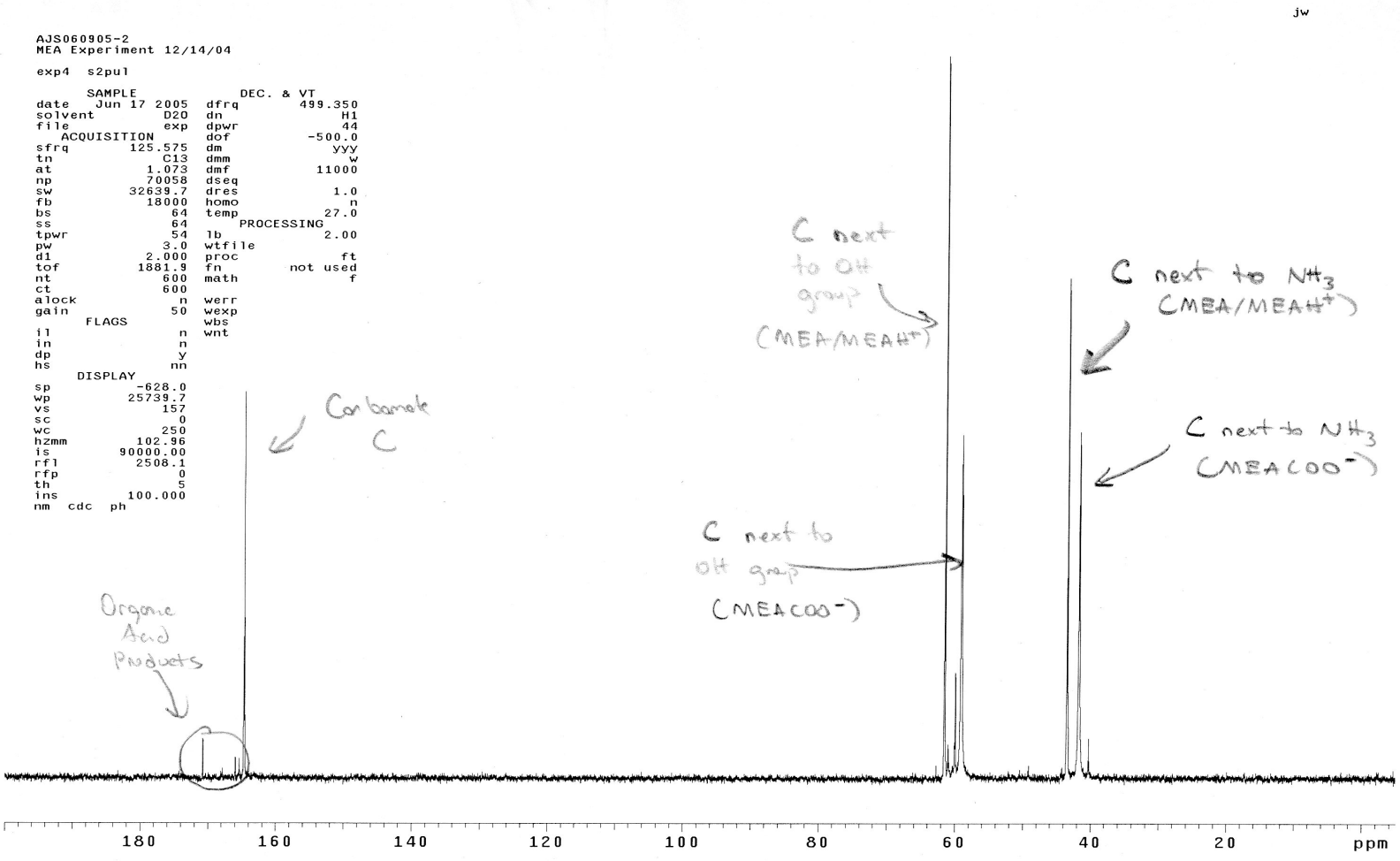

Figure B.4 ^{13}C NMR Analysis of Degraded 7 m MEA, 55°C, $\alpha = 0.40$, 0.6 mM Cu^{+2}, 1400 RPM

Table B.2 NMR Peak Summary for Degraded 7 m MEA, 55°C, α = 0.40, 0.6 mM Cu^{+2}, 1400 RPM

Sample Name	Retention Time (ppm)	NMR Type
DSS	0.00	^{1}H
Acetic Acid	2.00	^{1}H
MEA/MEAH+ (next to nitrogen)	3.15	^{1}H
MEACOO- (next to nitrogen)	3.40	^{1}H
MEA/MEAH+ (next to OH group)	3.60	^{1}H
MEACOO- (next to OH group)	3.65	^{1}H
Water	5.10	^{1}H
Unknown	5.40	^{1}H
Unknown Organic Acid	8.00	^{1}H
Unknown Organic Acid	8.10	^{1}H
Formic Acid	8.40	^{1}H
MEACOO- (next to nitrogen)	42.0	^{13}C
MEA/MEAH+ (next to nitrogen)	43.0	^{13}C
MEACOO- (next to OH group)	59.0	^{13}C
MEA/MEAH+ (next to OH group)	61.0	^{13}C
Carbamate C	164.5	^{13}C
Unknown Organic Acid	165.5	^{13}C
Unknown Organic Acid	166.0	^{13}C
Unknown Organic Acid	171.0	^{13}C

In order to attempt to qualitatively identify the four major carboxylic acid degradation products, an aqueous solution containing 200 mM of each of these four acids was added to an unloaded 7 m MEA solution. From the NMR scans, as shown in Figures B.5 and B.6, it appears that three of the four organic acids (formic, acetic, and glycolic) can be identified using the Aldrich Library. Oxalic acid does not show up on ^{1}H scans because there is only one type of hydrogen due to its symmetrical structure. Table B.3 quantifies the location of these peaks on ^{1}H and ^{13}C scans.

Table B.3 NMR Peak Summary for Unloaded 7 m MEA with 200 mM Carboxylic Acids Added

Sample Name	Retention Time (ppm)	NMR Type
DSS	0.00	^{1}H
Acetic Acid	1.90	^{1}H
MEA/MEAH+ (next to nitrogen)	2.80	^{1}H
MEA/MEAH+ (next to OH group)	3.60	^{1}H
Glycolic Acid	3.90	^{1}H
Water	4.85	^{1}H
Formic Acid	8.40	^{1}H
Acetic Acid	28.0	^{13}C
MEA/MEAH+ (next to nitrogen)	47.0	^{13}C
MEA/MEAH+ (next to OH group)	67.0	^{13}C
Unknown Organic Acid	176.0	^{13}C
Unknown Organic Acid	178.0	^{13}C
Unknown Organic Acid	184.5	^{13}C
Unknown Organic Acid	185.5	^{13}C

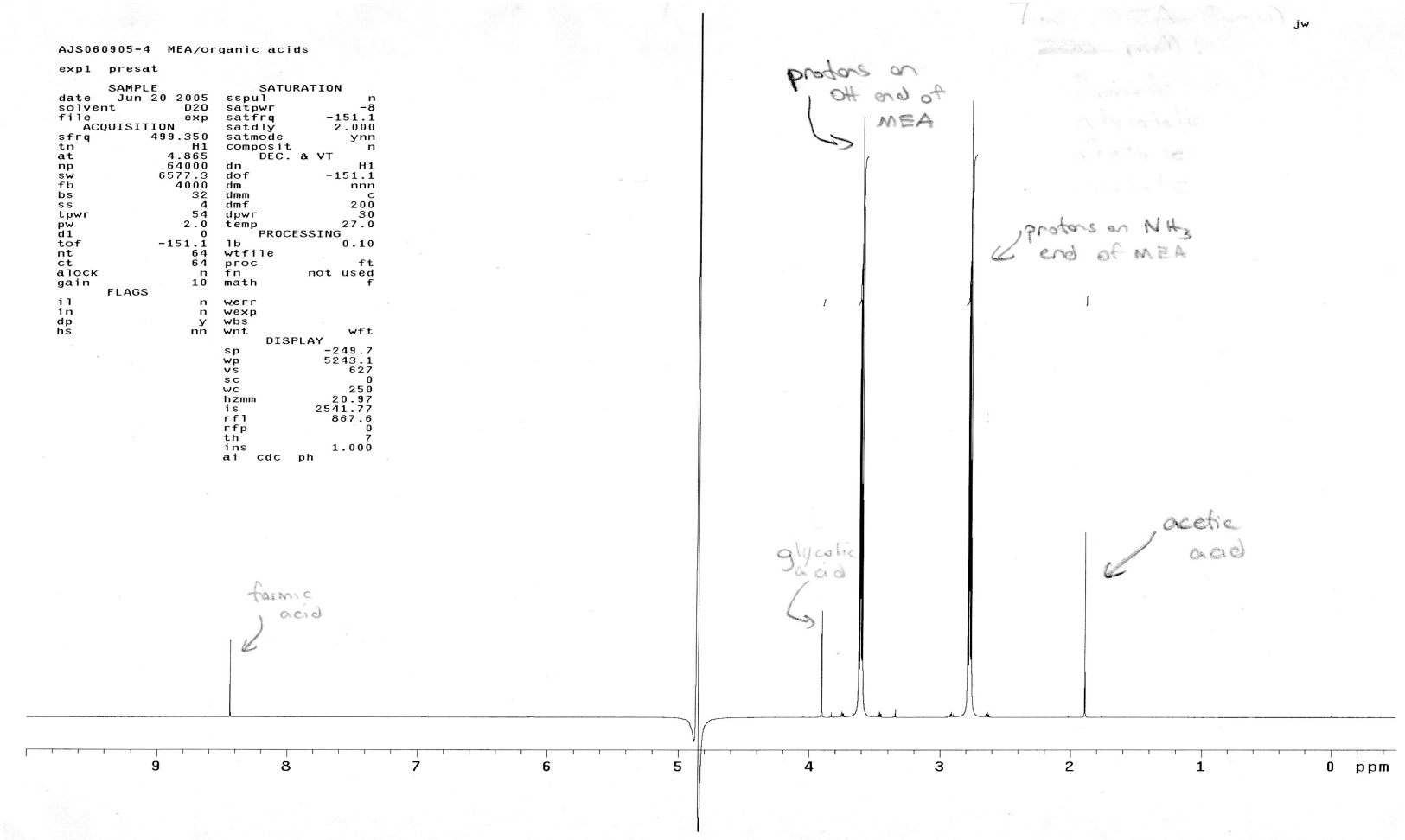

Figure B.5 ^{1}H NMR Analysis of 7 m MEA with 200 mM Acetic Acid, Formic Acid, Oxalic Acid and Glycolic Acid

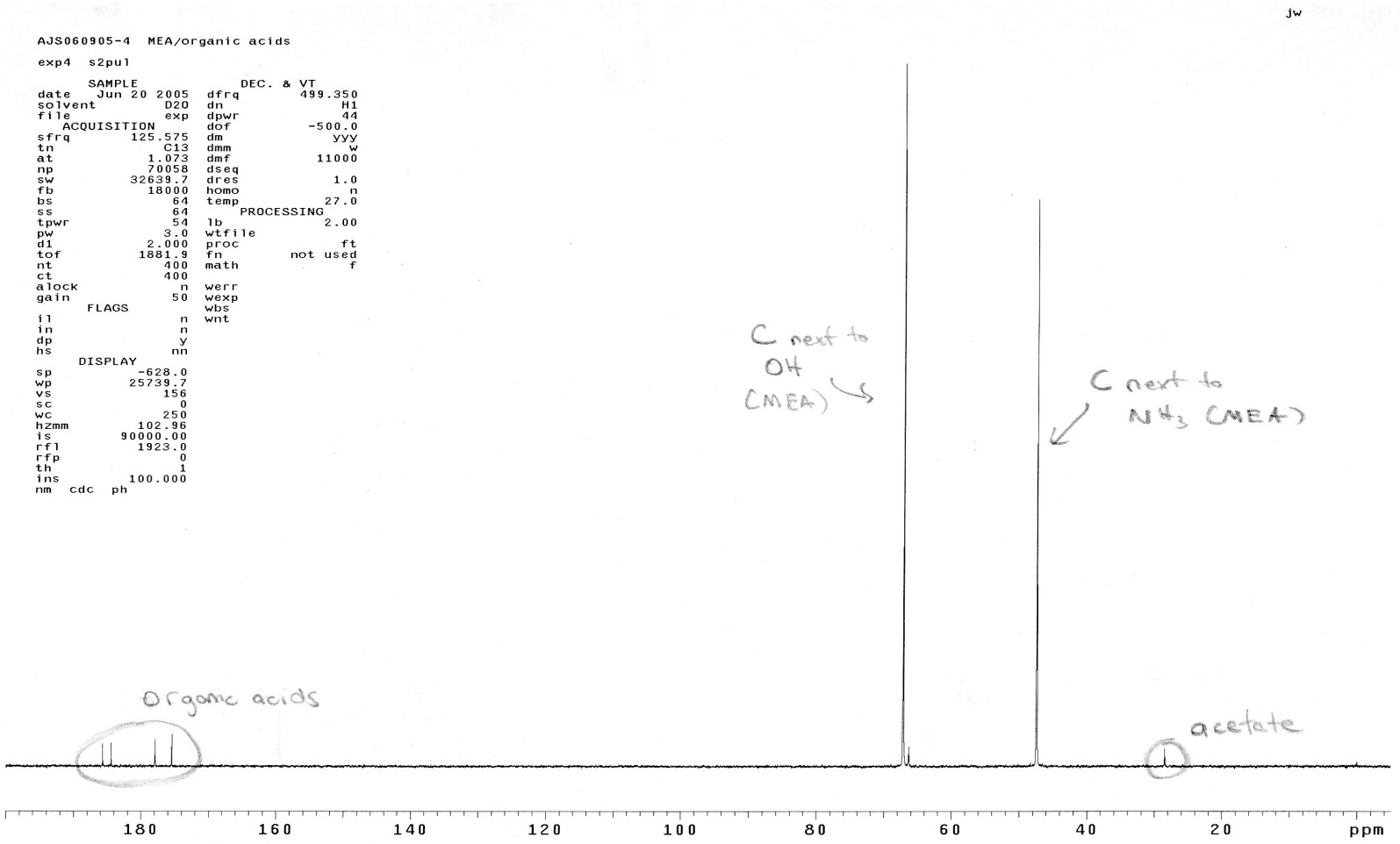

Figure B.6 ^{13}C NMR Analysis of 7 m MEA with 200 mM Acetic Acid, Formic Acid, Oxalic Acid and Glycolic Acid

Further NMR analysis was performed with the addition of formaldehyde to loaded and unloaded MEA solutions. The trends for unloaded (Figures B.7 and B.8) and loaded (Figures B.9 and B.10) MEA are similar. Four new, distinct peaks appear on the ^{13}C analysis for unloaded MEA with formaldehyde added and are correlated with something on the ^{1}H analysis, as shown in Figure B.7. However, it appears the peaks for the ^{1}H analysis that correlate with these ^{13}C peaks are hidden under the large MEA peaks. It is noteworthy that in Figure B.8 the peaks and their corresponding correlations do not appear on the 2-D plot.

This applies to the loaded solutions as well, but the loaded solutions are somewhat more difficult to interpret because they contain 5 mM Cu; the peaks on both scans are stretched a bit. The formaldehyde added sample (Figure B.9) shows three distinct peaks that do not appear in Figure B.10, which represents the sample with no formaldehyde added. The 2-D correlation supports what shows up on the ^{13}C; however, it appears once again that the peaks for ^{1}H analysis are hidden under the MEA peaks.

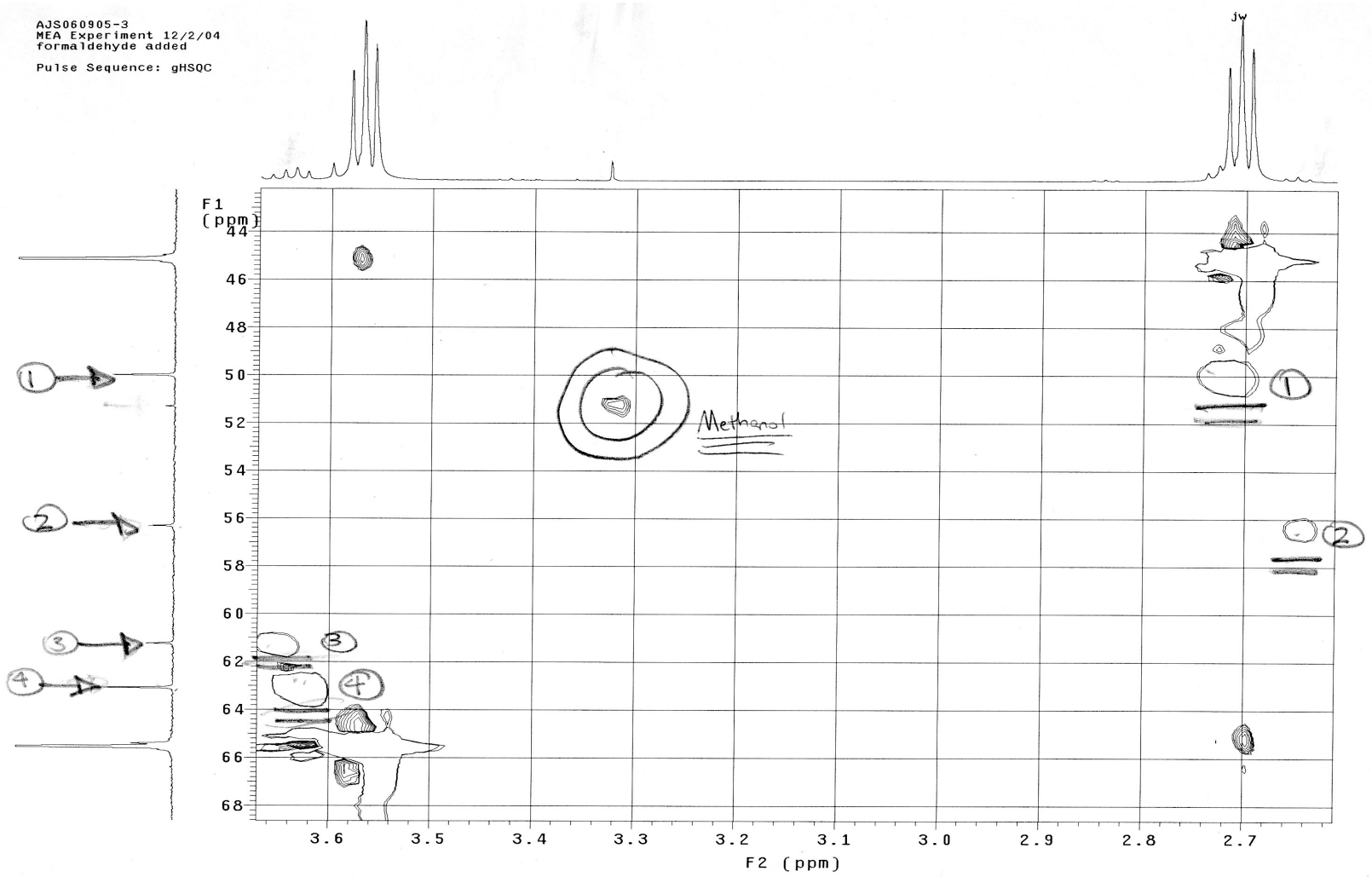

Figure B.7 2-D Correlation of 7 m MEA with 200 mM Formaldehyde ($\alpha = 0$)

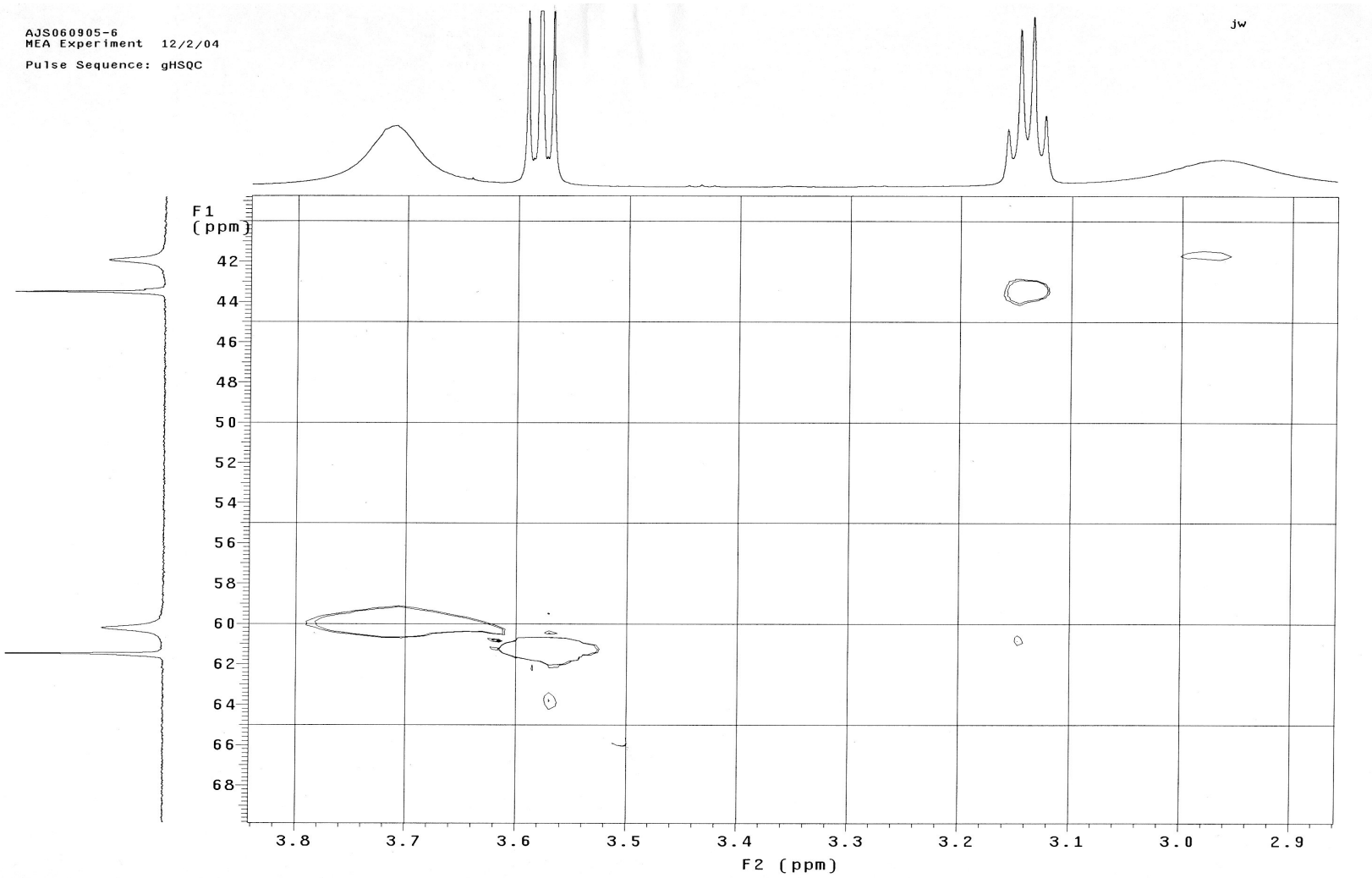

Figure B.8 2-D Correlation of 7 m MEA with no Formaldehyde ($\alpha = 0$)

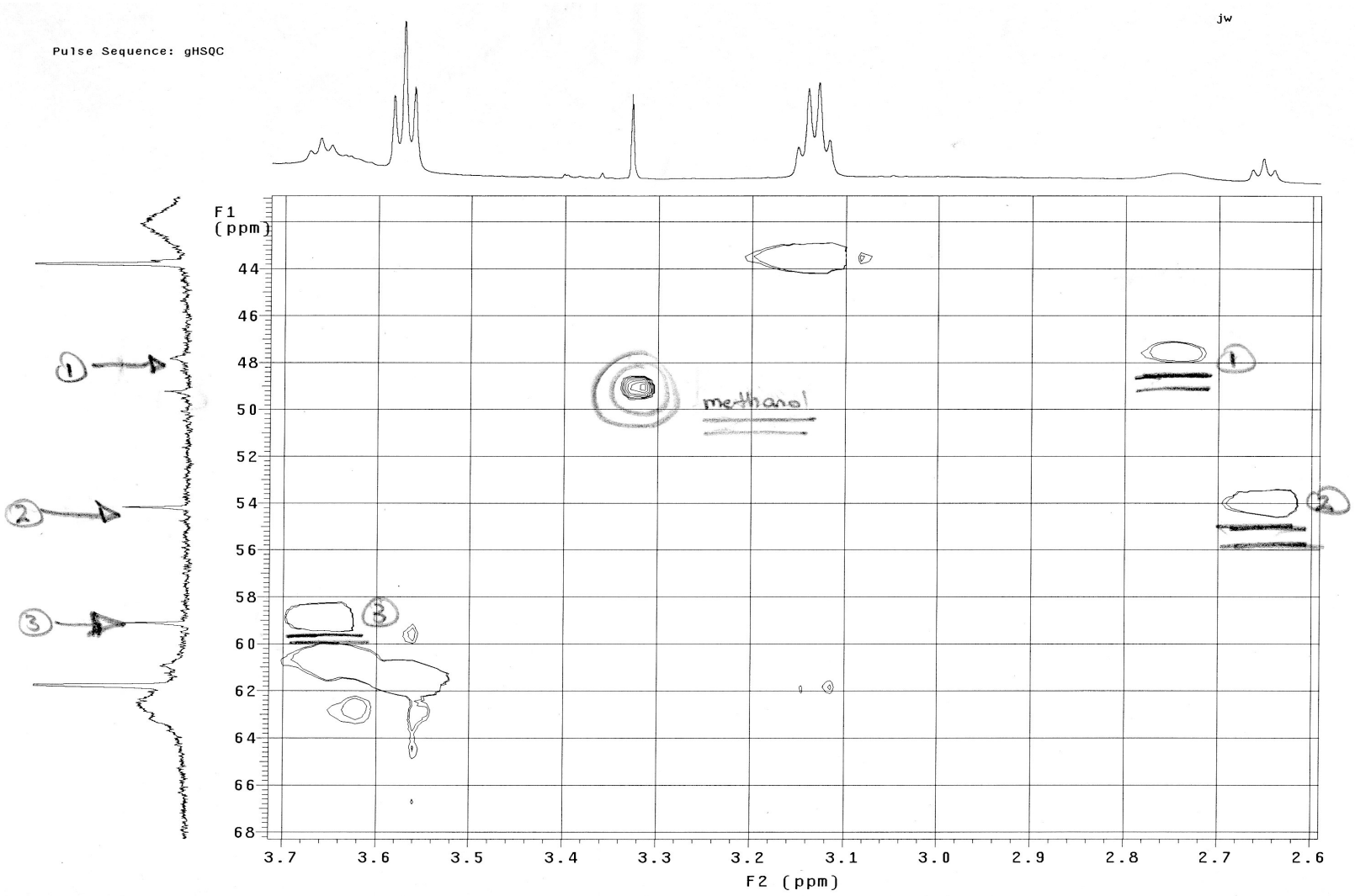

Figure B.9 2-D Correlation of 7 m MEA with 200 mM Formaldehyde ($\alpha = 0.15$)

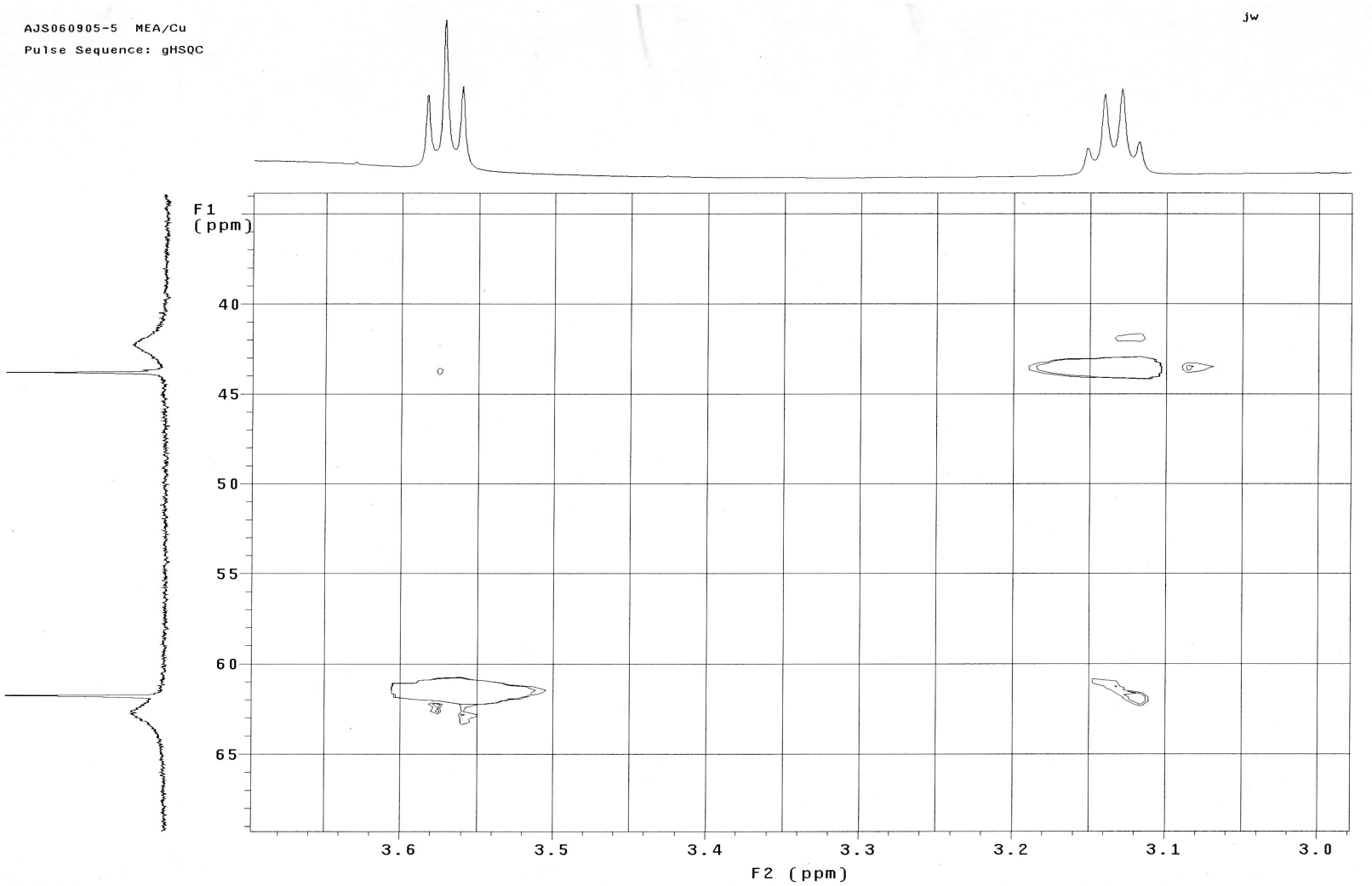

Figure B.10 2-D Correlation of 7 m MEA with no Formaldehyde ($\alpha = 0.15$)

NMR analysis was performed on experimentally degraded piperazine (PZ) samples to confirm the presence of ethylenediamine (EDA). Figures B.11 and B.12 below confirm the presence of EDA in these solutions.

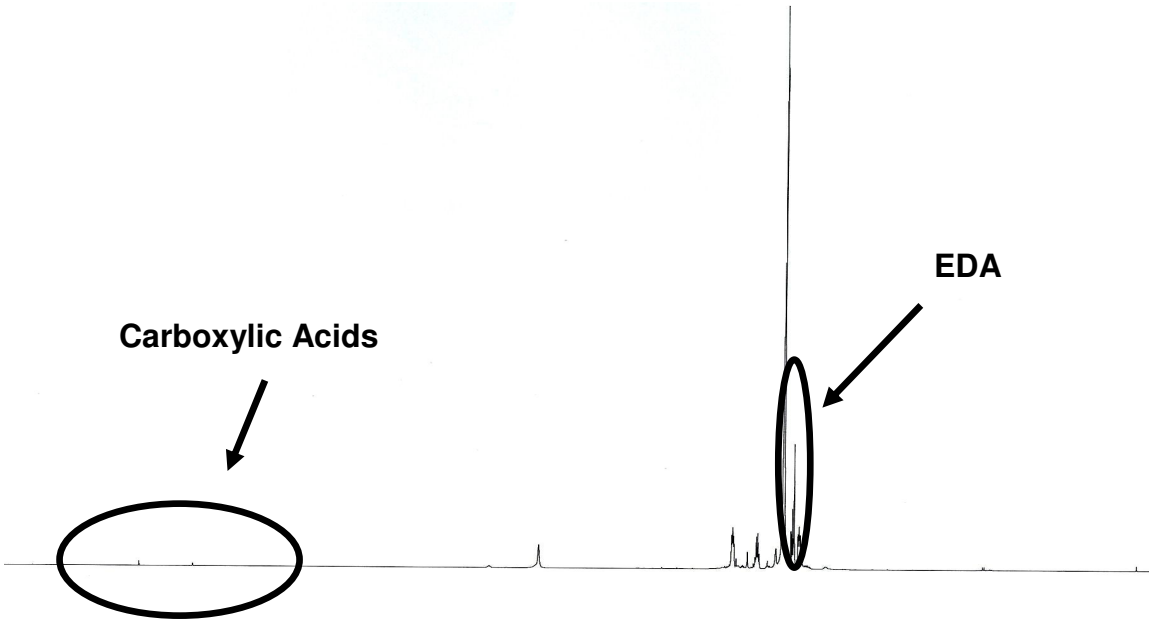

Figure B.11 ^{1}H NMR Analysis on Degraded 2.5 m PZ, 5 mM V^{+5}, 55°C, α = 0.30, 1400 RPM

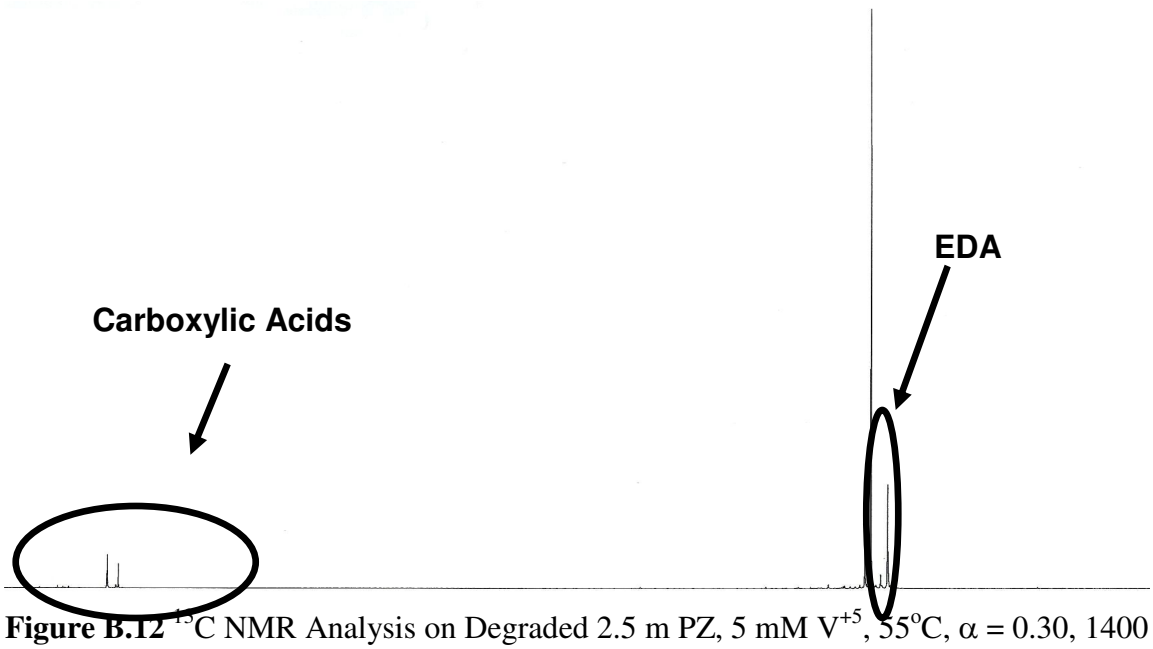

Figure B.12 ^{13}C NMR Analysis on Degraded 2.5 m PZ, 5 mM V^{+5}, 55°C, α = 0.30, 1400 RPM

Appendix C: Detailed Operational Procedures

This appendix gives detailed operating procedures for both cation and anion chromatography analysis on the Dionex ICS2500 and ICS3000 systems. This section also contains procedures on carrying out low and high gas flow experiments from startup to shutdown.

C.1. Anion Chromatography System Operation

Begin by checking to make sure that the Chromeleon server is running. The server monitor is found either in the Chromeleon startup menu or in the lower right corner of the desktop. If it is not running, start the server by clicking the "Start" button. The Chromeleon server is a background application that monitors and controls an instrument. It executes programs, sequences, and batches that are stored on a datasource, and saves data from an instrument as a channel into the same datatource. The status should read "Chromeleon Server is running idle" when the server is started. After the server monitor has been started, click the "Close" button. This will leave the server monitor icon in the Windows Services area of the task bar.

Click the Chromeleon icon on the desktop to begin the program. Chromeleon (Version 6.80) will open to the browser, where the sequences, programs, methods and control panels will be found. In the "Panels" folder, click on the ICS3000_IC panel. The ICS3000_IC panel is a tabset panel with the following headings: Home, Sequence Control, Status, Autosampler, Isocratic Pump, Eluent Generator, Detector Compartment, and Conductivity Detector. All of the important functions – eluent flowrate and concentration, suppressor current, cell heater, CR-ATC temperature and oven temperature – can be controlled from the "Home" tab.

Verify that the proper timebase is connected to the control panel. The timebase is a top level instrument container that is used to store all of the different module information simultaneously (from the isocratic pump, conductivity detector, chromatography oven, and autosampler). Click on the "Control" menu option. Select "Connect to Timebase" and choose the timebase under "My Computer". Confirm that the "connect" boxes are checked. The system is now ready to run a batch.

In order to set up the sample batch, press Ctrl-Tab, which will toggle the screen back to the browser. Under the folder "ICS3000_Anion Analysis" left-click the most recent date. Go to "File", click "Save As" and save the file as the date for the current day in the form of "MMDDYYYY". The status for all samples on the right side of the

browser should read “single”. Under the sample name, modify the names of all the samples accordingly. For each sequence, the following samples should be run initially: a blank sample of DDI water, then a calibration curve for the anion standards (10 through 50 ppm). After the calibration curve, then run the dilute experimentally degraded samples. The final sample is actually a placeholder that allows the shutdown command to turn off all of the modules after the sample batch has been run.

Modify the sample type, program, method, position, and injection volume for each sample. The blank sample and the shutdown sample should be saved as type “blank” from the drop-down menu, the calibration curve samples should be saved as “calibration”, and the experimentally degraded samples should be saved as “unknown”. Under the program category, choose “Anions” for all samples – with the exception of the final sample. Use the “Shutdown” program for the final sample. Under the method category, choose “Anions” for all samples. The injection volume for all samples should be 25.0 μL. Under the position column, enter the number on the autosampler tray where each sample was placed. The autosampler tray is a 10 by 10 grid numbered 1 through 100 (starting at the lower left corner, counting left to right for each row all the way to the upper right corner for 100). Save the sequence modifications.

Prior to beginning the batch, the cation IC system must be equilibrated at conditions used for “Anions”. These conditions are as follows: eluent generation at 2mM KOH, the CR-ATC turned on, a flowrate of 1.60 mL/min, chromatography oven temperature of 30^{o}C, and a suppressor current of 179 mA. The system pressure should be approximately 2200 psi. Allow approximately 30 minutes for the system to equilibrate.

To start the batch, click the “Batch” menu option from the top and select “Start”. Click the “Add” button and choose the sequence that was just modified. Click the “Ready Check” button to verify that there are no errors in the sequence you are trying to execute. If there are no errors impeding the batch from running, “ready check was successful” will appear in a dialog box on the screen. Click “OK”, then click the “Start” button to begin the batch. The autosampler needle will withdraw the blank from the appropriate vial and inject it into tubing that will carry the sample through the IC system.

The “Anions” program uses a 2 mM hydroxide eluent for the first 17 minutes of the program. The low concentration eluent helps to separate low molecular weight anions effectively. At time 17 minutes, a linear concentration gradient increases eluent concentration from 2 mM to 45 mM hydroxide from time 17 to 25 minutes. From time 25 to 35 minutes, 45 mM hydroxide elutes all of the high molecular weight anions off the column. At time 35 minutes, the program is finished. For a period of 6 minutes, the system returns to time zero conditions to re-equilibrate the system before the next sample is injected. After the final experimental sample has been run, the shutdown sequence turns off the eluent generator, CR-ATC, chromatography oven, eluent pump, and suppressor.

Once all samples in the batch have run, click on one of the five calibration standards from the browser panel. Switch to the method editor by clicking on the QNT-Editor icon on the toolbar. At the bottom of the screen, go to the “General” tab and type *ppm* in the “Dimension of Amounts” field and confirm that “Auto Recalibrate” is checked. Go to the “Detection” tab and set the integration parameters as needed. In most cases, several baseline noise peaks are integrated along with the main peaks. To eliminate the extra peaks, go to the “Detection” tab and add “Minimum Area” with a value of 0.010. Use the “Void Volume treatment” parameter to deal with the water dip.

Go to the “Peak Table” tab, right-click on the gray bottom half of the window, and choose “Autogenerate Peak Table”. Choose the “Enumerate peaks of current chromatogram” button. Read the warning in the dialog box and answer OK when it appears on the screen. Type in the peak names and retention times for the peaks displayed on the chromatogram. The peaks of interest are glycolate (Retention Time = 19.41 min), acetate (RT = 19.95 min), formate (RT = 20.61 min), nitrite (RT = 25.52 min), oxalate (RT = 28.80 min), and nitrate (RT = 32.29 min). Sulfate (RT = 28.18 min) and carbonate (RT = 26.60 min) are present as well, but are not important for degradation analysis. Sulfate concentration is a result of the degradation catalysts (which are added in the form of ferrous sulfate and cupric sulfate), and the carbonate peak is from the CO_2 loaded amine solution.

Go to the "Amount Table" tab. If the "Edit Amount Columns" dialog box does not appear automatically, right click in the empty gray space, and go to "Columns/Edit Amount Column". Click "OK" to the warning message about lack of amount columns. Click "Auto-Generate" and select the "Generate a separate amount column for EACH standard" option. Click "Apply" to execute the command. After columns for all standards have been created, click "OK" in the "Edit Amount Columns" dialog box.

Enter the amount of the actual anion concentrations for each of the five calibration standards (approximately 10, 20, 30, 40, and 50 ppm). Each anion stock concentration is needed to calculate the standard concentrations. For acetic acid, oxalic acid, sodium nitrite and sodium nitrate, divide the mass of the reagent (in grams) added to the 1-liter volumetric flask by the mass of water added to the flask (in grams) and multiply by 10^6. The resulting number is the concentration of the reagent in terms of parts of reagent per million parts of water (ppm_m). For formic acid (88 wt % in water) and glycolic acid (67 wt % in water), be sure to multiply the mass added to the stock solution by the weight percentage for the acids – since both acids are added in the form of aqueous solutions.

For each of the five calibration standards in the 100 mL volumetric flasks, take the mass of stock solution added (in grams) and divide it by total mass of the standard solution after water is added (in grams). Multiply this number by the stock concentration, and the output is the actual calibration standard concentrations. If all solutions were prepared correctly, then all of the concentrations should be very close to 10, 20, 30, 40, and 50 ppm.

After the calibration curve concentrations have been entered, click on the "Peak Table" tab and left-click on the "Calibration Type" column. Select "Quad" in the dialog box that appears and click "OK". Chromeleon will now automatically plot all calibration standard concentrations as a second-order function of peak area for each of the 6 anions of interest individually. Close the QNT-Editor and click "Yes" when asked if you want to save the changes. Once again, click on one of the standard chromatograms and click on the appropriate peaks. Click on the delimiter tool and use the tool to shape the peaks

and properly define their edges in an effort to eliminate including peak tailing in the overall area. Save the changes, close the chromatogram, and perform this procedure for all standard and unknown chromatograms.

After all of the peaks have been properly identified, reopen one of the chromatograms and click on the "Summary Table" tab at the bottom of the screen. This summary table lists the concentration of all anionic degradation products in every diluted sample in units of ppm_m. These concentrations, along with the dilution factor and molecular weight of the six reagents, are needed to calculate the concentration of the original samples. The dilution factor is self-explanatory – it tells by how much the original sample was diluted for analysis. It is calculated by dividing the total mass of the diluted sample (DDI water + original sample) by the mass of experimental sample added (in grams) to the screwtop vial. Most dilution factors range from 95 to 105.

The concentration of the original sample (in millimolar, or mM) is calculated by multiplying the dilute concentration (in ppm_m) of each anionic compound by the dilution factor, then dividing it by the molecular weight. This is done in an Excel template for every experimental sample run in each batch. The overall formation rate is calculated by subtracting the concentration (in mM) in the time zero sample from the concentration in the final experimental sample, and dividing it by the number of hours the degradation experiment had been running at the time the sample was taken.

C.2. Cation Chromatography System Operation

Begin by checking to make sure that the Chromeleon server is running. The server monitor is found either in the Chromeleon startup menu or in the lower right corner of the desktop. If it is not running, start the server by clicking the "Start" button. The Chromeleon server is a background application that monitors and controls an instrument. It executes programs, sequences, and batches that are stored on a datasource, and saves data from an instrument as a channel into the same datatource. The status should read "Chromeleon Server is running idle" when the server is started. After the

server monitor has been started, click the “Close” button. This will leave the server monitor icon in the Windows Services area of the task bar.

Click the Chromeleon icon on the desktop to begin the program. Chromeleon will open to the browser, where the sequences, programs, methods, and control panels can be found. In the “Panels” folder, click on the ICS2500 Panel. The panel displays information such as eluent composition, eluent flowrate, system pressure, oven temperature, and total conductivity signal. Verify that the proper timebase is connected to the control panel. The “timebase” is a top level instrument container that is used to store all of the different module information simultaneously (from the gradient pump, conductivity detector, chromatography oven and autosampler). Click on the “Control” menu option. Select “Connect to Timebase” and choose the timebase under “My Computer”. Confirm that the “connect” boxes are checked. The system is now ready to run a batch.

In order to set up the sample batch, press Ctrl-Tab, which will toggle the screen back to the browser. Under the folder “Cation IC Analysis” left-click the most recent date. Go to “File”, click “Save As” and save the file as the date for the current day in the form of “MMDDYYYY”. The status for all samples on the right side of the browser should read “single”. Under the sample name, modify the names of all the samples accordingly. For each sequence, the following samples should be run initially: a blank sample of DDI water, then a calibration curve for the appropriate amine or degradation product (10 through 50 ppm of the appropriate analyte). After the calibration curve, run the dilute experimentally degraded samples.

Approximately 3 mL of each sample must be transferred from its respective 15 mL screwtop vial to a 5 mL plastic vial that is used in conjunction with the AS40 Autosampler. After the vials have been loaded into the plastic racks and the racks have been placed in the autosampler, manually press the “Hold/Run” button on the front of the autosampler. That command should move the first vial into position for injection.

Modify the sample type, program and method for each sample. The blank sample should be saved as type “blank” from the drop-down menu, the calibration curve samples

should be saved as “calibration”, and the experimentally degraded samples should be saved as “unknown”. Under the program category, choose “Amine_Program”. Under the method category, choose “Amine_Method”. Save the sequence modifications.

Prior to beginning the batch, the cation IC system must be equilibrated at conditions used for “Amine_Program”. These conditions are as follows: 90% bottle A (6 mM MSA), 10% bottle C (55 mM MSA), a flowrate of 1.20 mL/min, and a suppressor current of 136 mA. The system pressure should be approximately 1400 psi. Allow 30 minutes for the system to equilibrate.

To start the batch, click the “Batch” menu option from the top and select “Start”. Click the “Add” button and choose the sequence that was just modified. Click the “Ready Check” button to verify that there are no errors in the sequence you are trying to execute. If there are no errors impeding the batch from running, “ready check was successful” will appear in a dialog box on the screen. Click “OK”, then click the “Start” button to begin the batch.

The “Amine_Program” employs a mobile phase of 11 mM methanesulfonic acid (MSA) from 0 to 7 minutes, with a step change to 16 mM at 7 minutes, then increases from 16 mM to 40 mM from time 12 to 17 minutes. The mobile phase remains at 40 mM until t = 20 minutes.

Once all samples in the batch have been injected, click on one of the five calibration standards from the browser panel. Switch to the method editor by clicking on the QNT-Editor icon on the toolbar. At the bottom of the screen, go to the “General” tab and type *ppm* in the “Dimension of Amounts” field and confirm that “Auto Recalibrate” is checked. Go to the “Detection” tab and set the integration parameters as needed. In most cases, several baseline noise peaks are integrated along with the main peaks. To eliminate the extra peaks, go to the “Detection” tab and add “Minimum Area” with a value of 0.010. Use the “Void Volume treatment” parameter to account for the water dip.

Go to the “Peak Table” tab, right-click on the gray bottom half of the window, and choose “Autogenerate Peak Table”. Choose the “Enumerate peaks of current chromatogram” button. Read the warning in the dialog box and answer “OK” when it

appears on the screen. Type in the peak names and retention times for the peaks displayed on the chromatogram. Depdending upon which solvent system was analyzed, peaks should appear at the following retention times: MEA – 4.69 minutes, Ethylene Glycol – 4.74 minutes, DEA – 4.95 minutes, AMP – 5.06 minutes, DGA – 5.28 minutes, EDA – 12.48 minutes, PZ – 13.96 minutes, DETA – 18.00 minutes.

Go to the "Amount Table" tab. If the "Edit Amount Columns" dialog box does not appear automatically, right click in the empty gray space, and go to "Columns/Edit Amount Column". Click "OK" to close the warning message about lack of amount columns. Click "Auto-Generate" and select the "Generate a separate amount column for EACH standard" option. Click "Apply" to execute the command. After columns for all standards have been created, click "OK" in the "Edit Amount Columns" dialog box.

Enter actual concentrations for each of the five calibration standards (approximately 10, 20, 30, 40, and 50 ppm). The stock concentration is needed to calculate these concentrations. Divide the mass of stock (in grams) added to the 1-liter volumetric flask by the mass of water added to the flask (in grams) and multiply by 10^6. The resulting number is the concentration of the compound in terms of parts of compound per million parts of water (ppm_m). For each of the five calibration standards in the 100 mL volumetric flasks, divide the mass of stock solution added (in grams) and divide it by total mass of the standard solution after water is added (in grams). Multiply this number by the stock concentration, to get the actual calibration standard concentrations. If all solutions were prepared correctly, then all of the concentrations should be very close to 10, 20, 30, 40, and 50 ppm.

After the calibration curve concentrations have been entered, click on the "Peak Table" tab and left-click on the "Calibration Type column". Select "Quad" in the dialog box that appears and click "OK". Chromeleon will now automatically plot amine concentration as a second-order function of peak area. Close the QNT-Editor and click "Yes" when asked if you want to save the changes. Once again, click on one of the standard chromatograms and click on the peak. Click on the delimiter tool and use the tool to shape the peak and properly define its edges so that any peak tailing is excluded.

Save the changes, close the chromatogram, and repeat this procedure for all standard and unknown chromatograms.

After all of the peaks have been properly identified, reopen one of the chromatograms and click on the "Summary Table" tab at the bottom of the screen. This summary table lists the concentration of amine in every diluted sample in units of ppm_m. These concentrations, along with the dilution factor and molecular weight, are needed to calculate the concentration of the original samples. The dilution factor is self-explanatory – it tells by how much the original sample was diluted. It is calculated by dividing the total mass of the diluted sample (DDI water + original sample) by the mass of experimental sample added (in grams) to the screwtop vial. Most dilution factors range from 95 to 105 for degradation products, and from 9500 to 10500 for samples analyzed for amine/solvent concentration.

The concentration of the original sample (in millimolar, or mM) is calculated by multiplying the dilute concentration (in ppm_m) of the component by the dilution factor, then dividing it by the molecular weight. This is done in an Excel spreadsheet for every experimental sample run in the batch. Overall degradation product formation rate is calculated by subtracting the concentration (in mM) in the time zero sample from the concentration in the final experimental sample, and dividing it by the number of hours the experiment had been running at the time the sample was taken.

Shutdown the Dionex system by opening the control panel and changing the suppressor current to zero. Click the "Off" button to stop eluent flow. Turn off the server by clicking the "Stop" button within the server monitor. Always turn off the server prior to powering down the computer.

C.3. Low Gas Flow Apparatus Operating Procedure

Each two low gas flow apparatus must be started independently. Low Gas Flow Apparatus #1 (without the flow controllers) sits on the left side of the fume hood. Take a sterilized 600 mL open-top Ace Glass jacked reactor and attach the 3/8" OD Tygon®

tubing from the Lauda circulator to the inlet and outlet ports on the reactor. Slide two metal clamps over the tubing and tighten them down over the ports to prevent heating fluid leakage. Fill the pre-saturator (Ace Glass vacuum adapter) to the top with DDI water; fill completely the 003 series stainless steel Lauda bath with boiler feedwater and turn on the power switch. Press the(·→) key to start the circulating pump on the Lauda E-100 heating circulator. Set the temperature setpoint at 55°C and allow the water to heat up.

Once the temperature has reached 55°C, use a 100 mL and a 250 mL volumetric flask to transfer 350 mL of loaded MEA (or the applicable amine) solution to the reactor. Record the mass of amine solution transferred to the reactor. Add the appropriate concentration of degradation catalyst (ferrous sulfate and/or cupric sulfate) and/or degradation inhibitor (inhibitor A) to the reactor via either solid or an aqueous dilute solution and record the mass of each added. Slide a rubber mat underneath the reactor so that the mat will absorb any vibrations from the reactor once the agitation begins.

Use a box cutter to cut two perpendicular slits through the middle of a rubber septum and coat the slits with vacuum grease. From the top down, thread the agitator shaft through the greased septum and the middle hole in the size 14 rubber stopper. Place the rubber stopper in the jacketed reactor and push down on it until there is a snug fit. Slide the agitator into the drive shaft and use the notched key to lock the agitator in place. Use the key to adjust the agitator height so that the impellers are 1" from the bottom of the reactor.

Turn the knob in on the upper right corner of the model SL1200 StedFast™ Stirrer to a speed of 9.5. Use a digital tachometer to confirm that the shaft is rotating at 1400 RPM. Adjust the knob setting if necessary. Agitate the solution for approximately 5 minutes – or until all of the catalysts/inhibitors have dissolved. Once they have dissolved, turn the agitator speed back to zero. Take a clean 15 mL screwtop vial. Through one of the two remaining holes in the rubber stopper, use a 5 mL glass pipette to remove 6 to 8 grams of solution from the reactor. Transfer the solution to the vial and record the mass of solution withdrawn from the sample. Label the sample with the date

and time the sample was taken, the mass of sample, and the amine/catalyst/inhibitor systems and concentrations used in the experiment. This is the initial sample from the experiment. Place another piece of tape on the outside of the reactor and mark the level of amine solution in the reactor.

Use the box cutter to cut perpendicular slits into two more rubber septa. Once again, cover the slits with vacuum grease. Slide a Fisherbrand glass thermometer into one of the rubber septa. Place the outlet tubing (1/4" Parker Perflex PE tubing) from the pre-saturator into the other rubber septum. In the cylinder corridor, open completely the gate valve on top of the 98% O_2/2% CO_2 cylinder purchased from Matheson. Set the regulator at 30 psig. Open the two gate valves along the flow path from the regulator to the reactor and inspect all threaded connections for gas leaks. Use the knob on the ColeParmer flowmeter to adjust the setting on the flowmeter to 13 (0-15 scale). Attach the PE outlet tubing to a 100 mL graduated burette to measure the displacement of soap bubbles as function of time. Adjust the flowmeter knob accordingly until the gas flow rate is approximately 100 cc/min (which corresponds to 6 seconds per a volume of 10 mL in the burette).

Once the knob has been properly set, disconnect the tubing from the graduated burette and insert the PE tubing into one of the remaining open holes in the rubber stopper. Adjust the tubing such that it extends 1" below the bottom of the rubber stopper. Insert the thermometer into the remaining hole in the rubber stopper and adjust the thermometer so that only the bottom ½" is submerged into the stationary batch solution (once the solution is agitated and vortexed, the outer vortex of the solution will submerge more of the thermometer). Use electrical tape to affix the rubber stopper to the outside of the jacketed reactor.

Turn the agitator knob back to the predetermined speed and use the digital tachometer to confirm the agitation speed of 1400 RPM. The experiment has been initialized and can run for a prolonged period of time with minimal monitoring. Some maintenance must be performed to keep the experiment running smoothly. Every 24 hours, the stainless steel Lauda baths must be refilled with boiler feedwater. Otherwise,

the gradual evaporation of water from the bath would cause the level to drop such that the low level alarm on the circulator would sound and the circulating pump would turn off. Moreover, every 48 hours, the Ace Glass pre-saturators must be refilled. This ensures that dry gas is never sent to the reactor; sending dry gas to the reactor would create an evaporative cooling effect, which would decrease the temperature and level of the solution in the reactor.

Approximately every 48 hours, a sample needs to be taken from the reactor. This allows for construction of a degradation profile as the experiment progresses. In order to withdraw a sample from the reactor, turn the speed of the agitator down to zero. Remove the thermometer from the rubber stopper. Insert the 5 mL glass pipette into the hole in the rubber stopper and withdraw approximately 5 grams of sample from the reactor. Transfer the degraded sample to a clean 15 mL screwtop vial and record the mass of solution. Cap the vial and label it with sample date and time, sample mass, and experiment description. Place the vial in the chemical storage refrigerator.

As previously mentioned, catalyst is added to the reactor as a sulfate salt. Sulfate is not consumed in any of the degradation reactions, so it is assumed that sulfate is conserved. Sulfate concentration is quantified and used as an internal standard using the anion chromatography analytical method. Sulfate appears on the anion chromatogram directly before oxalate.

If the water concentration in the reactor deviates from its initial value at any point during the degradation experiment, the sulfate concentration will change. Any increase in water concentration will result in a smaller sulfate peak area, while any decrease in water concentration will produce a larger sulfate peak area. Changes in water concentration result from the vapor pressure of water at 55^{o}C in the solution. Solution level in the reactor is monitored daily and DDI water is manually added to offset any evaporative losses.

It has been observed that even with the presaturator, on average approximately 7 mL of water evaporates from the reactor per day. Prior to collecting an intermediate sample, use the 2-10 mL Eppendorf autopipette to transfer DDI water to the amine

solution until level is at the mark on the outside of the reactor. After taking the sample, mark the new level in the reactor. Place the thermometer back into the rubber stopper and resume with solution agitation at 1400 RPM (if necessary, check the agitation speed with the digital tachometer). Repeat this process every 48 hours to collect intermediate experimental samples. Be sure to rinse the glass pipette several times with DDI water between sample collections.

After the solution has been degraded for approximately 14 days, the agitator can be turned off once again. Close the gate valves for CO_2/O_2 flow and completely close the gate valve on the gas cylinder. Remove the thermometer from solution and place it in the sink for washing and sterilization. Use the 5 mL glass pipette to transfer approximately 10g of degraded amine solution to a 15 mL screwtop vial and record the mass. Label the vial with sample date and time, sample mass and experimental conditions. This the final sample for the experiment.

Remove the gas tubing and agitator shaft from the rubber stopper as well. Remove the rubber septa from the thermometer, agitator shaft, and gas tubing and dispose of them. Place the agitator shaft and rubber stopper in the sink for cleaning. Transfer the remaining amine solution from the reactor to a beaker and record the mass of solution remaining. Carefully unhook the Tygon tubing from the reactor and drain the stainless steel Lauda bath of water. Empty the Ace Glass presaturator as well. Clean and sterilize the jacketed reactor.

The final step is to calculate the fractional mass loss from the reactor, which can be calculated by:

$$\text{Fractional Loss} = \{(\text{ISM} + \text{MCI}) - (\text{MSW} + \text{FSM})\}/\ \text{ISM} \qquad \text{C.1}$$

where: ISM = Initial Solution Mass

MCI = Mass of Catalysts and Inhibitors Added

MSW = Total Mass of Samples Withdrawn

FSM = Final Solution Mass

When this number is multiplied by 100%, it represents the percentage of water lost during the course of the experiment. This number is used in calculating the concentration of amine degradation products.

The procedure for constructing and operating Low Gas Flow Degradation Apparatus #2 only differs with respect to two components: the gas flow calibration and the agitator setting. The agitator on the second apparatus is a Maxima™ Stirrer manufactured by Fisher Scientific International. Unlike the Model SL1200 StedFast™, the Maxima™ is capable of agitation speeds of up to 2000 RPM. A setting of 6 for the Maxima™ achieves an agitation rate of 1400 RPM. This can be confirmed with the digital tachometer.

As mentioned previously, the gas flow for the second apparatus is operated using two Brooks 5850E mass flow controllers connected to a 4 channel Brose box. In the cylinder corridor, open completely the gate valves on top of the compressed oxygen (zero grade) and CO_2 cylinders purchased from Matheson. Set the regulator on the oxygen cylinder at 40 psig, and set the CO_2 cylinder at 60 psig. Open the two gate valves along the flow path from each regulator to the reactor and inspect all threaded connections for gas leaks. On the 4 channel Brose box, adjust the far left knob to channel 1. The digital readout now is displaying the % open for the channel 1 flowmeter valve (the O_2 flowmeter valve). Adjust the knob on the O_2 flowmeter until it reads 100% open. This represents an O_2 flow of approximately 95 mL/min based on the calibration curve. Now turn the far left knob to channel 2 (the CO_2 flowmeter). Adjust the channel 2 knob until the readout is 5.4% open. This represents a CO_2 flow of approximately 1.9 mL/min. Using the two flow controllers, a gas mix similar to that of the pre-mixed cylinder has been achieved. With the exception of the agitator and flow controller settings, follow the procedure for apparatus #1 for running a low gas flow experiment.

C.4. High Gas Flow Apparatus Operating Procedure

Turn on the FT-IR at least one hour prior to use to allow the analyzer sufficient time to warm up. Turn on the nitrogen purge to the FT-IR analyzer while making sure

the purge line is connected and open. Connect the sample line from the reactor to the pump inlet and plug in the sample pump power cord. Using channel 1 on the 4 channel Brose box, make sure air is flowing through the heated sample line – 30% open for the valve on the air flow controller should suffice. Gas must be flowing through the sample line at all times if the line is heated. This prevents the plastic tubing from melting and buildup of partial combustion products from accumulating in the sample line.

Set the "Umbilical Heater" and "Pump Heater" switches to 180°C. Flip the "Umbilical Heater" switch to turn on heat to the sample line. Open the CALCMET software application. Go to the "View" menu and open "Hardware Status". Table C.1 below lists the desired values for parameters under "Hardware Status". Once the temperature is 180°C the analyzer is ready to use. If any of the parameters are out of spec, the analyzer cannot be used. Call Mark Nelson of Air Quality Analytical to troubleshoot the issues.

Table C.1 FT-IR Hardware Status Parameters

Parameter	Desired Value(s)
Source Intensity	50 ± 25
Interferogram Height	| 1 to 4 | Volts
Interferogram Center	2400 ± 200
Interferometer Temperature	< 60°C

Once everything is up to temperature, it is time to make the background measurement. Turn the air on channel 1 of the control box to 0% and open up the nitrogen on channel 2 to approximately 25% open. Flowing pure nitrogen through the sample line flushes the line of any contaminants and helps to ensure a good background scan. Let the nitrogen flow through the system for 20 minutes. While the nitrogen purge is taking place, plug in the BriskHeat (Model #: UUTA10011NHN – 001, Serial #: 33264/1) insulating sleeve and turn on the IsoTemp and Lauda Heat Baths. Setpoints for both of the baths should be at 63°C.

Once the system has been purged, go to the "Options" menu and open the "Measuring Times" dialogue box. The background scan must be run at a longer integration time than the sample measurements, so choose a measuring time of 5 minutes

and click the OK button. Go to the "Measure" menu and choose "Zero Calibration". The analyzer will display a timer box that shows sample status.

After the background scan has been completed, CALCMET will display the results. A typical background scan is shown below in Figure C.1. Make sure there is no CO_2 or H_2O interference in the background scan. If there is, let the system purge with nitrogen for an additional 20 minutes and repeat the steps listed in the prior paragraph. Additionally, the maximum signal for the background scan should be above 25,000 counts and below 65,000 counts. If it is outside this range, contact Mark Nelson of Air Quality Analytical.

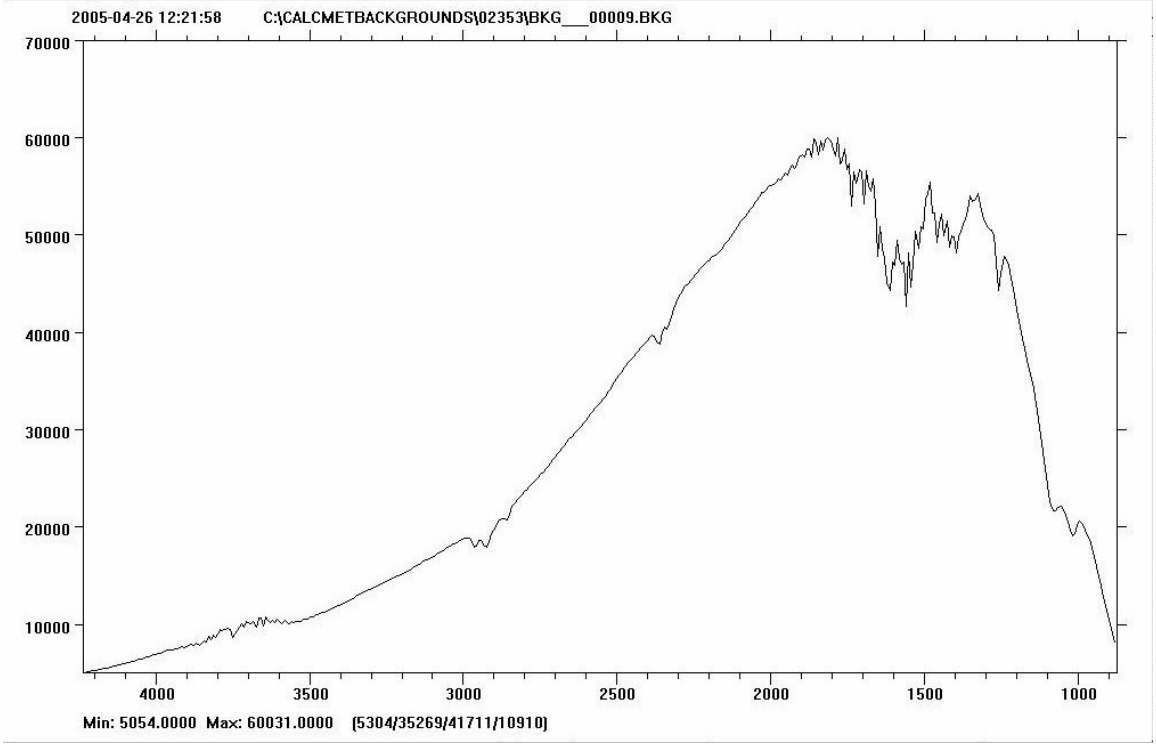

Figure C.1 Sample FT-IR Background Scan

If the background scan is successful, the FT-IR analyzer is ready for operation. Prepare the high gas flow apparatus by replacing the rubber septum that seals the reactor around the agitator shaft. Check the mist eliminator packing and replace it prior to beginning the experiment. Close the bottom drain valve on the reactor. Use a 100 mL and 250 mL volumetric flask to transfer 350 mL of the selected amine solution to the

reactor. Record the mass of amine solution transferred to the reactor. Add the appropriate degradation catalysts/degradation inhibitors (via addition of solids or in the form of an aqueous solution) and record the mass of each added.

Flip the power switch on the Maxima™ stirrer and turn the dial to "6", which represents an agitation rate of 1400 RPM. Agitate the solution until all of the degradation catalysts and inhibitors have dissolved. Once they have dissolved, turn the dial back to zero and turn the power switch on the agitator off. Insert a 10 mL glass pipette into one of the reactor openings and withdraw approximately 5 mL of solution from the reactor. Transfer the solution to a 15 mL screwtop vial and record the mass of solution. Label the vial (sample date and time, sample mass, experimental conditions) and cap it. This is the initial sample for the high gas flow experiment. After withdrawing the sample, place a piece of labeling tape on the outside of the reactor and mark the reactor level on the tape.

Fill the DDI reservoir on top of the Masterflex inlet peristaltic pump and turn on both of the pumps. Set the inlet pump to notch 4 out of 10 (which represents a flowrate of 1mL/min) and set the outlet pump to 10% (which represents a flowrate of 2 mL/min). Open the vent valve on the outlet gas line from the presaturator to the reactor and slightly crack the gate valve on the bottom outlet tube of the flash tank. Visually inspect the Tygon® tubing to ensure that flow is occurring through both of the peristaltic pumps. Insert the thermocouple plug into the reactor and cap all remaining openings on the reactor with the appropriate plugs.

Open the PicoLog Recorder program by clicking on the PicoLog icon on the desktop. Once the window has opened, left-click the "New File" icon. Go to "File", "Save As", and label the file with the appropriate date and experiment description. In the taskbar, go to "Settings" and click on "Recording". Make sure "real time continuous" is selected from the drop-down menu. Also in the "Settings" menu, click on "Sampling" and for the heading "sampling interval", make sure "5 minutes" is selected. Once this has been done, left-click the "start recording" icon. Temperature values will be logged by the PicoLog Recorder at 5 minute intervals.

Connect the sample line to the reactor while making sure the purge is open to drain condensate. Connect the air supply to the saturator bomb. Set the flowrate of air (channel 1) to 10%, while keeping the nitrogen (channel 2) and CO_2 (channel 3) at 0%. Close the vent valve on the outlet gas line and open the valves on the bottom of the reactor to slowly allow gas flow into the reactor. Once flow to the reactor has been established, set the flow controllers to the following settings: Air – 26.2%, N_2 – 4.5%, CO_2 – 19.0%. Turn the agitator switch on and set the speed to 6. Use the digital tachometer to confirm an agitator speed of 1400 RPM.

Return to the window with the CALCMET program. Click on "Options", then "Autosaving"; under the section "Autosave File Name", insert the date and description of the experiment and save this as a .SPE file (the default setting). Under "Result Output" in the "Options" menu, insert the same file name in the section "Save Results to File" and save as a .TXT file (default setting). The output files will automatically be exported to the location C:\CALCMET RESULTS\mmddyyyy. Under "Options", select "Measuring Times"; select "3 minutes" as the time interval. Left-click on the "continuous" icon to ensure that data will be collected every three minutes. Once the recording has begun, click on the "Trend" icon in the upper left corner. This allows the user view real-time concentration trends for up to five components.

During the course of the high gas flow experiment, the sample lines must be cleaned every 24 hours or so. In order to clean the lines, the CALCMET recording must be stopped. Turn down the agitator speed to 0 and flip the power switch to off. Close the valves on the bottom of the reactor to stop gas flow to the reactor and open the vent valve on the gas outlet of the pre-saturator. Disconnect the sample line from the pump inlet on the FT-IR and replace it with ¼" PE tubing. Connect the other end of the line to nitrogen supply line and crack the gate valve on the line. This will allow nitrogen gas to flow through the FT-IR, preventing damage to any of its components.

Disconnect the other end of the sample line from the top of the reactor and connect it to ¼" PE tubing. Insert the other end of the PE tubing to a hose coming off of the boiler feedwater supply line. Turn on the supply line and flush the sample line with

water for approximately 30 minutes. The water flush will remove the buildup of any organic contaminants from the sample line. Collect the water flush in a waste bucket and dispose of it properly. Disconnect the sample line from the PE tubing leading to the boiler feedwater and connect it to a second PE tubing line, which is connected to the building instrument air supply. Open the valve to allow the flow of instrument air and pass it through the sample line for approximately 20 minutes. This should dry the line and evaporate any residual water left in the line.

While the sample line is being flushed, the water reservoir for the DDI supply reservoir and Lauda water bath must be refilled (in fact, this should take place every 8 hours throughout the course of the experiment). If it isn't refilled, the low level alarm will sound and the heating circulator will stop heating the water in the bath. Moreover, an experimental sample should be taken from the reactor at this time. However, the level of the reactor must first be checked to ensure the peristaltic pumps are operating properly. If the level in the reactor is too low, then manually add DDI water until the level in the reactor is at the marking on the labeling tape. If the level is ok, use the 10 mL glass pipette to remove approximately 5 mL of sample from the reactor. Transfer this sample to a screwtop vial and record the mass of solution taken from the reactor. Label the vial with appropriate information and cap it. Remove the labeling tape from the outside of the reactor and mark it with the new level.

Once the sample line has been dried adequately, unhook the instrument air line from the sample line. Close the nitrogen supply valve and unhook the bypass line. Reconnect the sample line to the pump inlet on the FT-IR. While bypassing the presaturator and reactor, connect the reaction gas line directly to the sample line and turn the nitrogen to 25% open while keeping the air and CO_2 flow controllers at zero. Purge the FT-IR with N_2 for 15 minutes and repeat the aforementioned process for a background scan on the FT-IR. If the background scan is successful, repeat the steps to hook the sample line to the reactor and the reaction gas line to the presaturator to route gas flow back through the reactor.

Appendix D: Miscellaneous Low Gas Experiments

This appendix details low gas flow experiments not contained within the body of the report. Agitation rate and CO_2 concentration were altered from standard experimental conditions to test their effect on MEA degradation rates.

As stated in Chapter 3, standard experimental conditions for the low gas flow degradation apparatus were 100 cc/min of a saturated gas mixture of 98% O_2/2%CO_2 vortexed at 1400 RPM into an amine solution kept at 55^oC using a heated water passed through the jacket of the reactor. Two low gas flow experiments were run outside of these standard experimental conditions to test the effect of these variables. One experiment tested the effect of changing the CO_2 concentration in the vapor space, while the other experiment tested the effect of changing agitation rate. The results of these two experiments are shown in Table D.1.

Table D.1 Effect of Changing Experimental Conditions on Degradation Rates (mM/hr)

Catalyst Concentration (mM)	**1mM Fe**	**1mM Fe**	**0.1mM Fe / 5mM Cu**	**0.1mM Fe / 5mM Cu**
Variable Experimental Condition	**2% CO_2**	**6% CO_2**	**1400 RPM**	**700 RPM**
Hydroxyethylimidazole	**0.66**		**1.70**	
Hydroxyethyl-formamide	**0.77**	**0.76**	**3.25**	**2.83**
Formate	**0.29**	**0.30**	**0.73**	**0.43**
Oxamide	**0.09**	**0.73**	**0.42**	**1.57**
Oxalate	**0.02**	**0.04**	**0.04**	**0.05**
Nitrite	**0.21**	**0.32**	**0.29**	**0.17**
Nitrate	**0.09**	**0.12**	**0.10**	**0.08**
Glycolate	**0.01**	**0.04**	**0.00**	**0.11**
Acetate	**0.00**	**0.01**	**0.01**	**0.00**
Carbon Products (mM/hr C)	**6.3**	**5.7**	**20.0**	**15.5**
Nitrogen Products (mM/hr N)	**2.5**	**1.9**	**7.1**	**4.6**
MEA Loss	**3.8**	**6.4**	**10.3**	**15.9**
O_2 Rate	**1.9**	**3.1**	**5.6**	**6.2**

Table D.1 shows results from four low gas flow degradation experiments: two experiments whose results have been discussed in Chapter 6, and the two experiments whose experimental conditions have been altered from standard conditions. The first two columns list results from two experiments of which the gas composition has been altered from 98% O_2/2% CO_2 to 94% O_2/2% CO_2. In each case 7 m MEA was degraded in the presence of 1 mM of Fe catalyst. HPLC analysis was not performed on the experiment degraded in the presence of 6% CO_2, which equates to a loading of approximately 0.46

(as opposed to a loading of 0.4 for 2% CO_2). The hydroxyethyl-formamide production rate reported for this experiment is calculated from the NaOH hydrolysis analytical technique.

The only observed product that showed any dramatic difference between the two experiments was oxamide. Its production rate increased by a factor of 8 for the low gas experiment run at higher CO_2 loading. Nitrite and nitrate increased by 55% and 25% respectively. Carbon and nitrogen formation rates are slightly lower, but that is because hydroxyethylimidazole is not accounted for in the experiment with higher CO_2 concentration. On the other hand, according to cation analysis, MEA losses are 65% greater, and O_2 consumption is 60% greater (even without the hydroxytethylimidazole being accounted for). This disputes Goff's finding that MEA solutions were more susceptible to oxidative degradation at lower loadings. These results suggest that oxygen mass transfer is greater at higher CO_2 loadings.

In the second set of experiments, the agitation rate was decreased from 1400 RPM to 700 RPM to measure the effects of changing the rate at which oxygen is vortexed into solution. Both 7 m MEA solutions were degraded in the presence of Fe and Cu catalyst. HPLC analysis was not carried out on the experiment performed at 700 RPM; hydroxyethyl-formamide concentration was calculated using NaOH hydrolysis.

Similar to the experiment carried out at higher CO_2 concentration, the only observed species that increased in concentration (0.42 mM/hr at high agitation rate to 1.57 mM/hr at low agitation rate). Despite lower carbon and nitrogen formation rates (because of the absence of hydroxyethylimidazole in the analysis), MEA losses were 60% greater and the oxygen consumption rate was 15% greater.

The explanation for this phenomenon is relatively straightforward. At 1400 RPM in the low gas flow degradation apparatus, MEA (and most other amine systems tested in the apparatus) began to foam as it degraded. In fact, if the agitator was turned off in the middle of the experiment, a layer of foam ranging from ½" to 1" could be observed. This layer of foam could be observed even as the solution was vortexed. However, 700 RPM was not great enough to create foaming in the low gas apparatus as the MEA degraded.

The layer of foam produced at high agitation rate actually provided a physical barrier for the diffusion of oxygen (and carbon dioxide) from the bulk gas to the gas/liquid interface (or foam/liquid interface). This extra layer of resistance actually decreases the mass transfer capabilities of the apparatus.

Appendix E: Miscellaneous High Gas Experiments

This appendix details high gas flow experiments not contained within the body of the report. All high gas flow experiments were conducted for 6 to 14 hours for MEA, PZ and blended MEA/PZ systems. All results are reported in terms of NH_3 evolution (mM/hr), analogous to the findings reported by Goff (2005).

E.1. MEA and MEA/PZ Systems

Several short-term experiments were run using the high gas flow degradation apparatus on MEA and blended MEA/PZ solutions. All solutions were degraded for 6 to 14 hours in the high gas flow apparatus and the off-gas was continuously analyzed using the FT-IR. Figures E.1 through E.5 detail the ammonia evolution rates these experiments. From viewing these figures, it is interesting to note that the experiments with lower concentrations of metal catalysts (either 0.1 mM Fe or 1 mM Fe) reached steady state ammonia rates within five to ten hours. However, the experiments with an increased concentration of metal catalysts (0.1 mM Fe and 5 mM Cu) did not come close to reaching steady state after fourteen hours. Ammonia evolution rates for the experiments were still around 4 mM/hr. Figure E.6 details the ammonia evolution rate for an experiment where Ni and Cr were sequentially added to a 7 m MEA system in order to determine which catalyst had a greater effect on the ammonia evolution rate. Experimental results show that neither catalyst had any effect on NH_3 production.

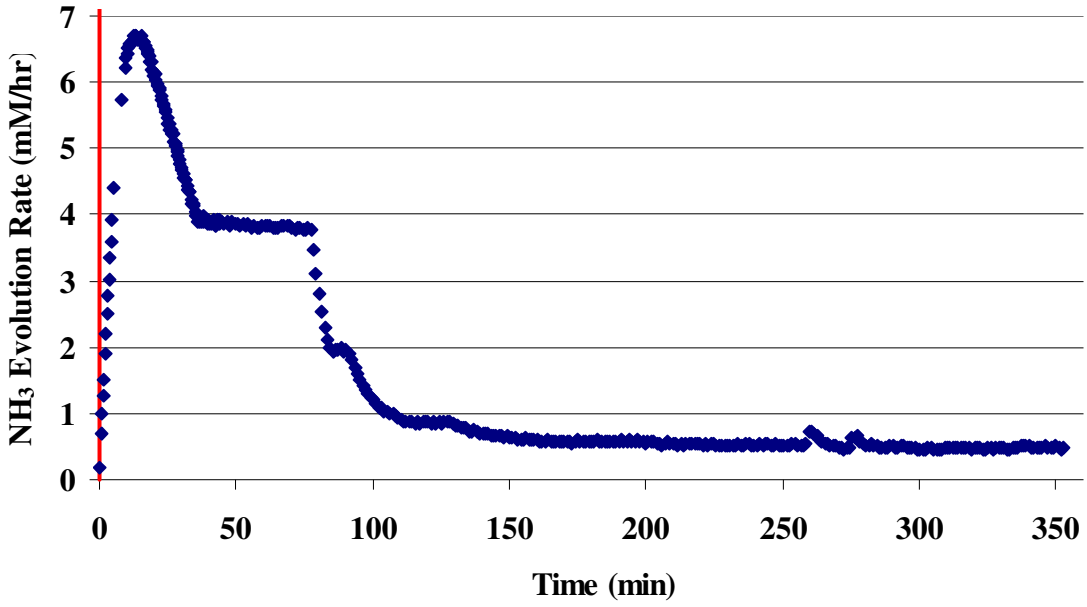

Figure E.1 Ammonia Evolution Rate for Degraded 7 m MEA, 55°C, 0.1 mM Fe^{+2}, 7.5 L/min 15% O_2/2% CO_2, 1400 RPM, 5/18/06, High Gas Apparatus

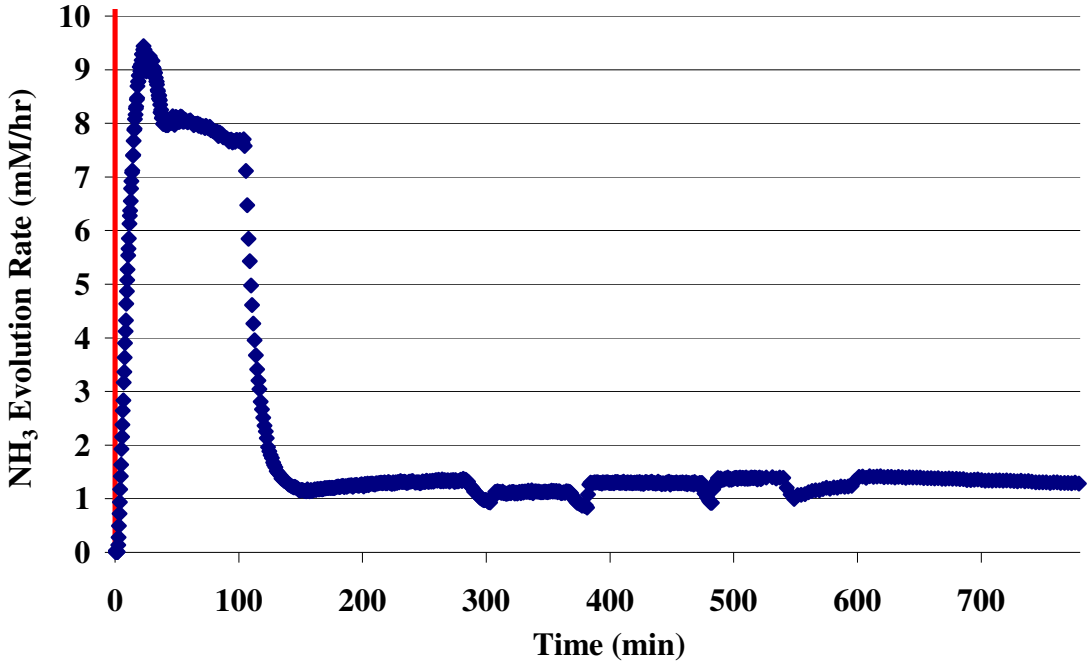

Figure E.2 Ammonia Evolution Rate for Degraded 7 m MEA, 55°C, 1 mM Fe^{+2}, 7.5 L/min 15% O_2/2% CO_2, 1400 RPM, 9/27/06, High Gas Apparatus

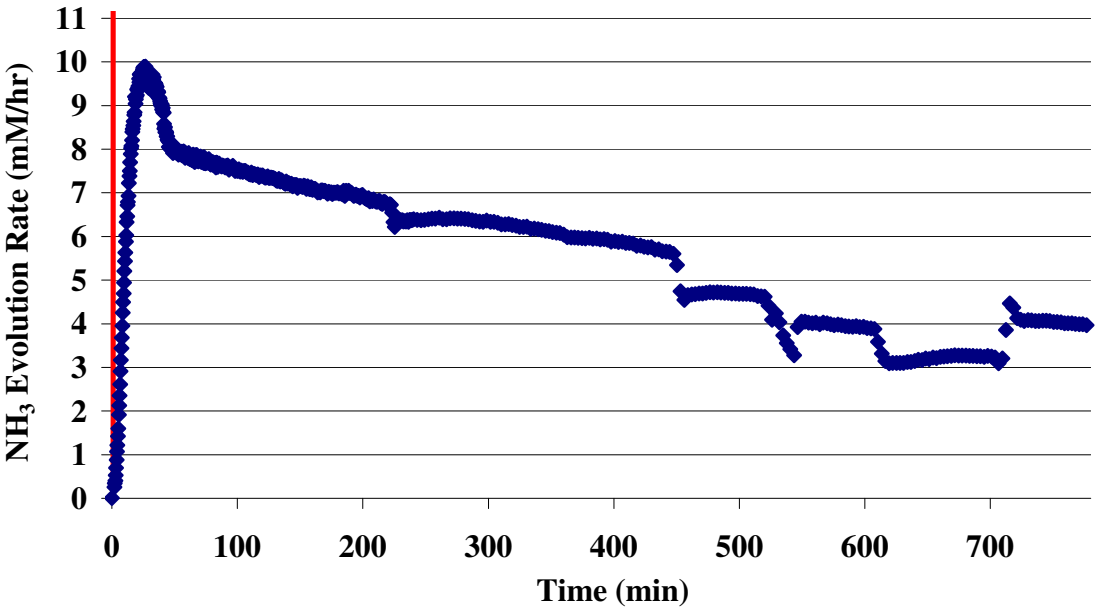

Figure E.3 Ammonia Evolution Rate for 7 m MEA, 55°C, 0.1 mM Fe^{+2}, 5 mM Cu^{+2}, 7.5 L/min 15% O_2/2% CO_2, 9/28/06, High Gas Apparatus

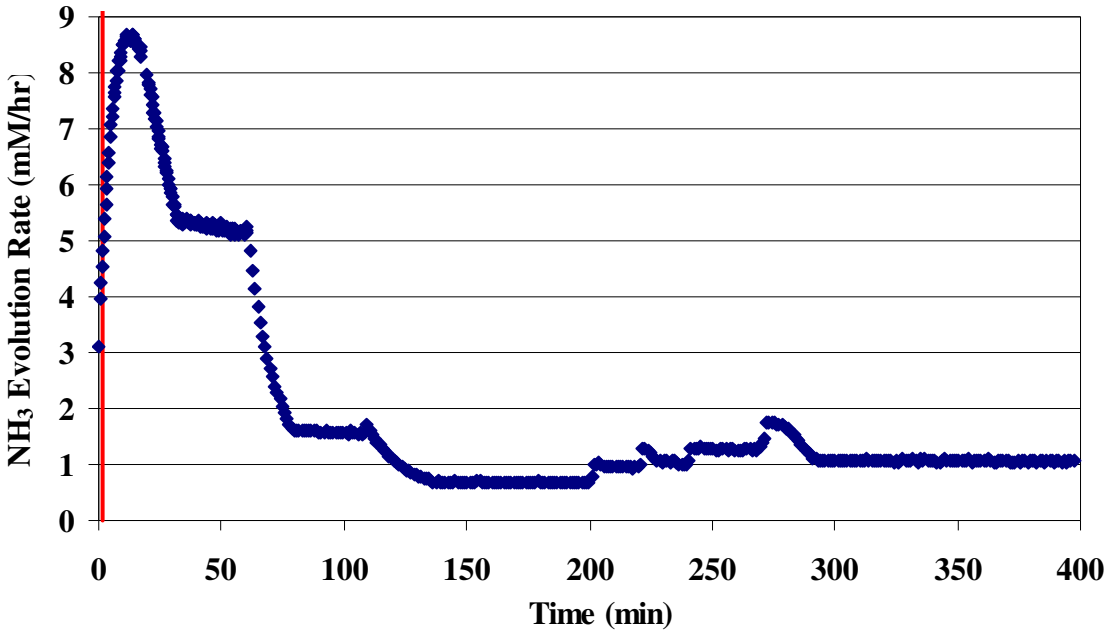

Figure E.4 Ammonia Evolution Rate for 22 wt% MEA/8 wt% PZ, 55°C, 0.1 mM Fe^{+2}, 7.5 L/min 15% O_2/2% CO_2, 6/7/06, High Gas Apparatus

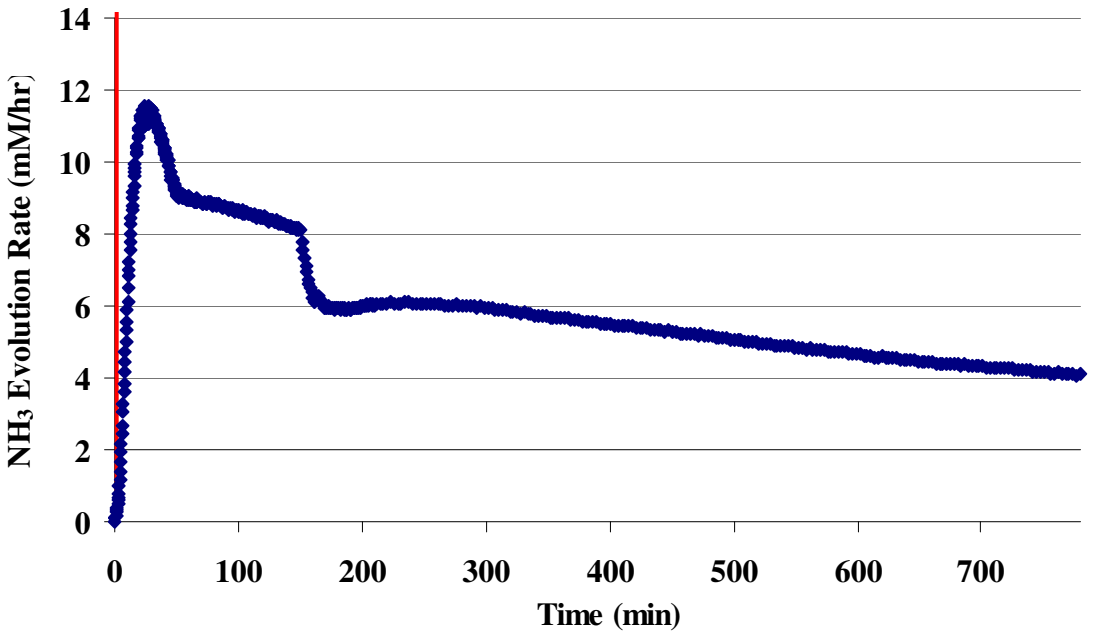

Figure E.5 Ammonia Evolution Rate for 22 wt% MEA/8 wt% PZ, 55°C, 0.1 mM Fe^{+2}, 5mM Cu^{+2}, 7.5 L/min 15% O_2/2% CO_2, 9/29/06, High Gas Apparatus

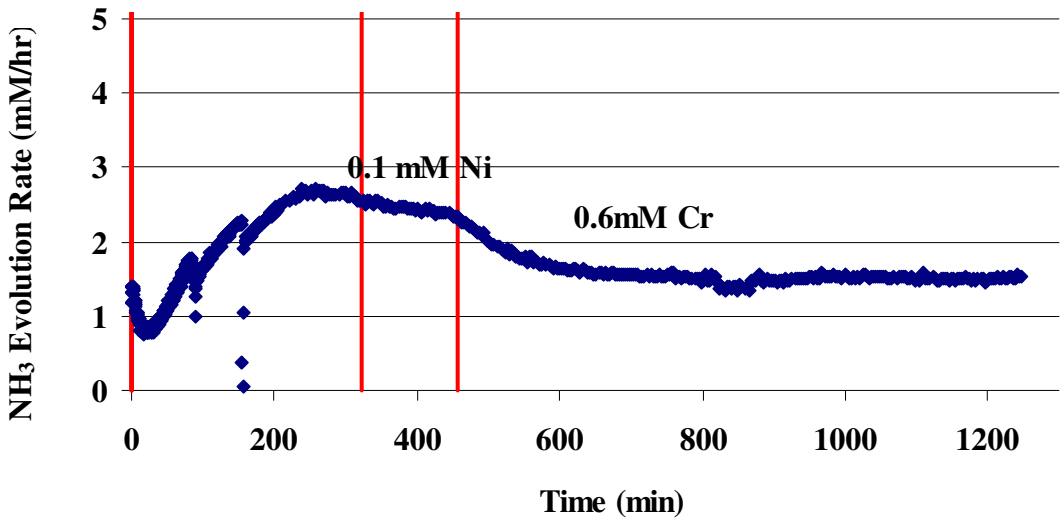

Figure E.6 Ammonia Evolution Rate for 7 m MEA, 55°C, 0.1 mM Ni^{+2}, 0.6 mM Cr^{+3}, 7.5 L/min 15% O_2/2% CO_2, 7/31/08, High Gas Apparatus

Table E.1 lists ammonia evolution rates for experiments represented in Figures E.1 through E.6. As the iron concentration was increased from 0.1 mM to 1 mM, the NH_3 rate increased from 0.77 mM/hr to 1.28 mM/hr. The MEA system catalyzed by Cr and Ni experienced a slightly higher ammonia evolution rate. Furthermore, on a 30 wt% amine basis (30 wt% MEA versus 22 wt% MEA/8 wt% PZ), the replacement of some MEA with PZ decreases the ammonia evolution rate. The substitution of 8 wt% with MEA with PZ (a 26.7% reduction in amine concentration by weight) reduced NH_3 evolution by 36.7% from 0.77 mM/hr to 0.48 mM/hr. This suggests that the PZ is degrading in addition to the MEA.

Table E.1 Ammonia Evolution Rates (mM/hr) for MEA and MEA/PZ Systems

Amine Solution	Fe (mM)	Cu (mM)	NH_3 Rate (mM/hr)
30 wt% MEA	0.1		0.77
30 wt% MEA	1		1.28
30 wt% MEA	0.1	5	3.97
30 wt% MEA	0.1 (Ni)	0.6(Cr)	1.54
22 wt% MEA/8 wt% PZ	0.1		0.48
22 wt% MEA/8 wt% PZ	0.1	5	4.09

E.2. Concentrated Piperazine Systems

Two short-term degradation experiments were also run in the high gas flow apparatus using concentrated piperazine at two different concentrations: 5 m PZ and 8 m PZ. Both experiments began with only aqueous piperazine solution – no catalyst added. Once ammonia evolution reached a presumed steady-state level, aqueous cuprous sulfate was added such that 1 mM Cu was present in the solution. After ammonia evolution reached steady-state levels once again, aqueous cuprous sulfate was added to increased catalyst concentration in the reactor to 5 mM Cu.

Figures E.7 and E.8 show that in the absence of catalyst, concentrated piperazine solutions produce very little volatile ammonia in its off-gas. In each experiment, after approximately 4 hours, ammonia evolution was non-existent. As cuprous sulfate was added in each experiment, NH_3 production spiked and began to approach zero levels once again. The NH_3 production is explained by the oxidation of cuprous-PZ complex oxidizing to a cupric-PZ complex. Once that finite amount of cuprous is oxidized to cupric, ammonia does not evolve from the degraded solution.

Volatility measurements were also taken during the experiment; these measurements show piperazine volatility to be approximately 50 ppm for the 5 molal solution, and approximately 70 ppm for the 8 molal solution. These volatility

measurements are consistent with the prediction from the Hilliard VLE model (Hilliard 2007).

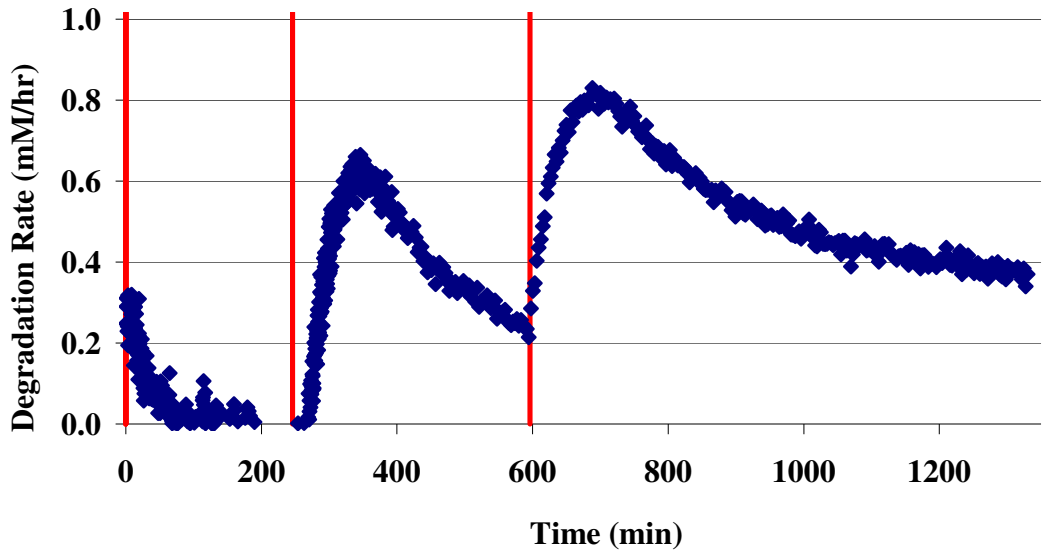

Figure E.7 Ammonia Evolution Rate for 5 m PZ, 55°C, 7.5 L/min 15% O_2/2% CO_2, High Gas Apparatus

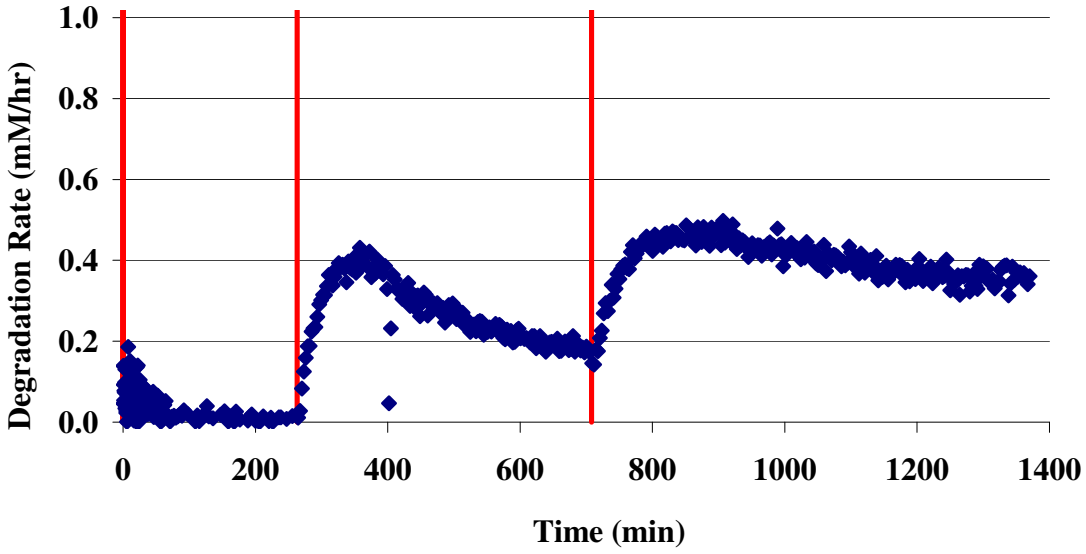

Figure E.8 Ammonia Evolution Rate for 8 m PZ, 55°C, 7.5 L/min 15% O_2/2% CO_2, High Gas Apparatus

Appendix F: Acid-Base Titration and pH Analysis

Appendix F details results of acid-base titration analysis to calculate total amine losses for selected low and high gas flow degradation experiments. Additionally, the pH was measured and analyzed for several of the low gas flow degradation experiments.

F.1. Acid-Base Titration Operating Procedure

Titration analysis is carried out using a Metrohm-Peak 835 Titrando (Serial#: 11040208) equipped with an automatic dispenser, Metrohm-Peak 801 Stirrer and 3 M KCl pH Probe (Temperature: 0-60^{o}C, pH: 0-13). Two 1-liter reservoirs contain 0.2 N H_2SO_4 and 0.1 N NaOH, which are used for the titrations; both glass reservoirs are equipped with desiccant to absorb any excess moisture.

Prepare a sample for pH titration by adding approximately 0.5 g of degraded amine sample to 60 g of DDI water. Record the masses of amine solution and water added to the beaker. Make sure that the H_2SO_4 reservoir is attached to the Titrando. Access the PC Control software on the attached computer by double-clicking the PC Control software icon. Place an empty beaker (labeled "waste beaker") underneath the dosing device. Click on the "manual" button, then click "dosing". When the next screen appears, hold down the "dosing" button until approximately 10 mL of acid has been dispensed into the beaker. Rinse both the pH probe and the manual dosing device with DDI water.

Place the beaker with the diluted amine onto the 801 Stirrer and lower the pH probe and dosing device into the liquid. Click on "Programs" and select "Total Alkalinity Mono – Acid". Under "Identification 1", insert a sample description that will identify the degraded amine sample. Under the heading "Identification 2", state the mass of water used to dilute the degraded amine solution; next to "sample size", insert the mass of degraded amine solution added to the beaker. After all of the information has been filled in, click the "start" button. The Titrando will continue to add H_2SO_4 in 0.1 mL increments until the pH reaches 2.0. The PC Control software will automatically identify the appropriate equivalence points.

Remove the sulfuric acid reservoir from the Titrando unit and insert the 0.1 N NaOH reservoir. Place the waste beaker underneath the dosing device. Click on the "manual" button, then click "dosing". When the next screen appears, hold down the

"dosing" button until approximately 10 mL of base has been dispensed into the beaker. Rinse both the pH probe and the manual dosing device with DDI water.

Place the beaker with the acid-titrated amine onto a hot plate set at 100°C. Allow the beaker to set on the plate until all the CO_2 has been evolved from the solution. Do not allow the solution to come to a boil. After the solution has cooled, place the beaker onto the 801 Stirrer and lower the pH probe and dosing device into the liquid. Click on "Programs" and select "Piperazine Determination – Base". Under "Identification 1", insert a sample description that will identify the degraded amine sample. Under the heading "Identification 2", state the mass of water used to dilute the degraded amine solution; next to "sample size", insert the mass of degraded amine solution that was added to the beaker. After all of the information has been filled in, click the "start" button. The Titrando will continue to add NaOH in 0.1 mL increments until the pH reaches 10.5; furthermore, the PC Control software will automatically identify the appropriate equivalence points.

Three numbers are needed from the two titrations in order to calculate amine concentration(s): the amount of H_2SO_4 (in mL) necessary to reach the equivalence point around a pH of 4.5, the amount of NaOH (in mL) needed to reach the first equivalence point during back titration around a pH of 4.5 and the amount of NaOH (in mL) needed to reach the second equivalence point. In order to calculate total amine concentration (in mol/kg solution), multiply the volume of H_2SO_4 by the concentration (in molarity), and divide by the mass of amine sample added (in grams). The result is the total amine/base concentration.

In order to calculate total piperazine concentration (in mol/kg solution), calculate the difference in NaOH volume between the two equivalence points for the base titration. Multiply this volume by the concentration of the NaOH titrant (in molarity), and divide by the mass of amine sample added (in grams). This gives the piperazine concentration in mol PZ/kg solution. In order to determine MEA concentration, subtract two times the PZ concentration from the total base concentration (it is necessary to multiply the PZ concentration by two because PZ is a diprotonated species at a pH of 2).

F.2. Acid-Base Titration Analysis

Acid-base titration was investigated as a means to determine total amine concentration in experimentally degraded samples. Initial (if one was preserved) and final samples from several high gas flow experiments were diluted and titrated for total base concentration as well as specific amine concentration.

Figures F.1 and F.2 show titration curves for the initial sample of a 7 m MEA/2 m PZ high gas flow experiment. Figure F.1 illustrates the initial titration with 0.1 N sulfuric acid. From the graph the two equivalence points can be seen: the first one (unmarked) occurs at a pH of 7 when CO_2 is liberated, and the second one is at pH 4.5 (designated with the purple square) when all base has been neutralized. Figure F.2 shows the back titration with 0.1 N sodium hydroxide. The two equivalence points are marked with a purple square (when all amine, MEA + PZ, has been titrated) and a yellow triangle (when all base, MEA + 2*PZ, has been titrated).

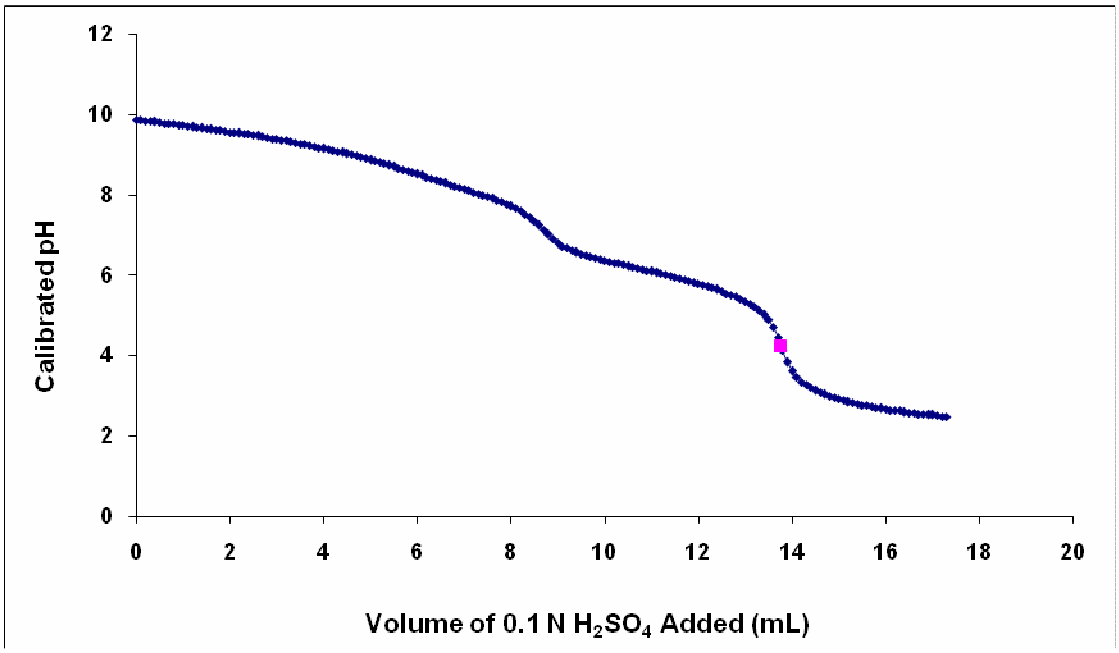

Figure F.1 Acid Titration Curve for Undegraded 7 m MEA/2 m PZ Initial Sample

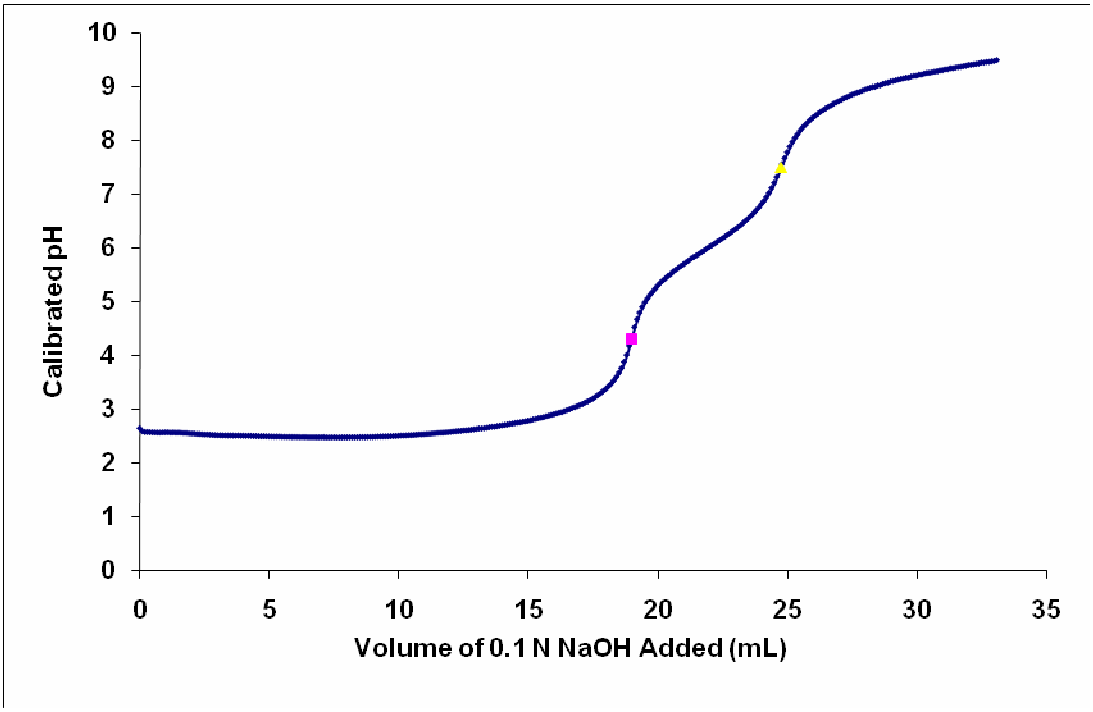

Figure F.2 Base Titration Curve for Undegraded 7 m MEA/2 m PZ Initial Sample

All degraded samples containing MEA only was acid titrated for total base concentration; for these samples it was assumed that all the base present in the sample was MEA. All degraded samples containing a mixture of MEA and PZ was titrated with sulfuric acid, then back titrated with sodium hydroxide to determine MEA and PZ concentrations individually (in mol/kg solution). In addition to the titration method, all of these samples were diluted and analyzed for amine concentration using cation IC methods.

Tables F.1, F.2, and F.3 tabulate the results of the titration and cation IC analysis. Table F.1 lists three key pieces of information for samples from the high gas flow experiments: the MEA and PZ molalities (if applicable) as determined from titration analysis, MEA and PZ molalities as determined from cation IC analysis, and the calculated absolute error between the two analyses. Table F.2 only gives MEA and PZ concentrations as determined by acid-base titration for selected low gas experiments. Table F.3 tabulates the percentage of MEA and PZ degraded during experiments where the final and initial samples are available.

The error in MEA concentration between the two analysis methods ranged from 1.6% to 33.0%, while the error in piperazine concentration ranged from 25.8% to 52.9%. This could be accounted for by several factors, notably the presence of degradation products, water balance error from the experiments and free amine tied up as other compounds (amides, for example) during cation IC analysis.

Table F.1 Total Amine Concentration of Samples at High Gas Flow

Experimental Conditions	Titration		IC		Analysis	
High Gas Flow	MEA Concentration (molality)	PZ concentration (molality)	MEA Concentration (molality)	PZ concentration (molality)	% MEA Difference	% PZ Difference
5/3/05, 7m MEA, 4 mM Cu, 200 mM "A", α=0.15	6.00		5.90		1.6	
5/9/05, 7m MEA, 4 mM Cu, 0.2 mM Fe, 200 mM "A", α=0.15	5.85		5.61		4.1	
5/16/05, 7m MEA, 4 mM Cu, 0.2 mM Fe, 200 mM "A", α=0.40	4.42		5.88		33.0	
5/18/06 (Initial), 25% MEA, 8% PZ, 5 ppm Fe	4.44	1.61	4.83		8.7	
5/18/06 (Final), 25% MEA, 8% PZ, 5 ppm Fe	3.63	1.54	3.53	1.14	2.6	25.8
6/6/06, 7m MEA, 5 ppm Fe	5.17		4.58		11.3	
6/7/06, 7m MEA, 2m PZ, 5 ppm Fe	4.10	1.67	3.72	1.17	9.2	30.1
7/24/06, 35% MEA	8.39		7.49		10.8	
8/9/06, 35% MEA, 5% PZ	9.24	1.82	6.42	0.86	30.5	52.9
9/27/06, 7m MEA, 50 ppm Fe	5.90		5.34		9.5	
9/28/06 (Initial), 7m MEA, 5 ppm Fe, 250 ppm Cu	6.22		6.58		5.8	
9/28/06 (Final), 7m MEA, 5 ppm Fe, 250 ppm Cu	5.00		3.88		22.4	
9/29/06, 7m MEA, 2m PZ, 5 ppm Fe, 250 ppm Cu	3.91	1.66	3.54	1.03	9.4	37.9

Any data from Table F.2 with a line through it represents concentrations generated from titration analysis that I believe are incorrect. In the case of the MEA/PZ/Fe/Cu experiment, the initial concentration of the sample is reported as 3.57 m MEA, when it should be 7 m MEA. It is believable that some degradation has occurred from sample storage, but 50% degradation is too much. The MEA/PZ/Fe and MEA/Cu/Fe/A experiments were called into question because the analysis concluded that the final MEA concentration was greater that the initial concentration. A logical explanation is that a significant amount of water evaporated from these samples during the course of the experiment, thereby increasing the concentration of the amines (while the amount remained the same).

Table F.2 Total Amine Concentration of Samples at Low Gas Flow

Experimental Conditions	Titration	
Low Gas Flow	MEA Concentration (molality)	PZ concentration (molality)
12/06 (Initial), 2.5m PZ, 500 ppm V, 100 mM "A"		2.49
12/06 (Final), 2.5m PZ, 500 ppm V, 100 mM "A"		1.94
11-12/06 (Initial), 2.5m PZ, 5m K, 500 ppm V		2.53
11-12/06 (Final), 2.5m PZ, 5m K, 500 ppm V		2.34
9-10/06 (Initial), 7m MEA, 2m PZ, 0.1 mM Fe, 4 mM Cu	~~3.57~~	2.26
9-10/06 (Final), 7m MEA, 2m PZ, 0.1 mM Fe, 4 mM Cu	~~0.69~~	1.18
8/06 (Initial), 35% MEA	7.72	
8/06 (Final), 35% MEA	5.70	
5/06 (Initial), 7m MEA, 2m PZ, 5 ppm Fe	~~4.07~~	~~2.63~~
5/06 (Final), 7m MEA, 2m PZ, 5 ppm Fe	~~6.98~~	~~4.55~~
3-4/06 (Initial), 2.5m PZ, 5m K, 500 ppm V		2.50
3-4/06 (Final), 2.5m PZ, 5m K, 500 ppm V		0.63
3/06 (Initial), 7m MEA, 0.2 mM Fe	6.21	
3/06 (Final), 7m MEA, 0.2 mM Fe	5.95	
1/06 (Initial), 7m MEA, 0.2 mM Fe, 0.2 mM Cu, 100 mM "A"	~~5.80~~	
1/06 (Final), 7m MEA, 0.2 mM Fe, 0.2 mM Cu, 100 mM "A"	~~8.33~~	
10/05 (Initial), 2.5m PZ, 500 ppm V		2.88
10/05 (Final), 2.5m PZ, 500 ppm V		6.96
8/05 (Initial), 7m MEA, 0.2 mM Fe, 0.2 mM Cu	4.60	
8/05 (Final), 7m MEA, 0.2 mM Fe, 0.2 mM Cu	1.51	
12/04 (Initial), 7m MEA, 0.2 mM Cu	5.18	
12/04 (Final), 7m MEA, 0.2 mM Cu	4.61	

Table F.3 Total Amine Losses from Degradation via Acid-Base Titration

Experimental Conditions	Titration		Analysis	
High Gas Flow	**MEA Concentration (molality)**	**PZ concentration (molality)**	**% MEA Degradation**	**% PZ Degradation**
5/18/06 (Initial), 25% MEA, 8% PZ, 5 ppm Fe	4.44	1.61		
5/18/06 (Final), 25% MEA, 8% PZ, 5 ppm Fe	3.63	1.54	18.24	4.35
9/28/06 (Initial), 7m MEA, 5 ppm Fe, 250 ppm Cu	6.22			
9/28/06 (Final), 7m MEA, 5 ppm Fe, 250 ppm Cu	5.00		19.61	
Low Gas Flow	**MEA Concentration (molality)**	**PZ concentration (molality)**	**% MEA Degradation**	**% PZ Degradation**
12/06 (Initial), 2.5m PZ, 500 ppm V, 100 mM "A"		2.49		
12/06 (Final), 2.5m PZ, 500 ppm V, 100 mM "A"		1.94		22.09
11-12/06 (Initial), 2.5m PZ, 5m K, 500 ppm V		2.53		
11-12/06 (Final), 2.5m PZ, 5m K, 500 ppm V		2.34		7.51
8/06 (Initial), 35% MEA	7.72			
8/06 (Final), 35% MEA	5.70		26.17	
3-4/06 (Initial), 2.5m PZ, 5m K, 500 ppm V		2.50		
3-4/06 (Final), 2.5m PZ, 5m K, 500 ppm V		0.63		74.80
3/06 (Initial), 7m MEA, 0.2 mM Fe	6.21			
3/06 (Final), 7m MEA, 0.2 mM Fe	5.95		4.19	
8/05 (Initial), 7m MEA, 0.2 mM Fe, 0.2 mM Cu	4.60			
8/05 (Final), 7m MEA, 0.2 mM Fe, 0.2 mM Cu	1.51		67.17	
12/04 (Initial), 7m MEA, 0.2 mM Cu	5.18			
12/04 (Final), 7m MEA, 0.2 mM Cu	4.61		11.00	

Where the appropriate data was available, a percent MEA and percent PZ loss due to degradation were calculated for high and low gas experiments; these results are shown in Table F.3. Even for the initial samples, it is very clear that some degradation has occurred from the samples aging. Therefore, in the future, it is imperative to perform this type of quantitative analysis shortly after the samples have been collected. In the high gas flow apparatus, MEA losses were 18 to 19%, while PZ piperazine losses were 4.4%. In the low gas flow apparatus, MEA losses ranged from 4 to 67%, while piperazine losses ranged from 7 to 75%. Acid-base titration appears to be unreliable for the analysis of degraded samples due to interference from degradation products.

F.3. pH Analysis

The pH of dilute amine species was determined using a Cole Parmer pH probe and Cole Parmer pH/mV/^{o}C meter (Model # 59003-00, Serial # EP1000/5411). A calibration curve was constructed using pH buffers (range: 2-12) produced by Fisher Chemical. A curve of actual pH versus measured pH was constructed so that measured pH could be correlated to actual pH accurately. For each low gas flow experiment, all samples (initial, final, intermediate) were diluted by a factor of approximately 120 (0.5 g amine sample + 60 g DDI water) in 60 mL plastic bottles.

Rinse the pH probe with DDI water above a waste beaker, and then insert it into the dilute initial sample. Insert the probe in the solution for five minutes and allow it to equilibrate. Record the pH displayed on the meter. Rinse the probe with DDI water and place in the first intermediate sample. Repeat this process for the remaining samples and record the measured pH values. Convert the measured pH values to actual pH values using the calibration and construct a pH profile for the experiment.

Figure F.3 details pH profiles for several of the older low gas flow experiments: 5 MEA experiments, 1 PZ experiment, and 1 MEA/PZ experiment. The experiment times varied, so the times at which samples were taken were normalized such that 0 represents the initial experimental sample and 1 represents the time at which the final sample was taken. All of the initial diluted samples have a pH level in the range of 9.0 to 9.5 (concentrated samples would be in the range of 10.5 to 11.0). The pH level of all the final samples ranges from 8.7 to 9.2 (10.2 to 10.7 for the concentrated samples). These results are logical because the pure amine solutions are highly basic, and become slightly more acidic as degradation products accumulate as the solution degrades. However, the pH of the degraded samples is still highly basic.

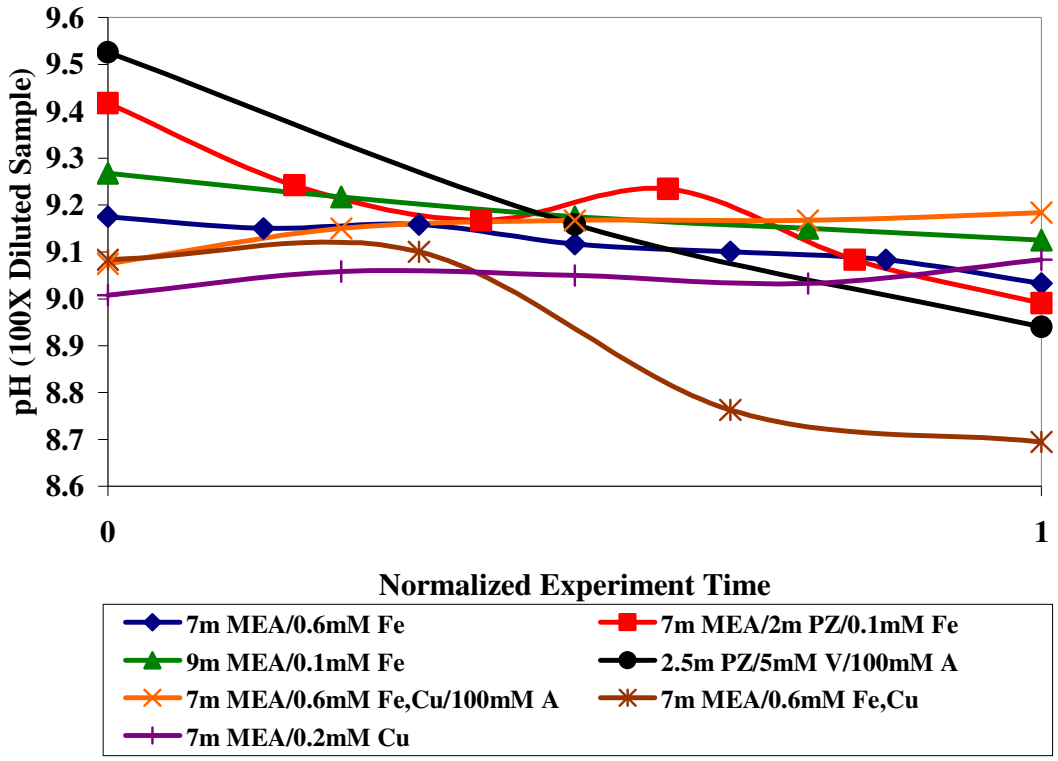

Figure F.3 pH Profiles of Low Gas Flow Experiments

Bibliography

ABB *CO2 Recovery from Flue Gas/Turbine Exhaust Gas: Kerr-McGee/Lummus Carbon Dioxide Recovery Technology.* ABB Lummus Global: 1998; 12.

Alawode, A. Oxidative Degradation of Piperazine. Masters Thesis, The University of Texas at Austin, Austin, TX, 2005.

Alejandre, J.; Rivera, J. L.; Mora, M. A.; De la Garza, V. Force Field of Monoethanolamine. *Journal of Physical Chemistry B* **2000,** *104*(6), 1332-1337.

Anslyn, E. Personal Communication to Andrew J. Sexton. Austin, TX, 2008.

Arnold, D. S.; Barrett, D. A.; Isom, R. H. Carbon Dioxide Can be Produced from Flue Gas. *Oil and Gas Journal* **1982,** *80*(47), 130-136.

Aroua, M. K.; Salleh, R. M. Solubility of CO_2 in Aqueous Piperazine and Its Modeling Using the Kent-Eisenberg Approach. *Chem. Eng. Tech.* **2004***,* 27(1), 65-70.

Asperger, R. G.; Tebbal, S.; Kane, R. D. (CLI International, Inc.) Corrosion Inhibitor and Its Use; Patent Application WO 9828381 A1 19980702, 1998.

Astarita, G. Regimes of Mass Transfer with Chemical Reaction. *Journal of Industrial and Engineering Chemistry (Washington, D. C.)* **1966,** *58*(8), 18-26.

Austgen, D. M., Jr A Model of Vapor-Liquid Equilibria for Acid Gas-Alkanolamine-Water Systems. Doctoral Thesis, The University of Texas at Austin, Austin, 1989.

Barron, C. H.; O'Hern, H. A. Reaction Kinetics of Sodium Sulfite Oxidation by the Rapid Mixing Method. *Chemical Engineering Science* **1966,** *21*, 397-404.

Bello, A.; Idem, R. O. Pathways for the Formation of Products of the Oxidative Degradation of CO_2-Loaded Concentrated Aqueous Monoethanolamine Solutions during CO_2 Absorption from Flue Gases. *Industrial & Engineering Chemistry Research* **2005,** *44*(4), 945-969.

Bengtsson, S.; Bjerle, I. Catalytic Oxidation of Sulphite in Diluted Aqueous Solutions. *Chemical Engineering Science* **1975,** *30*, 1429-1435.

Bishnoi, S. Carbon Dioxide Absorption and Solution Equilibrium in Piperazine Activated Methyldiethanolamine. Doctoral Thesis, The University of Texas at Austin, Austin, TX, 2000.

Bishnoi, S. and G. T. Rochelle. Absorption of Carbon Dioxide into Aqueous Piperazine: Reaction Kinetics, Mass Transfer and Solubility. *Chem. Eng. Sci.* **2000***,* 55(22), 5531-5543.

Blachly, C. H.; Ravner, H. *The Effect of Trace Amounts of Copper on the Stability of Monoethanolamine Scrubber Solutions.* NRL-MR-1482; U.S. Naval Research Laboratory: Washington, D.C., December, 1963, 1963; 9.

Blachly, C. H.; Ravner, H. *The Stabilization of Monoethanolamine Solutions for Submarine Carbon Dioxide Scrubbers.* AD609888; NRL-FR-6189; NRL-6189; Naval Research Laboratory: Washington, D.C., 1964.

Blachly, C. H.; Ravner, H. Stabilization of Monoethanolamine Solutions in Carbon Dioxide Scrubbers. *Journal of Chemical Engineering Data* **1966,** *11*(3), 401-3.

Blachly, C. H.; Ravner, H. *Studies of Submarine Carbon Dioxide Scrubber Operation: Effect of an Additive Package for the Stabilization of Monoethanolamine*

Solutions. NRL-MR-1598; U.S. Naval Research Laboratory: Washington, D.C., March, 1965, 1965.

Blezard, Michael; Jones, Glyn R. Nitrosamine inhibition. United States Patent Application No. 5,223,644. 1993.

Button, J. K.; Gubbins, K. E.; Tanaka, H.; Nakanishi, K. Molecular Dynamics Simulation of Hydrogen Bonding in Monoethanolamine. *Fluid Phase Equilib.* **1996,** *116*(1-2), 320-325.

Calle, Emilio; Casado, Julio; Cinos, Jose L.; Garcia Mateos, Francisco J.; Tostado, Manuel. Formation of nitrosamines in alkaline conditions: a kinetic study of the nitrosation of linear and cyclic secondary amines by nitroalkanes. Journal *of the Chemical Society*, Perkin II, 1559-1564, **1992**.

Chakma, A.; Meisen, A. Identification of Methyl Diethanolamine Degradation Products by Gas Chromatography-Mass Spectrometry. *J. Chromatography* **1988***,* 457, 287-297.

Chakma, A.; Meisen, A. Methyl-Diethanolamine Degradation – Mechanism and Kinetics. *The Canadian Journal of Chemical Engineering* **1997**, 75, 861-871.

Chakravarti, S.; Gupta, A. Carbon Dioxide Recovery Plant. US-20010026779, 2001. Chapman, C. M.; Gibilaro, L. G.; Nienow, A. W. A Dynamic Response Technique for the Estimation of Gas-Liquid Mass Transfer Coefficients in a Stirred Vessel. *Chemical Engineering Science* **1982,** *37*(6), 891-6.

Challis, B.C.; Kyrtopoulos, S.A. The Chemistry of Nitroso-compounds. Part 11. Nitrosation of amines by the two-phase interaction of amine in solution with gaseous oxides of nitrogen. *J. Chem. Soc.*, Perkin I, **1979**.

Challis, B.C.; Challis, J.A. *N*-nitrosamines and *N*-nitrosoimines, p. 1151-1223, The chemistry of amino, nitroso and nitro compounds and their derivatives, Supplement F, Part 2, edited by S. Patai, John Wiley and Sons, New York, 1982.

Chen, E. Carbon Dioxide Absorption into Piperazine Promoted Potassium Carbonate using Structured Packing. Doctoral Thesis, The University of Texas at Austin, Austin, TX, 2007.

Chen, T.-I.; Barron, C. H. Some Aspects of the Homogeneous Kinetics of Sulfite Oxidation. *Industrial & Engineering Chemistry Fundamentals* **1972,** *11*(4), 466-470.

Chi, Q. S. Oxidative Degradation of Monoethanolamine. Masters Thesis, The University of Texas at Austin, Austin, TX, 2000.

Chi, S.; Rochelle, G. T. Oxidative Degradation of Monoethanolamine. *Industrial & Engineering Chemistry Research* **2002,** *41*(17), 4178-4186.

Choy, E. T.; Meisen, A. Gas Chromatographic Detection of Diethanolamine and Its Degradation Products. *Journal of Chromatography* **1980**, 187, 145-152.

Comeaux, R. V. The Mechanism of MEA (Monoethanolamine) Corrosion. *Proc. Am. Petrol. Inst., Sect. III* **1962,** *42*(3), 481-489.

Conklin, M. H.; Hoffmann, M. R. Metal Ion-Sulfur(IV) Chemistry. 2. Kinetic Studies of the Redox Chemistry of Copper(II)-Sulfur(IV) Complexes. *Environmental Engineering Science* **1988,** *22*(8), 891-898.

Cringle, D. C.; Pearce, R. L.; Dupart, M. S. Method for Maintaining Effective Corrosion Inhibition in Gas Scrubbing Plant. 4690740, 1987.

Critchfield, J. E.; Jenkins, L. Evidence for MDEA degradation in tail gas treating plants. *Petroleum Technology Quarterly* 1999.

Cullinane, J. T. Carbon Dioxide Absorption in Aqueous Mixtures of Potassium Carbonate and Piperazine. Masters Thesis, The University of Texas at Austin, 2002.

Cullinane, J. T. Thermodynamics and Kinetics of Aqueous Piperazine with Potassium Carbonate for Carbon Dioxide Absorption. Doctoral Thesis, The University of Texas at Austin, Austin, 2005.

Dang, H. CO_2 Absorption Rate and Solubility in Monoethanolamin/Piperazine/Water. Master of Science of Engineering Thesis, The University of Texas at Austin, Austin, TX, 2001.

Daptardar, S. D. et al. On degradation of chemical solvents for bulk removal of CO_2. *Gas Separation & Purification* **1994**, 8(2), 115-121.

Davis, J. D. Thermal Degradation of Amines. Doctoral Thesis, The University of Texas at Austin, Austin, TX, 2009 (in progress).

Davison, J.; Freund, P.; Smith, A. *Putting Carbon Back into the Ground.* IEA Greenhouse Gas R&D Programme: 2001; 28.

Dawson, B. A.; Lawrence, R. C. Analysis of piperazine drug formations for *N*-nitrosamines. *Journal – Association of Official Analytical Chemists*, 70(5), p. 840-841, **1987**.

Dawodu, O. F.; Meisen, A. Degradation of Alkanolamine Blends by Carbon Dioxide. *The Canadian Journal of Chemical Engineering* **1996**, 74, 960-966.

Dean, J. A. *Lange's Handbook of Chemistry*. 14 ed.; 1992.

Dennis, W. H., Jr.; Hull, L. A.; Rosenblatt, D. H. Oxidations of Amines. IV. Oxidative Fragmentation. *Journal of Organic Chemistry* **1967***,* 32(12): 3783-3787.

Denisov, E. T.; Mitskevich, N. L.; Agabekov, V. E. *Liquid-Phase Oxidation of Oxygen-Containing Compounds*. Consultants Bureau, New York, 1977.

Elespuru, R.K.; Lijinsky, W. Mutagenicity of cyclic nitrosamines in *Escherichia coli* following activation with rat liver microsomes. *Cancer Research*, p. 4099-4101, **1976**.

Energy Information Administration *Emisssions of Greenhouse Gases in the United States 2003*. 2004a ftp://ftp.eia.doe.gov/pub/oiaf/1605/cdrom/pdf/ggrpt/057303.pdf (Accessed July 2008).

Energy Information Administration *International Energy Annual 2002*. 2004b http://www.eia.doe.gov/iea/contents.html (Accessed July 2008).

EPA *Technology Transfer Network Air Toxics Website, The original list of hazardous air pollutants*. 1990 http://www.epa.gov/ttn/atw/orig189.html (Accessed July 2008).

Ermatchkov, V; Kamps, A.; Maurer, G. Chemical Equilibrium Constants for the Formation of Carbamates in (Carbon Dioxide + Piperazine + Water) from 1H-NMR-Spectroscopy. *J. Chem. Thermodyn.* **2003***,* 35(8), 1277-1289.

Fessenden, R. J.; Fessenden, J. S. *Organic Chemistry*. 5th ed.; Brooks/Cole Publishing Company: Pacific Grove, CA, 1994.

Freguia, S. Modeling of CO_2 Removal from Flue Gases with Monoethanolamine. Masters Thesis, The University of Texas at Austin, Austin, TX, 2002.

Gaddis, E. S. Mass Transfer in Gas-Liquid Contactors. *Chemical Engineering and Processing* **1999,** *38*(4-6), 503-510.

Garcia-Ochoa, F.; Gomez, E. Mass Transfer Coefficient In Stirred Tank Reactors for Xanthan Gum Solutions. *Biochemical Engineering Journal* **1998,** *1*(1), 1-10.

Girdler Corporation *Carbon Dioxide Absorbants.* Contract No. 50023; Girdler Corporation, Gas Processes Division: Louisville, KY, June, 1, 1950.

Goff, G. S.; Rochelle, G. T. Monoethanolamine Degradation: O_2 Mass Transfer Effects under CO_2 Capture Conditions. *Industrial & Engineering Chemistry Research* **2004,** *43*(20), 6400-6408.

Goff, G. S.; Rochelle, G. T. *Oxidative Degradation of Aqueous Monoethanolamine in CO_2 Capture Systems Under Absorber Conditions*, 6th International Conference on Greenhouse Gas Control Technologies, Kyoto, Japan, 2003; Gale, J., et al., Eds. Elsevier: Oxford UK: Kyoto, Japan, 2003; 115-120.

Goff, G. S. Oxidative Degradation of Aqueous Monoethanolamine in CO_2 Capture Processes: Iron and Copper Catalysis, Inhibition, and O_2 Mass Transfer. Doctoral Thesis, The University of Texas at Austin, 2005.

Goff, G. S.; Rochelle, G. T. Oxidation Inhibitors for Cu Catalyzed Degradation of Monoethanolamine in CO_2 Capture Processes. *Industrial & Engineering Chemistry Research* **2006**, *45*(8), 2513-2521.

Grace, J. Understanding and Managing the Global Carbon Cycle. *Journal of Ecology* **2004,** *92*(2), 189-202.

Grigsby, R. Personal Communication to Andrew J. Sexton. Austin, TX, 2008.

Hakka, L. E.; Ouimet, M. A. Recovery of CO_2 from Waste Gas Streams Using Amines as Absorbents. US-2004253159, 2004.

Hall, W. D.; Barron, J. G. Solving Gas Treating Problems – A Different Approach. Presented at the Laurence Reid Gas Conditioning Conference, Norman, OK, 1981.

Hilliard, M. A Predictive Thermodynamic Model for an Aqueous Blend of Potassium Carbonate, Piperazine, and Monoethanolamine for Carbon Dioxide Capture from Flue Gas. Doctoral Thesis, The University of Texas at Austin, Austin, TX, 2008.

Ho, F. *The Effect on the Stability of Monoethanolamine by Vanadium Metal.* Submitted to Gary T. Rochelle at The University of Texas at Austin: 2003.

Hofmeyer, B. G.; Scholten, H. G.; Lloyd, W. G. Contamination and Corrosion in Monoethanolamine Gas Treating Solutions. *Am. Chem. Soc., Div. Petrol. Chem., Preprints-Symposia* **1956,** *1*(2), 91-99.

Holub, P. E.; Critchfield, J. E.; Su, W-Y. Amine Degradation Chemistry in CO_2 Service. Presented at the 48th Annual Laurence Reid Gas Conditioning Conference, Norman, OK, 1998.

Hook, R. J. An Investigation of Some Sterically Hindered Amines as Potential Carbon Dioxide Scrubbing Compounds. *Ind. Eng. Chem. Res.* **1997**, 36, 1779-1790.

Hsu, C. S.; Kim, C. J. Diethanolamine (DEA) Degradation Under Gas-Treating Conditions. *Ind. Eng. Chem. Prod. Res. Dev.* **1985**, 24, 630-635.

Hull, L. A.; Davis, G. T.; Rosenblatt, D. H.; Mann, C. K. Oxidations of Amines. VII. Chemical and Electrochemical Correlations. *J. Phys. Chem.* **1969,** *73*(7), 2142-6.

Hull, L. A.; Davis, G. T.; Rosenblatt, D. H.; Williams, H. K. R.; Weglein, R. C. Oxidations of Amines. III. Duality of Mechanism in the Reaction of Amines with Chlorine Dioxide. *J. Am. Chem. Soc.* **1967,** *89*(5), 1163-1170.

IEA *Carbon Dioxide Capture from Power Stations.* IEA Greenhouse Gas R&D Programme: http://www.ieagreen.org.uk/capt1.htm (Accessed July 2008), 1999.

IEA *CO2 Capture at Power Stations and Other Major Point Sources.* International Energy Agency, Working Party on Fossil Fuels: Paris, France, 2003; 13.

IPCC *Climate Change 2001: The Scientific Basis.* Published for International Panel on Climate Change by Cambridge University Press: New York, 2001.

Jones, T. Oxidative Degradation of Piperazine in Aqueous Potassium Carbonate. Masters Thesis, The University of Texas at Austin, Austin, TX, 2003.

Jou, F.-Y.; Mather, A. E.; Otto, F. D. The Solubility of CO_2 in a 30 Mass Percent Monoethanolamine Solution. *Canadian Journal of Chemical Engineering* **1995,** *73*(1), 140-7.

Kamps, A.; Xia, J.; Maurer, G. Solubility of CO_2 in (H_2O + Piperazine) and in (H_2O + MDEA + Piperazine). *AIChE J.* **2003***,* 49(10), 2662-2670.

Keefer, L.K.; Roller, P.P. *N*-Nitrosation by Nitrite Ion in Neutral and Basic Medium, Science 181, 1245-47, **1973**.

Keeling, C. D.; Whorf, T. P. Atmospheric CO_2 Records from Sites in the SIO Air Sampling Network. In *Trends: A Compendium of Data on Global Change*; Carbon Dioxide Information Analysis Center, Oak Ridge National Laboratory, U.S. Department of Energy: Oak Ridge, Tenn., U.S.A., 2004.

Kennard, M. L.; Meisen, A. Mechanism and Kinetics of DEA Degradation. *Ind. Eng. Chem. Fund.* **1985**, 24, 129-140.

Kim, C. J.; Sartori, G. Kinetics and Mechanism of DEA Degradation in Aqueous Solutions Containing Carbon Dioxide. *Int. J. Chem. Kin*. **1984**, 16, 1257-1266.

Kim, C. J. Degradation of Alkanolamines in Gas Treating Solutions: Kinetics of Di-2-propanolamine Degradation in Aqueous Solutions Containing Carbon Dioxide. *Ind. Eng. Chem. Res*. **1988**, 27, 1-3.

Kindrick, R. C.; Atwood, K.; Arnold, M. R. The Relative Resistance to Oxidation of Commercially Available Amines. Girdler Report No. T2.15-1-30, in "Report: Carbon Dioxide Absorbents", Contract No. NObs-50023, by Girdler Corp., Gas Processes Division, Louisville, KY, for the Navy Department, Bureau of Ships, Washington, DC (Code 649P), 1950a.

Kindrick, R. C.; Reitmweier, R. E.; Arnold, M. R. A Prolonged Oxidation Test on Amine Solutions Resistant to Oxidation. Girdler Report No. T2.15-1-31, in "Report: Carbon Dioxide Absorbents", Contract No. NObs-50023, by Girdler Corp., Gas Processes Division, Louisville, KY, for the Navy Department, Bureau of Ships, Washington, DC (Code 649P), 1950b.

Kirsch, Michael; Korth, Hans-Gert; Sustmann, Reiner; De Groot, Herbert. Carbon Dioxide but Not Bicarbonate Inhibits *N*-Nitrosation of Secondary Amines.

Evidence for Amine Carbamates as Protecting Entities. *Chemical Research in Toxicology*, 13(6), p. 451-461, **2000**.

Klein, R.G. Calculations and measurements on the volatility of *N*-nitrosamines and their aqueous solutions. *Toxicology*, 23(2-3), 135-147, **1982**.

Kohl, A.; Nielsen, R. *Gas Purification*. 5th ed.; Gulf Publishing Co.: Houston, 1997.

Koike, L. et al. N-Formyldiethanolamine: a new artifact in diethanolamine solutions. *Chemistry and Industry* **1987**, 626-627.

Kyoto Protocol *The United Nations Framework Convention on Climate Change*. 2004 http://unfccc.int/resource/convkp.html. (Accessed July 2008).

Lawal, A. O.; Idem, R. O. Effects of Operating Variables on the Product Distribution and Reaction Pathways in the Oxidative Degradation of CO_2-Loaded Aqueous MEA-MDEA Blends during CO_2 Absorption from Flue Gas Streams. *Industrial & Engineering Chemistry Research* **2005,** *44*(4), 986-1003.

Lawal, O.; Bello, A.; Idem, R. The Role of Methyl Diethanolamine (MDEA) in Preventing the Oxidative Degradation of CO_2 Loaded and Concentrated Aqueous Monoethanolamine (MEA)-MDEA Blends during CO_2 Absorption from Flue Gases. *Industrial & Engineering Chemistry Research* **2005,** *44*(6), 1874-1896.

Lee, Y. J.; Rochelle, G. T. Oxidative Degradation of Organic Additives for Flue Gas Desulfurization: Products, Kinetics, and Mechanism. *Environmental Science and Technology* **1987**, 21, 266-272.

Lee, Y. J. Oxidative Degradation of Organic Acids Conjugated with Sulfite Oxidation in Flue Gas Desulfurization. Doctoral Thesis, The University of Texas at Austin, Austin, 1986.

Lewis, W. K.; Whitman, W. G. Principles of Gas Absorption. *Journal of Industrial and Engineering Chemistry (Washington, D. C.)* **1924,** *16*, 1215-20.

Linek, V.; Vacek, V. Chemical Engineering Use of Catalyzed Sulfite Oxidation Kinetics for the Determination of Mass Transfer Characteristics of Gas-Liquid Contactors. *Chemical Engineering Science* **1981,** *36*(11), 1747-68.

Lloyd, W. G. The Low-Temperature Autoxidation of Diethylene Glycol. *Journal of the American Chemical Society* **1956,** *78*, 72-75.

Love, L.A.; Lijinsky, W.; Keefer, L.; Garcia, H. Chronic oral administration of 1-nitrosopiperazine in high doses to MRC rats. *Z. Krebsforsch*., p. 69-73, **1977**.

Lovejoy, D.J.; Vosper, A.J. Part VI. The Reaction of Dinitrogen Trioxide with Primary and Secondary Amines, *J. Chem. Soc. (A)*, 2325-2328, **1968**.

Mago, B. F.; et al. Corrosion Inhibitors for Alkanolamine Gas Treating System. U.S. Patent 3 959 170, 1984.

McGinnis, B. D.; Adams, V. D.; Middlebrooks, E. J. Degradation of Ethylene Glycol in Photo Fenton Systems. *Wat. Res.* **2000**, 34(8), 2346-2354.

McGinnis, B. D.; Adams, V. D.; Middlebrooks, E. J. Degradation of Ethylene Glycol using Fenton's reagent and UV. *Chemosphere* **2001**, 45, 101-108.

Nakayanagi, M. Formation of $FeCO_3$ Scale Layer and Corrosion of Carbon Steel in CO_2-loaded Aqueous Alkanolamine Solutions. *Sekiyu Gakkaishi* **1996,** *39*(5), 322-329.

Nascimento, R. F. et al. Qualitative and quantitative high-performance liquid chromatographic analysis of aldehydes in Brazilian sugar cane spirits and other distilled alcoholic beverages. *Journal of Chromatography A* **1997**, 782(1), 13-23.

Nelson, M. Personal Communication to Andrew J. Sexton. Austin, TX, 2008.

NRC *Climate Change Science: An Analysis of Key Questions.* 0-309-07574-2; National Research Council Committee on the Science of Climate Change, National Academy Press: Washington, D.C., 2001.

Okoye, C. Rate and Solubility in MEA/PZ/Water. Masters Thesis, The University of Texas at Austin, Austin, TX, 2005.

Olivieri, A. C.; Escandar, G. M. Random Error Analysis in the Determination of Equilibrium Constants of Very Stable Metal Complexes. *Analytical Letters* **1997**, 30(10), 1967-1980.

Onda, K.; Takeuchi, H.; Okumoto, Y. Mass Transfer Coefficients Between Gas and Liquid Phases in Packed Columns. *Journal of Chemical Engineering of Japan* **1968,** *1*(1), 56-62.

Pearce, R. L. Removal of Carbon Dioxide From Industrial Gases. U.S. Patent 4440731, 1984.

Pearce, R. L.; Pauley, C. R.; Wolcott, R. A. Recovery of Carbon Dioxides from Gases. U.S. Patent 2135900, 1984.

Petryaev, E. P.; Pavlov, A. V.; Shadyro, O. I. Homolytic Deamination of Amino Alcohols. *Zh. Org. Khim.* **1984,** *20*(1), 29-34.

Polderman, L. D.; Dillon, C. P.; Steele, A. B. Why Monoethanolamine Solution Breaks Down in Gas-Treating Service. *Oil and Gas Journal* **1955,** *54*(No. 2), 180-3.

Polderman, L. D.; Steele, A. B. Degradation of diethanolamine in gas treating service**.** *Proc. Gas Conditioning Conf.* **1956**, 49-56.

Ranney, M. W. *Corrosion Inhibitors - Manufacture and Technology*. Noyes Data Corporation: Park Ridge, NJ, 1976.

Rao, A. B.; Rubin, E. S. A Technical, Economic, and Environmental Assessment of Amine-Based CO2 Capture Technology for Power Plant Greenhouse Gas Control. *Environmental Science and Technology* **2002,** *36*(20), 4467-4475.

Riggs, O. L., Jr. Theoretical Aspects of Corrosion Inhibitors and Inhibition. In *Corrosion Inhibitors*, Nathan, C. C., Ed.; National Association of Corrosion Engineers: Houston, 1973; 7-27.

Rochelle, G. T.; Bishnoi, S.; Chi, S.; Dang, H.; Santos, J. *Research Needs for CO_2 Capture from Flue Gas by Aqueous Absorption/Stripping.* DE-AF26- 99FT01029; U.S. Departmnt of Energy - Federal Energy Technology Center: Pittsburgh, PA, 2001.

Rooney, P. C.; DuPart, M. S.; Bacon, T. R. Oxygen's Role in Alkanolamine Degradation. *Hydrocarbon Process., Int. Ed.* **1998,** *77*(7), 109-113.

Rosenblatt, D. H.; Hayes, A. J., Jr.; Harrison, B. L.; Streaty, R. A.; Moore, K. A. Reaction of Chlorine Dioxide with Triethylamine in Aqueous Solution. *Journal of Organic Chemistry* **1963,** *28*(10), 2790-2794.

Rosenblatt, D. H.; Hull, L. A.; DeLuca, D. C.; Davis, G. T.; Weglein, R. C.; Williams, H. K. R. Oxidations of Amines. II. Substituent Effects in Chlorine Dioxide Oxidations. *J. Am. Chem. Soc.* **1967,** *89*(5), 1158-1163.

Rossiter, W. J. et al. An investigation of the degradation of aqueous ethylene glycol and propylene glycol solutions using ion chromatography. *Solar Energy Materials* **1985**, 11(5-6), 455-467.

Rouchaud, J. P.; Decallonne, J. R.; Meyer J. A. Metabolism of the Fungicide Triforine in Barley Plants. *Pestic. Sci*. **1977**, 8, 65-70.

Rouchaud, J. P.; Decallonne, J. R.; Meyer J. A. Metabolism of [2,5-^{14}C]Piperazine in Barley Plants. *Pestic. Sci.* **1978a**, 9, 139-145.

Rouchaud, J. P.; Moons, C.; Decallonne, J. R.; Meyer J. A. Photodecomposition of Piperazine in Water by 'Sunlight' Ultraviolet Radiation. *Pestic. Sci.* **1978b**, 9, 305-309.

Ruddiman, W. F. How Did Humans First Alter Global Climate. *Scientific American* **2005,** *292*(3), 46-53.

Russell, G. A. Peroxide Pathways to Autoxidation, p. 107-128 in Peroxide Reaction Mechanism ed. By J. O. Edwards, Interscience Publishers, New York, 1960.

Sajus, L.; Seree De Roch, I. The Liquid Phase Oxidation of Aldehydes. *Comprehensive Chemical Kinetics* **1980**, 16, 89-124.

Seader, J. D.; Henley, E. J. *Separation Process Principles*. 1st ed.; John Wiley & Sons: 1997.

Seibig, S.; van Eldik, R. Kinetics of [FeII(EDTA)] Oxidation by Molecular Oxygen Revisited. New Evidence for a Multistep Mechanism. *Inorganic Chemistry* **1997,** *36*(18), 4115-4120.

Shoulders, B. Personal Communication to Andrew J. Sexton. Austin, TX, 2008.

Smith, P.A.S.; Loeppky, R.N. Nitrosative Cleavage of Tertiary Amines, *J. ACS*, 89, 1147-1157, **1967**.

Somogyi, L. P. Kirk-Othmer Encyclopedia of Chemical Technology, *Food Additives in Kirk-Othmer Encyclopedia of Chemical Technology*. 2008 http://www.mrw.interscience.wiley.com/kirk/articles/foodfrie.a01/frame.html (Accessed July 2008).

Sorensen, M.; Zurell, S.; Frimmel F. H. Degradation Pathway of the Photochemical Oxidation of Ethylenediaminetetraacetate (EDTA) in the UV/H_2O_2 Process. *Acta Hydrochim* **1998**, 26(2), 109-115.

Strazisar, B. R.; Anderson, R. R.; White, C. M. Degradation Pathways for Monoethanolamine in a CO_2 Capture Facility. *Energy & Fuels* **2003,** *17*(4), 1034-1039.

Stumm, W.; Lee, G. F. Oxygenation of Ferrous Iron. *Ind. Eng. Chem.* **1961**, *53*, 143-146.

Sunda, W.; Huntsman, S. Effect of pH, light, and temperature on Fe-EDTA chelation and Fe hydrolysis in seawater. *Marine Chemistry* **2003**, 84(1-2), 35-47.

Supap, T. Kinetic Study of Oxidative Degradation in Gas Treating Unit Using Aqueous Monoethanolamine Solution. MS Thesis, University of Regina, Regina, Saskatchewan, 1999.

Supap, T.; Idem, R.; Veawab, A.; Aroonwilas, A.; Tontiwachwuthikul, P.; Chakma, A.; Kybett, B. D. Kinetics of the Oxidative Degradation of Aqueous Monoethanolamine in a Flue Gas Treating Unit. *Industrial & Engineering Chemistry Research* **2001,** *40*(16), 3445-3450.

Tanthapanichakoon, W.; Veawab, A. Heat Stable Salts and Corrosivity in Amine Treating Units. *Greenhouse Gas Control Technologies, Proceedings of the International Conference on Greenhouse Gas Control Technologies, 6th, Kyoto, Japan, Oct. 1-4, 2002* **2003,** *2*, 1591-1594.

Tricker, A.R.; Kumar, R.; Siddiqi, M.; Khuroo, M.S.; Preusmann, R. Endogenous formation of *N*-nitrosamines from piperazine and their urinary excretion following antihelmintic treatment with piperazine citrate. *Carcinogenesis*, 12(9), p. 1595-1599, **1991**.

Ulrich, R. K. Sulfite Oxidation Under Flue Gas Desulfurization Conditions: Enhanced Oxygen Absorption Catalyzed by Transition Metals. Doctoral Thesis, The University of Texas at Austin, Austin, 1983.

United States EPA National Exposure Research Laboratory. Total Kjeldahl Nitrogen by Ion Selective Electrode. 351.4-1 – 351.4-3. 1978.

van Holst, J.; Politiek, P. P.; Niederer, J. P. M.; Versteeg, G. F.; Feron, P. H. M. CO_2 Capture from flue gas using amino acid salt solutions. Presented at the 8th International Conference on Greenhouse Gas Control Technologies, Trondheim, Norway, 2006.

Van't Riet, K. Review of Measuring Methods and Results in Nonviscous Gas-Liquid Mass Transfer in Stirred Vessels. *Industrial & Engineering Chemistry Process Design & Development* **1979,** *18*(3), 357-364.

Vazquez, G.; Alvarez, E.; Navaza, J. M.; Rendo, R.; Romero, E. Surface Tension of Binary Mixtures of Water + Monoethanolamine and Water + 2-Amino-2- methyl-1-propanol and Tertiary Mixtures of These Amines with Water from 25^{o}C to 50^{o}C. *Journal of Chemical and Engineering Data* **1997,** *42*(1), 57-59.

Veawab, A.; Aroonwilas, A. Identification of Oxidizing Agents in Aqueous Amine-CO_2 Systems Using a Mechanistic Corrosion Model. *Corrosion Science* **2002,** *44*(5), 967-987.

Veawab, A.; Tontiwachwuthikul, P.; Chakma, A. Influence of Process Parameters on Corrosion Behavior in a Sterically Hindered Amine-CO_2 System. *Industrial & Engineering Chemistry Research* **1999,** *38*(1), 310-315.

Vorobyov, I.; Yappert, M. C.; DuPre, D. B. Hydrogen Bonding in Monomers and Dimers of 2-Aminoethanol. *Journal of Physical Chemistry A* **2002,** *106*(4), 668-679.

Weiland, R. H. *Physical Properties of MEA, DEA, MDEA, and MDEA-Based Blends Loaded with CO_2*. GPA Research Report No. 152; Gas Processors Association: Tulsa, OK, 1996.

Weiland, R. H.; Dingman, J. C.; Cronin, D. B.; Browning, G. J. Density and Viscosity of Some Partially Carbonated Aqueous Alkanolamine Solutions and Their Blends. *Journal of Chemical and Engineering Data* **1998,** *43*(3), 378-382.

White, J. C. Deaerator Providing Control of Physicochem. Oxygen Scavenging in Boiler Feedwaters. US-20010045396, 2001.

Wolcott, R. A.; Pauley, C. R.; Pearce, R. L. Recovery of copper inhibitor in the recovery of carbon dioxide from flue gases. 8502555, 1985.

Wong, H. A.; Kohler, R.; Kosseim, A. J.; Kubek, D. J.; McCullough, J. G. Corrosion-Inhibition System Passes Severest Test at Chevron's Princess MEA Plant. *Oil and Gas Journal* **1985,** *83*(45), 100-108.

Yazvikova, N. V.; Zelenskaya, L. G.; Balyasnikova, L. V. Mechanism of Side Reactions During Removal of Carbon Dioxide from Gases by Treatment with Monoethanolamine. *Zhurnal Prikladnoi Khimii* **1975,** *48*(3), 674-676.

Vita

Andrew James Sexton was born on May 20, 1981 in Somerset, Kentucky to Carol and Samuel Sexton. The author graduated from Pulaski Southwestern High School in Somerset, Kentucky in May 1999. The author entered the chemical engineering program at the University of Louisville in Louisville, Kentucky in the fall of 1999. He graduated with a Bachelor of Science in May 2003 and a Masters of Engineering (both in chemical engineering) in August 2004. While attending the University of Louisville, the author worked for DuPont Fluoroproducts in Louisville, Kentucky from 2001 to 2002. He entered the Graduate School at The University of Texas at Austin in the fall of 2004.

Permanent Address: 407 Murphy Avenue
Ferguson, Kentucky 42533

This dissertation was typed by Andrew J. Sexton.